

**Processing of O⁶ - methylguanine in mammalian cells:
involvement of DNA double strand break repair proteins
and cytokine stimulation**

**Dissertation
Zur Erlangung des Grades
Doktor der Naturwissenschaften**

**Am Fachbereich Biologie
Der Johannes Gutenberg -Universität Mainz**

**Malgorzata Debiak
geb. am 16.02.1976 in Krakow, Polen**

Mainz, 2006

Tag der Prüfung: 13.07.2006

Table of contents

Table of contents

	Table of contents	I
	Table of figures	IV
	Abbreviations	VI
1	Introduction	1
1.1	Processing of DNA damage induced by alkylating agents	1
1.2	Role of ATM in signaling of DNA damage	5
1.3	Cytokines as modulators of DNA repair and apoptosis	10
1.3.1	IGF-I	11
1.3.1.1	The physiological role and regulation of the IGF-I system	11
1.3.1.2	IGF-I system in cancer	12
1.3.1.3	IGF-I modulation of apoptosis and DNA repair	13
1.3.2	IL-1	13
1.3.2.1	Physiological functions of IL-1	15
1.3.2.2	IL-1 in cancer biology	16
1.3.2.3	IL-1 in apoptosis and DNA repair	16
1.4	Aims	18
2	Materials and methods	19
2.1	Equipment	19
2.2	Assays, chemicals, materials and recombinant proteins	20
2.3	Cell Culture Reagents	21
2.4	Bacteria	22
2.5	Cell lines	22
2.6	Oligonucleotides	22
2.7	Antibodies	24
2.8	Buffers	25
2.9	Cell culture	26
2.9.1	Treatment with genotoxic agents and cytokines	27
2.9.2	Transfection of eukaryotic cells	27
2.10	Viability assays	28
2.10.1	WST-1 assay	28
2.10.2	Clonogenic survival	28
2.11	Apoptosis determination	29
2.11.1	Annexin V/propidium iodide double staining	29
2.11.2	Flow cytometric analysis of SubG1 fraction	29
2.11.3	Caspase activity detection with FITC-VAD-FMK	30
2.11.4	DNA laddering	30
2.12	FACS analysis of cell cycle distribution	30
2.13	Protein analysis	31
2.13.1	Protein extracts	31
2.13.1.1	Whole cell extracts	31
2.13.1.2	Nuclear extracts	31
2.13.1.3	Fractionation of cytosolic and mitochondrial proteins	31
2.13.1.4	Whole cell extracts for western blot with phospho-specific antibodies	32
2.13.1.5	Extracts for western blot with anti-caspase antibodies	32
2.13.1.6	Nuclear extracts for Electro Mobility Shift Assay (EMSA)	32
2.13.1.7	Extracts for MGMT activity assay	33
2.13.2	Determination of protein concentration	33
2.13.2.1	Protein concentration determination using the Bradford method	33

Table of contents

2.13.2.2	Protein concentration determination using the Lowry method	33
2.13.3	Polyacrylamide gel electrophoresis (SDS PAGE)	33
2.13.4	Western blot transfer and protein detection with antibodies	34
2.13.5	Electro Mobility Shift Assay (EMSA)	34
2.13.6	IL-6 elisa assay	35
2.13.7	Caspase assay	35
2.13.8	MGMT assay	36
2.14	Gene expression analysis	36
2.14.1	RNA isolation and RNA electrophoresis	36
2.14.2	Reverse transcription	37
2.14.3	PCR	37
2.14.3.1	Semi quantitative PCR	37
2.14.3.2	Real Time PCR	37
2.14.4	DNA electrophoresis	38
2.14.5	DNA microarray analysis	38
2.15	Cloning of DNA	39
2.15.1	Cloning with Topo vectors	39
2.15.2	Transformation of E. coli	39
2.15.3	Isolation of plasmid DNA	40
2.15.3.1	“Mini” preparation	40
2.15.3.2	“Midi” and “Maxi” preparation	40
3	Results	41
3.1	DNA double-strand break repair in processing of O ⁶ MeG lesions	42
3.1.1	Phenotypic characteristics of ATM knockout cells	42
3.1.2	Sensitivity of ATM deficient cells to DNA methylating chemotherapeutic drugs	44
3.1.3	Role of O ⁶ MeG in methylating agents toxicity towards ATM -/- cells	46
3.1.4	Effect of caffeine on cell death induced by MNNG and MMS	52
3.1.5	Effect of O ⁶ -benzylguanine and MGMT cDNA transfection on O ⁶ MeG induced cell death	53
3.1.6	ATM in the apoptotic pathway evoked by methylating agents	60
3.1.7	JNK and p38 kinase activation in ATM +/+ and ATM -/- cells	65
3.1.8	AP-1 binding activity upon methylating agents treatment	67
3.1.9	Expression of AP-1 and NFκB target genes in ATM +/+ and ATM -/- cells	68
3.1.10	Cell cycle checkpoint activation upon treatment with methylating agents	69
3.2	Influence of cytokines on DNA repair and sensitivity of cells to alkylating agents	77
3.2.1	Modulation of cell survival by IGF-I and IL-1 after MMS treatment in ATM -/- and ATM +/+ background	77
3.2.2	Influence of IGF-I and IL-1 on DNA repair gene expression	80
3.3	IL-1 regulates APEX2 gene in human keratinocytes	84
3.3.1	IL-1 gene up-regulation was specific for APEX2 and did not occur for other BER genes	87
3.3.2	IL-1 increases survival of KB cells exposed to oxidative stress	89
3.3.3	Influence of APEX2 over-expression on survival of HeLa cells	93
3.3.4	Sensitivity of HeLa cells over-expressing APEX2 to DNA damaging agents	94
4	Discussion	97

Table of contents

4.1	ATM is involved in O ⁶ MeG processing	97
4.1.1	ATM deficient cells are hypersensitive to methylating agents	97
4.1.2	O ⁶ MeG is the DNA lesion causing hypersensitivity of ATM -/- cells to DNA methylating agents	99
4.1.3	ATM is dispensable for apoptosis induced by O ⁶ MeG	100
4.1.4	Apoptosis induced by O ⁶ MeG is a late effect	102
4.1.5	Apoptosis induced by O ⁶ MeG is executed via the mitochondrial pathway	103
4.2	ATM protects cells against O ⁶ MeG induced apoptosis	104
4.2.1	ATM interactions within the apoptotic pathway upon treatment with O ⁶ MeG inducing agents	104
4.2.2	ATM does not activate cell cycle checkpoints following methylating agent treatment	105
4.3	Influence of cytokines on DNA repair capacity and sensitivity to DNA methylating agents	105
4.3.1	IGF- I protects cells against MMS in an ATM dependent manner	107
4.3.2	IL-1 induces APEX2 in human keratinocytes	108
4.4	Outlook	110
5	Summary	112
6	References	113
	Publications, abstracts and oral presentations	136
	Curriculum vitae	138
	Acknowledgements	139

Table of figures

Table of figures

Fig. 1	Positions of alkylating adducts substitution within DNA	1
Fig. 2	Processing of O ⁶ MeG in Mex ⁺ and Mex ⁻ cells	5
Fig. 3	ATM phosphorylates number of proteins involved in genomic stability	7
Fig. 4	Role of ATM in activation of cell cycle checkpoints	8
Fig. 5	IGF-IR signaling pathway	12
Fig. 6	IL-1 signaling cascade	14
Fig. 7	MGMT activity in ATM +/+ and ATM -/- mouse fibroblasts	42
Fig. 8	Expression of MMR and p53 in ATM wild type and mutated cells	43
Fig. 9	Clonogenic survival and programmed cell death in ATM +/+ and ATM -/- cells upon γ -irradiation	44
Fig. 10	Clonogenic survival of ATM +/+ and ATM -/- cells exposed to temozolomide or fotemustine	45
Fig. 11	Induction of programmed cell death in ATM +/+ and ATM -/- cells upon treatment with temozolomide and fotemustine	46
Fig. 12	Clonogenic survival of ATM +/+ and ATM -/- cells exposed to MNNG and MMS	47
Fig. 13	Viability of ATM +/+ and ATM -/- cells as measured by WST-1 metabolic assay as a function of dose upon pulse treatment with MNNG and MMS	48
Fig. 14	Viability of ATM +/+ and ATM -/- cells as a function of dose measured by the metabolic WST-1 assay upon treatment with MMS	49
Fig. 15	Apoptosis and necrosis induced by MNNG and MMS in ATM +/+ and ATM -/- cells	51
Fig. 16	Frequency of apoptosis and necrosis in ATM +/+ and ATM -/- treated with MNNG and MMS in combination with 1 mM caffeine	53
Fig. 17	MGMT activity in ATM +/+ and ATM -/- cells	54
Fig. 18	Sensitivity of ATM +/+ and ATM -/- cells to MNNG and MMS upon depletion of residual MGMT activity with O ⁶ BG	56
Fig. 19	Colony formation of clones transfected with MGMT cDNA upon MNNG and MMS treatment	57
Fig. 20	Induction of apoptosis and necrosis by MNNG and MMS in ATM +/+ and ATM -/- cells over-expressing MGMT	59
Fig. 21	Time course of apoptosis and caspase activation in ATM +/+ and ATM -/- cells after treatment with 10 μ M MNNG	61
Fig. 22	Time course of apoptosis and caspase activation in ATM +/+ and ATM -/- cells after treatment with 1 mM MMS	62
Fig. 23	Caspase activation and expression of apoptotic proteins in ATM +/+ and ATM -/- cells upon MNNG and MMS treatment	64
Fig. 24	MAPK activation in ATM +/+ and ATM -/- cells upon treatment with 10 μ M MNNG or 1 mM MMS	66
Fig. 25	MAPK activation as a function of dose of MNNG and MMS 1 h after mutagen treatment in ATM +/+ and ATM -/- cells	67
Fig. 26	AP-1 binding activity in ATM +/+ and ATM -/- cells upon treatment with 10 μ M MNNG and 1 mM MMS	68
Fig. 27	RT-PCR analysis of JNK and NF κ B dependent genes in ATM +/+ and ATM -/- cells upon treatment with 10 μ M MNNG and 1 mM MMS	69
Fig. 28	Cell cycle distribution of ATM +/+ and ATM -/- cells after treatment with 10 μ M MNNG	71
Fig. 29	Cell cycle distribution of ATM +/+ and ATM -/- cells after treatment with 1 mM MMS	72

Table of figures

Fig. 30	Cell cycle distribution of ATM +/+ and ATM -/- cells as a function of dose 24 h after MNNG treatment	73
Fig. 31	Cell cycle distribution of ATM +/+ and ATM -/- cells 24 h after treatment with different doses of MMS	74
Fig. 32	Chk-1 kinase activation in ATM -/- and ATM +/+ cell upon treatment with 5 Gy ionising radiation, 10 µM MNNG and 1 mM MMS	76
Fig. 33	ATM +/+ and ATM -/- cells possess functional IGF-I and IL-1 receptors	78
Fig. 34	Survival of ATM +/+ and ATM -/- cells treated for 24 h with different concentrations of MMS in presence or absence of IGF-I or IL-1	79
Fig. 35	Apoptosis and necrosis analysed in ATM +/+ and ATM -/- cells treated with 0.6 mM MMS for 24 h with and without IGF-I stimulation	80
Fig. 36	DNA repair gene expression upon stimulation of KB cells with 50 ng/ml IGF-I	82
Fig. 37	Regulation of IL-6 on RNA and protein level in KB cells treated with 10 ng/ml IL-1	83
Fig. 38	Microarray analysis of DNA repair gene expression in KB cells 2 h after stimulation with 10 ng/ml IL-1	84
Fig. 39	Induction of <i>NFκB</i> , <i>IκB</i> , <i>p21</i> and <i>APEX2</i> in KB cells after IL-1 stimulation was confirmed by semi-quantitative RT-PCR	85
Fig. 40	<i>APEX2</i> expression on RNA and protein level after stimulation of cells with 10 ng/ml IL-1	86
Fig. 41	Influence of actinomycin D on <i>APEX2</i> expression in IL-1 stimulated KB cells	88
Fig. 42	BER gene expression in KB cells stimulated with 10 ng/ml IL-1	89
Fig. 43	Western blot analysis of BER proteins in whole and nuclear extracts of KB cells stimulated with 10 ng/ml IL-1	90
Fig. 44	Frequency of apoptosis in KB cells treated with different genotoxic agents with and without IL-1 stimulation	90
Fig. 45	Cell cycle distribution of KB cells treated with IL-1 and genotoxins	91
Fig. 46	Influence of IL-1 on major apoptotic proteins in KB cells treated with 1 mM MMS or 1 mM H ₂ O ₂	92
Fig. 47	<i>APEX2</i> expression in HeLa cells stably and transiently transfected with pcDNA3.1- <i>APEX2</i>	93
Fig. 48	Apoptosis induced by different genotoxins in HeLa cells transfected with pcDNA3.1-neo and pcDNA3.1- <i>APEX2</i> vector	95
Fig. 49	Frequency of apoptosis measured by SubG1 in HeLa -MR cells transiently transfected with pcDNA3.1 empty or pcDNA3.1- <i>APEX2</i> vector	96

Abbreviations

Abbreviations:

APS	Ammonium persulfate
ACNU	(1-(4-amino-2-methyl-5-pyrimidyl)methyl-3-(2-chloroethyl)-3-nitrosourea
AP-1	Activator protein 1
APE1	Apurinic endonuclease 1
APEX2	Apurinic endonuclease 2
A-T	Ataxia telangiectasia
ATM	Ataxia-telangiectasia mutated
ATR	Ataxia-telangiectasia and Rad3-related protein
Bax	“Bcl-2 associated protein X”
Bcl-2	“B cell lymphoma 2”
BCNU	(1,3- <i>bis</i> (2-chloroethyl)-1-nitrosourea
BER	Base excision repair
BRCA1	Breast cancer associated 1
BSA	Bovine serum albumin
Cis-Pt	Cisplatin
DMSO	Dimethyl sulfoxide
DNA-PK	DNA-dependent protein kinase
DSB	Double strand break
DTT	Dithiothreitol
EDTA	Ethylenediaminetetraacetic acid disodium salt
E2F1	E2 promoter binding factor 1
EGF	Epidermal growth factor
EMS	Ethyl methanesulphonate
ENU	N-ethyl-N-nitrosourea
ERCC1	Excision repair cross complementation group 1
ERK2	Extracellular signal receptor regulated kinase 2
FACS	Fluorescence activated cell sorting
FCS	Foetal calf serum
FEN-1	Flap endonuclease 1
GAPDH	Glyceraldehyde 3- phosphate dehydrogenase
GH	Growth hormone
HEPES	N-(2-Hydroxyethyl)piperazine-N’-(2-ethanesulfonic acid)
HNSCC	Head and neck squamous cell carcinoma
HR	Homologous recombination
IAP	Inhibitor of apoptosis protein
IGFBP3	IGFI binding protein 3
IGF-I	Insulin-like growth factor I
IGF-IR	IGFI receptor
IL-1	Interleukin 1
IL-1R	Interleukin 1 receptor
IL-6	Interleukin 6
IR	Ionising radiation
JNK	c-Jun NH ₂ -terminal kinase
MAPK	Mitogen-activated protein kinase
MDC1	Mediator of damage checkpoint 1
MDM2	“Mouse double minute”
MGMT	O ⁶ -methylguanine-DNA methyltransferase
MMR	Mismatch repair
MMS	Methyl methansulfonate

Abbreviations

MNNG	N-Methyl-N'-nitro-N-nitrosoguanidine
MNU	N-Methyl-N-Nitrosourea
MRN	Mre11/Rad50/Nbs-1 complex
NBS-1	Nijmegen breakage syndrome
NER	Nucleotide excision repair
NFκB	Nuclear factor-κB
NHEJ	Non-homologous end joining
O ⁶ BG	O ⁶ - Benzylguanine
O ⁶ MeG	O ⁶ - Methylguanine
PBS	Phosphate buffered saline
PCNA	Proliferating cell nuclear antigen
PI	Propidium iodide
PI3K	Phosphatidylinositol 3-kinase
PMSF	Phenylmethylsulfonylfluorid
SCE	Sister chromatide exchange
SDS	Sodium dodecyl sulphate
SSB	Single strand break
TBS	Tris buffered saline
TEMED	N,N,N',N'-Tetramethylethylendiamin
TNF-α	Tumour necrosis factor - α
Tris	Tris(hydroxymethyl)aminomethane
UV	Ultraviolet light
XRCC1	X-Ray cross complementing factor 1
Z-VAD-FMK	Benzyloxycarbonyl -Val-Ala-Asp-fluoromethyl ketone

1 Introduction

1.1 Processing of DNA damage induced by alkylating agents

Alkylating agents belong to a structurally diverse group of compounds that include natural and industrial environmental pollutants. They interact with DNA, transferring an alkyl group onto the different nucleotides by a nucleophilic substitution reaction. Examples of simple alkylating agents are methylating and ethylating agents. On the basis of their chemical structure, they are divided into 4 groups: the alkyl sulfates, the alkyl alkanesulfonates, the nitrosamides and the nitrosamines (Beranek, 1990). Alkylating agents are highly mutagenic, carcinogenic and clastogenic. By taking advantage of their high toxicity against proliferating tissues, they are frequently used as anti-cancer drugs. Therapeutic methylating agents include temozolomide, streptozotocin, procarbazine and dacarbazine, which are administered for the treatment of gliomas, melanomas, carcinoid tumours and Hodgkin's lymphomas. Chloroethylating agents, such as carmustine (BCNU), nimustine (ACNU), and fotemustine, are widely used to treat brain tumours and melanomas (Gerson, 2004).

Exposure of cells to alkylating agent produce 15 different nitrogen and oxygen adducts within the bases of DNA while also forming 2 phosphotriesterisomers (**Fig. 1**). The differences in amounts of the products formed are determined by the nature of the alkylating agent (O'Connor and Saffhill, 1979).

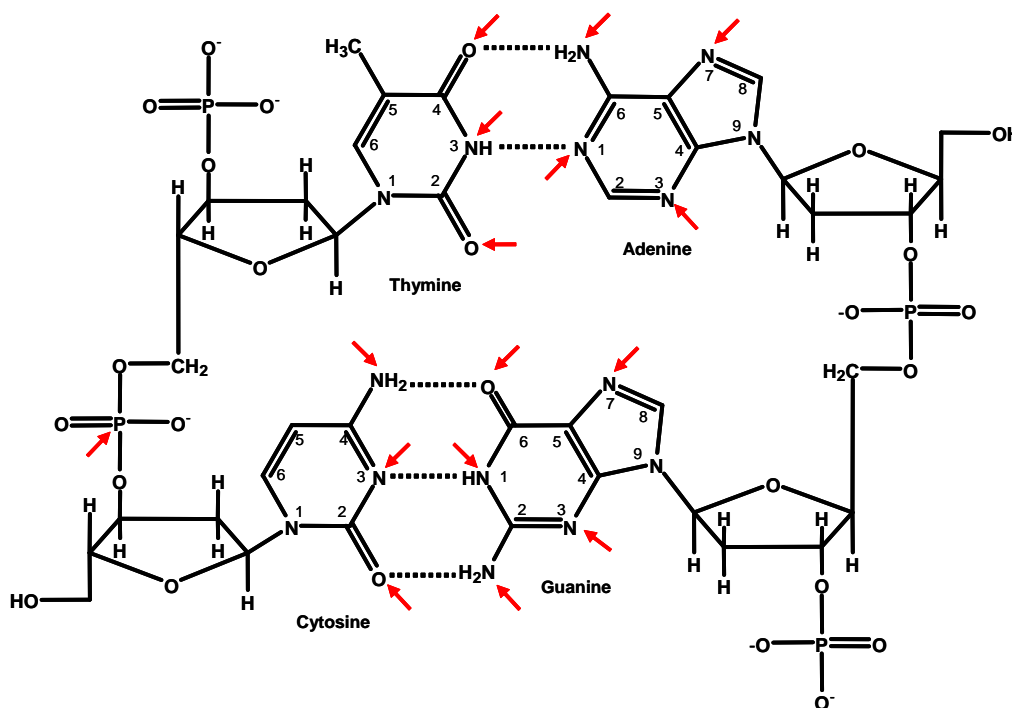


Fig. 1 Positions of alkylating adducts substitution within DNA

Introduction

Although the vast majority of adducts are formed at the N7 position of guanine (about 62 % of alkylating products formed), O⁶-alkylguanine is the lesion responsible for the most severe biological effects of alkylating agents, which include mutagenesis and toxicity. This lesion is induced in minor amounts not exceeding 8% of total alkylation products (Beranek, 1990). Attention will be focused on the methyl version of this lesion, namely O⁶-methylguanine (O⁶MeG).

O⁶MeG is repaired in a one step reaction by the repair protein O⁶-methylguanine-DNA methyltransferase (MGMT) [EC2.1.1.64] (Pegg, 1990; Pegg et al., 1995). To initiate repair, MGMT binds DNA and scans individual bases for evidence of O⁶-methylation, flipping each base into its active-site pocket (Daniels et al., 2000). Once found, the methyl group binds to cysteine within the active site of MGMT. This reaction is known as the so called “suicide” reaction since MGMT becomes irreversibly inactivated by the covalent transfer of the methyl group from the oxygen in guanine to the sulphur in the cysteine of the MGMT protein (Moore et al., 1994; Wibley et al., 2000). The methylated protein disassociates from DNA, becomes ubiquitinated and is then degraded. Degradation of inactive, methylated MGMT protein is much faster than degradation of the active MGMT protein (Srivenugopal et al., 1996). The kinetics of O⁶MeG repair is quite rapid, occurring within minutes; more than 90% of adducts are removed within the first 10 minutes after they were formed (Gerson, 2002). Beside O⁶MeG, MGMT also recognises longer alkyl adducts at the O⁶ position of guanine and O⁴ of thymine but the repair process occurs with lower efficiency.

MGMT expression is cell type specific. In most species, the liver has the highest expression level followed by lung and kidney. The nervous system and mammary gland exhibit the lowest MGMT expression level (Citron et al., 1991; Gerson et al., 1986). Mean MGMT activity is usually higher in malignant tissues than in their normal counterpart (Preuss et al., 1996; Silber et al., 1993). High MGMT activities have been detected in colon cancer, lung tumours, breast and ovarian cancer (Kaina and Christmann, 2002; Povey et al., 2000). However, several human tumours lack MGMT. This is due to abnormal MGMT promoter methylation accompanying malignant transformation. Among glioblastomas the percentage of MGMT deficient tumours is particularly high (Kaina and Christmann, 2002; Preuss et al., 1996; Silber et al., 1998).

MGMT expression is regulated by different mechanisms involving transcription factor binding and methylation of DNA within the gene or promoter region. Within the MGMT promoter region, several transcription-factor-recognition sequences have been identified,

Introduction

which include SP1, GRE and AP-1 sites. Transcriptional activation of MGMT has been shown for glucocorticoids, cAMP and protein kinase C activators (Biswas et al., 1999; Grombacher et al., 1996; Pegg, 1999). Additionally, MGMT expression can be induced by DNA damaging agents. *In vivo* and *in vitro* studies reported MGMT up-regulation after treatment with γ -irradiation and alkylating agents such as MNNG, MMS, EMS and MNU (Chan et al., 1992; Fritz and Kaina, 1992; Lefebvre and Laval, 1986; Lefebvre and Laval, 1989; Lefebvre et al., 1993). Up-regulation of MGMT expression regulated by transcription factors occurs in normal and malignant tissues. Contrary to this, MGMT regulation by promoter methylation is limited to tumours and is associated with promoter methylation of other cancer-related genes, including p21, p16, and MLH1. The methylation takes place on the cytosine of CpG islands, which are located in two distinct regions of the MGMT promoter (regions from -249 to -103 and +107 to +196) (Harris et al., 1991). Hypermethylation of the CpG islands leads to chromatin condensation within the promoter region, preventing binding of DNA polymerases and transcription factors, finally leading to gene silencing (Watts et al., 1997). Treatment of cells with the demethylating agent, 5-azacytosine, which de-methylates the promoter region, reactivates transcription and restores MGMT activity (von Wronski and Brent, 1994). Comparison of MGMT proficient and deficient cell lines showed that MGMT regulation may also involve the methylation of DNA in the coding region (Fritz et al., 1991; Lage et al., 1999). Unlike the promoter region, methylation of the gene facilitates MGMT transcription (Wang et al., 1992).

Studies with MGMT transgenic cells and mice revealed a direct correlation between MGMT activity and sensitivity to alkylating agents. As expected, MGMT knockout mice are more sensitive to methylating (MNU) and chloroethylating (BCNU) agents due to high bone marrow toxicity (Glassner et al., 1999; Shiraishi et al., 2000). Opposed to this MGMT over-expression protects against the toxic effects of methylating and chloroethylating agents as well as carcinogenesis. Thus, tissue-targeted MGMT over-expression reduced development of thymic lymphomas, liver and lung tumours. Over-expression of MGMT in epidermal cells protected against tumour initiation in the two stage skin carcinogenesis model following MNU and ACNU treatment (Becker et al., 1996; Becker et al., 1997). Furthermore, tumour progression was also delayed in these mice (Becker et al., 2003). Cells with high MGMT activity (phenotype described also as Mex⁺) are resistant to alkylating agents induced cell death and apoptosis and maintain their genomic stability (Kaina et al., 1993; Kaina et al., 1991; Kokkinakis et al., 1997; Preuss et al., 1996).

Introduction

In MGMT deficient cells (Mex⁻), O⁶MeG remains unrepaired within DNA what leads to mutations, chromosomal aberrations, SCE's and apoptosis. These processes are dependant on cell proliferation and a functional mismatch repair system (MMR). Non-proliferating cells are highly resistant to both alkylation induced mutations as well as apoptosis (Kaina and Christmann, 2002; O'Neill, 2000; Roos et al., 2004). MGMT and MMR deficient cells produce mutations with high frequency upon alkylating agent treatment but are resistant to O⁶MeG induced cell death. This is known as the “tolerant phenotype” as these cells can tolerate high levels of un-repaired O⁶MeG in their DNA (Branch et al., 1993; Dosch et al., 1998; Goldmacher et al., 1986). O⁶MeG does not distort the double helix to a great extent, although it does alter the hydrogen bonding of guanine with cytosine. Thus, during DNA synthesis, O⁶MeG is misread by DNA polymerase as adenine that results in preferential incorporation of thymine instead of cytosine. Unless repaired, O⁶MeG:T mispairs result in G to A point mutations during a subsequent replication round (**Fig. 2**) (Loechler et al., 1984; Rossi and Topal, 1991; Saffhill and Hall, 1985). Alternatively, O⁶MeG:T mispairs are recognised by the MutS α complex of MMR (Duckett et al., 1996; Karran and Bignami, 1992). Processing of O⁶MeG:T is aberrant because MMR targets the newly synthesised DNA strand containing the thymine, leaving O⁶MeG behind. This results in several rounds of failure MMR that gives rise to pro-apoptotic secondary lesions. Increased frequency of recombination and chromosomal aberrations indicated that DNA double-strand breaks (DSB) might be involved in processing of O⁶MeG (Kaina et al., 1997; Ochs and Kaina, 2000). Single-strand breaks (SSB) are repair intermediates of the MMR system. DSB are suspected to be the result of two SSB forming in close proximity of each other on opposite DNA strands or a SSB converted to a DSB because of replication fork progression during the next round of replication. If toxicity is mediated via DSB's, DSB repair deficient cells should be highly sensitive to alkylating agents. The main protein responsible for DSB's detection and initiation of the DSB repair process is Ataxia Telangiectasia Mutated protein (ATM).

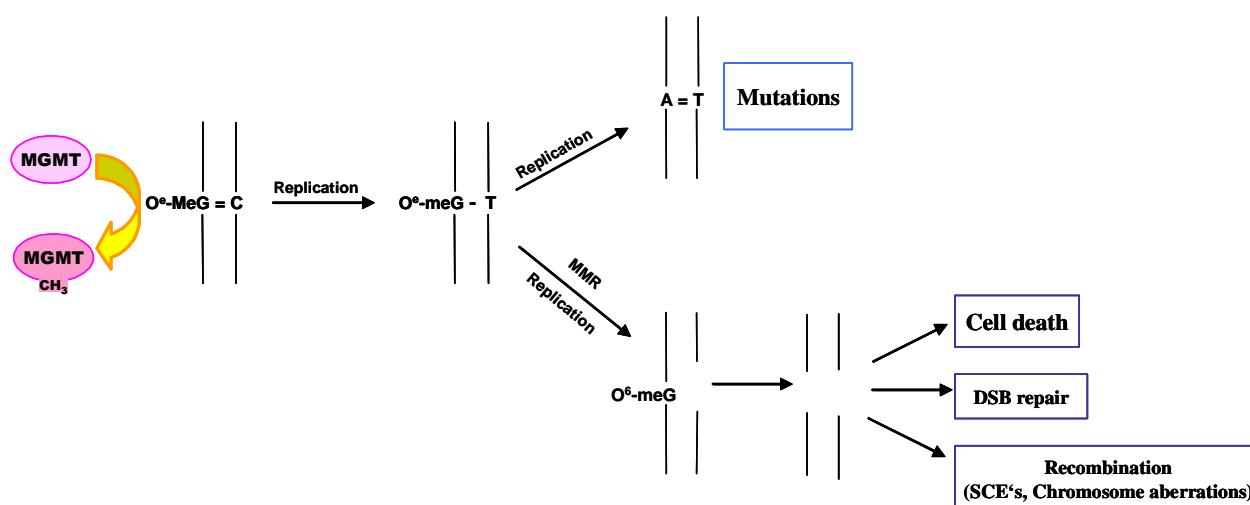


Fig. 2 Processing of O⁶MeG in Mex⁺ and Mex⁻ cells

1.2 Role of ATM in signaling of DNA damage

ATM is the product of the gene mutated in the human genetic disorder ataxia telangiectasia (A-T) (Savitsky et al., 1995a). A-T patients suffer from progressive neuronal degeneration, immunodeficiency, radiosensitivity and increased cancer risk, particularly the development of lymphoid malignancies. The cellular phenotype includes chromosomal instability, hypersensitivity to DSB inducing agents, radioresistant DNA synthesis and inadequate cell cycle control in response to DNA damage (Lavin and Shiloh, 1997). ATM knockout mice are viable and show a phenotype remarkably similar to A-T, except for progressive neurodegeneration. Mice homozygous for the disrupted *atm* allele display growth retardation, neurologic dysfunction, infertility, defects in T lymphocyte maturation, and extreme sensitivity to γ -irradiation. Animals develop malignant thymic lymphomas very early and die by the age of 6 month (Barlow et al., 1996; Elson et al., 1996; Xu et al., 1996).

The *atm* gene is positioned on the chromosome 11q22-23 (Gatti et al., 1988). It extends over 160kb of genomic DNA and is composed of 66 exons, from which 62 are coding sequences. There is only one functional splice variant known within the open reading frame (Savitsky et al., 1995b). The ATM protein consists of 3056 aminoacids (ca 350 kDa) and is ubiquitously expressed in embryonic and adult tissues. Expression is particularly high in the developing nervous system as well as in the spleen, thymus and testes, tissues in which active gene rearrangement occurs (Brown et al., 1997; Chen and Lee, 1996; Soares et al., 1998).

Introduction

ATM is a member of the phosphatidylinositol 3-kinase family (PI3K) that also includes the catalytic subunit of DNA-dependent protein kinase (DNA-PKcs) and ATM and Rad3-related protein (ATR). Despite the homology to PI3K, all these proteins are protein kinases and express no lipid kinase activity. The consensus phosphorylation motif is a serine or threonine followed by glutamine (the 'SQ/TQ motif') (Kim et al., 1999; Lavin et al., 1995; O'Neill et al., 2000). ATM plays a central role in DNA damage recognition, initiation of cell cycle checkpoints and repair processes. It is primarily involved in recognition of DSB's caused by ionising radiation and radiomimetic drugs (Khanna et al., 1998; Smith et al., 1999; Suzuki et al., 1999), although it can also be activated by other stimuli that do not cause DSBs directly, including UV light (Hannan et al., 2002), chromium VI (Ha et al., 2003), nitric oxide (Hofseth et al., 2003), nutrient deprivation (Suzuki et al., 2003) and insulin (Yang and Kastan, 2000).

ATM is mostly a nuclear protein. 10 % of the protein is located in the cytoplasm in peroxisomes or endosomes. The function of the cytoplasmic fraction is unknown (Lim et al., 1998; Watters et al., 1999). In nuclei, ATM molecules are present as inactive dimers or higher multimers. Upon DNA damage, ATM dimers are converted into active monomers displaying kinase activity. This process is accompanied by ATM auto-phosphorylation at Ser1981. Whether auto-phosphorylation is necessary for ATM activation is still controversial. Bakkenist & Kastan presented a model postulating that the phosphorylation event is the initial step in ATM dimer dissociation and activation. ATM activation is not dependent on direct binding to DNA strand breaks but rather involves changes in chromatin structure and histone modifications that results from DNA damage (Bakkenist and Kastan, 2003; Kozlov et al., 2003). However, this model is challenged by Lee & Paull who observed that ATM mutated at Ser1981 can still be activated to the same extent as wild - type protein. In addition, the kinase activity of ATM is stimulated *in vitro*, by the Mre11-Rad50-Nbs1 (MRN) complex in the presence of damaged DNA. The MRN complex acts as a sensor for DSB's and recruits ATM to DNA (Lee and Paull, 2004; Lee and Paull, 2005). This model is supported by the finding that the MRN complex is required for ATM activation *in vivo* (Uziel et al., 2003). Thus, the MRN complex appears to be an up- and downstream target of ATM. Once activated, ATM phosphorylates a number of different substrates that take part in cell cycle control, DSB repair, transcription control and apoptosis (**Fig. 3**).

Introduction

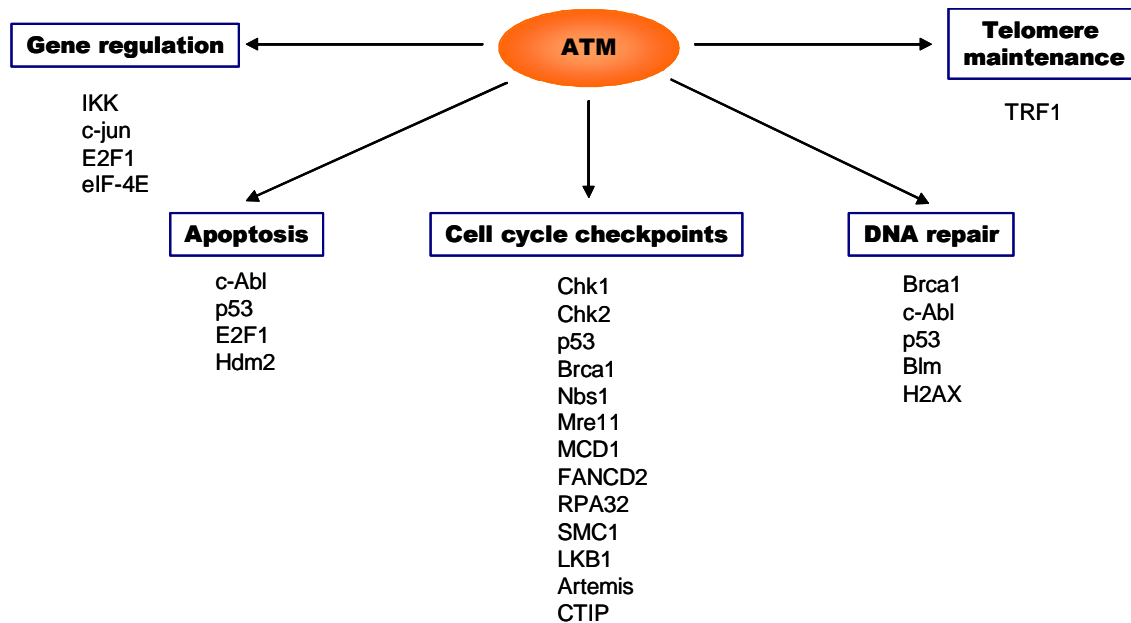


Fig. 3 ATM phosphorylates number of proteins involved in genomic stability

ATM plays a part in G1/S, S and G2 checkpoint control in eukaryotic cells. Following DNA damage induction, ATM activates the checkpoint signaling cascade, resulting in delay of cell cycle progression. This provides additional time for the cell to remove the DNA damage before entering the next cell cycle phase. The arrest at the G1/S checkpoint is mediated by the tumour suppressor protein p53. In non-stimulated cells, p53 is complexed with the proto-oncogene MDM2. The binding of MDM2 promotes the ubiquitination of p53 and its subsequent degradation by the proteasome. Following formation of DSBs, for example by exposing cells to ionising radiation, ATM phosphorylates p53 on Ser15 and MDM2 on Ser395, that are within the MDM2-p53 binding region (Banin et al., 1998; Canman et al., 1998; Khanna et al., 1998; Maya et al., 2001). These phosphorylation events lead to liberalization of the complex and prevent the degradation of p53, which becomes transcriptionally activated. A consequence of the p53 stabilisation and activation is transcriptional up-regulation of p21 (CDK2 inhibitor). Inhibition of CDK2 by p21 stops the cells at the G1/S border (el-Deiry et al., 1994; Harper et al., 1993). A-T cells exhibit a reduced and delayed induction of p53 and consequently an impaired G1/S block following exposure to γ -irradiation (Kastan et al., 1992; Khanna and Lavin, 1993). ATM also initiates the second pathway linking DNA damage to the G1/S checkpoint. In response to γ -irradiation, ATM phosphorylates Chk2 at the regulatory site Thr68, which enhances its kinase activity towards Cdc25A phosphatase. Phosphorylated Cdc25A becomes degraded, thereby is no longer able to activate Cdk2 by dephosphorylation (Matsuoka et al., 2000; Melchionna et al., 2000; Zhou et al., 2000). This ATM dependent checkpoint pathway also operates in S-phase. In absence

Introduction

of ATM, DNA synthesis persists despite irradiation evoked DSBs. This phenotype is described as radioresistant DNA synthesis (RDS). A-T patients share RDS with patients suffering from ataxia-telangiectasia-like syndrome, which results from NBS1 deficiency and is indicative of the involvement of the MRN complex in S-phase checkpoint regulation (Carney et al., 1998; Stewart et al., 1999; Varon et al., 1998). ATM dependent NBS1 phosphorylation is required for γ -irradiation induced DNA damage tolerance and the delay in S-phase progression (Lim et al., 2000; Wu et al., 2000a; Wu et al., 2000b; Zhao et al., 2000). In response to DSBs, ATM also phosphorylates Mre11 and the MRN binding protein MDC1, that participate in the mediation of the S-phase checkpoint (Goldberg et al., 2003; Yuan et al., 2002). A definite role of the MRN complex in S-phase checkpoint signal transduction remains to be elucidated. The G2/M checkpoint also depends on ATM-mediated signaling via Chk1 and Chk2. Chk1 triggers the G2/M arrest by phosphorylation of Cdc25C, whereas Chk2 has a supportive role in G2/M block maintenance (Gatei et al., 2003; Zhou et al., 2000).

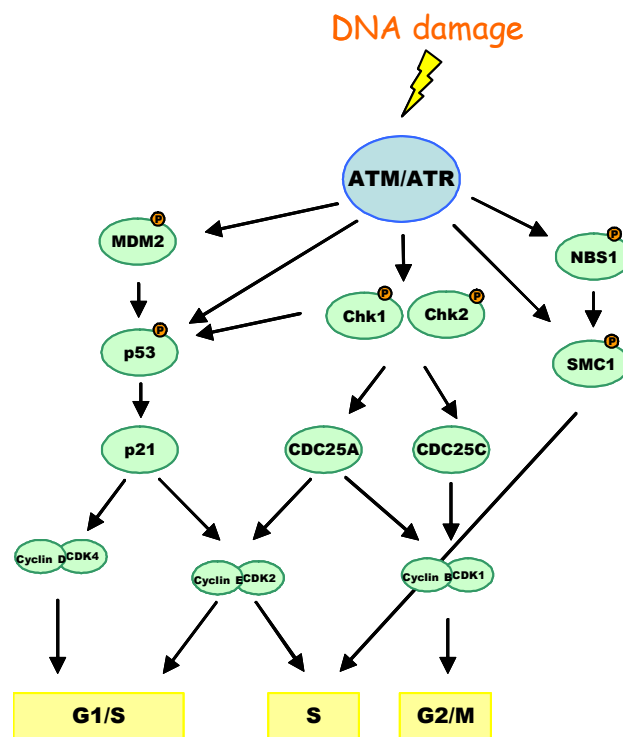


Fig. 4 Role of ATM in activation of cell cycle checkpoints

Introduction

Besides regulation of cell cycle control, ATM has been shown to participate in DSB repair by homologous recombination (HR). ATM is required for the activation of the tyrosine kinase activity of c-Abl and does this by phosphorylation of c-Abl at Ser465 (Baskaran et al., 1997; Shafman et al., 1997). c-Abl phosphorylates RAD51 *in vitro* and *in vivo*, thereby enhancing the complex formation between RAD51 and RAD52 that cooperate during HR (Chen et al., 1999a; Yuan et al., 2003a; Yuan et al., 2003b). Another possible way that ATM may assist DSB repair is by the phosphorylation of histone H2AX (this phosphorylated form of H2AX is known as γ -H2AX), which opens the chromatin structure, thereby allowing DNA repair proteins to gain access to DSBs (Burma et al., 2001).

As a general rule, ATM protects against DNA damage triggered apoptosis by slowing down the progression of the cell cycle and stimulating DNA repair. However, murine ATM^{-/-} thymocytes are more resistant to γ -irradiation induced-apoptosis than their wild type counterparts, implying a role for ATM in the induction of apoptosis (Bhandoola et al., 2000; Xu and Baltimore, 1996). Following irradiation, ATM phosphorylates c-Abl that in turn phosphorylates and activates p73, which is responsible for the induction of apoptosis (Shaul, 2000). P73 is under transcriptional control of the E2 promoter binding factor 1 (E2F1). E2F1 is phosphorylated by ATM in response to DNA damage that leads to E2F1 stabilization and enhancement of its transcriptional activity. Thus, ATM reinforce the signal leading to p73 accumulation and apoptosis (Irwin et al., 2000; Lin et al., 2001; Lissy et al., 2000).

However, beside the fact that ATM is the main signaling protein for genotoxins like γ -irradiation that induce DSBs directly, the data obtained for the role of ATM in relation to DNA alkylating damage are still contradictory. There is some evidence that A-T fibroblasts are hypersensitive to simply ethylating (EMS, ENU) and methylating agents (MMS, MNNG) (Barfknecht and Little, 1982; Hoar and Sargent, 1976; Scudiero, 1980; Teo and Arlett, 1982), whereas other authors report no differences in clonogenic survival between normal and A-T cells after treatment with alkylating agents (Barfknecht and Little, 1982; Shiloh and Becker, 1981; Teo and Arlett, 1982). The reason for this might be that the authors failed to address the contribution of MGMT or MMR in the cell systems they were working with.

1.3 Cytokines as modulators of DNA repair and apoptosis

Cytokines are intercellular mediators of numerous cellular processes including cell proliferation and differentiation in normal tissues and tumours. Several cytokines possess anti-tumour potential and are tested in immunotherapy. Nevertheless, the influence of cytokines on DNA repair (determining the efficiency of anticancer drugs) has hardly been investigated. Here we started a systematic study on influence of two cytokines: IGF-I and IL-1 on DNA repair.

IGF-I is a growth hormone with high mitogenic and anti-apoptotic potential. IGF-I stimulation leads to increased survival following γ -irradiation. IGF-I signaling is also deregulated in ATM deficient cells, which is partly responsible for the hypersensitive phenotype of these cells to ionising radiation. The IGF-I receptor (IGF-IR) is under transcriptional control of the ATM protein. The basal expression level of IGF-IR is drastic reduced in ATM cells, and can be restored by transfection of ATM cDNA. Enhanced expression of IGF-IR in ATM mutated cells increased survival after ionising radiation and inhibition of IGF-I signaling caused radiosensitisation in ATM wild type cells (Peretz et al., 2001; Shahrabani-Gargir et al., 2004). IGF-I stimulates ATM phosphorylation at both threonine and tyrosine residues, although the direct interaction partner responsible for the ATM phosphorylation after cytokine treatment has not been identified (Suzuki et al., 2004).

IL-1 is a multifunctional cytokine, playing a key role in inflammation. Additional functions are regulation of insulin and growth hormone (GH) metabolism. GH is the strongest stimulator of IGF-I synthesis. IL-1 inhibits GH induced IGF-I secretion by liver cells *in vitro* and *in vivo* (Shumate et al., 2005; Thissen and Verniers, 1997; Wolf et al., 1996). IL-1 also directly antagonizes IGF-I signaling, by blocking IGF-I receptor tyrosine kinase activity (Costantino et al., 1996). Interestingly, the IL-1 pathway seems to be impaired in the A-T disorder. Sikpi et al. showed that ATM mutated lymphoblasts are defective in c-Jun transcription regulation, not only in response to IR damage but also after mitogenic stimuli like IL-1 and EGF (Sikpi et al., 1999).

1.3.1 IGF-I

1.3.1.1 The physiological role and regulation of the IGF-I system

IGF-I is a single chain peptide that shares characteristics of both an endocrine hormone and a tissue growth factor. It exhibits 50% homology to insulin and binds also to insulin receptor. Insulin also interacts with the IGF-I receptor, nevertheless the binding of the heterologous ligand occurs with approximately 100 times lower affinity. The *IGF-I* gene is expressed in many tissues however, liver and, to a lesser extent, bone are the main sources of plasma IGF-I. The major factor regulating the blood concentration of IGF-I is GH (Olivecrona et al., 1999). In fibroblasts, the synthesis of IGF-I is stimulated by PDGF and FGF. Serum levels of IGF-I are age-dependent, increasing slowly from birth to puberty and thereafter declining with age. Average serum concentrations in adults are 100-200 ng/ml (Collett-Solberg and Cohen, 2000). Over 75 % of plasma IGF-I is complexed with insulin-like growth factor binding protein-3 (IGFBP-3) and the acid-labile subunit (ALS) (Binoux, 1997; Holman and Baxter, 1996). Complex formation extends IGF-I half-life and forms a circulating reservoir. Modification of IGFBP-3 liberates IGF-I, enabling its interaction with IGF-IR. IGF-IR is a trans-membrane tyrosine kinase, structurally similar to the insulin receptor. It is composed of two extra-cellular α subunits and two intracellular β subunits. IGF-I binding to IGF-IR signals a conformational change of the intracellular domain, which causes receptor clustering, autophosphorylation and stimulation of the receptor's tyrosine kinase activity. Downstream signaling cascade involves the PI3K and MAPK pathways (Jerome et al., 2003), which are linked to cell growth, proliferation and apoptosis suppression (see **Fig. 5**).

The IGF-I system plays a pivotal role in normal growth throughout fetal and childhood development. In adult life, this system continues to function by regulating normal cellular metabolism, proliferation, differentiation and apoptosis suppression. The major role of IGF-I is the regulation of bone growth and remodelling. Several studies have also shown the participation of IGF-I and IGF-IR in hematopoiesis. IGF-I stimulates erythropoiesis (Kurtz et al., 1982). It maintains the survival and enhances the maturation of erythroid cells (Muta et al., 1994; Sawada et al., 1989). IGF-I also effects lymphocyte development and function. IGF-IR expression is down-regulated during T lymphocytes differentiation, so that immature thymocytes show a 3- to 4-fold higher expression of IGF-IR than CD4/CD8 double-positive or single-positive cells (Kooijman et al., 1995). Additionally, IGF-I promotes B cell proliferation and immunoglobulin production (Kimata and Fujimoto, 1994; Soon et al., 1999).

Introduction

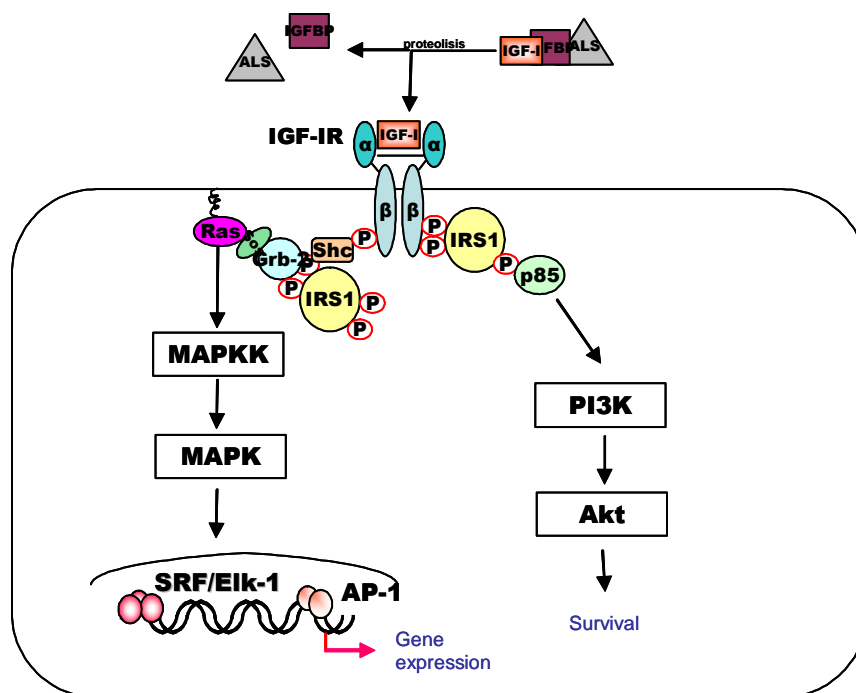


Fig. 5 IGF-IR signaling pathway

Modification of IGF-BP-3 liberates IGF-I, enabling its interaction with IGF-IR. Ligand binding activates the tyrosine kinase activity of the IGF-IR, which phosphorylates itself and adaptor proteins IRS-1 and SHC. Phosphorylated IRS-1 interacts with p85 subunit of PI3K and leads to activation of downstream survival factors. The Ras-MAPK cascade is activated by IGF-IR phosphorylated IRS-1 and SHC, via interaction with Grb-2/Sos.

1.3.1.2 IGF-I system in cancer

IGF-I is highly mitogenic and an effective survival factor. Disruption in the balance of IGF-I system components leads to development and progression of malignant growth. Epidemiological studies have shown that high levels of circulating IGF-I, low levels of IGF-BP-3, or an elevated ratio of IGF-I to IGF-BP-3, are associated with increased risk for developing several common cancers, particularly breast (Hankinson et al., 1998; Li et al., 2001), prostate (Chan et al., 2002), lung (London et al., 2002) and colon cancer (Giovannucci, 2001). Hyper-stimulation of the IGF-I pathway is also accomplished by over-expression of IGF-IR. IGF-IR levels are elevated in breast cancer cell lines and this is also often the case in fresh tumour biopsies (Rubin and Baserga, 1995). Activation of IGF-I signaling promotes tumour growth by rescuing cancer cells from apoptosis induced by different groups of cytotoxic stimuli such as TNF- α , topoisomerase inhibitors and taxol (Dunn et al., 1998; Fischer-Posovszky et al., 2004; Rozen et al., 1998; Sell et al., 1995). Up-regulation of IGF-I pathway also leads to radioresistance (Macaulay et al., 2001; Peretz et al., 2001; Turner et al., 1997).

1.3.1.3 IGF-I modulation of apoptosis and DNA repair

Most of the abilities of IGF-I to promote cell survival is ascribed to its high anti-apoptotic potential. IGF-I stimulation leads to PI3K phosphorylation, which in turn activates Akt/PKB (Kulik et al., 1997). The final step is the phosphorylation of Bad, a member of the Bcl-2 family (Datta et al., 1997). Phosphorylated Bad does not complex with Bcl-x_L, allowing the homodimer of Bcl-x_L to suppress mitochondrial apoptosis and therefore caspase-9 activation (Zha et al., 1996).

Several reports indicate that IGF-I activation may influence survival not only by modulation of apoptotic pathway but also by stimulation of DNA repair. These include enhanced DNA repair via IGF-I activated p38 MAPK signaling pathway in response to UV-mediated DNA damage. IGF-I in physiological concentrations significantly increased DNA repair capacity of 3T3 cells over-expressing IGF-IR and treated with the UV-mimetic drug 4-nitroquinoline N-oxide (4-NQO). Better DNA repair of cells treated with IGF-I was related to activation of p38 kinase and down-stream regulation of MDM2 protein levels. The consequence of MDM2 up-regulation following IGF-I treatment is that p53 translocates into the cytoplasm and is degraded (Heron-Milhavet et al., 2001; Heron-Milhavet and LeRoith, 2002). A relationship between IGF-I and ATM, a major regulator of cell cycle and DNA repair, is well established (Peretz et al., 2001; Shahrabani-Gargir et al., 2004). However, a direct link connecting these two proteins is still missing.

Finally, IGF-I treatment increased survival of Cis-Pt treated mouse fibroblasts expressing human IGF-IR. The authors postulated that survival of IGF-I stimulated cells resulted from better repair of DSB, which are Cis-Pt intermediates. Increased DSB repair by HR of IGF-I treated cells has been shown by an *in vivo* assay. The model, supported by experimental data, proposes a direct interaction of phosphorylated Irs-1 with Rad51 that facilitates Rad51 translocation to the nucleus and Rad51 foci formation at DSB (Trojanek et al., 2003).

1.3.2 IL-1

IL-1 is the general name for two distinct proteins coded for by different genes: IL-1 α and IL-1 β . The homology between the proteins is about 25%, but both perform nearly the same functions (March et al., 1985). IL-1 α is active as pro-cytokine, whereas IL-1 β precursor needs to be cleaved in order to attain enzymatic activity by the IL-1 β -converting enzyme (ICE) (Kurt-Jones et al., 1985; Mosley et al., 1987; Thornberry et al., 1992). In humans IL-1 β is the dominant form while in mice IL-1 α dominates.

Introduction

The receptors for both IL-1 proteins are IL-1RI (CD121a) and IL-1RII (CD121b), with IL-1RI displaying higher affinity for IL-1 α , and IL-1RII for IL-1 β (Chizzonite et al., 1989; Dower et al., 1992; Jobling et al., 1988). IL-1RI is characterized by trans-membrane immunoglobulin-like domains and a Toll/Interleukin-1 domain, which is required for intracellular signaling (Sims et al., 1988). IL-RII is a decoy receptor, consisted of only an Ig-like molecule (Colotta et al., 1993; McMahan et al., 1991). IL-1, once bound to IL-1RI, is recognised by the IL-1R accessory protein (IL-1Ra) (Greenfeder et al., 1995), which initiates the intracellular signaling cascade, finally activating the NF κ B and the MAPK pathways (Fig. 6).

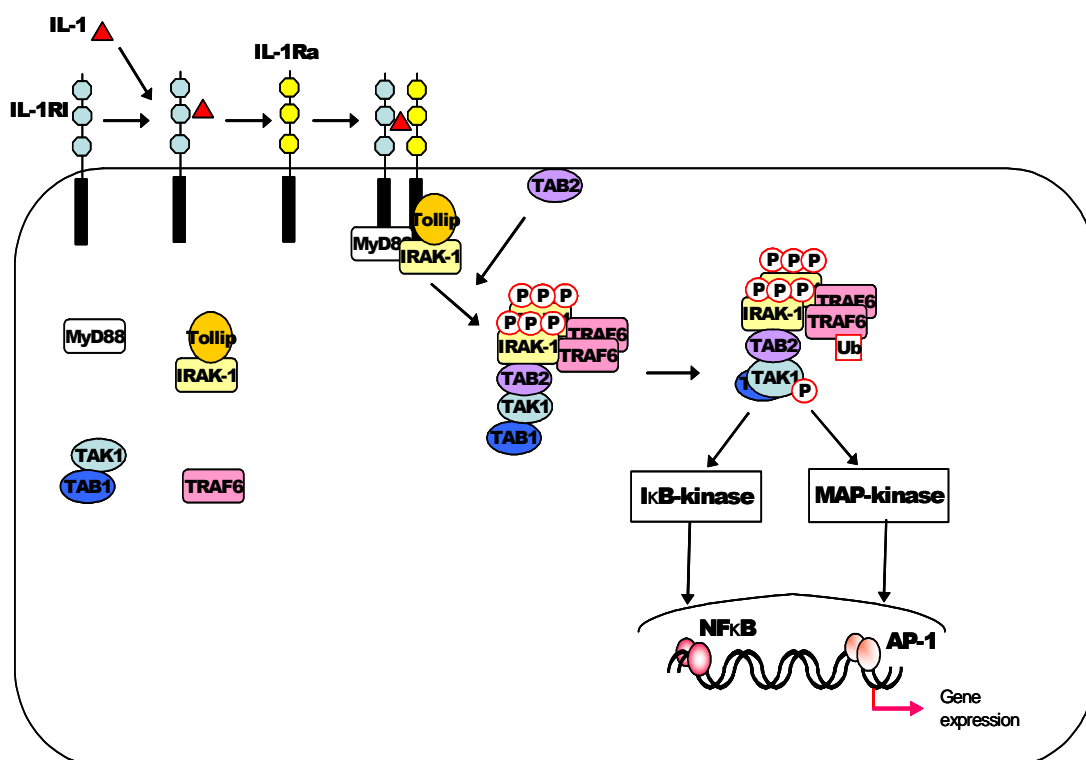


Fig. 6 IL-1 signaling cascade

The IL-1 binds to IL-1R and mediates its association with IL-1RA. The heterodimeric signaling receptor complex creates the scaffold for the association of MyD88 and Tollip and recruitment of IRAK-1. Hyperphosphorylated IRAK-1 dissociates from the receptor complex and presumably dimerizes. The adapter protein TAB2 is transported by IRAK-1 from the membrane to the forming signalosome. IRAK-1 as multimer allows dimerization of TRAF6, that becomes ubiquitinated and together with TAB2 triggers autophosphorylation of TAK1. TAK1 phosphorylates I κ B-kinase and MKK's (Martin and Wesche, 2002).

1.3.2.1 Physiological functions of IL-1

Interleukin-1 is a multifunctional cytokine that affects nearly all cell types, often in concert with other cytokines or small mediator proteins (Dinarello, 1996). It is produced mainly from monocytes and macrophages upon stimulation of CD14 receptor with LPS or CD64 with immunoglobulins (Ellingsen et al., 2002; van de Winkel and Capel, 1993). In skin a potent activator of IL-1 expression is UV irradiation (Corsini et al., 1997; Griswold et al., 1991). The most pronounced role of IL-1 is attributed to the local inflammatory response, which takes place in a synergistic manner with TNF- α . Once released, IL-1 has an impact on a number of different cells in the local environment. First it stimulates endothelial cells to produce chemokins such as IL-8 and MCP-1 and to express vascular adhesion molecules E-Selektin, ICAM-1 and VCAM-1, which facilitates the passage of leukocytes from the blood stream into the tissue (Kupper and Groves, 1995). Moreover IL-1 induces its own expression in newly arriving monocytes, thus reinforcing the overall inflammatory response (Dinarello et al., 1987). Furthermore, IL-1 is needed for the efficient production of IFN- γ by NK cells that proceeds to IFN- γ induced activation of macrophages (Billiau, 1996). During the progression of the inflammatory process, IL-1 stimulates B lymphocytes to proliferate and to produce antibodies (Koyama et al., 1988). IL-1 also participates in the activation of granulocytes and the expansion of T lymphocytes by up regulation of IL-2 and IL-2 receptor. Additional genes under IL-1 expressional control during the local inflammation response include platelet-activating factor (PAF), type II phospholipase A₂ (PLA₂) (Bomalaski et al., 1992; Kol et al., 1997) and the inducible nitric oxide synthase (iNOS) (Chao et al., 1997; Corbett et al., 1996; Ellingsen et al., 2002). Finally, IL-1 affects the central nervous system resulting in fever (Endres et al., 1987; Wang et al., 1997) and causes production of acute phase proteins in liver during systemic inflammation (Zhang and Fuller, 1997).

It is important to note that IL-1 function is not limited to the inflammatory response. Aside from monocytes and macrophages, IL-1 is also produced to a lesser extent in many other cell types, which include some tumours such as melanoma, sarcoma, hepatoblastoma (Anasagasti et al., 1997; Chen et al., 1999b; Huang et al., 1999; Lazar-Molnar et al., 2000; Woods et al., 1998). It also takes part in processes such as bone formation and remodelling (Kumar et al., 2001; Kusano et al., 1998), insulin secretion (Ling et al., 1998), proliferation of fibroblasts (Bachus et al., 1995) and muscle development.

1.3.2.2 IL-1 in cancer biology

IL-1 exhibits stimulating as well as inhibitory effects on tumour progression, depending on tumour type and local environment. Chronic inflammation caused by IL-1 over-expression leads to accumulation of DNA and protein damage in tissues exposed to oxidative stress, resulting in increased proliferation, and finally development of tumours, with high frequency of colon cancer (Ambs et al., 1998; Singer et al., 1996), hepatocellular cancer (Garcia-Monzon et al., 1990; Hata et al., 1992; Majano et al., 1998) and breast cancer (Jin et al., 1997; Verhasselt et al., 1992). Tumour promotion by IL-1 is achieved by up-regulation of genes involved in angiogenesis and growth factors for particular types of tumours. As an example, in multiple myeloma IL-1 stimulates myeloid and megakaryocytic cells to increase IL-6 production, which is a survival and proliferation factor (Costes et al., 1998). Similarly IL-1 contributes to progression of HNSCC by activation of IL-8 secretion (Bancroft et al., 2002; Liss et al., 2001; Thomas et al., 2004; Wolf et al., 2001) and enhanced progression of melanoma and breast cancer by IL-6 (Honma et al., 2002). Some breast cancer cells are characterised by high expression of IL-1RI and IL-1 levels that were correlated with increased malignancy (Knupfer et al., 2001; Miller et al., 2000; Singer et al., 2003). In chronic and acute myelogenous leukaemia, IL-1 leads to uncontrolled production of colony stimulating factors, working as autocrine and paracrine growth hormone (Estrov et al., 1999; Kurzrock et al., 1995). IL-1 also appears to be an autocrine growth modulator for human gastric (Ito et al., 1993) and thyroid carcinoma cells and a paracrine growth hormone for melanoma (Lazar-Molnar et al., 2000).

Anti tumour activity of IL-1 is due to its anti-proliferative, cytotoxic and cytotoxic activities. IL-1 applied in tumour area provokes high expression of chemokins and supports monocyte mediated tumour cytotoxicity, resulting in tumour regression (Bjorkdahl et al., 1997; Lovett et al., 1986; Onozaki et al., 1985; Takikawa et al., 1993).

1.3.2.3 IL-1 in apoptosis and DNA repair

Depending on the cell type and local environment, IL-1 operates as apoptotic inducer or apoptosis inhibitor. It is cytotoxic on its own to insulin-producing beta cells, osteoclasts, astrocytes and some cancer cells (Ehrlich et al., 1999; Hu et al., 1997; Lachman et al., 1986; Ralston and Grabowski, 1996; van't Hof et al., 2000; van't Hof and Ralston, 1997; Xie et al., 1996; Yamada et al., 1996). IL-1 stimulation leads to NF κ B dependent induction of iNOS and production of NO, which is genotoxic and provokes apoptosis (Dupraz et al., 2000; Ehrlich et al., 1999; Nikulina et al., 2003). Recently, it was reported that IL-1 elevates UVB induced

Introduction

apoptosis in human keratinocytes. Cells stimulated with IL-1 prior to UVB irradiation secreted high amounts of TNF- α , that additionally activated the receptor dependent apoptotic pathway. Additionally, IL-1 down-regulates anti-apoptotic proteins such as inhibitor of apoptosis proteins (IAPs), Flice-inhibitory protein (FLIP) and TNF receptor associated proteins (TRAF-1,-2,-6) (Poppelmann et al., 2005).

IL-1 may also promote cell survival by NF- κ B controlled up-regulation of anti-apoptotic proteins such as IAP's and Bcl-2 (Jimi et al., 1998). High expression of IAP's was reported in keratinocytes and osteoclasts treated with IL-1, and it protected keratinocytes against toxicity of TNF and TRAIL (Kothny-Wilkes et al., 1998). IL-1 increased the Bcl-2 level in chondrocytes, which protected them against FasL induced apoptosis (Kuhn et al., 2000). The same effect was observed in Kaposi's sarcoma cells, where IL-1 elevated the survival upon serum deprivation (Simonart and Van Vooren, 2002). Another anti-apoptotic mechanism is dependent on the activation of PI3K by IL-1 and subsequent phosphorylation of the Akt kinase, which in turn phosphorylates Bad. IL-1mediated Akt activation was found in osteoclasts, neurons and endothelial cells exposed to IL-1, resulting in increased cell survival (Diem et al., 2003; Lee et al., 2002; Madge and Pober, 2000).

Although IL-1 has been intensively investigated during the last twenty years, surprisingly no attention has been focus on its effect on DNA repair. The only repair related study concerns the interaction of IL-1 with Cis-Pt resistance of ovarian carcinoma cells. IL-1 showed an *in vitro* and *in vivo* synergistic killing effect in combination with Cis-Pt when treating human ovarian cancer cells, and this was accompanied by increased drug uptake and Pt-DNA adducts formation. The maximal effect was obtained, when IL-1 was added in combination or 24h prior to Cis-Pt treatment. IL-1 increased the sensitivity of cells by interaction with the nucleotide excision repair process (NER). Upon Cis-Pt treatment, the cells over-expressed the key NER protein ERCC-1, that results in higher repair capacity of Pt-DNA adducts. IL-1 pre-treatment led to inhibition of ERCC-1 up-regulation and, therefore, increased Cis-Pt induced cell death (Benchekroun et al., 1995; Li et al., 1998; Wang et al., 1996).

1.4 Aims

O⁶MeG - inducing compounds are potent anticancer chemotherapeutics. Nevertheless, little is known about the cellular processing of O⁶MeG. The understanding of the mechanism by which this lesion induces cell death may lead to the improvement of cancer therapy. This study is aimed at investigation of involvement of DNA double strand breaks in the processing of O⁶MeG. The investigation concerns the participation of ATM kinase that is primarily involved in DSB recognition, in the signaling of O⁶MeG triggered cell cycle checkpoints, apoptosis and DNA repair processes. Moreover, the modulation of O⁶MeG cytotoxicity by cytokines will be investigated in dependence of ATM background. The following questions are addressed:

1. Are ATM mutated cells more sensitive to methylating agents than ATM proficient cells?
2. Which apoptosis pathway is activated by O⁶MeG? Is ATM involved in this process?
3. Does ATM modulate the apoptotic signalling cascade by activation of pro- or anti – apoptotic factors upon treatment with methylating agents?
4. Is the cell cycle progression disturbed by O⁶MeG? Is the cell cycle checkpoint activation ATM dependent?
5. Can we modulate the cell survival after methylating agents treatment by stimulation with cytokines such as IL-1 and IGF-I? Do they regulate DNA repair gene expression?

2 Materials and methods

2.1 Equipment

Array Hybridizer Lucidea Slide Pro	Amersham Bioscience, Freiburg
Array Scanner Affymetrix 428	Affymetrix, Santa Clara, USA
Bacteria Incubator	Heraeus, München
Bacteria incubator Ceromat R/TC2	Braun Biotech, Int., Melsungen
Balance	Sarorius, Göttingen
Biophotometer	Eppendorf, Hamburg
Centrifuge 5417	Eppendorf, Hamburg
Centrifuge Sorvall RC-5B	DuPont, Bad Homburg
Centrifuge, Megafuge 1.0, rotor 3360	Heraeus, München
CO ₂ incubator	Heraeus, München
Concentrator 5310	Eppendorf, Hamburg
Elisa Reader Multiscan Ex	Thermo Electron, Vantaa, Finland
FACS Calibur	BD Bioscience, Heidelberg
FACS Vantage SE	BD Bioscience, Heidelberg
Gel Documentation System Ingenius	Syngene, Cambridge, UK
Gel Dryer Mode 543	Bio-Rad, München
Kinetic Imaging Komet 4.0.2 Software	BFI Optilas, Puchheim
Lamin Air HB 2448	Heraeus, München
LightCycler	Roche, Mannheim
Liquit Scintillation Analyzer TRI-CARB 2100 TR	Canberra-Packard, Dreieich
Microscope BX 50 F	Olympus, Hamburg
Microscope, Wilovert A	Hund, Wetzlar
Power supply Power Pac 300	Bio-Rad, München
SDS electrophoresis chamber	Biometra, Göttingen
Semi-dry transfer chamber	Bio-Rad, München
Sonifier 250	Branson, Danbury, USA
Thermocycler	Biometra, Göttingen
Thermostat 5322	Eppendorf, Hamburg
Waterbath, GFL 1092	GFL, Burgwedel

2.2 Assays, chemicals, materials and recombinant proteins

Chemicals were purchased from Roche (Mannheim), Roth (Karlsruhe), Serva (Heidelberg), Sigma (München) and Merck (Darmstadt). Restriction enzymes were provided by Fermetas (St. Leon-Rot). Cytokines were obtained from TebuBio (Offenbach)

[³ H]-MNU (18,7 Ci/mmol)	Ammersham Pharmacia, Freiburg
[γ - ³² P]ATP, 3000Ci/mmol	NEN DuPont, Boston, USA
Agarose	Sigma -Aldrich, Deisenhofen
Annexin V-FITC	PharMingen, Heidelberg
Bradford reagent	Bio-Rad, München
Caspase activity assay	R&D systems, Minneapolis, USA
Complete, Mini EDTA - free	Roche, Mannheim
Cover slides 24x60 mm	Roth, Karlsruhe
Cyanine 3-dCTP	NEN DuPont, Boston, USA
Cyanine 5-dCTP	NEN DuPont, Boston, USA
DNA ladder	Fermentas, St. Leon-Rot
ECL + detection system	Ammersham Pharmacia, Freiburg
ECL detection system	Ammersham Pharmacia, Freiburg
Effecten Transfection Kit	Qiagen, Hilden
FITC-VAD-FMK	Promega, Mannheim
Fotemustine	Les Laboratoires Servier, Gildy, France
Glass slides 26x76 mm	Roth, Karlsruhe
Hyperfilm ECL	Ammersham Pharmacia, Freiburg
LabelStar Array Kit	Qiagen, Hilden
Lipofectamine 2000	Invitrogene, Karlsruhe
Low Melting Point Agarose	Appligene, Heidelberg
Microarrays	MWG-Biotech, Ebersberg
MMS	Sigma -Aldrich, Deisenhofen
MNNG	Sigma -Aldrich, Deisenhofen
Mycoplasma Detection Kit	Roth, Karlsruhe
Nitrocellulose membrane	Schleicher&Schuell, Dassel
Non-fat dry milk	Reformhaus, Mainz
Nonidet P40	Fluka, Darmstadt
NucleoSpin Extract II Kit	Machery & Nagel, Düren

Materials and Methods

NucleoSpin RNA II	Machery & Nagel, Düren
O ⁶ BG	Sigma -Aldrich, Deisenhofen
PI	Sigma -Aldrich, Deisenhofen
PNK	Roche, Mannheim
Prestained protein marker	Fermentas, St. Leon-Rot
Qiagen HiSpeed Plasmid Kit	Qiagen, Hilden
Quantikine Human IL-6 Immunoassay	R&D Systems, Minneapolis, USA
REDTaq ReadyMix PCR Reaction Mix	Sigma -Aldrich, Deisenhofen
Salmon sperm DNA	Roche, Mannheim
SuperScript First-Strand Synthesis System	Invitrogene, Karlsruhe
SYBR Green I PCR kit	Roche, Mannheim
T4-DNA-Ligase	Fermentas, St. Leon-Rot
Temozolomide	Essex Pharma, München
Topo pcDNA3.1	Invitrogene, Karlsruhe
Whatmann 3 MM filter paper	Schleicher&Schuell, Dassel
WST-1	Roche, Mannheim

2.3 Cell Culture Reagents

Ampicillin	Sigma -Aldrich, Deisenhofen
Bacto Agar	Difco Laboratories, Detroit, USA
DMEM	Cambrex, Verviers, Belgium
DMEM/F12	Cambrex, Verviers, Belgium
DMSO	Fluka, Darmstadt
Foetal Calf Serum	Biowest, Nuaville, France
G418	GIBCOBRL, Karlsruhe
Hepes buffer solution	PAA Laboratories, Pasohing, Austria
HygromycinB	Calbiochem, Darmstadt
Luria Broth Base (LB)	Lab M, Burry, U.K.
Opti-MEM I	GIBCOBRL, Karlsruhe
PBS	Biochrom AG, Berlin
Pen/Strep	Cambrex, Verviers, Belgium
Plasmocin	Invivogene, Karlsruhe
RPMI	PAA Laboratories, Pasohing, Austria

Materials and Methods

SOC-Medium	Invitrogene, Karlsruhe
Sodium pyruvate	GIBCOBRL, Karlsruhe
Trypsine 250	Cambrex, Verviers, Belgium

2.4 Bacteria

<i>E. coli</i> DH5 α	F80 <i>lacZ</i> Δ (<i>lacZYA-argF</i>)U169 <i>endA1recA1hsd</i> R17(rk-mk+) <i>deoR supE44thi-1λ-gyrA96relA1</i>
-----------------------------	---

2.5 Cell lines

ATM -/-	Mouse embryonic fibroblasts, double knockout for ATM and p53 (Elson et al., 1996)
ATM +/+	Mouse embryonic fibroblasts, ATM wild-type, p53 knockout (Elson et al., 1996)
BK4	Mouse fibroblastoid cell line, p53 proficient (Haas and Kaina, 1995)
CHO-9	Chinese hamster ovary epithelial cell line
HaCaT	Human normal keratinocytes
HeLa MR	Human epithelial carcinoma, <i>mex</i> ⁻
HeLa S3	Human epithelial carcinoma, <i>mex</i> ⁺
KB	Human epithelial carcinoma

2.6 Oligonucleotides

Oligonucleotides were synthesised and purified by MWG-Biotech (Ebersberg).

Gene	Sequence	Application
AP-1 3'	5' AGTGGTGACTCATCACT 3'	EMSA
AP-1 5'	5' AGTGATGAGTCACCACT 3'	EMSA
<i>ape1</i> 3' (human)	5' CCGAGGGCCTTGGAACG 3'	RT-PCR
<i>ape1</i> 5' (human)	5' CCGGCAGCGCTGGGATGAA 3'	RT-PCR
<i>apex2</i> 3' (human)	5' GTACCCGGGTTTGATTGTTGTGCT 3'	RT-PCR
<i>apex2</i> 5' (human)	5' CAGGGCGCAAGTGGATGGAC 3'	RT-PCR
<i>apex2</i> -gene 3'	5' GAATTCATGTTGCGCGTGGTGAGC 3'	<i>apex2</i> cloning
<i>apex2</i> -gene 5'	5' GGTTTCAGCTGGGCCTGCTCCAG 3'	<i>apex2</i> cloning
<i>c-jun</i> 3' (mouse)	5' CGATCCGCTCCAGCTTCCTTTTC 3'	RT-PCR
<i>c-jun</i> 5' (mouse)	5' GCTCCCGCGGTGGCCTCAGTAG 3'	RT-PCR

Materials and Methods

Gene	Sequence	Application
<i>fasL</i> 3' (mouse)	5' GAGCGGTTCCATATGTGTCTTCC 3'	RT-PCR
<i>fasL</i> 5' (mouse)	5' GGGCTCCTCCAGGGTCAGTT 3'	RT-PCR
<i>fasR</i> 3' (mouse)	5' TGCCCTCCTTGATGTTATTTTCTC 3'	RT-PCR
<i>fasR</i> 5' (mouse)	5' TGGAAACAAACTGCACCCTGAC 3'	RT-PCR
<i>fen-1</i> 3' (human)	5' TGCTGCAGAATGAGGAGGGTGAGA 3'	RT-PCR
<i>fen-1</i> 5' (human)	5' ACAGGGCTGCCGAAGGTGAGG 3'	RT-PCR
<i>gapdh</i> 3' (human)	5' GAAGATGGTGATGGGATTTC 3'	RT-PCR
<i>gapdh</i> 3' (mouse)	5' GGTGGAAGAGTGGGAGTTGCTGTTGA 3'	RT-PCR
<i>gapdh</i> 5' (human)	5' GAAGGTGAAGGTCGGAGT 3'	RT-PCR
<i>gapdh</i> 5' (mouse)	5' CCCCTCTGGAAAGCTGTGGCGTGAT 3'	RT-PCR
<i>iap</i> 3' (mouse)	5' ATCTGCCGCTGAACCGTCTGT 3'	RT-PCR
<i>iap</i> 5' (mouse)	5' TTGCCTGTGGTGGGAAACTGA 3'	RT-PCR
<i>il-6</i> 3' (human)	5' CTGCGCAGAATGAGATGAGTTGTC 3'	RT-PCR
<i>il-6</i> 5' (human)	5' CCCAGTACCCCCAGGAGAAGAT 3'	RT-PCR
<i>ikba</i> 3' (human)	5' TTCAGCCCCTTTGCACTCATAACG 3'	RT-PCR
<i>ikba</i> 5' (human)	5' GCCGACTGCCCTTCACCTC 3'	RT-PCR
<i>ligIII</i> 3' (human)	5' TTGGGGAAGGTTAGTGGCAGATTT 3'	RT-PCR
<i>ligIII</i> 5' (human)	5' GAGGGGCTGGTGCTGAAGGATG 3'	RT-PCR
<i>nfkb1</i> 3' (human)	5' AGGGACAACAGCAATGACAACAGA 3'	RT-PCR
<i>nfkb1</i> 5' (human)	5' TAGACGAGCTCCGAGACAGTGACA 3'	RT-PCR
<i>p21</i> 3' (human)	5' CTCCCCATCATATACCCCTAACA 3'	RT-PCR
<i>p21</i> 5' (human)	5' GTGGGGGCATCATCAAAAATT 3'	RT-PCR
<i>pcna</i> 3' (human)	5' GAGAGTGGAGTGGCTTTTGTA 3'	RT-PCR
<i>pcna</i> 5' (human)	5' ACCTTGCGCTAGTATTTGAA 3'	RT-PCR
<i>polβ</i> 3' (human)	5' GGGTTCCCGGTATTTCCACT 3'	RT-PCR
<i>polβ</i> 5' (human)	5' GACCCATCCCAGCTTCACTTC 3'	RT-PCR
<i>xrcc1</i> 3' (human)	5' ACGAATGCCAGGGAGGGGTTGTC 3'	RT-PCR
<i>xrcc1</i> 5' (human)	5' AGCGGTGGCAGCGGAGATGAAG 3'	RT-PCR

2.7 Antibodies

anti Akt	Cell Signalling, Frankfurt	9272
anti Ape1	Novus Biologicals, Littleton, USA	NB 100-116
anti Apex2	Abcam, Cambridge, UK	13691
anti Bax	Santa Cruz Biotechnology, Heidelberg	sc493
anti Bcl-2	Santa Cruz Biotechnology, Heidelberg	Sc7382
anti Caspase 3	Cell Signalling, Frankfurt	Sc 9664
anti Caspase 9	Cell Signalling, Frankfurt	Sc 9502
anti Cyclin A	Santa Cruz Biotechnology, Heidelberg	Sc596
anti Cytochrome c	Santa Cruz Biotechnology, Heidelberg	Sc7159
anti ERK2	Santa Cruz Biotechnology, Heidelberg	Sc7383
anti FasR	Transduction Laboratories, Lexington	F22120
anti Fen1	BD Bioscience, Heidelberg	611294
anti JNK	Cell Signalling, Frankfurt	9252
anti MLH1	Pharminen, Lexington	13271A
anti MSH2	Oncogene, Cambridge	NA27
anti MSH6	Transduction Laboratories, Lexington	G70220
anti p38	Cell Signalling, Frankfurt	9212
anti p53	Santa Cruz Biotechnology, Heidelberg	Sc 99
anti p-Akt	Cell Signalling, Frankfurt	9271
anti p-Chk1	Cell Signalling, Frankfurt	2341
anti PCNA	Calbiochem, Schwalbach	NA03
anti p-JNK	Cell Signalling, Frankfurt	9251
anti PMS2	Pharminen, Lexington	65861A
anti Pol β	NeoMarkers, Asbach	MS 669 P1
anti p-P38	Cell Signalling, Frankfurt	9211
anti XRCC1	NeoMarkers, Asbach	MS 434
anti mouse (HRP conjugated)	Amersham Pharmacia, Freiburg	NA931
anti rabbit (HRP conjugated)	Amersham Pharmacia, Freiburg	NA934

Materials and Methods

2.8 Buffers

Denhardt's Solution (50x)	1 % Ficoll (Type 400) 1 % Polyvinylpyrrolidon 1 % BSA (Fraction V)
MOPS buffer (10x)	0.2 M MOPS 80 mM Na-acetate 10 mM EDTA, pH 8.0
PBST	1 x PBS 0.2 % Tween-20
PBS	137 mM NaCl 2.7 mM KCl 0.7 mM CaCl ₂ 0.6 mM MgCl ₂ 6.5 mM Na ₂ HPO ₄ 1.5 mM KH ₂ PO ₄
RNA denaturing buffer	500 µl Formamid 100 µl 10 x MOPS buffer 150 µl Formaldehyde
RNA loading buffer	50 % Glycerol 1mM EDTA, pH 8.0 0.25 % Bromphenolblue 0.25 % Xylen- Cyanol FF
SDS electrophoresis buffer	25 mM Tris-HCl, pH 8.3 192 mM Glycine 0.1 % SDS
SDS running gel	7.5 – 12 % PAA 375 mM Tris-HCl, pH 8.8 0.1 % SDS 0.05 % APS 0.005 % TEMED
SDS sample buffer (4x)	250 mM Tris- HCl, pH 6.8 8 % SDS 40 % Glycerol 20 % 2-Mercaptoethanol 0.04 % Bromphenolblue
SDS stacking gel	5 % PAA 125 mM Tris-HCl, pH 6.8 0.1 % SDS 0.05 % APS 0.005 TEMED

Materials and Methods

SSC (20x)	3 M NaCl 0.25 M Na-Citrat, pH 6.5
TBE (10x)	0.9 mM Tris-HCl 0.9 M Boric acid 12.5 mM Na ₂ EDTA
TBS	24.2 g Tris-HCl, pH 7.6 80.0 g NaCl ad 1l with H ₂ O
TBST	1 x TBS 0.1 % Tween-20
TE	10 mM Tris-HCl 1mM EDTA, pH 8.0
RIPA buffer	50 mM Tris-HCL, pH 7.4 1 % NP40 0.25 % Na-deoxycholol 150 mM NaCl 2 mM EDTA 1 mM EGTA 1 mM PMSF
TELT- buffer	62.8 mM Na ₂ EDTA 4 % Triton X-100 50 mM Tris-HCl, pH 8.0 2.5 M LiCl
Western blot transfer buffer	25 mM Tris-HCl 100 mM Glycine 25 % Methanol, pH 8.0

2.9 Cell culture

Cells were cultivated in plastic cell culture flasks at 37°C and 7 % CO₂ in humidified atmosphere. CHO-9 cells were maintained in F12/DMEM (1:1) supplemented with 5 % FCS. Mouse embryonic fibroblasts and HaCaT cells were maintained in DMEM with 10 % FCS. HeLa cells were cultivated in DMEM/F12 medium with 5 % FCS. KB cells were cultivated in RPMI medium supplemented with 10 % FCS, 100 mM HEPES pH 7.4 and 10 mM sodium pyruvate. Cells were propagated twice a week in dilution 1:10. All cultures were routinely screened for *Mycoplasma sp.* (*M. arginini*, *M. hyorhinis*, *M. laidlawii*, *M. orale*) contamination with Mycoplasma Detection Kit in 2 month time periods. 2 ml of medium was

Materials and Methods

subtracted from confluent cells and the ELISA assay was performed according to the manufactory's protocol. In case of contamination, the culture was treated for 14 days with Plasmocin (25 µg/ml). Cryo-preserved cell culture stocks were prepared from *Mycoplasma* free, exponentially growing cultures. Cells were harvested from 10 cm culture dish, centrifuged, suspended in chilled culture medium containing 10 % DMSO and aliquoted per 10⁶ cells in cryo-tubes. Stocks were frozen stepwise in evaporating liquid nitrogen. Frozen stocks were fast thawed in a water bath at 37°C, washed with pre-warmed culture medium and cultured under standard conditions.

2.9.1 Treatment with genotoxic agents and cytokines

Cells were seeded in cell culture dishes in appropriate numbers, assuring for exponential growth during the experiment. They were left to recover for 24 h after seeding, and then medium was replaced with fresh medium containing mutagen. After 1h treatment, medium was removed cells were washed with PBS and fresh medium was added to the cells. MMS and MNNG aquatic solutions were stored frozen in aliquots as highly concentrated stocks (300 and 10 mM respectively). Temozolomide was dissolved in 70 % ethanol to a final concentration of 35 mM and stored in aliquots at -80°C. Fotemustine was dissolved in 70 % ethanol directly before treatment. Treatment with O⁶BG was performed 1 h before alkylating drug addition; than mutagen was added to the medium for 1 h. Cells were washed with PBS and supplemented with new medium containing MGMT inhibitor. O⁶BG was not removed from the experiment. Treatment with caffeine was performed similarly to O⁶BG with the exception; medium with PI3K inhibitor was replaced by fresh medium 24 h after drug treatment. γ -irradiation was carried out through the medium on attached cells. Experiments involving cytokines were performed in serum free medium (0.2 % FCS). Cells were seeded and left to recover for 24 h, than washed with PBS and supplemented with serum free medium for next 24 h. Afterwards cells were treated according to the experimental setup.

2.9.2 Transfection of eukaryotic cells

Transfection was performed with Effecten Transfection Kit according to the manufacture's protocol. Cells were seeded in 5 cm cell culture dishes in the appropriate numbers, resulting in 80 % confluency after 24 h cultivation. DNA-lipid complexes were added to the medium. Cells were incubated for the next 24 h, and then reseeded at low density in selection medium. Cells over-expressing *mgmt* were selected with 300 µg/ml hygromycin B. HeLa cells transfected with pcDNA3.1-APEX2 were selected with G418 (1mg/ml). Resistant clones

Materials and Methods

were picked and propagated. The efficiency of DNA transfer was checked by enzyme activity assay or PCR. Newly established cell lines were maintained in selection medium but selection reagent was omitted during experiments.

Transient transfection was performed with Lipofectamine 2000 reagent. 4×10^5 cells were plated in 5 cm culture plate a day prior to transfection experiment. 8 μg DNA was diluted in 0.5 ml Opti-MEM I Reduced Serum Medium without serum. 20 μl Lipofectamine 2000 was mixed with 0.5 ml Opti-MEM I medium. After 5 min incubation at room temperature, DNA was combined with Lipofectamine 2000 solution and left for the next 20 min. The DNA: Lipofectamine 2000 complexes were added to the plates. The gene transfer was checked following 24 h cultivation of cells under standard conditions.

2.10 Viability assays

2.10.1 WST-1 assay

The assay quantifies the amount of metabolically active cells, based on overall activity of mitochondrial dehydrogenases. WST-1 reagent is a tetrazolium salt (4-[3-(4-iodophenyl)-2-(nitrophenyl)-2H-5-tetrazolio]-1,3-benzene disulfonate) that is cleaved into formazan in cellular enzymatic reaction. The amount of accumulated formazan dye is measured. Cells were seeded in 96-well microtiter plate (2000 cells per well), incubated for 24 h and then treated according to the experimental setup. After treatment, cells were incubated for a further 24 to 72 h. Medium was discarded and cells were supplemented with 100 μl medium containing 10 % WST-1 reagent. Cells were placed in a cell culture incubator for optimal colour development and the absorbance was measured at 450 nm and 600 nm for reference. Results were expressed as the absorbance ratio (%) of sample versus control.

2.10.2 Clonogenic survival

Depending on plating efficiency, 500 - 1000 cells were seeded in 5 cm cell culture plate and treated when attached, 6 h later. Following treatment, cells were incubated for up to 10 days until colonies appeared. Thereafter plates were rinsed with PBS, fixed with 100 % methanol and stained with 1.25 % crystal violet/0.125 % Giemza solution. Excessive dye was washed out with water. Clonogenic survival was expressed as percentage of colonies grown upon treatment compared with the control.

2.11 Apoptosis determination

2.11.1 Annexin V/propidium iodide double staining

Annexin V is a phospholipid-binding protein with high affinity to phosphatidylserine. In apoptotic cells, the membrane phospholipid phosphatidylserine residues are translocated from the inner to the outer leaflet of the plasma membrane, thereby exposing them to the external cellular environment. Since phosphatidylserine is also detectable during necrosis, Annexin V is used in conjunction with a vital dye propidium iodide (PI) to distinguish apoptotic from necrotic cells. Cells that stain positive for Annexin V and negative for PI are undergoing apoptosis. Cells that are positive for both Annexin V and PI are undergoing necrosis, or are in the end stage of apoptosis. Viable cells remain unstained.

Cells were harvested with trypsin/EDTA, washed with PBS and centrifuged (1000 rpm, 5 min, 4°C). The cell pellet was re-suspended in annexin binding buffer (10 mM HEPES/NaOH, pH 7.4, 140 mM NaCl, 2.5 mM CaCl₂) to an end concentration of 1 x 10⁶ cells/ml. 50 µl of cell suspension was transferred into FACS tube and incubated with 2.5 µl Annexin V conjugated to fluorescein isothiocyanate (Annexin V-FITC) for 15 min on ice. 245 µl annexin binding buffer and 5 µl PI (50 µg/ml) were added and samples were analysed by flow cytometry using the FLH-1 and FLH-3 channels. Analysis was performed by means of Cell Quest Pro software.

2.11.2 Flow cytometric analysis of SubG1 fraction

Cells were harvested, added to the collected culture medium and centrifuged (1000 rpm, 5 min, 4°C). Cell pellet was re-suspended in 5 ml PBS. PBS was discarded after the second centrifugation round (1000 rpm, 5 min, 4°C). Cells were re-suspended in 0.5 ml PBS and fixed in ice cold ethanol (70 %) over night at -20°C. Cells were then centrifuged (1500 rpm, 6 min, 4°C) and re-suspended in PBS to the end concentration of 1 x 10⁶ cells/ml. 0.5 ml of cell suspension was transferred into a FACS tube. RNA digestion was performed with RNaseA (100 µg/ml end concentration) for 1h at room temperature. 10 µl propidium iodide (1 mg/ml) was added for DNA staining. Samples were subjected to flow cytometry analysis using the FLH-2 channel followed by quantification of SubG1 fraction with Cell Quest Pro software.

2.11.3 Caspase activity detection with FITC-VAD-FMK

FITC-VAD-FMK is a FITC conjugate of the cell membrane permeable caspase inhibitor VAD-FMK. It binds to activated caspases, serving as an *in situ* marker for apoptosis. The bound marker is visualised by fluorescence detection. Cells were seeded in 24 well plates and supplied with 1 ml medium. 10 pmol FITC-VAD-FMK was added to the medium and cells were incubated for 20 min in cell culture incubator. Cells were harvested with trypsin/EDTA together with culture medium and washed with 5 ml PBS. They were collected by centrifugation (1000 rpm, 5 min, 4°C), re-suspended in 0.5 ml PBS and immediately analysed by flow cytometry.

2.11.4 DNA laddering (Ioannou and Chen, 1996)

Cells were harvested, washed with PBS and centrifuged (1000 rpm, 5 min, 4°C). 5×10^6 cells were suspended in 150 μ l PBS. Cells were lysed by the addition of 600 μ l hypotonic solution (5 mM Tris-HCl, pH 8.0, 20 mM EDTA, 0.1 % Triton X-100). High molecular weight DNA was precipitated with 50 μ l PEG 8000 (50 %) and 200 μ l 5 M NaCl. After 10 min incubation on ice and centrifugation with maximum speed for 10 min supernatant was transferred to a new 1.5 ml micro-centrifuge tube and nucleic acids were purified by phenol/chlorophorm extraction. DNA was precipitated with ethanol at -80°C over night. DNA was air dried and suspended in 40 μ l TE buffer. Following RNA digestion by RNase A (100 μ g/ml, 37°C, 30 min), DNA was subjected to agarose gel electrophoresis (1.5 %, 25V, over night) and visualised with ethidium bromide.

2.12 FACS analysis of cell cycle distribution

Cells were harvested using trypsin/EDTA, washed with 5ml PBS and collected by centrifugation. Cell pellet was re-suspended in 500 μ l PBS and cells were fixed with ice cold 70 % ethanol over night at -20°C. After centrifugation (1500 rpm, 5 min, 4°C) cells were re-suspended in 0.5 ml PBS and transferred into FACS tubes. RNase A (100 μ g/ml end concentration) was added and samples were incubated for 1 h at room temperature. DNA was stained with propidium iodide (20 μ g/ml) and cells were subjected to flow cytometry analysis. Cell cycle distribution was analysed with ModFitLT 3.0 software.

2.13 Protein analysis

2.13.1 Protein extracts

All steps were performed on ice unless stated otherwise. Cells were harvested by trypsinisation and combined with previously collected cell culture medium in 50 ml centrifuge tubes. Following centrifugation (1000 rpm, 5 min, 4°C) cells were re-suspended in 1 ml pre-chilled PBS and transferred into 1.5 ml micro-centrifuge tubes. Cells were pelleted by centrifugation (2500 rpm, 5 min, 4°C) and subjected to protein extraction by selected protocol. Protein extracts were flash-frozen in aliquots using liquid nitrogen and stored at -80°C. Thawing of extracts was performed on ice and refreezing of extracts was avoided. All extracts were prepared in buffer containing the proteases inhibitor cocktail. Stock solution was prepared by dissolving 1 tablet Complete Mini EDTA-free cocktail in 1 ml water. The working dilution of the cocktail in extraction buffer was 1: 50.

2.13.1.1 Whole cell extracts

Cell pellets were re-suspended in ice-cold modified RIPA buffer (50mM Tris-HCl, pH 7.4, 1 % NP40, 0.25 % Na-deoxycholate, 150 mM NaCl, 2 mM EDTA, 1 mM EGTA, 1 mM PMSF). Samples were incubated on ice for 15 min and centrifuged (14000 rpm, 15 min, 4°C). Supernatants were transferred to fresh micro-centrifuge tubes, aliquoted and flash-frozen using liquid nitrogen.

2.13.1.2 Nuclear extracts

Cell pellets collected from 10 cm culture plates were re-suspended in 0.5 ml NP40-lysis buffer (10 mM Tris-HCl, pH 7.4, 10 mM NaCl, 3 mM MgCl₂, 0.5 % NP40). Samples were incubated on ice for 5 min. Nuclei were spun at 3200 rpm for 5 min and washed with NP40-lysis buffer where NP40 has been omitted. Nuclei were again centrifuged (3200 rpm, 5 min, 4°C) and re-suspended in 100 µl map-kinase buffer (20 mM Tris-HCl, pH 7.4, 40 mM Na-phosphate, 50 mM NaF, 5 mM MgCl₂, 100 µM NaVO₄, 10 mM Na₂EDTA, 1 % Triton X-100, 0.5 % Na-deoxycholate, 0.1 % SDS). Samples were sonicated 3 x 10 sec on ice and then centrifuged (10000 rpm, 10 min, 4°C). Proteins in the supernatant were transferred to a new 1.5 ml tube and flash-frozen in aliquots using liquid nitrogen.

2.13.1.3 Fractionation of cytosolic and mitochondrial proteins

Cell pellets were re-suspended in 200 µl lysis buffer (20 mM HEPES-KCl, pH 7.5, 250 mM sucrose, 20 mM KCl, 1.5 mM MgCl₂, 1 mM EGTA, 1 mM EDTA, 1 mM DDT, 0.1 mM

Materials and Methods

PMSF). After incubation on ice for 10 min, samples were passed through an 18 G needle, 10 times, and centrifuged at 10000 rpm for 15 min at 4°C. Cytosolic fractions in the supernatant were then subjected to ultracentrifugation (100000g, 15 min, 4°C), aliquoted and flash-frozen using liquid nitrogen. The pelleted membrane/mitochondria fraction was re-suspended in 200 µl lysis buffer and sonicated 3 x 10 sec on ice. Cell debris was removed by centrifugation (10000 rpm, 30 min, 4°C). Mitochondrial extracts, in supernatant, were placed in new micro-centrifuge tubes and flash-frozen in aliquots using liquid nitrogen.

2.13.1.4 Whole cell extracts for western blot with phospho-specific antibodies

Medium was aspirated from the culture plates and cells were washed with PBS. Cells were then directly lysed on the cell culture plates by adding hot SDS sample buffer (100 - 500 µl for 5 cm plate, depending on cell density). The cell lysate were removed from the culture plate and transferred to a micro-centrifuge tube. Samples were then chilled on ice. DNA was fragmented by sonication for 10 sec. Extracts were heated to 95°C for 5 min and then placed on ice. 10 µl extracts was loaded onto SDS-PAGE gel.

2.13.1.5 Extracts for western blot with anti-caspase antibodies

Cells were harvested by trypsinisation and reunited with cells in the culture medium, centrifuged and washed with PBS. Following centrifugation (1000 rpm, 5 min, 4°C) cell pellets were re-suspended in one volume of chaps lysis buffer (50 mM Pipes-NaOH, pH 6.5, 2 mM EDTA, 0.1 % Chaps, 5 mM DTT, 1 mM PMSF). Cell membranes were disrupted by repeated cycles, 3 times, of shock freezing, thawing and vortexing (liquid N₂ and 37°C). Finally, cell debris was pelleted by centrifugation (14000 rpm, 5 min, 4°C). Supernatants were transferred to new micro-centrifuge tubes and flash-frozen using liquid nitrogen.

2.13.1.6 Nuclear extracts for Electro Mobility Shift Assay (EMSA)

Cells pooled from two 10 cm cell culture plates were suspended in 1 ml lysis buffer (10 mM Tris-HCl, pH 7.4, 10 mM NaCl, 3 mM MgCl₂, 1 mM DTT, 2 mM PMSF). Following 10 min incubation on ice, 53 µl 10 % NP40 was added to the samples. Samples were again incubated on ice for 2 min. After incubation, samples were centrifuged (2500 rpm, 5 min, 4°C) and the supernatant was discarded. Pellets, containing the nuclei, were washed with 1 ml lysis buffer and centrifuged (2500 rpm, 5 min, 4°C). Nuclei were re-suspended in 2 volumes of nuclei lysis buffer (Hepes-KCl, pH 7.9, 600 mM KCl, 0.2 mM EDTA, 1 mM DTT, 2 mM PMSF). Suspensions were incubated on ice for 30 min and than centrifuged for 10 min at maximum

Materials and Methods

speed (4°C). Supernatants were transferred to fresh micro-centrifuge tubes and mixed with one volume of nuclei lysis buffer where KCl was omitted. Glycerol was added to the extracts to a final concentration of 20 %. Extracts were flash-frozen in aliquots using liquid nitrogen.

2.13.1.7 Extracts for MGMT activity assay

Cells from two 10 cm culture plates were harvested by trypsinisation, washed with PBS and centrifuged (900 rpm, 5 min, 4°C). Cell pellets were re-suspended in 400 µl sonication buffer (20 mM Tris-HCl, pH 8.5, 1 mM EDTA, 1 mM 2-mercaptoethanol, 5 % glycerol) and sonicated on ice 3 x 10 sec. Cell debris was removed by centrifugation (14000 rpm, 10 min, 4°C). Extracts were aliquoted and flash-frozen using liquid nitrogen.

2.13.2 Determination of protein concentration

2.13.2.1 Protein concentration determination using the Bradford method (Bradford, 1976)

Protein concentration was measured with Commasie blue G250. Commasie blue G250 binds to amino groups of proteins that result in a shift of the absorption maximum of the dye from 465 nm to 595 nm. Protein extracts (10 µl) were pipetted in 96-wells microtiter plate. Samples were incubated with 200 µl Bradford Reagent (8.5 % phosphor acid, 4.75% ethanol, 1 % Commasie blue G250) for 10 min at room temperature. Absorbance was measured at 595 nm. The protein concentration was read from a calibration curve generated for each experiment using known concentrations of bovine serum albumin (BSA) (0 - 5 µg/µl).

2.13.2.2 Protein concentration determination using the Lowry method (Lowry et al., 1951)

Protein extracts (5 µl) were mixed with 145 µl Lowry Reagent I (2 % Na₂CO₃, 0.1 NaOH). 250 µl Lowry Reagent II (2 % Na₂CO₃, 0.1 NaOH, 0.02 % Na-K-tartrat 0.01 % CuSO₄) and then 30 µl 50% Folin Reagent was added to the samples. Absorbance was measured at 600 nm following the incubation of the samples for 90 min in the dark at room temperature. Protein concentration was determined based on a calibration curve generated with known concentrations of BSA (0 - 60 µg/µl).

2.13.3 Polyacrylamide gel electrophoresis (SDS PAGE) (Laemmli, 1970)

Protein extracts (30 µg in 15 µl) were mixed with 5 µl 4 x SDS sample buffer (250 mM Tris-HCl, pH 6.8, 8 % SDS, 40 % Glycerol, 20 % 2-mercaptoethanol, 0.04 % 2-bromophenol blue)

Materials and Methods

and denatured for 5 min at 95°C. Samples were chilled, on ice, and loaded on the polyacrylamide gels. Proteins were concentrated in an 5 % stacking gel (5 % PAA, 125 mM Tris-HCl, pH 6.8, 0.1 % SDS, 0.05 % APS, 0.005 % TEMED) and separated in a running gel (7.5-12 % PAA, 375 mM Tris-HCl, pH 8.8, 0.1 % SDS, 0.05 % APS, 0.005 % TEMED). Proteins were separated using a constant electric field of 120 V in SDS electrophoresis buffer (25 mM Tris-HCl, pH 8.3, 192 mM glycine, 0.1 % SDS).

2.13.4 Western blot transfer and protein detection with antibodies

Following SDS-PAGE protein separation, proteins were transferred onto a nitrocellulose membrane in a semi-dry transfer chamber. Four sheets of filter paper and a nitrocellulose membrane were cut to the size of the polyacrylamide gel and presoaked in transfer buffer (48 mM Tris, pH 9.2, 39 mM glycine, 20 % methanol). Two sheets of presoaked filter paper and membrane were placed on the anode. The gel was placed on top of the membrane and covered with the remaining presoaked filter paper. Air bubbles were removed from the stack and it was covered with the cathode assembly. The transfer was performed for 35 min at 12 V. To check the accuracy of the transfer, the membrane was placed in PonceauS solution (0.1 % ponceauS, 3 % TCA) for 1 min. After protein staining, the membrane was washed with TBS for 5 min and then incubated in blocking buffer (5 % w/v non-fat milk powder in TBST or 5 % w/v BSA in TBST depending on primary antibodies) for 1 h at room temperature. The membrane was incubated over night with primary antibodies diluted in blocking buffer in the ratio 1: 500. It was washed three times with TBST for 5 min and incubated with horseradish peroxidase-conjugated secondary antibodies (1: 2000 dilutions in blocking buffer) with gentle agitation for 1h at room temperature. Following 3 washing steps with TBST (5 min each with gentle agitation), blots were developed with the chemoluminescence detection system (ECL or ECL+) and exposed to x-ray film in the dark.

2.13.5 Electro Mobility Shift Assay (EMSA)

Double-stranded DNA oligonucleotides (3.5 pmol) containing an AP-1 binding sequence were incubated with 10 Units of polynucleotide kinase, 1 µl 10 x reaction buffer (700 mM Tris-HCl, pH 7.6, 100 mM MgCl₂, 50 mM DTT, 1 mM spermidin, 1 mM EDTA) and 3 µl γ ³²P-dATP (10 µCi/µl) in total volume of 10 µl. The radioactive labelling was carried out for 1 h at room temperature. Water was added to sample to a final volume of 100 µl and 25 µl 5 M ammonium acetate was added. DNA was precipitated with 70 % ethanol over night at -20°C, re-suspended in 1 M ammonium acetate and again precipitated with ethanol. Following

Materials and Methods

centrifugation (14000 rpm, 30 min, 4°C) oligonucleotides were washed with 70 % ethanol to remove the remaining salt. Labelled DNA was dissolved and stored in TE buffer, pH 7.5.

Protein extracts (4 µg in 4 µl) were mixed with 15 µl of reaction buffer (10 mM Hepes-KCl, pH 7.9, 10 % glycerol, 50 mM KCl, 4 mM MgCl₂, 4 mM Tris-HCl, 0.5 mM EDTA, 0.005 % BSA, 0.005 % poly(dI-dC)) and 2 µl of the radioactive labelled oligonucleotide. Samples were incubated for 30 min at room temperature. Proteins, and nucleotides, were separated in a 4 % polyacrylamide gel (4 % PAA, 0.25 % TBE, 0.05 % APS, 0.005 % TEMED) in 0.25 % TBE buffer by 100 mV. Electrophoresis was preceded by pre-equilibration of gel for 1h by 100 mV. Electrophoresis was stopped before the front reached the end of the gel to avoid chamber contamination with unbound radioactive nucleotides. Gels were dried at +80°C and exposed over night to x-ray film.

2.13.6 IL-6 elisa assay

Quantification of IL-6 protein level in cell culture supernatants upon stimulation with IL-1 was performed with the Quantikine Human IL-6 Immunoassay. The assay employs the quantitative sandwich enzyme immunoassay technique. Cell culture medium was collected in 1.5 ml micro-centrifuge tubes, centrifuged at 14000 rpm for 5 min at 4°C and frozen in aliquots. Samples were stored at -80°C. Standards and samples were probed on 96-well micro-titer plate pre-coated with a monoclonal antibody specific for IL-6. IL-6 present in samples was bound by the immobilized antibody. After discarding unbound substances by washing, horseradish peroxidase conjugated polyclonal antibody specific for IL-6 was added to the wells. Following removal of any unbound antibody-enzyme reagent by additional washing, a substrate solution was added to the wells. The colour development was proportional to the amount of IL-6 bound by primary antibodies. The reaction was stopped and the absorbance was measured at 450 nm and 600 nm for reference. The IL-6 concentration was quantified based on calibration curve generated during the experiment.

2.13.7 Caspase assay

Caspase activity assays were purchased from R&D Systems. 2×10^6 cells per measure point were collected by trypsinisation and combined with culture medium. Cells were pelleted (2500 rpm, 5 min, 4°C) and lysed for 10 min on ice with supplied buffer. Lysates were centrifuged (14000 rpm, 5 min, 4°C) and kept on ice. The enzymatic reaction was carried out in 96-well micro-titer plate. The cell lysat was incubated with caspase-specific peptides that were conjugated to the colour reporter molecule p-nitroanilide. The cleavage of the peptide by

the caspase resulted in release of the chromophore that was detected spectrophotometrically at 405 nm.

2.13.8 MGMT assay

MGMT activity was determined by the transfer of ^3H -labelled O^6MeG from a DNA template to the active site of the MGMT protein. Salmon sperm DNA was labelled with [^3H]methyl-N-nitrosourea. 30 ml of DNA solution (6.3 mg/ml) was incubated with [^3H]-MNU (16.5 Ci/mmol) in reaction buffer (0.2 M NaCacodylat, pH 7.5, 1 mM EDTA) for 2 h at 37°C. DNA was precipitated with 2 volumes of ethanol and dialysed against TE buffer. DNA was again precipitated, washed with ethanol and finally diluted in TE buffer to the final concentration of 6600 cpm/ μl . In a standard reaction, 200 μg protein of a cell extract was incubated at 37°C with 80000 cpm ^3H -labelled DNA in 70 mM Hepes, 1mM DTT, 5 mM EDTA, pH 7.8. After 90 min the reaction was stopped by addition of 1 volume TCA (13 %) and the DNA was hydrolyzed by incubation for 15 min at 95°C. The precipitated protein was collected by centrifugation (14000 rpm, 10 min, 4°C) and washed three times with 5 % TCA. The protein was solubilised in 200 μl NaOH (0.1 N) and the radioactivity was determined in a liquid scintillation counter. The MGMT activity was calculated as fmol of [^3H]methyl transferred to TCA-insoluble material per mg total protein cell extract.

2.14 Gene expression analysis

2.14.1 RNA isolation and RNA electrophoresis

RNA preparation was performed with NucleoSpin RNA II kit according to the manufacture's protocol. Cells were harvested and collected by centrifugation. Lysis was carried out in a solution containing RNases inhibitors. Than nucleic acids were bound onto silica membrane and DNA was removed by DNase I digestion. Following washing steps RNA was eluted with RNase-free water. The integrity of RNA, isolated for microarray experiments, where the highest quality of material is required, was examined by denaturing agarose gel electrophoresis. RNA samples were prepared by adding 15 μl RNA denaturing buffer to 5 μg RNA of minimal concentration 1 $\mu\text{g}/\mu\text{l}$. 1 μl ethidium bromide (10 mg/ml) was added to the samples for visualisation of RNA after electrophoresis. Directly prior to loading, RNA samples were heated to 65°C for 10 min in order to denature any secondary structures. Samples were cooled on ice for 2 min and 2 μl RNA loading buffer was added. Samples were loaded onto 1 % agarose gel (1 % agarose in 1 x MOPS buffer containing 2.2 M formaldehyde) and electrophoretically separated at 30 mA in MOPS/formaldehyde buffer.

2.14.2 Reverse transcription

Reverse transcription was performed with SuperScript First-Strand Synthesis System for RT-PCR with 2 µg of RNA template. The cDNA synthesis reaction was primed with Oligo (dT) of 12 to 18 nucleotide length. RNA template was mixed with Oligo (dT) primers (0.5 µg) and dNTP's (1mM), and then incubated at 65°C for 5 min in order to release any secondary structures. Samples were chilled on ice. The mixture of Reverse Transcription buffer, MgCl₂ (5 mM), DTT (10 mM) and recombinant RNase inhibitor was added and samples were heated to 42° C for 2 min. The reverse transcription was carried out at 42° C for 50 min with 50 units of SuperScript II reverse transcriptase. Reaction was stopped by heat inactivation of RT (70° C, 15 min). The RNA template was digested with 1 unit RNase H (37° C, 20 min). Water was added to samples to a final volume of 40 µl.

2.14.3 PCR

2.14.3.1 Semi quantitative PCR

PCR was carried out using 15 µl REDTaq ReadyMix PCR Reaction Mix and 2 µl cDNA template. Pre-synthesized specific primers (1 µM final concentration) were added and reaction was filled with A. dest. up to 30 µl. 20 µl of amplified DNA was loaded on 1 % agarose gel. The PCR parameters were:

Initial denaturation	94°C, 2 min	1 cycle
Denaturation	94°C, 45 sec	
Annealing	Variable 50-65°C, 1 min	20-35 cycles
Extension	72°C, 1 min	
Final extension	72°C, 10 min	1 cycle

2.14.3.2 Real Time PCR

The method is based on the incorporation of fluorescent dye SYBR Green I into DNA. SYBR Green I binds specific to double-stranded DNA that enhances its fluorescence signal. During each phase of DNA synthesis, SYBR Green I binds to the amplified PCR product that enables detection of the amplicon by fluorescence. A ready- to use reaction mix was purchased from LaRoche and reaction was mixed according to the manufacture's protocol with 2 µl cDNA template and 10 µM of desired primers. Specificity of PCR reaction was proven by melting curve analysis.

Materials and Methods

The PCR conditions were:

Initial DNA denaturation and activation of DNA polymerase	95°C, 10 min	1 cycle
Denaturation	95°C, 10 sec	
Amplification	63-52°C gradient with step size 0.5°C, 10 sec	45 cycles
Elongation	72°C, 20 sec	
Melting	60-90°C, continuous increase	1 cycle

2.14.4 DNA electrophoresis

Agarose (1 % w/v) was melted in TBE buffer, cooled down and ethidium bromide (1 µg/ml) was added. Agarose solution was poured into electrophoresis tray and let to set. DNA was applied on the gel and separated in an electric field (100 mA) in TBE buffer. Gels were photographed and analyzed with Gene Snap and Gene Tools software.

2.14.5 DNA microarray analysis

RNA was isolated with NucleoSpin RNA II kit and tested for integrity by denaturing gel electrophoresis. 20 µg RNA was labelled with fluorescent dye using the LabelStar Array Kit. RNA was treated with supplied denaturation solution to ensure denaturation of the RNA template and neutralization of inhibitors of reverse transcription. Incorporation of modified nucleotides (Cyanine 3-dCTP and Cyanine 5-dCTP) was performed during reverse transcription of the denatured RNA. Reaction was stopped after 2 h and DNA was purified on silica membrane. DNA of sample was combined with DNA of control and air dried. DNA was re-dissolved in 220 µl hybridization buffer (50 mM Na-phosphate, pH 8.0, 50 % formamide, 6 x SSC, 5 x Denhardt's solution, 0.5 % SDS) and denatured for 5 min at 95°C. Custom made DNA-oligo microarrays were obtained from MWG – Biotech. Hybridization was performed for 20 h at 37°C upon permanent shaking in Amersham Array Hybridizer. Arrays were washed for 5 min with 2 x SSC containing 0.1 % SDS, and then 2 x 5 min with 1 x SSC and 0.5 x SSC at 30°C. Afterwards arrays were flushed with 2-propanol and air dried. Slides were read with Affymetrix 428 array scanner and then analysed with Imagine 4.2 software.

2.15 Cloning of DNA

2.15.1 Cloning with Topo vectors

The activated vector (pcDNA3.1 and Topo blue) were purchased from Invitrogene. The system employs topoisomerase I from *Vaccinia* virus that cleaves the phosphodiester backbone after 5'-CCCTT in one DNA strand. The energy from the broken phosphodiester backbone is conserved by formation of a covalent bond between the 3' phosphate of the cleaved strand and a tyrosine-274 of topoisomerase. The phosphor-tyrosyl bound is subsequently attacked by the 5' hydroxyl group of the added PCR product. The vector is supplied in activated form that means linearized with single 3'thymidine overhangs and topoisomerases covalently bound to the vector. Single 3'thymidine overhangs ensure high affinity of plasmid to inserts as Taq polymerase adds a single adenosine to the 3'ends of PCR products. PCR products were pulled on agarose gel electrophoresis and subsequently purified with NucleoSpin Extract II Kit. 2 µl insert was incubated with activated plasmid DNA for 5 min at room temperature. The religated plasmid was transformed into *E. coli*.

2.15.2 Transformation of *E. coli*

The competent bacteria stocks were prepared from 250 ml over night culture with OD600 in the range of 0.35- 0.45. The procedure was carried out on ice at 0°C. The bacteria culture was centrifuged at 9000g for 2 min and re-suspended in 70 ml 50 mM CaCl₂ solution. The suspension was incubated for 20 min on ice and, following centrifugation (9000g, 2 min), bacteria were taken in 12.5 ml 50 mM CaCl₂/10 % glycerol solution. Bacteria stock was aliquoted and frozen in liquid nitrogen and stored at -80°C.

The *E. coli* transformation was performed using the heat shock method. 10 µl ligated DNA sample was incubated with a well of competent bacteria for 45 sec on ice. Afterwards the culture was immediately transferred to 42°C water bath and incubated for 45 sec. 250 µl pre-warmed LB medium was added and bacteria were placed on the shaker for 30 min at 37°C. 100 µl of reaction was plated on pre-warmed agar plates containing 100 µg/ml ampicillin and let to grow over night at 37°C.

2.15.3 Isolation of plasmid DNA

2.15.3.1 “Mini” preparation

Single bacteria clones were picked up from the agar plates and subjected to over night culture in 4 ml LB-medium supplemented with 40 µl ampicillin (10 mg/ml). 1.5 ml culture was pelleted by centrifugation (14000 rpm, 10 min, 4°C) and re-suspended in 100 µl TELT-buffer (50 mM Tris-HCl pH 8.0, 62.8 mM Na₂EDTA, 4 % Triton X-100, 2.5 M LiCl). Plasmid was extracted from bacteria lysats by phenol-chlorophorm-isoamylalkohol (25:24:1) separation. The hydrophilic phase containing DNA was collected and DNA was precipitated with 2.5 volume of 100 % ethanol. DNA was washed with 70 % ethanol, air dried and dissolved in TE buffer, pH 8.0.

2.15.3.2 “Midi” and “Maxi” preparation

Amplification of plasmid DNA was carried out by over night bacteria culture (50 and 250 ml for “midi” and “maxi” preparation respectively). Bacteria were spun down (4000 rpm, 30 min, 4°C) and placed on ice. Plasmid isolation was performed with Qiagen HiSpeed Plasmid Kits according to the manufacture’s protocol. Following re-suspension of bacteria and alkaline lysis in the presence of RNase A (NaOH-SDS lysis buffer), DNA was applied on pre-equilibrated anion exchange column under appropriate low-salt and pH conditions. RNA, proteins and low molecular weight impurities were removed by a medium salt wash. Plasmid DNA was eluted in high-salt buffer and then concentrated and desalted by isopropanol precipitation. DNA pellet was washed with 70 % ethanol, air dried and re-dissolved in TE buffer, pH 8.0.

3 Results

3.1 DNA double-strand break repair in processing of O⁶MeG lesions

O⁶MeG inducing agents, such as temozolomide, streptocotocin, prozarbazine and dacarbazine, are widely used as anti-cancer chemotherapeutics. Their application is gradually growing and presently they are administered in the treatment of gliomas, melanomas, carcinoid tumours and Hodgkin's lymphoma. However, the mechanism of O⁶MeG induced cytotoxicity remains unclear. So far, it is known that O⁶MeG is not toxic to cells as long as it is not processed during proliferation. The current model suggests that O⁶MeG mispairs with thymine in the first round of DNA replication after drug exposure. In the subsequent cell cycle the O⁶MeG/T mispairs are subjected to erroneous MMR, forming a secondary DNA lesion, which interferes with DNA replication. High frequency of SCE's and chromosomal aberrations, which appear after the 2nd mitosis, point out that the secondary DNA lesion might be DSB as suggested previously (Kaina, 2004; Ochs and Kaina, 2000). If this is the case, cells deficient in the repair of DSB should be more sensitive to alkylating agent treatment. A key protein responsible for sensing and processing of DSB in eukaryotic cells is the ATM kinase. The A-T (ATM deficient) phenotype is characterised by hypersensitivity to DSB inducing agents such as ionising radiation and topoisomerase poisons. Following those treatments, A-T cells lack adequate cell cycle control and do not accomplish efficient DNA repair (Shiloh, 2001). This study is aimed at answering the question of whether ATM is involved in the processing of the alkylating lesion O⁶MeG. The investigation concerns the participation of ATM in the signaling of O⁶MeG triggered cell cycle checkpoints, apoptosis and DNA repair processes.

3.1.1 Phenotypic characteristics of ATM knockout cells

Eukaryotic cells possess multiples mechanisms for repairing alkylating DNA lesions. O⁶MeG is directly repaired by the nuclear protein MGMT. MGMT recognises alkylating DNA lesions at guanine and transfers the alkyl group to its own active site. In this one step reaction, the DNA integrity is restored. In order to investigate the role of ATM in O⁶MeG processing, it was necessary to clarify the cells repair capacity mediated by MGMT.

The MGMT expression was determined using a functional activity assay. ATM +/+ and ATM -/- cell lines were characterised by comparable, very low residual MGMT activity (**Fig. 7**). The enzymatic activity was 67 and 78 fmol/mg protein in wild - type and ATM knockout cells

Results

respectively. This is a very low level. In Mex⁺ proficient control cells (HeLa S3), the activity was approximately 10 times higher and reached 800 fmol/mg protein, whereas HeLa MR did not express MGMT at all. The MGMT activity in ATM^{+/+} and ATM^{-/-} cells was neither increased by ionising radiation nor by treatment with methylating agent MNNG. Treatment with MNNG resulted in saturation of MGMT and complete depletion of basal MGMT activity in the investigated ATM cell pair (**Fig. 8**).

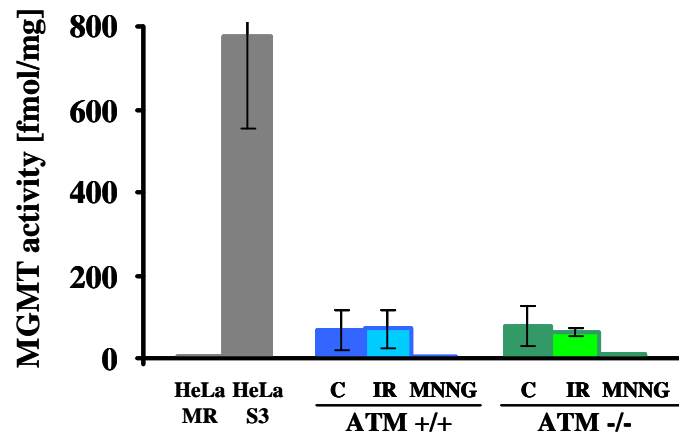


Fig. 7 MGMT activity in ATM^{+/+} and ATM^{-/-} mouse fibroblasts

Protein extracts were prepared from exponentially growing cells. Cells exposed to 4 Gy of γ -radiation or 10 μ M of MNNG, were cultivated in serum free medium 24 h prior to the treatment. Protein extracts were prepared 24 h after irradiation and 6 h after MNNG treatment. During the post-treatment time cells were further maintained in medium without serum. 200 μ g protein was used for the assay. Results are mean values of three independent experiments. HeLa MR and HeLa S3 served as Mex⁻ and Mex⁺ control cell lines, respectively.

In the absence of MGMT, O⁶MeG enters replication and mispairs with thymine. This lesion is subjected to MMR. The mammalian MMR system consists of two functional complexes that are homologues to prokaryotic MutS and MutL. Detection of DNA mispairs occurs by the MutS α complex consisting of MSH2 and MSH6. Following mispair recognition, MutS α associates with an additional heterodimer (MutL α) composed of MHL1 and PMS2, which is homologue to bacterial the MutL (Christmann et al., 2003). MMR deficient cells are highly resistant to O⁶MeG inducing agents. Treatment with alkylating agents leads to accumulation of mutations in these cells but does not evoke cell death. For this reason MMR mutated cells are described as having the “tolerant phenotype” (Kaina and Christmann, 2002). To analyse the MMR status of ATM^{-/-} and ATM^{+/+} mouse fibroblasts, the expression of MMR proteins was assayed by western blotting. Both cell lines expressed all relevant MMR proteins

Results

(Fig. 8A). There was no difference in the nuclear expression of MSH2, MSH6 and MLH1 between the two cell lines. Only the level of PMS2 protein was higher in ATM knockout cells. Nevertheless, as PMS2 acts only in complex with MLH1, PMS2 upregulation on its own should not influence the efficiency of MMR.

Another factor that interferes with the sensitivity of cells to alkylating agents is the p53 protein. Wild - type p53 becomes stabilised upon genotoxic treatment and participates in activation of the cell cycle checkpoint in the G1/S phase and in the activation of DNA repair mechanisms or apoptosis. p53 mutated rodent cells are hypersensitive to O⁶MeG and this hypersensitivity is paralleled by a high rate of apoptosis (Dunkern et al., 2003; Lackinger and Kaina, 2000). p53 was undetectable by Western Blotting in untreated and irradiated ATM -/- and ATM +/+ cells. In contrast, in a mouse control cell line BK4, p53 was detected in irradiated cells 6 h after exposure. Therefore we conclude that ATM -/- and ATM +/+ cells are mutated for p53 (Fig. 8B).

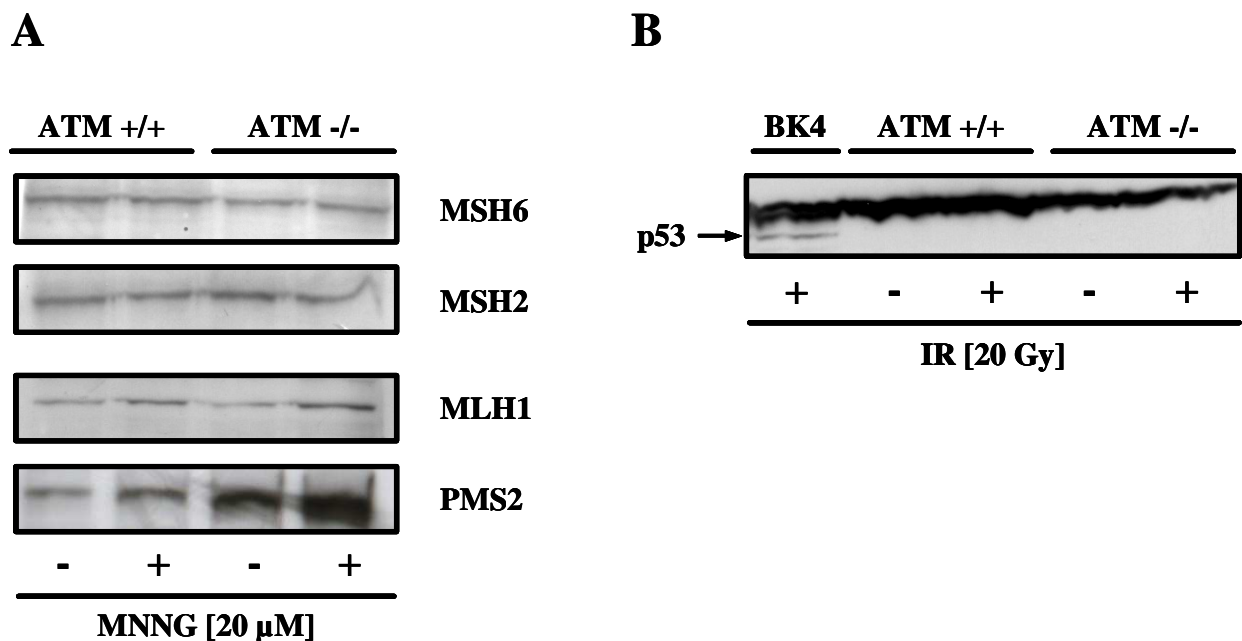


Fig. 8 Expression of MMR and p53 in ATM wild type and mutated cells

- A) Western blot with MMR proteins. Nuclear extracts were isolated from cells untreated or treated with 20 μM MNNG after 6 h incubation. 20 μg of cell extracts were subjected to SDS PAGE.
- B) Western blot analysis of p53 expression. Cells were harvested 6 h after irradiation with 20 Gy. 20 μg nuclear extracts were loaded on SDS PAGE (arrow indicates specific band). The mouse cell line BK4 was used as ap53 wild – type control.

3.1.2 Sensitivity of ATM deficient cells to DNA methylating chemotherapeutic drugs

The A-T phenotype is characterised by extreme sensitivity to ionising radiation. ATM $-/-$ cells are defective in the detection of irradiation induced DSB and are not able to perform effective DSB repair. A consequence, ATM $-/-$ fibroblasts undergo apoptosis with high frequency. In order to confirm the data in the mouse ATM plus and minus system employed, apoptosis and survival upon γ -irradiation was analysed. The clonogenic survival of ATM $-/-$ cells was clearly lower than the corresponding wild type cell line (**Fig. 9A**). After irradiation with 1 Gy survival of ATM $-/-$ cells was reduced by 50%, whereas the survival of wild type cells was hardly influenced. With further increase of the applied dose, the difference in sensitivity was even more pronounced. The sensitivity to ionising radiation correlated with high rate of programmed cell death in ATM $-/-$ cells (**Fig. 9B**). 50 % of ATM $-/-$ cells died 72 h after irradiation with 20 Gy, while the wild type cells remained viable (80 %).The cells underwent both apoptotic and necrotic cell death. None of the death pathways was preferably induced.

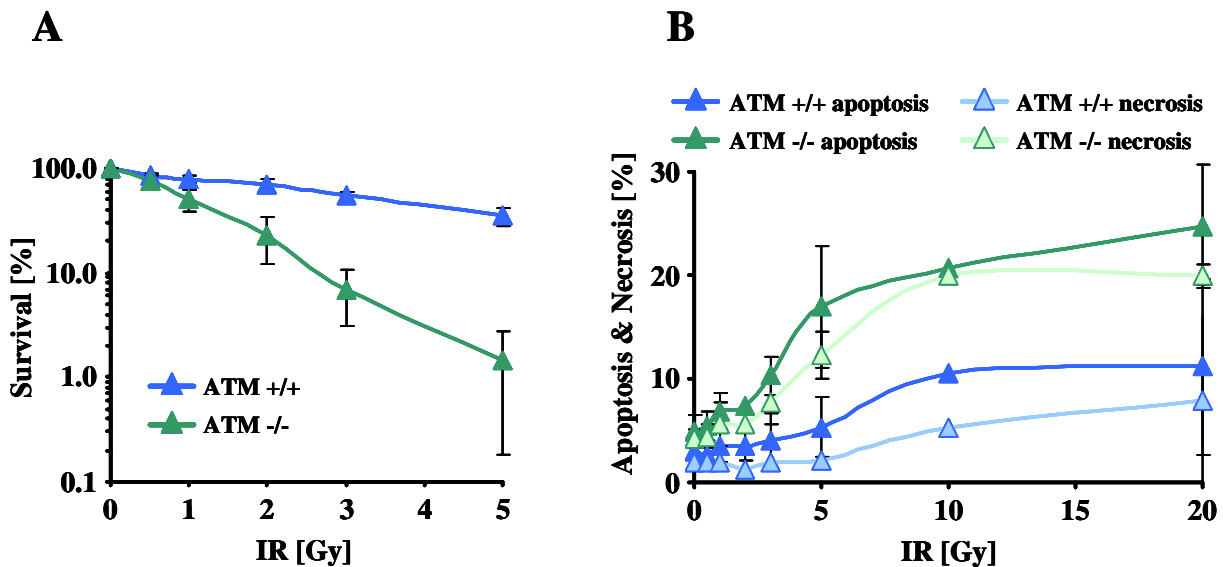


Fig. 9 Clonogenic survival and programmed cell death in ATM +/+ and ATM -/- cells upon γ -irradiation

- A) Clonogenic survival of ATM wild - type and knockout MEF's. 500 cells were seeded in 5 cm culture plates and treated in a dose dependent manner 6 h later. Number of colonies was determined after 7 days cultivation.
- B) Dose response of apoptosis and necrosis after ionising radiation treatment as measured by Annexin V/PI double staining and FACS analysis. Acquisition was performed 72 h after treatment. The data are mean values of 3 independent experiments \pm SD.

To elucidate if ATM participates in the processing of alkylating DNA lesions, ATM $-/-$ cells were assayed in clonogenic survival assays upon treatment with the chemotherapeutic drugs

Results

temozolomide and fotemustine. Temozolomide is a simple DNA methylating agent which therapeutic action is mediated via the formation of O⁶MeG lesions. Fotemustine also alkylates DNA at O⁶ positions of guanine with forming chloroethyl adduct. Most of O⁶-chloroethylguanine adducts is converted to G-C interstrand crosslinks within 8-12 hours following alkylation. These crosslinks are thought to be responsible for the fotemustine-mediated therapeutic effect (Kaina and Christmann, 2002).

ATM ^{-/-} cells were more sensitive to the simple methylating agent temozolomide, but not to the cross-linking agent fotemustine, as shown by clonogenic survival data (Fig. 10). Upon treatment with 50 μ M temozolomide, which is comparable to temozolomide plasma levels achieved in the patient during cancer therapy, survival of ATM ^{-/-} cells was reduced to 50 % (Fig. 10A). The difference in sensitivity between mutated and wild - type cells increased with elevation of the applied drug dose, similar to ionising radiation (Fig. 9). After treatment with 0.5 mM temozolomide, the survival of ATM ^{-/-} cells decreased to 2 %, while 30 % of ATM ^{+/+} cells still formed colonies. The survival after treatment with fotemustine decreased in a dose dependent manner (Fig. 10B). There were no significant differences in sensitivity between the cell lines. The colony formation capacity of ATM ^{-/-} cells was slightly lower than in ATM wild - type cells.

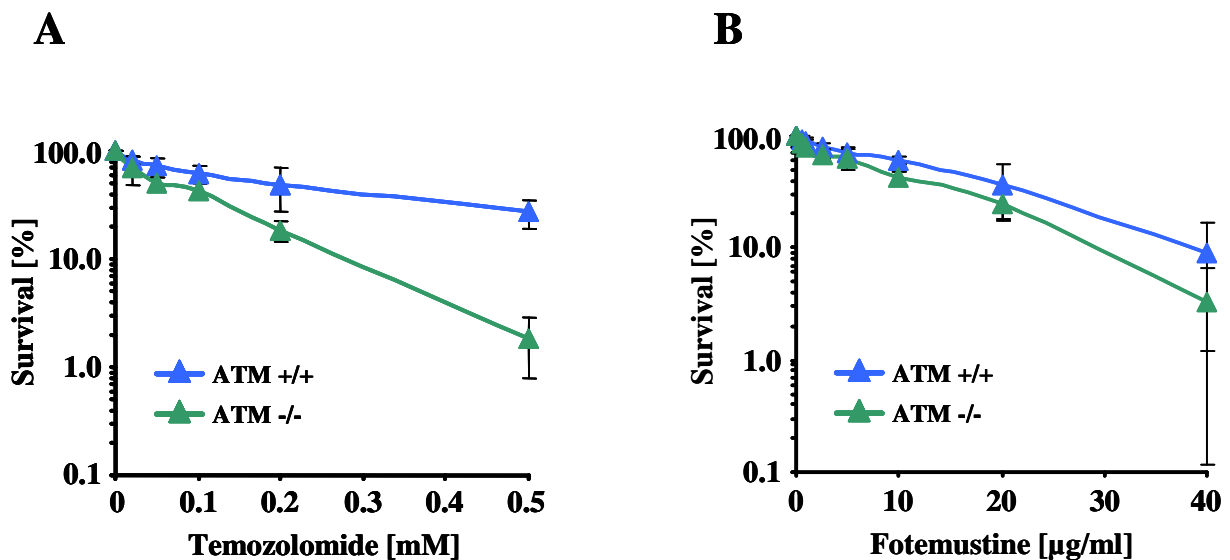


Fig. 10 Clonogenic survival of ATM ^{+/+} and ATM ^{-/-} cells exposed to temozolomide (A) or fotemustine (B)

Pulse treatment with the agents (for 60 min) was performed 6 h after plating. Colonies of at least 50 cells were counted 7 days after drug treatment. The data are mean values of 3 independent experiments \pm SD.

Results

The higher sensitivity of ATM $-/-$ cells to temozolomide was due to the induction of apoptosis (Fig. 11A). Temozolomide provoked apoptosis in the mutated cells even at the lowest dose, which was 10 μ M. Increasing the drug concentration to 40 μ M increased the apoptotic response by a factor of 4 compared to untreated control. The toxicity of 40 μ M temozolomide in ATM $-/-$ cells, as determined by apoptosis, was comparable to the effect of 5 Gy γ -rays (Fig. 9B). Contrary to ionising radiation that induced both apoptosis and necrosis, temozolomide killed cells exclusively by triggering apoptosis. Necrosis was not induced in ATM $-/-$ or wild - type cells. ATM $+/+$ cells were resistant to temozolomide induced apoptosis up to the maximum dose used. Fotemustine induced apoptosis in a dose dependent manner in both ATM $-/-$ and ATM $+/+$ cells (Fig. 11B). At low dose, the apoptotic response was higher in ATM $-/-$ cells than in the wild - type, nevertheless at higher doses no difference was observed. Again, cell death was mainly due to the induction of apoptosis because only a marginal increase in necrosis was observed.

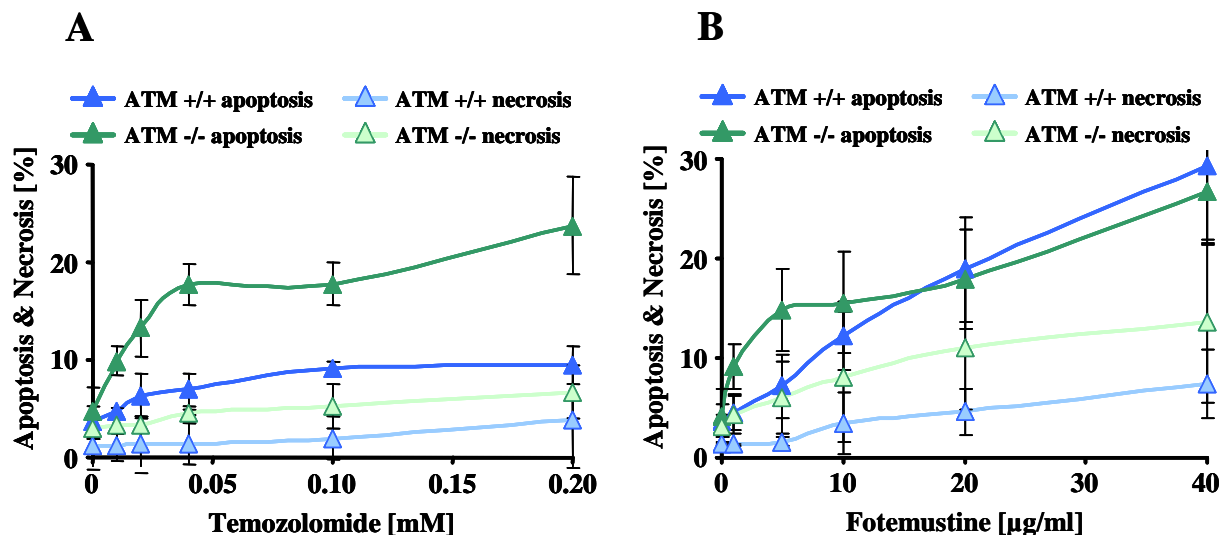


Fig. 11 Induction of programmed cell death in ATM $+/+$ and ATM $-/-$ cells upon treatment with temozolomide (A) and fotemustine (B)

Analysis of apoptosis and necrosis was carried out by Annexin V/PI double staining and subsequent FACS analysis. Acquisition was performed 96 h after treatment. The results are the means of three independent experiments \pm SD.

3.1.3 Role of O^6 MeG in methylating agents toxicity towards ATM $-/-$ cells

ATM is thought to be involved in the processing of DNA damage induced by the chemotherapeutic drug temozolomide because ATM $-/-$ were more sensitive to temozolomide than the corresponding wild-type in both cell survival and apoptosis induction. Unfortunately, due to the unavailability of temozolomide, further studies on the involvement of ATM in the

Results

processing of O⁶MeG were performed with the non-therapeutic agents MMS and MNNG. Both are widely used as a model mutagens. Apart from the availability of these agents, an additional advantage over temozolomide is that the exact frequencies of induced DNA adducts are known. When considering the total DNA methylations, O⁶MeG is formed at a frequency of 7% and not exceeding 0.3% when treating cells with MNNG or MMS respectively. The main product within DNA, for both compounds, is N7 methylguanine comprising between 60 – 80 % of total DNA alkylations. The second most frequent adduct is N3 methyladenine. The remaining DNA alkylations are N1- and N7- adenine, N3- cytosine, N3- guanine and N3- thymidine (Beranek, 1990).

ATM ^{-/-} cells were more sensitive than the corresponding wild type cells to MNNG and MMS as shown by colony forming assays after 1 h pulse treatment (Fig. 12). The difference in colony formation between ATM ^{-/-} and ATM ^{+/+} cells was much more pronounced after treatment with MNNG than with MMS. The survival of ATM ^{-/-} decreased rapidly upon treatment with MNNG in a dose range of 1 – 10 μM, whereas ATM ^{+/+} cells were only slightly affected (Fig. 12A). ATM ^{-/-} cells were also more sensitive than ATM ^{+/+} cells to MMS, although to a lesser degree (Fig. 12B). The difference in MMS sensitivity only becomes apparent at high doses (>0.5 mM) and was never as pronounced as seen after treatment with MNNG.

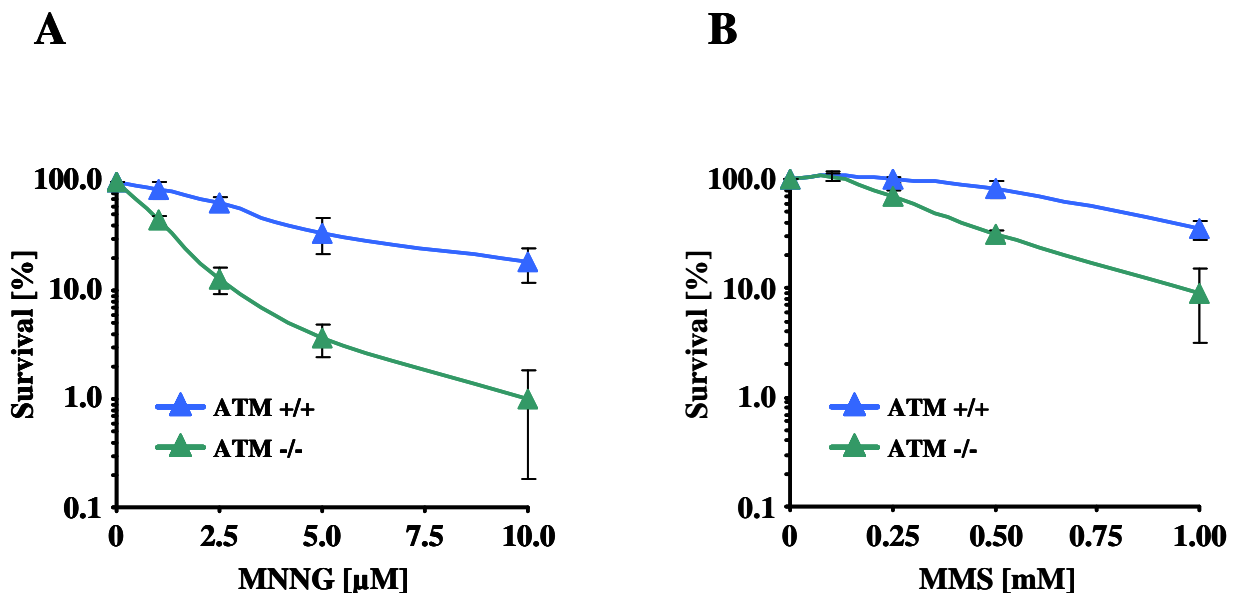


Fig. 12 Clonogenic survival of ATM ^{+/+} and ATM ^{-/-} cells exposed to MNNG (A) and MMS (B)

Colony formation as a function of dose. The treatment occurred for 1 h. Afterwards, cells were incubated for 7 days until colonies appeared. The data are the mean of three independent experiments ± SD.

Results

Hypersensitivity of ATM $-/-$ cells to the O⁶MeG inducing agent MNNG was confirmed in WST-1 viability assays (**Fig. 13**). The cells were seeded in 96 wells micro-titer plate and treated for 1h with MNNG (**Fig. 13A**) or MMS (**Fig. 13B**). The metabolic assay was performed 72 h after drug application. The viability of ATM $-/-$ cells was strongly reduced after low dose MNNG treatment. A linear decrease in ATM $-/-$ cell survival for doses up to 2.5 μ M was observed. At higher doses the survival curve reached the characteristic plateau at 50 % survival. The viability of wild - type cells was not influenced by MNNG even at the highest concentration of 20 μ M. The relative survival after MMS treatment measured with the WST-1 assay confirmed the previous data obtained with colony building assays. Toxicity in ATM $-/-$ cells was observed starting at concentrations 0.5 mM MMS and higher. The viability of wild - type cells remained at 100 % for the applied dose range.

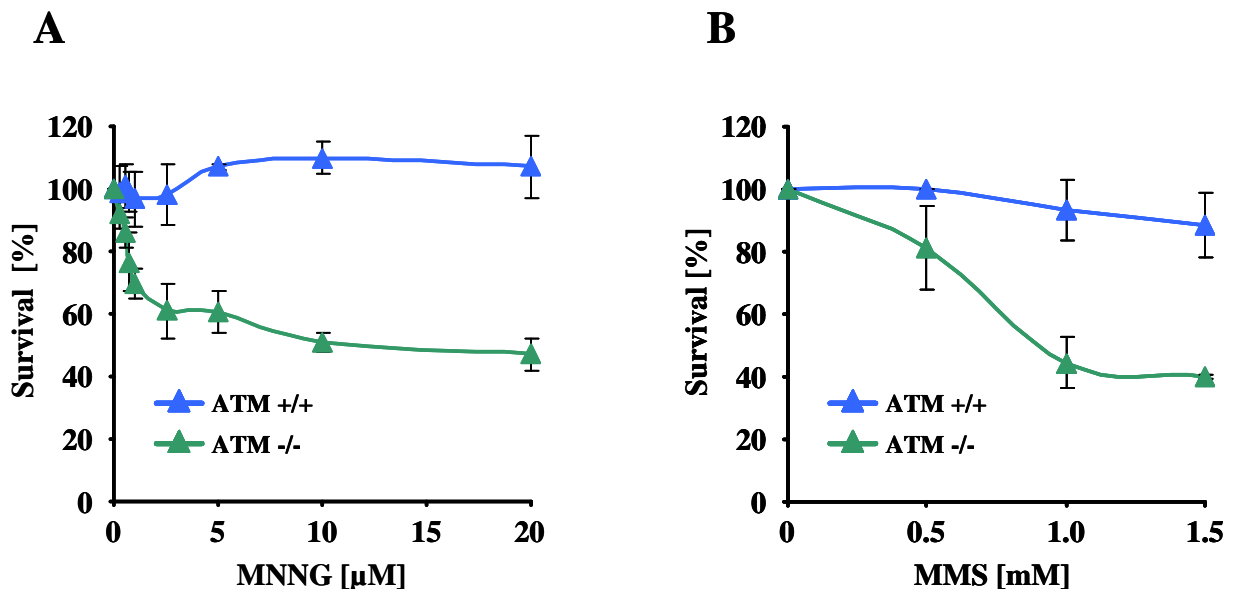


Fig. 13 Viability of ATM $+/+$ and ATM $-/-$ cells as measured by WST-1 metabolic assay as a function of dose upon pulse treatment (for 60 min) with MNNG (A) and MMS (B)

2000 cells were seeded in a 96-well micro-titer plate and cultivated for 48 h. Cells were treated with different doses of MNNG or MMS for 1h and then washed with PBS. The metabolic assay was performed 72 h later. Each measure point was analysed in triplicate. The data are mean values of three independent experiments \pm SD.

Hypersensitivity of ATM $-/-$ cells to MMS was observed after permanent treatment with MMS (**Fig. 14**). ATM $+/+$ cells did not show any reduction in viability up to a dose of 0.4 mM MMS. In this dose range the survival of ATM $-/-$ cells decreased gradually and at 0.4 mM MMS was as low as 25 %.

Results

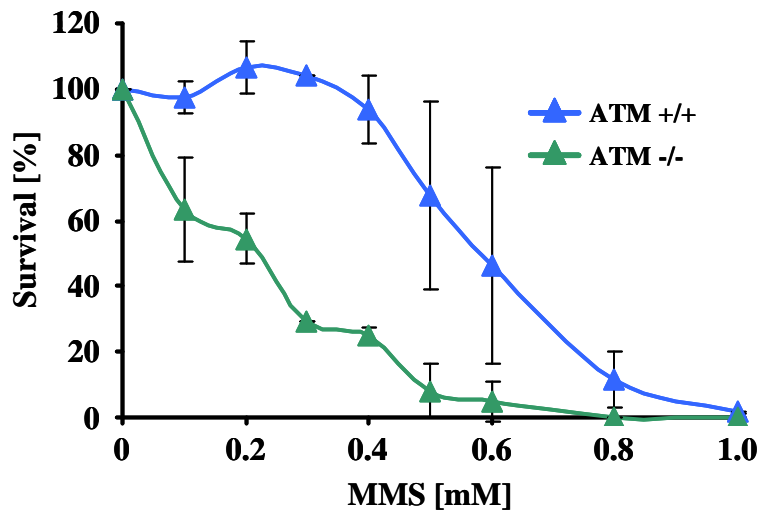


Fig. 14 Viability of ATM +/+ and ATM -/- cells as a function of dose measured by the metabolic WST-1 assay upon treatment with MMS

2000 cells were seeded in 96-well micro-titer plate and cultivated for 48 h. Cells were treated with MMS in a dose dependent manner and the medium containing the mutagen not replaced for the next 72 h. After that the metabolic assay was performed. Each measure point was analysed in triplicates. The data are mean values of three independent experiments \pm SD.

Decreased viability and cellular survival of ATM -/- cells after MNNG treatment was due to the induction of apoptosis, as shown by Annexin V/ PI double staining and DNA laddering (**Fig. 15**). Low dose MNNG treatment ($< 20 \mu\text{M}$) effectively induced apoptosis in ATM -/- but not in ATM +/+ cells (**Fig. 15A**). $1 \mu\text{M}$ MNNG increased apoptosis in ATM -/- cells by a factor of two, compared to the untreated control. Doubling of the apoptotic response (15%) in ATM +/+ cells was only observed after a dose of $20 \mu\text{M}$ MNNG. At this dose, 50 % of ATM -/- cells were undergoing apoptosis. Similar to temozolomide, MNNG induced almost no necrosis. At the highest dose ($20 \mu\text{M}$ MNNG), 15% of ATM -/- cells were necrotic while ATM +/+ cells showed similar necrosis levels as untreated cells.

MMS was less effective in triggering apoptosis in ATM -/- cells than MNNG (**Fig. 15C**). Apoptosis was only observed at high MMS doses ($>1\text{mM}$). ATM +/+ cells were slightly more resistant to MMS triggered apoptosis than ATM -/- cells but the difference was not as dramatic as observed following MNNG treatment. In the dose range used, necrosis was only detected in ATM -/- cells and never exceeded 15 %.

Results

Apoptosis induction in cells treated with MNNG and MMS was confirmed by DNA laddering (**Fig. 15B and 15D**). Cells undergoing apoptosis activate nuclear endonucleases that cleave genomic DNA. The intact genomic DNA of high molecular weight have difficulty entering the agarose gel and form a single compaction zone at the top of the gel. The smaller cleaved DNA of different lengths enters the gel and forms the distinctive apoptosis “DNA ladder”. The appearance of the DNA ladder corresponded to 10% apoptosis, as determined by Annexin V/PI double staining. MNNG and MMS induced apoptotic DNA laddering in ATM $+/+$ and ATM $-/-$ cells in a dose dependent manner. The ATM $+/+$ cells were much more resistant to treatment with both methylating agents and DNA laddering was only observed after a dose of 20 μ M MNNG or 1 mM MMS. DNA fragmentation was shown in ATM $-/-$ cells already after treatment with 5 μ M MNNG and 0.5 mM MMS (**Fig. 15B and 15D**).

Results

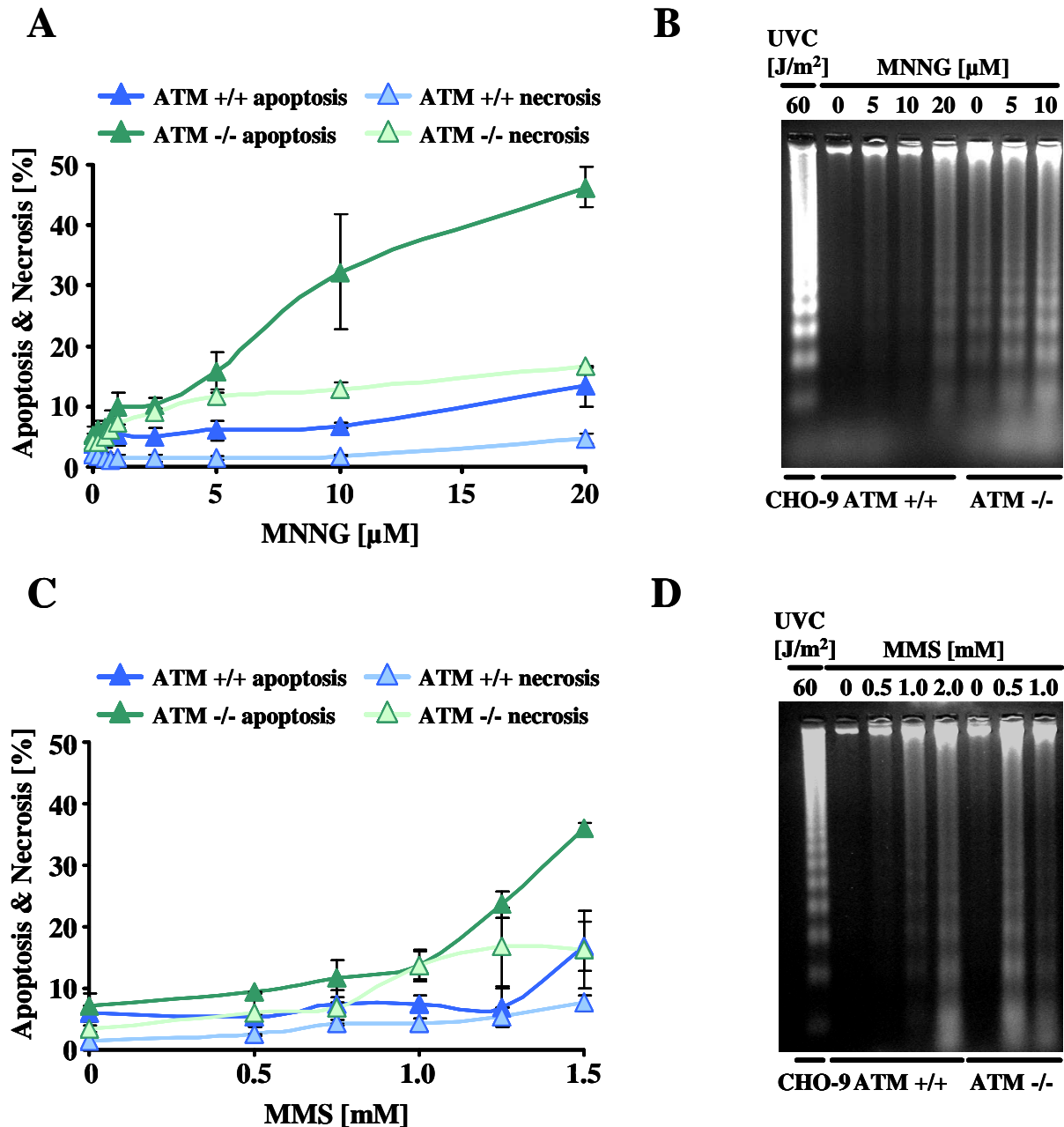


Fig. 15 Apoptosis and necrosis induced by MNNG and MMS in ATM +/+ and ATM -/- cells

- A) Frequency of apoptosis and necrosis upon MNNG treatment quantified by Annexin V/PI staining and subsequent FACS analysis. The acquisition was carried out 96 h after treatment. Data are mean of three independent experiments \pm SD.
- B) DNA fragmentation analysed by agarose gel electrophoresis as a function of dose 96 h after MNNG treatment. A representative experiment is shown and UVC was used as positive control.
- C) Apoptosis and necrosis rate 72 h after pulse treatment with MMS analysed by Annexin V/PI staining. Data are mean of three independent experiments \pm SD.
- D) DNA laddering after MMS treatment as a function of dose. Cells were collected 72 h after 1 h MMS exposure. A representative experiment is shown and UVC was used as positive control.

3.1.4 Effect of caffeine on cell death induced by MNNG and MMS

Caffeine is an unspecific inhibitor of PI3K family proteins and aside from ATM, it also inhibits ATR and DNA-PK at higher doses. For ATM, the inhibitory concentration of caffeine that inhibits 50% of ATMs kinase activity (IC_{50}) is 0.2 mM, for ATR the IC_{50} is 1.1 mM, and for DNA-PK the IC_{50} is 10mM. Wild - type cells treated with 1 mM caffeine exhibit A-T phenotype such as radiosensitivity, radioresistant DNA synthesis and lack of S and G2 checkpoint induction (Blasina et al., 1999; Sarkaria et al., 1999).

ATM $+/+$ and ATM $-/-$ cells were treated with 1 mM caffeine in order to inhibit ATM and partially ATR. Following 1 h incubation MNNG or MMS was added to the medium and left for an additional hour. After that cells were washed with PBS and supplied with fresh medium containing 1 mM caffeine. Because of the high cytotoxicity of the ATM inhibitor, exposure of cells to caffeine was limited to 24 h. Caffeine was therefore removed by medium replacement and the cells were cultivated for an additional 72 h and 48 h after MNNG and MMS treatment, respectively. Cell death was measured by Annexin V-FITC and PI double staining. Caffeine did not affect apoptosis in ATM $-/-$ cells (**Fig. 16**). However in wild type cells, the ATM inhibitor increased apoptosis after both MNNG and MMS treatment. MNNG, in combination with caffeine, induced apoptosis in ATM $+/+$ cells with nearly the same frequency as in ATM $-/-$ cells. The apoptosis triggered by MMS was doubled by caffeine in ATM $+/+$ cells and reached the same level induced in the ATM knockouts at all doses applied. The frequency of necrosis was not influenced by caffeine upon MNNG or MMS treatment; it never exceeded 15 %.

Results

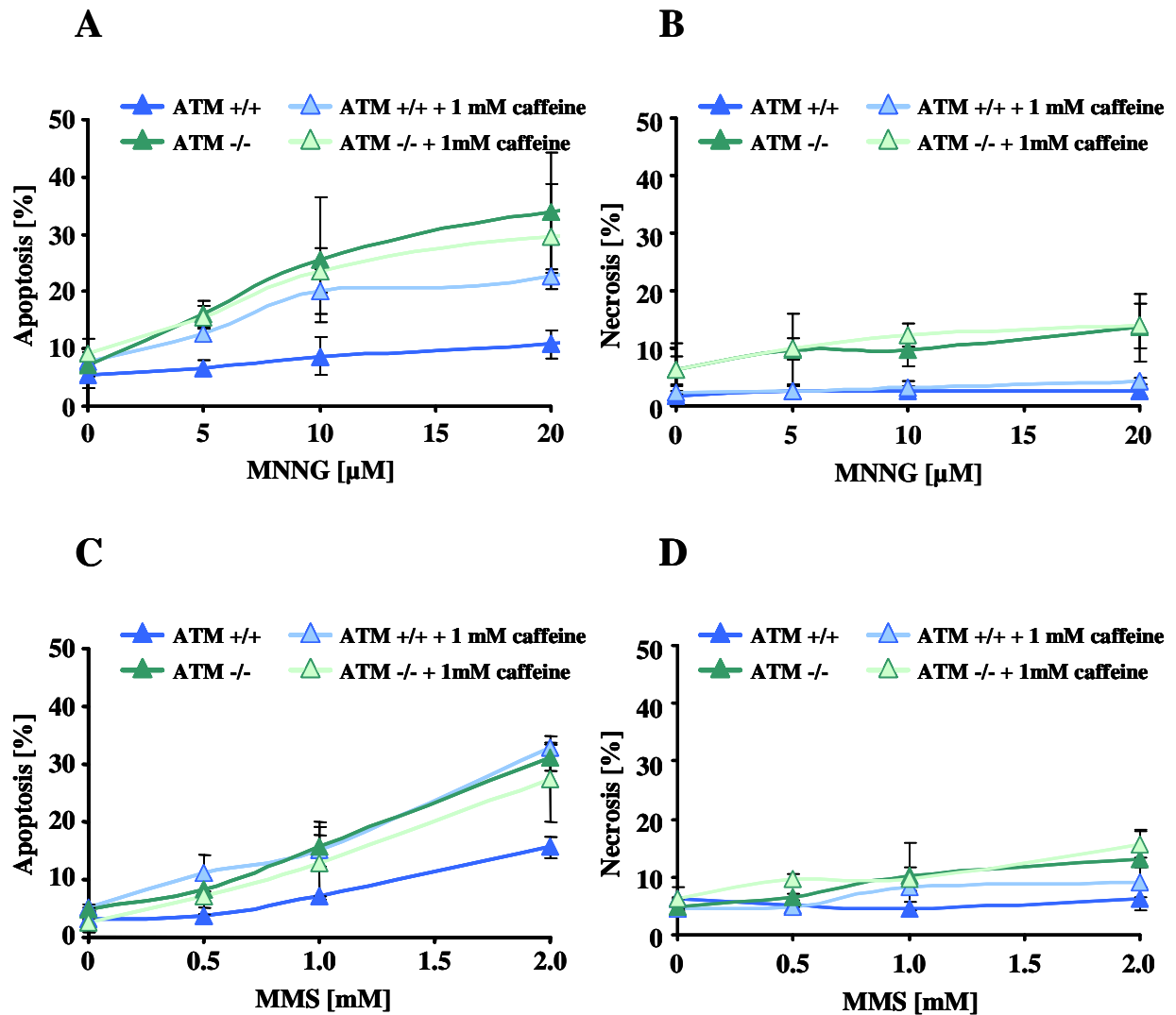


Fig. 16 Frequency of apoptosis and necrosis in ATM +/+ and ATM -/- treated with MNNG and MMS in combination with 1 mM caffeine

Cells were pre-treated with 1 mM caffeine for 1 h. MNNG and MMS at different concentrations were added to the medium containing caffeine and left on the plates for 1 h. Mutagens were removed and the cells were supplied with new medium containing caffeine. Caffeine post-treatment was applied for 24 h and then the medium was exchanged for standard culture medium. Acquisition was carried out by Annexin V/PI staining and FACS analysis. The analysis of apoptosis (A) and necrosis (B) was performed 96 h after MNNG treatment. Apoptosis (C) and necrosis (D) after MMS were analysed 72 h after treatment. The data are means of three independent experiments \pm SD.

3.1.5 Effect of O^6 -benzylguanine and MGMT cDNA transfection on O^6 MeG induced cell death

Increased cytotoxicity induced in ATM -/- cells by methylating agents might be due to deficient repair or erroneous processing at either N7- or O^6 – guanine methylation lesions. To prove the involvement of O^6 MeG in toxicity, the MGMT activity of the cells was

Results

manipulated. MGMT specifically repairs O⁶ alkylations and has no influence on N7 adduct repair. O⁶BG is a non-cytotoxic, competitive MGMT inhibitor. 10 μM O⁶BG added to the medium for 1 h depleted the MGMT activity to a non-detectable level (**Fig. 17**). In order to increase the O⁶MeG repair capacity, the cells were transfected with human MGMT cDNA. The MGMT gene was cloned under control of the SV40 promoter in the pSV2-neo vector (Kaina et al., 1991). Because the cell lines were already neomycin resistant, co-transfection with pSV2-hygro was required. ATM -/- and ATM +/+ cells were transfected with Effectene reagent (Qiagen). The transfection was carried out with 1 μg pSV2-MGMT vector and 0.05 μg pSV2-Hygro. The control cells were transfected with 1 μg pSV2-hygro vector alone. Stable transfected clones were selected with 300 μg/ml hygromycin B. Two cell clones were selected that expressed comparable MGMT activity, which was approximately 10 times higher than in parental cell lines (**Fig. 17**).

MGMT activity [fmol/mg]	ATM +/+	ATM -/-
Parental cell line	67.5	78.5
MGMT inhibitor	Not detected	Not detected
Hygro transfected line	31.0	14.0
MGMT transfected line	776.0	635.0

Fig. 17 MGMT activity in ATM +/+ and ATM -/- cells

MGMT activity assay was performed with protein extracts isolated from exponentially growing cells. MGMT inhibition was carried out for 60 min with 10 μM O⁶BG. Cells were transfected with pSV2- MGMT and pSV2-hygro (designed as ATM +/+ MGMT and ATM -/- MGMT) or with pSV2-hygro alone (designed as ATM+/+ Hygro and ATM -/- Hygro). The MGMT over-expressing clones were selected with 300 μg/ ml hygromycin B.

Results

O⁶BG added to the medium completely depleted the residual MGMT activity. To prevent any effect that newly synthesised MGMT may have, O⁶BG was present throughout the experiment. Inhibition of MGMT decreased clonogenic survival in both ATM +/+ and ATM -/- cell lines after MNNG treatment (**Fig. 18A**). The survival of ATM -/- cells, after 1 μ M MNNG, decreased from 50 % to 10 % in the absence of MGMT. The decrease in survival of ATM +/+ cells, after MGMT inhibition and MNNG treatment, was between 10 and 20 %. Interestingly, survival of ATM -/- cells after MMS treatment was also reduced by O⁶BG co-treatment (**Fig. 18C**).

The decrease in survival of ATM -/- cells upon combined treatment with the methylating agent and the MGMT inhibitor was due to higher level of apoptosis, as shown by Annexin V-FITC and PI staining followed by FACS analysis (**Fig. 18B and 18D**). The acquisition was done 96 h after treatment with 1 μ M MNNG and 72 h after treatment with 0.5 mM MMS. Because of low dose treatment, apoptosis was observed only in ATM mutated cells. Viability of ATM +/+ cells was not influenced by MNNG or MMS and the toxicity was not increased by additional reduction of O⁶MeG repair capacity. In ATM -/- cells, O⁶BG increased MNNG induced apoptosis from 12 to 22 % without affecting necrosis. Compared to MNNG, MMS induces only low amounts of O⁶MeG (~ 0.3 % of total DNA methylations), nevertheless this small portion still contributed to MMS - induced cell death in MGMT depleted ATM -/- cells. The frequency of apoptosis in cells treated with MMS plus O⁶BG was almost twice as high as in ATM -/- cells treated with MMS alone.

Results

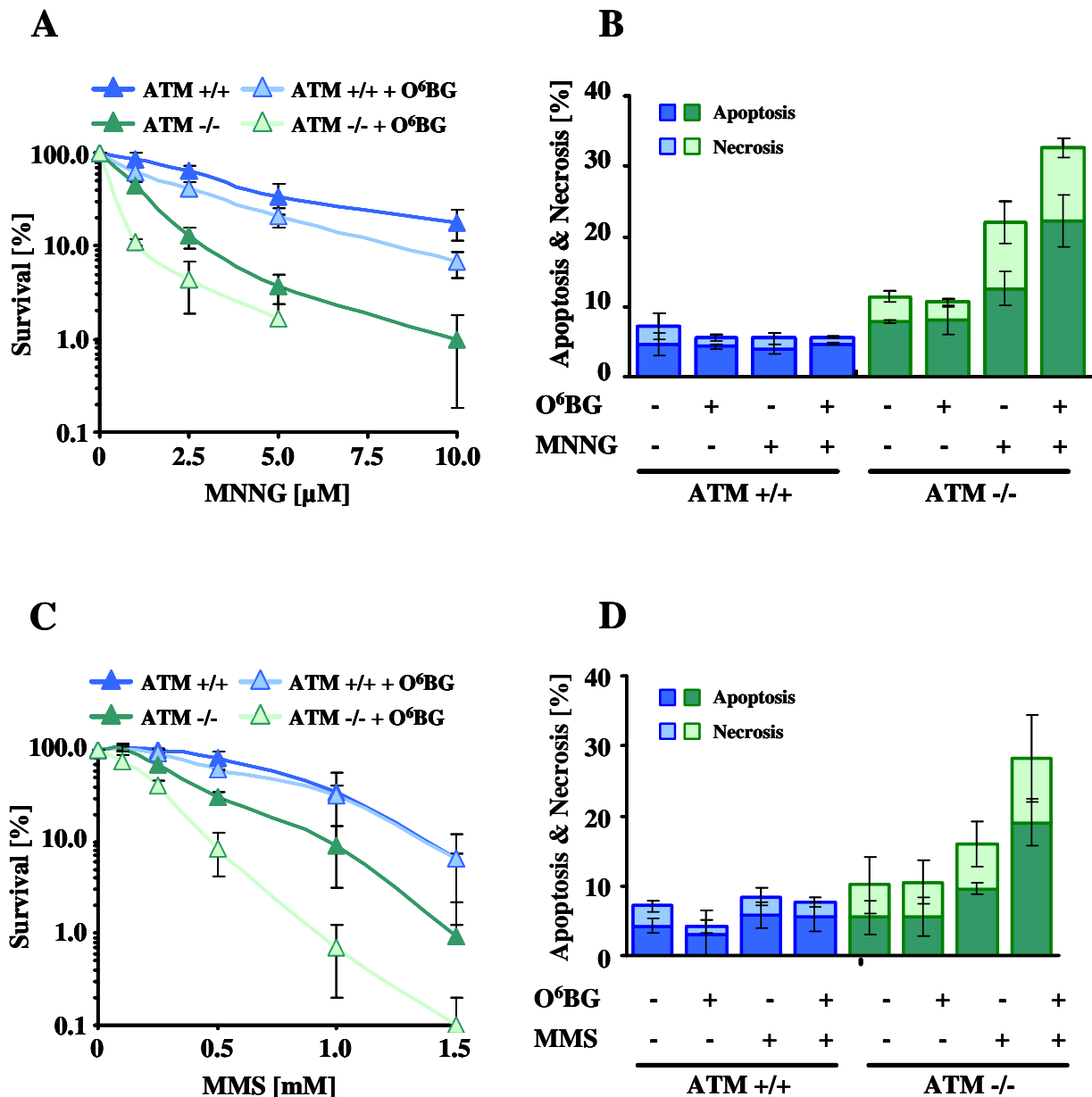


Fig. 18 Sensitivity of ATM +/+ and ATM -/- cells to MNNG and MMS upon depletion of residual MGMT activity with O⁶BG

O⁶BG (10 μM) was added to the culture medium 1 h prior methylating agents treatment. Thereafter cells were treated with different doses of MNNG or MMS in presence of inhibitor. Following 1 h incubation, the medium containing mutagens was replaced with fresh medium supplemented with 10 μM O⁶BG. O⁶BG was left in culture medium to the end of experiment. Survival was quantified by colony formation (A and C). Apoptosis and necrosis was measured by Annexin V-FITC/PI staining and FACS analysis 96 h after MNNG (B) and 72 h after MMS (D) exposure. Data are means of three independent experiments \pm SD.

Results

The potentiating effect of O⁶BG on MNNG and MMS cytotoxicity indicated that the hypersensitivity of ATM^{-/-} cells is due to non-repaired O⁶MeG lesions. If this was the case, increased MGMT activity would protect the ATM deficient cells against MNNG and MMS. To analyse this, ATM^{-/-} and ATM^{+/+} cells were transfected with an expression vector for MGMT (pSV2-MGMT). Indeed ATM^{-/-} cells over-expressing MGMT became much more resistant to both agents, as shown by colony formation experiments (Fig. 19). Over-expression of MGMT led to stronger protection of ATM^{-/-} than ATM^{+/+} fibroblasts. The protection was much more pronounced after MNNG than MMS treatment. The colony formation of ATM^{-/-} MGMT^{-/-} control cells (transfected with pSV2-hygro) was reduced by 2.5 μ M MNNG to 15 % that was similar to the colony forming ability of the non transfected cell line. MGMT over-expression in ATM^{-/-} cells provoked 100% protection against MNNG in the dose range up to 5 μ M. MNNG at higher concentration induced only a slight reduction in survival of ATM^{-/-} MGMT^{+/+} cells. MNNG in the dose range of up to 20 μ M did not provoke any cytotoxic effect in ATM^{+/+} MGMT^{+/+} cells.

Over-expression of MGMT protected ATM^{-/-} cells also against MMS (Fig. 19B). The clonogenic survival of ATM^{-/-} was enhanced by MGMT expression to the level of ATM^{+/+} cells in the dose range up to 2.0 mM MMS.

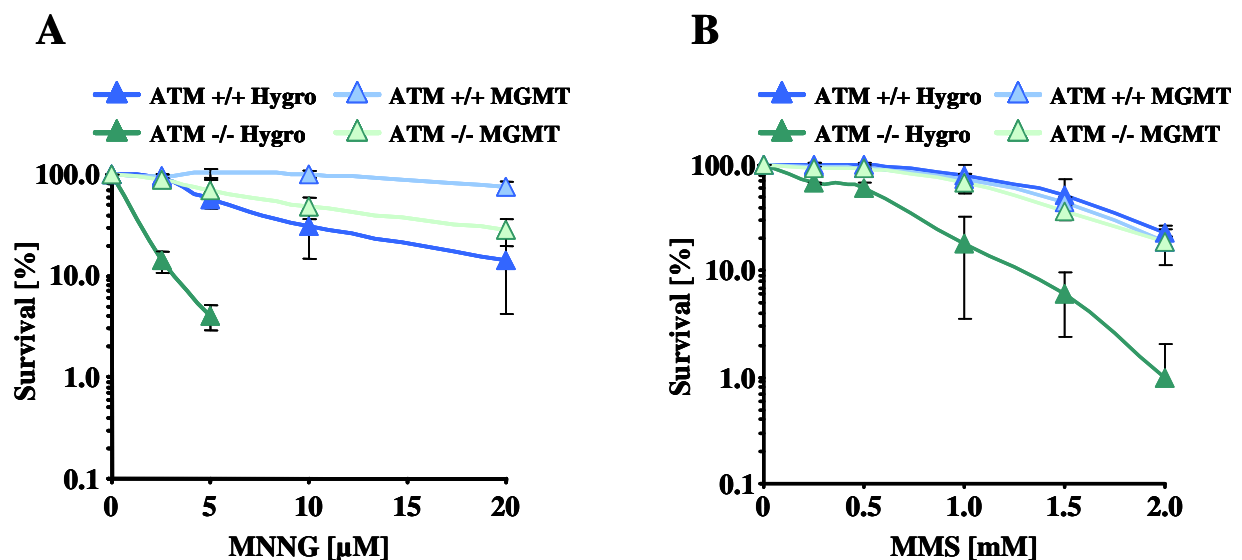


Fig. 19 Colony formation of clones transfected with MGMT cDNA upon MNNG (A) and MMS (B) treatment

ATM^{+/+} and ATM^{-/-} cells were stably transfected with pSV2-hygro alone (designated as Hygro) or together with pSV2-MGMT (designated as MGMT). Colonies were counted 7 days after pulse treatment with the mutagen (for 60 min). Data are means of three independent experiments \pm SD.

Results

The protective effect against MNNG and MMS mediated by MGMT over-expression was confirmed by determination of apoptotic rate (**Fig. 20**). The ATM ^{-/-} Hygro clone was sensitive to MNNG already within the low dose range with a level of apoptosis > 40 % after application of 20 μM MNNG. It was also more sensitive than ATM ^{+/+} Hygro cells to MMS in a dose range up to 2 mM. Apoptosis in ATM ^{+/+} Hygro cells was hardly influenced by any of the agents. MGMT over-expression completely protected ATM ^{-/-} cells against cell death induced by low dose MNNG and MMS treatment. Apoptosis was first detected after application of more than 10 μM MNNG or 1.5 mM MMS reaching 20 %, in both ATM ^{-/-} and ATM ^{+/+} cells. The strong protective effect of over-expressed MGMT in ATM ^{-/-} but not in ATM ^{+/+} cells supported the conclusion that the hypersensitivity of ATM ^{-/-} cells to methylating agents such as MNNG and MMS was due to O⁶MeG, which remained unrepaired within the DNA.

Results

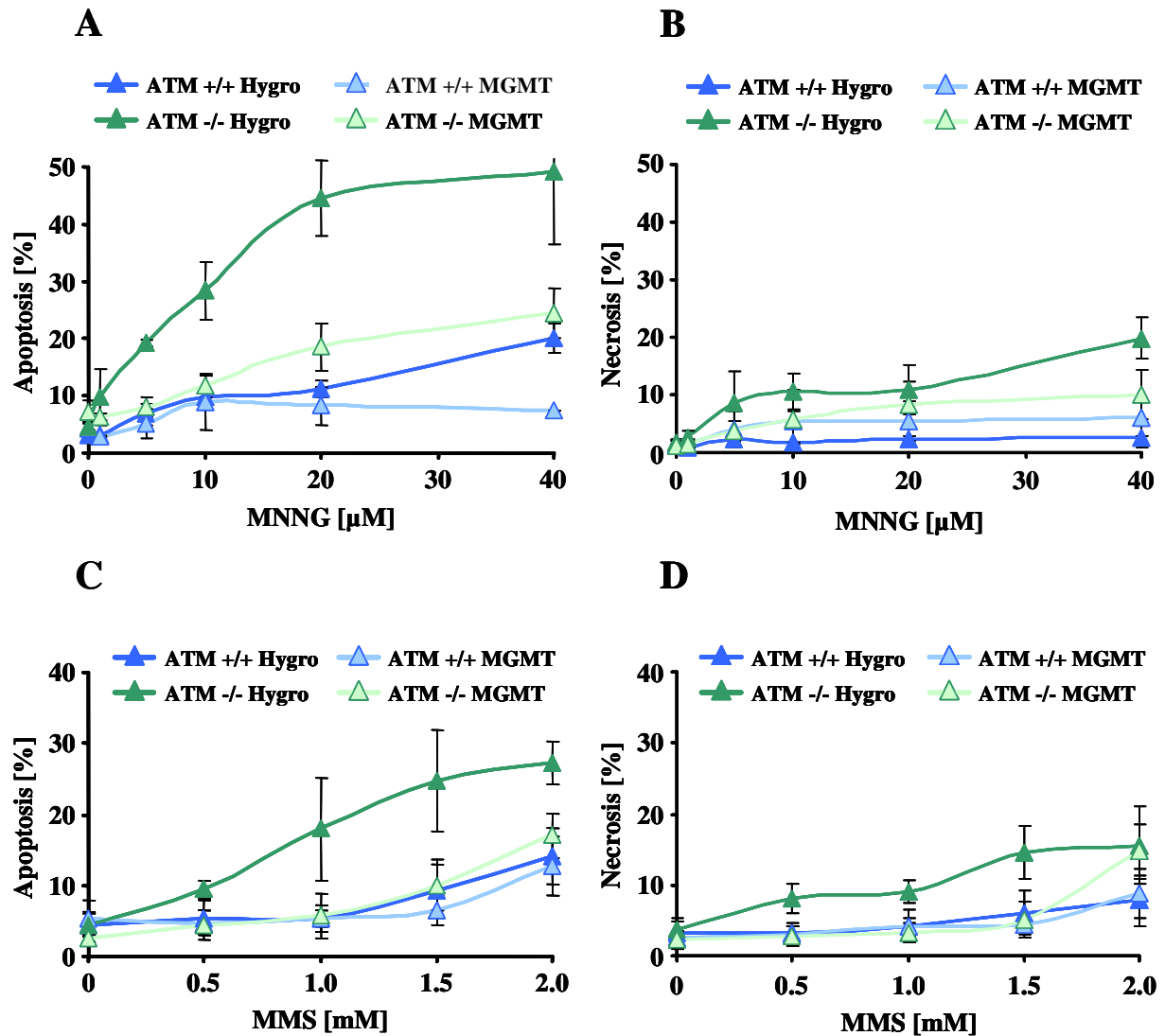


Fig. 20 Induction of apoptosis and necrosis by MNNG (A-B) and MMS (C-D) in ATM +/+ and ATM -/- cells over-expressing MGMT

ATM +/+ and ATM -/- cells were stably transfected with pSV2-hygro alone (designated as Hygro) or together with pSV2-MGMT (designated as MGMT). Cell death was analysed by Annexin V-FITC and PI double staining followed by FACS. The apoptosis and necrosis frequency was quantified 96 h after MNNG and 72 h after MMS treatment. Data are means of three independent experiments \pm SD.

3.1.6 *ATM in the apoptotic pathway evoked by methylating agents*

It was previously shown that ATM $-/-$ cells are sensitive to O⁶MeG inducing agents. The sensitivity of ATM $-/-$ cells corresponded to a high level of apoptosis induced already by low dose mutagen treatment (**Fig. 20**). In murine fibroblasts ATM was not required for cell death initiation after methylating agent treatment. In opposite, ATM $+/+$ cells were protected against apoptosis. The protective role of ATM might result from repair of pro-apoptotic DNA lesions. Alternatively it is due to activation of an anti-apoptotic signaling cascade. Thus, it has been shown that upon genotoxic stress ATM regulates apoptosis through NF κ B as well as through the MAPK pathway. ATM $-/-$ cells are impaired in the activation of c-Jun, ATF2 and Stat-3 transcription factors in response to DNA damage, which is dependent on the stress-activated MAP kinases JNK and p38 (Bar-Shira et al., 2002; Kool et al., 2003; Lee et al., 2001; Weizman et al., 2003). Upon DSB induction, ATM also activates the NF κ B pathway via I κ B- α phosphorylation (Jung et al., 1997; Li et al., 2001; Panta et al., 2004; Piret et al., 1999).

Apoptosis induced by methylating agents such as MNNG and MMS is a late event starting first 48 h after treatment as revealed by time course experiments (**Fig. 21 - 22**). In these experiments apoptosis was quantified by FACS analysis of the SubG1 fraction (cell population with DNA content less than 2n, resulting from apoptotic DNA cleavage). Cells were treated for 60 min with 10 μ M MNNG or 1 mM MMS. Consistent with data obtained with Annexin V staining survival of ATM $+/+$ was nearly not affected (**Fig. 21A**). 10 μ M MNNG induced 15 % apoptosis in the wild type cells 96 h after treatment whereas half of the ATM $-/-$ population underwent nuclear fragmentation. Apoptosis started 48 h after exposure. MMS induced apoptosis with much lower frequency than MNNG (**Fig. 22A**). Apoptosis in ATM $+/+$ cells did not exceed 10 % whereas SubG1 fraction of ATM $-/-$ cells reached 30 % after 96 h. Apoptosis after MMS treatment was observed in ATM $-/-$ cells already after 24 h post-treatment, that might be due to higher participation of N-alkylations among DNA adducts. Apoptosis induction was paralleled by caspase activation (**Fig. 21B and 22B**). Overall caspase activity was measured with a paninhibitor of caspases, VAD-FMK, coupled to fluorophore. Cells were treated with 10 μ M MNNG or 1 mM MMS. 30 min prior harvest cells were incubated with FITC-VAD-FMK and then subjected to FACS analysis. Increased caspase activity was measured 48 h after MNNG and 24 h after MMS treatment. The activities were higher in ATM $-/-$ cells than ATM $+/+$. The results were confirmed in western blot experiments with antibodies against the cleavage product of caspase 3 (**Fig. 21C and 22C**).

Results

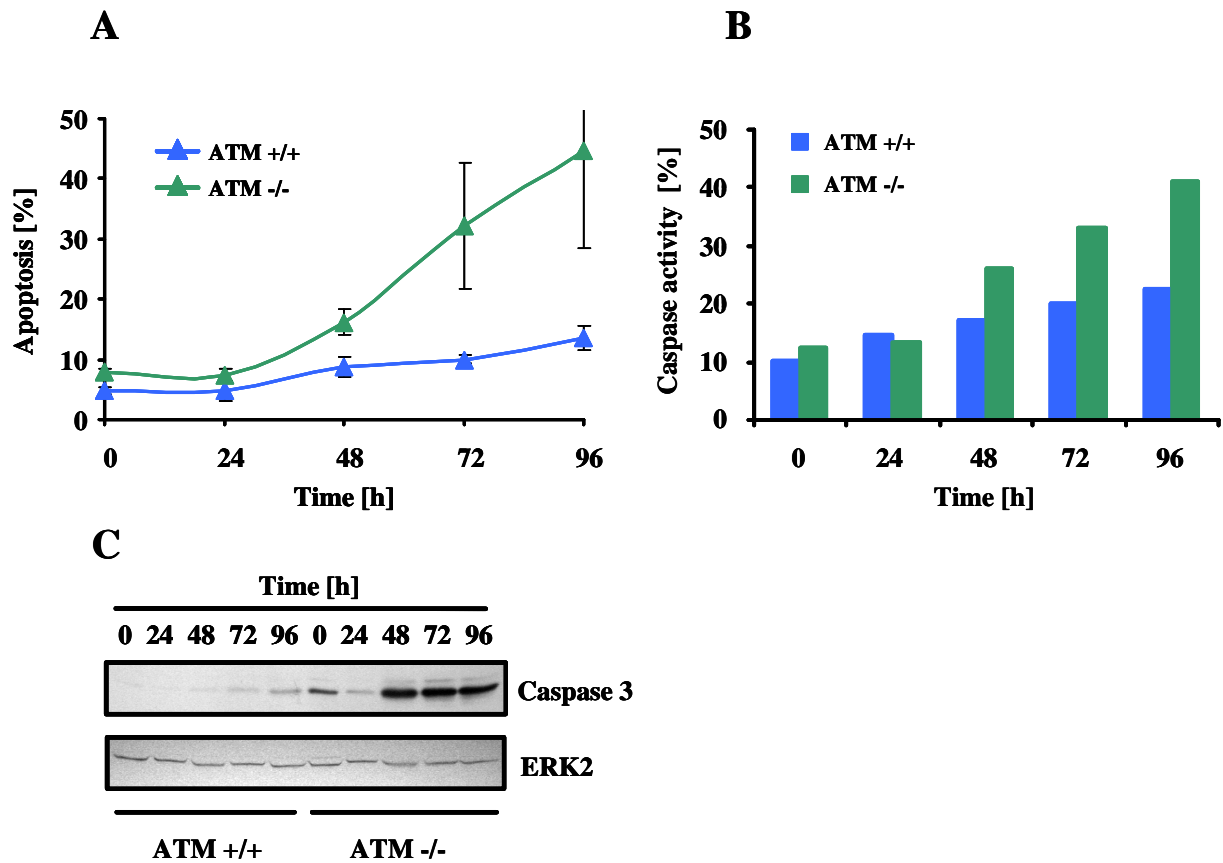


Fig. 21 Time course of apoptosis and caspase activation in ATM +/+ and ATM -/- cells after treatment with 10 μ M MNNG

- A) Apoptosis quantified by SubG1 fraction
- B) Overall caspase activity measured by FACS analysis of cells stained with FITC-VAD-FMK.
- C) Western blot analysis of caspase 3 activation. Antibodies were directed against cleavage product of caspase 3.

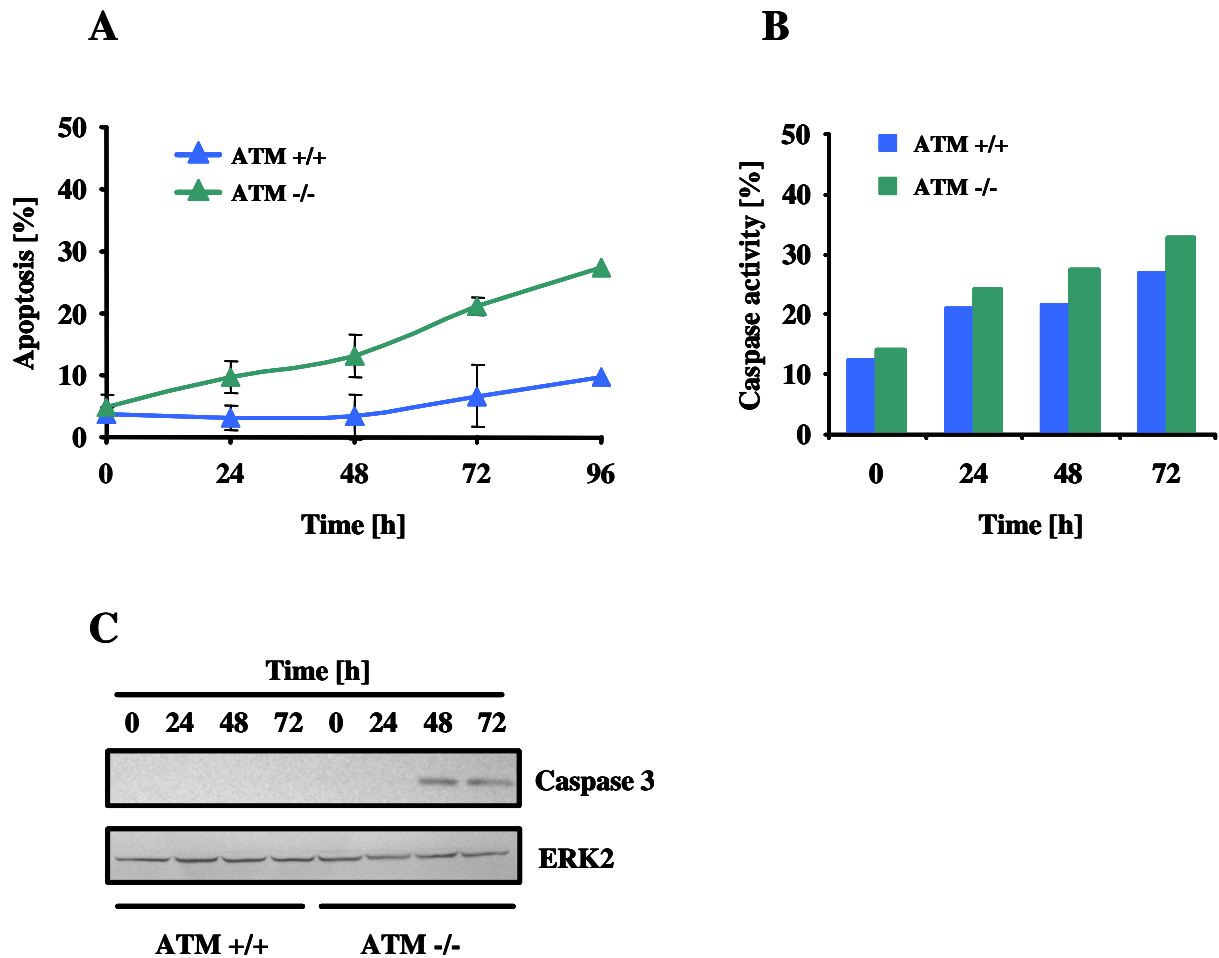


Fig. 22 Time course of apoptosis and caspase activation in ATM +/+ and ATM -/- cells after treatment with 1 mM MMS

- A) Apoptosis quantified by SubG1 fraction
- B) Overall caspase activity measured by FACS analysis of cells stained with FITC-VAD-FMK.
- C) Western blot analysis of caspase 3 activation. Antibodies were directed against cleavage product of caspase 3.

Apoptosis can be mediated by two distinct signaling pathways: extrinsic, dependent on activation of membrane receptors such as FasR (CD95), or intrinsic activated by DNA damage and executed via the mitochondrial pathway. To find out which pathway is dominating in mouse fibroblasts treated with methylating agents, cell extracts were subjected to caspase activity assays (**Fig. 23A and 23C**). Cells were treated with 1 mM MMS or 10 μ M MNNG, harvested 72 h later and apoptosis was measured by the caspase activity assays. Treatment induced apoptosis in ATM -/- cells and the effector caspase - 3 activity was induced by a factor of 3 by MMS and a factor of 5 by MNNG. This treatment did not activated caspase 3 in ATM +/+ cells. In order to induce caspase - 3 in ATM +/+ cells to the

Results

level observed in ATM $-/-$ cells higher doses have to be applied (1.25 mM and 15 μ M for MMS and MNNG respectively). Despite activation of caspase - 3, the transducer caspases - 8 and - 9 were only marginally activated (factor 1.0 – 1.3). This does not allow any conclusion as to the signaling pathway involved.

In further experiments, cells were treated in a dose dependent manner and harvested 96 and 72 h after treatment with MNNG and MMS respectively. Detection of cleaved caspase - 3 and - 9, as well as FasR was performed by western blot of whole cell extracts (**Fig. 23B and 23D**). The expression of Bcl-2 and Bax was determined in mitochondrial extracts, while cytochrome c was detected in the cytosolic fraction. Caspase - 3 became activated in ATM $-/-$ cells already by the lowest applied dose of the mutagens (1 μ M MNNG and 0.5 mM MMS). It was accompanied by cytochrome c release from mitochondria. In ATM $+/+$ cells, cleavage of caspase - 3 and cytochrome c release were limited to a high dose of MNNG and MMS. The levels of cleaved caspase - 9 remained not changed in ATM $-/-$ and ATM $+/+$ cells after both MNNG and MMS treatment (**Fig. 23B and 23D**). ATM $+/+$ and ATM $-/-$ cells differ drastically according to the Fas R expression. ATM $+/+$ cells expressed very high level of the death receptor (lower band) and the expression was stimulated neither by MMS nor MNNG. In ATM $-/-$ cells the basal level of Fas R was under the detection limit and the expression was induced by high dose methylating agent treatment. The Bcl-2/Bax ratio decreased only in ATM $+/+$ cells upon MMS treatment in a dose dependent manner. In ATM $-/-$ cells the Bcl-2/Bax ratio remained overall unchanged as a slight decline in expression was observed for both proteins. Data indicate on the involvement of mitochondrial pathway in methylating agents induced apoptosis.

Results

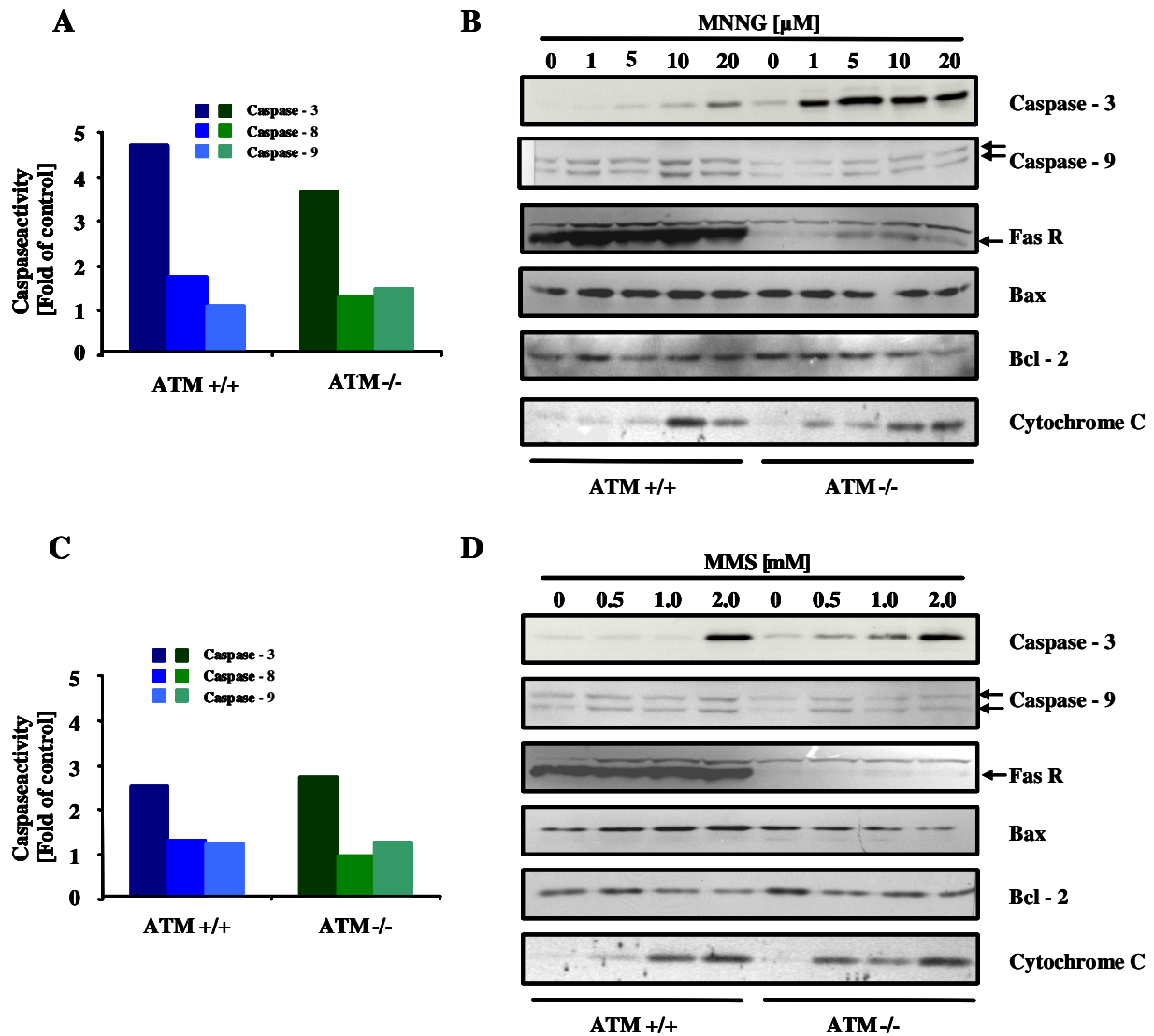


Fig. 23 Caspase activation and expression of apoptotic proteins in ATM +/+ and ATM -/- cells upon MNNG and MMS treatment

- Caspase - 3, - 8 and - 9 activity assays upon treatment with MNNG. ATM +/+ and ATM -/- cells were treated with 15 μ M and 10 μ M MNNG respectively. Cells were harvested after 72 h.
- Western blot analysis of apoptotic proteins. Cells were treated with different doses of MNNG for 60 min and harvested 96 h after treatment. Caspase - 3, caspase - 9 and FasR were detected in whole cell extracts, Bax and Bcl-2 in mitochondria and cytochrome c in cytosol. 20 μ g proteins per lane were loaded on 10% SDS PAGE.
- Caspase - 3, - 8 and - 9 activity assay upon treatment with MMS. ATM +/+ and ATM -/- cells were treated with 1.25 mM and 1.0 mM MMS respectively. Cells were harvested 48 h after treatment.
- Western blot analysis of apoptotic proteins. Cells were treated with different doses of MMS for 60 min and harvested 72 h later. Caspase - 3, caspase - 9 and FasR were detected in whole cell extracts, Bax and Bcl-2 in mitochondria and cytochrome c in cytosol. 20 μ g proteins per lane were loaded on 10% SDS PAGE.

3.1.7 JNK and p38 kinase activation in ATM +/+ and ATM -/- cells

Having shown that ATM -/- cells are hypersensitive to methylating agents, a potential activation of the MAPK pathway was investigated. The MAPK is thought to operate upstream in the signaling cascade leading to apoptosis. Therefore, the experiments were performed before the onset of apoptosis i.e. 0- 36 h after mutagen treatment. Activation of MAPK was examined by phosphospecific antibodies raised against Thr183/Tyr185 p44/42 MAPK (described as JNK) and Thr180/Tyr 182 p38 MAPK. The phosphorylation is known to correspond with kinase activation. Cells were treated with 10 μ M MNNG or 1 mM MMS. Increased MAPK kinase phosphorylation was observed already 1 h after treatment with the methylating agents (**Fig. 24**). At this early time point, there were no differences were observed between ATM -/- and ATM +/+ cells. Interestingly in ATM -/- cells JNK activity persisted longer than in the ATM +/+ cells. Phosphorylated JNK was detected in ATM-/- cells up to 18 h after treatment, while in ATM +/+ cells it was not observed for longer periods than 3 h and 9 h after MMS and MNNG treatment, respectively. Phosphorylation of p38 MAPK was not influenced by the ATM status. In both cell lines the control level of p38 phosphorylation was restored 9 h after mutagen treatment.

Furthermore, MAPK activation was determined in dose dependent manner 1 h after MNNG and MMS treatment. p38 and JNK kinase phosphorylation was observed upon treatment with 5 μ M MNNG (**Fig. 25A**) or 0.5 mM MMS (**Fig. 25B**). It further increased in a dose dependent manner. The early MAPK activation is ATM independent.

Results

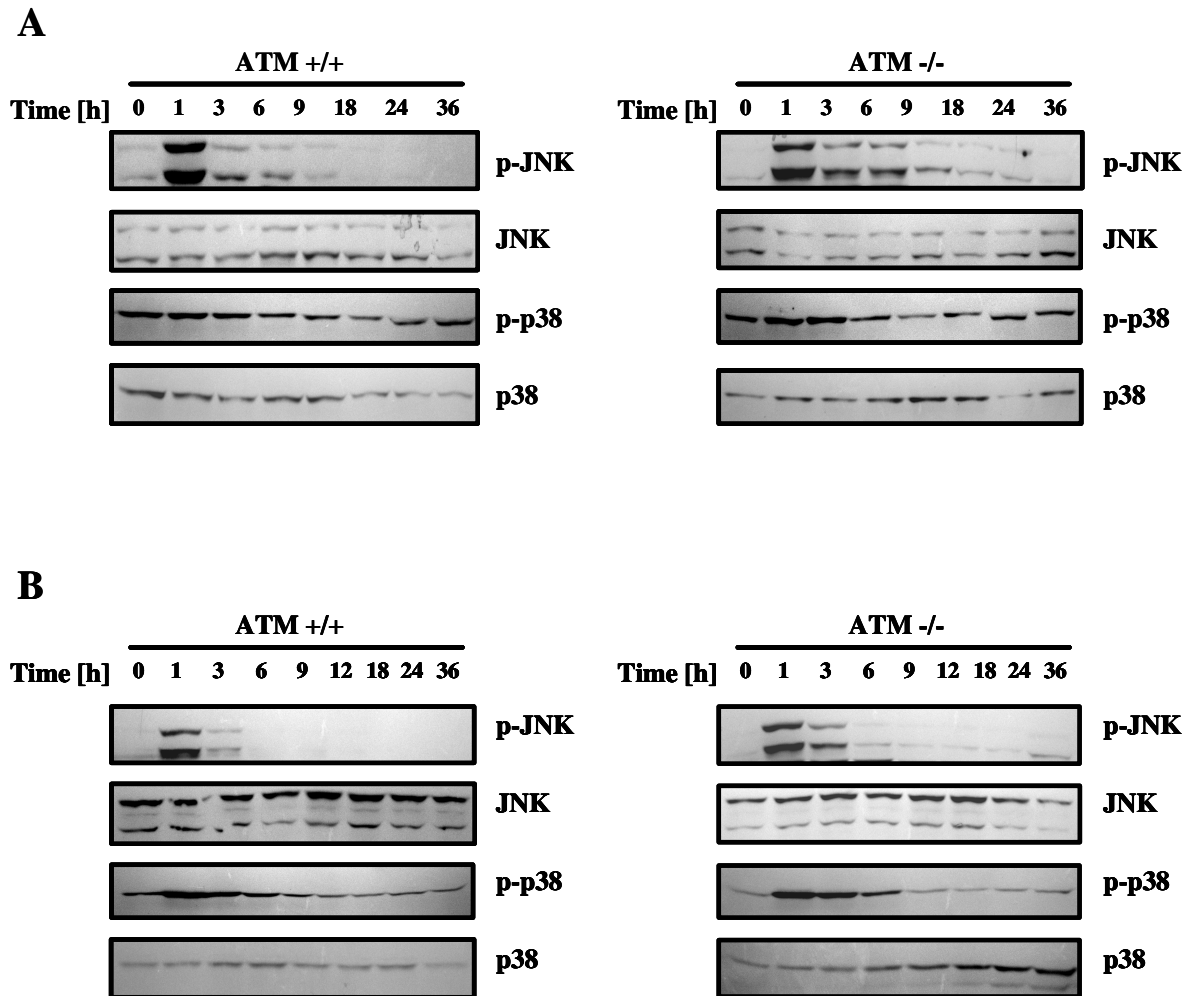


Fig. 24 MAPK activation in ATM +/+ and ATM -/- cells upon treatment with 10 μ M MNNG (A) or 1 mM MMS (B)

Cells were seeded in 6 cm culture plates and cultivated for 48 h, then treated for 60 min. Cells were harvested directly on the plates with hot loading buffer. 10 μ l protein extracts were separated on 10 % SDS gels. Membranes were incubated over night with primary antibodies against phospho Thr183/Tyr185 p44/42 MAPK (p-JNK), p44/42 MAPK (JNK), Thr180/Tyr182 p38 MAPK (p-p38) or p38 MAPK.

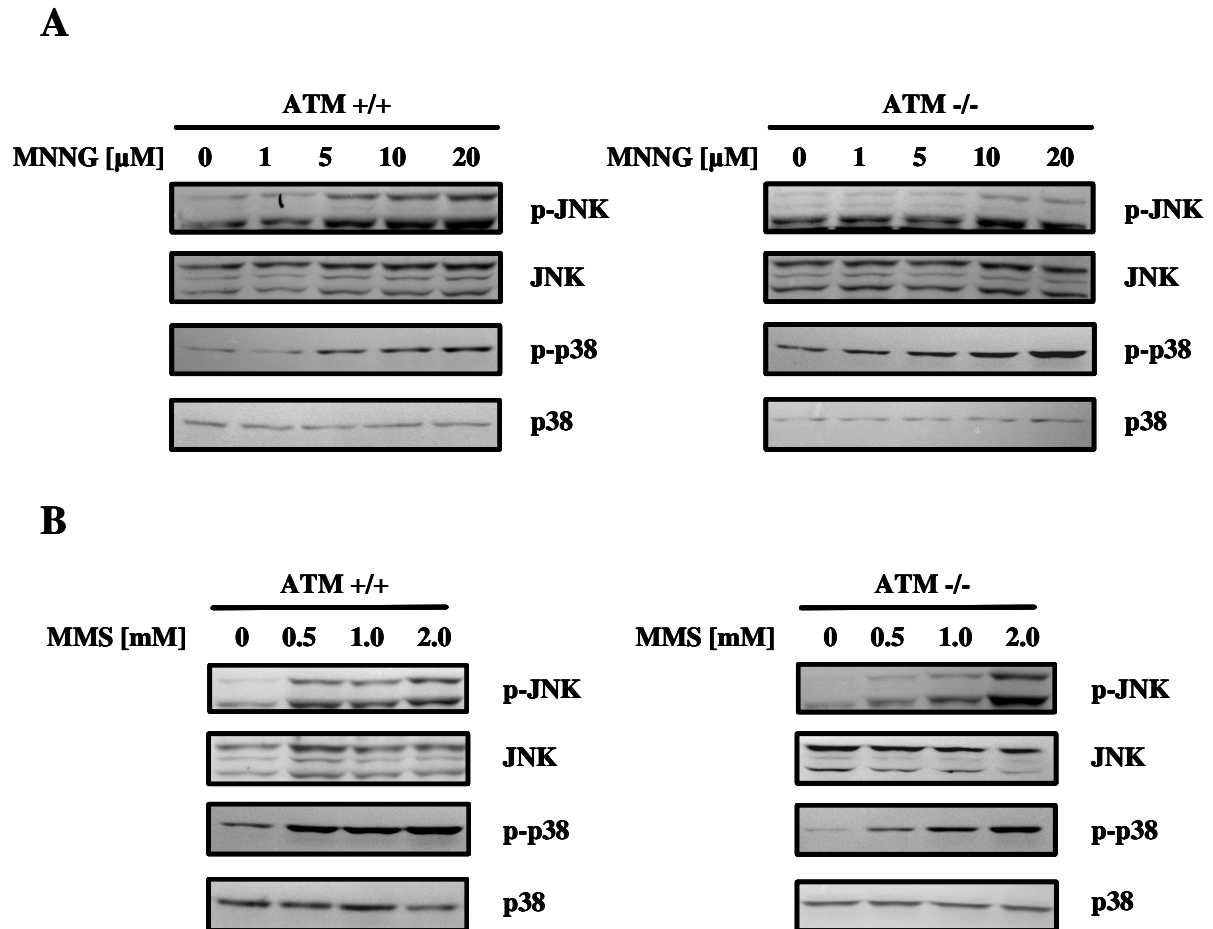


Fig. 25 MAPK activation as a function of dose of MNNG (A) and MMS (B) 1 h after mutagen treatment in ATM +/+ and ATM -/- cells

Cells were seeded in 6 cm culture plates and cultivated for 48 h, then treated for 60 min. 10 μ l protein extracts were separated on 10 % SDS gels. Western Blot membranes were overnight incubated with antibodies against phospho Thr183/Tyr185 p44/42 MAPK (p-JNK), p44/42 MAPK (JNK), Thr180/Tyr 182 p38 MAPK (p-p38) and p38 MAPK.

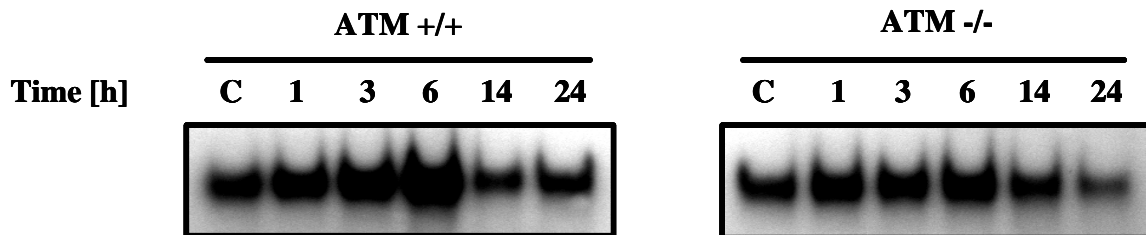
3.1.8 AP-1 binding activity upon methylating agents treatment

Activated JNK phosphorylates and thereby activates several proteins including c-Jun and ATF-2, which form the heterodimeric transcription factor AP-1. AP-1 activation in turn gives rise to increased expression of AP-1 target genes, among them the gene encoding the proapoptotic FasL protein. To investigate if the persisting activity of JNK in ATM -/- cells influences the binding activity of the AP-1 complex, EMSA analysis with an oligonucleotide derived from mouse collagenase promoter as performed (Fig. 26). Cells were treated with 10 μ M MNNG or 1 mM MMS and harvested at the time points indicated. Increased AP-1 binding activity was observed in ATM +/+ and ATM -/- cells 1 h after MNNG and MMS

Results

treatment. Maximal signal intensity was observed 3 h after treatment. Thereafter the binding capacity gradually returned to the control level.

A



B

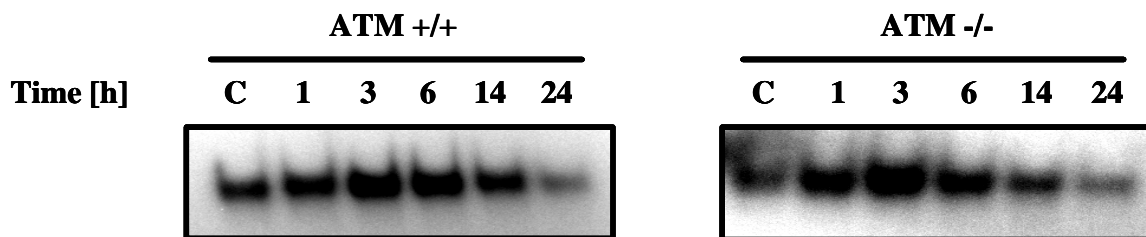


Fig. 26 AP-1 binding activity in ATM +/+ and ATM -/- cells upon treatment with 10 μ M MNNG (A) and 1 mM MMS (B)

EMSA with oligonucleotide containing AP-1 binding site derived from mouse collagenase promoter. 2 μ g protein extracts were incubated with 32 P labelled oligonucleotide. The reaction products were separated on 5 % polyacrylamide gels and subjected to autoradiography.

3.1.9 Expression of AP-1 and NF κ B target genes in ATM +/+ and ATM -/- cells

The influence of mutagen – induced AP-1 activation on gene expression in ATM +/+ and ATM -/- cells was analysed by semi quantitative RT-PCR. The cells were treated with 10 μ M MNNG or 1 mM MMS. Primers were specific for genes controlled by JNK (*c-jun*, *fasL*) and the NF κ B pathways (*fasR* and *c-iap*). Expression in ATM +/+ cells of the JNK dependent genes, *c-jun* and *fasL*, was enhanced 24 h after methylating agent treatment and was increasing further with time (**Fig. 27**). The NF κ B pathway was down-regulated by both agents. 14 h after treatment the amount of *fasR* and *c-iap* mRNA was clearly reduced and then gradually restored to reach the control level 72 h after treatment. In ATM -/- cells the expression of all genes analysed was unchanged upon mutagen treatment (**Fig. 27**).

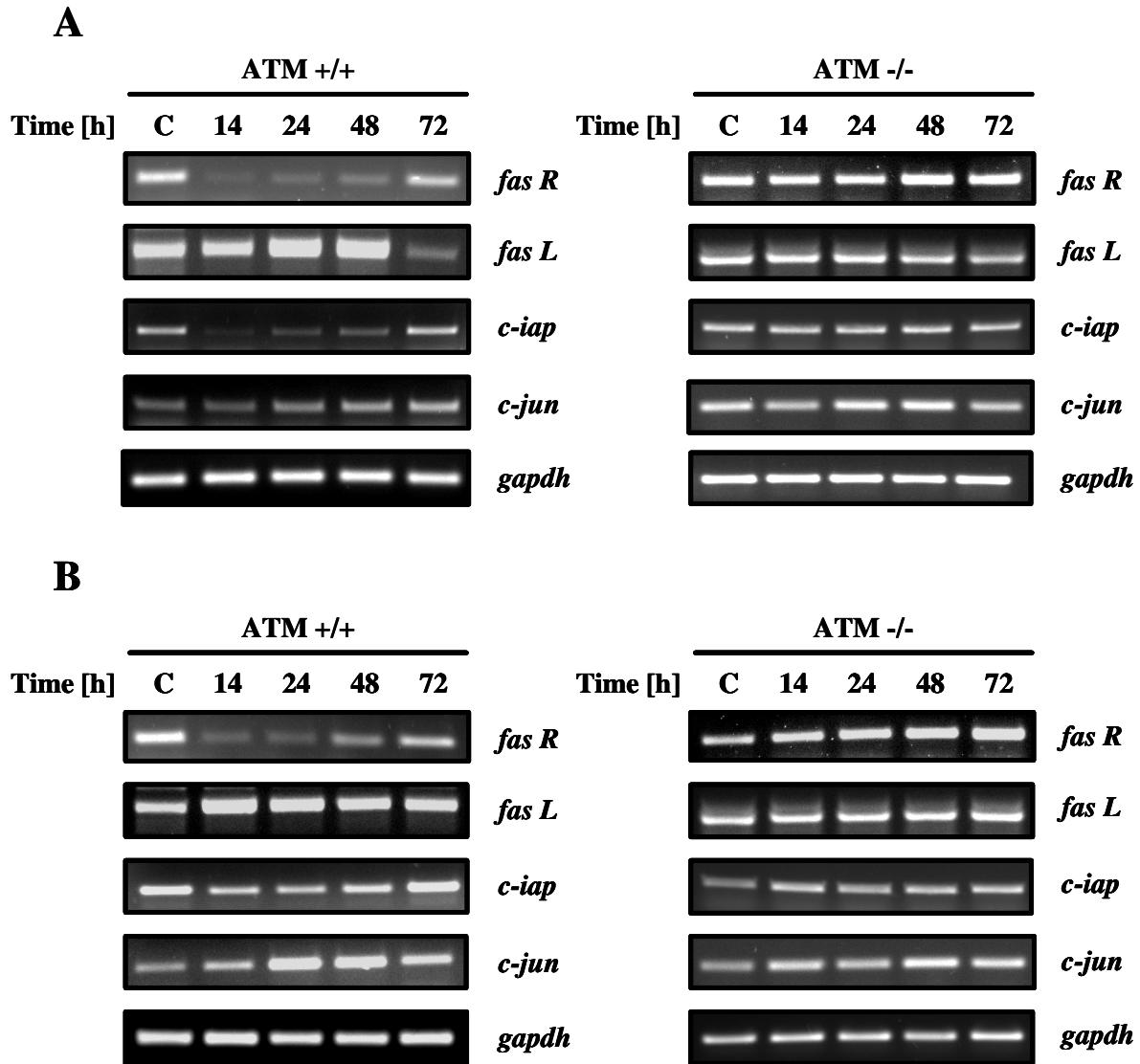


Fig. 27 RT-PCR analysis of JNK and NFκB dependent genes in ATM +/+ and ATM -/- cells upon treatment with 10 μM MNNG (A) and 1 mM MMS (B)

Cells were treated with mutagens for 60 min. 1 μg RNA was used for the RT reaction. PCR conditions: *fasR* 22 cycles x 55.2°C; *fasL* 35 x 57°C; *c-iap* 27 x 57.2°C; *c-jun* 25 x 64.2 C ; *gapdh* 21 x 56°C

3.1.10 Cell cycle checkpoint activation upon treatment with methylating agents

Cell cycle checkpoints can be activated in response to genotoxic stress. They coordinate cell cycle progression with DNA repair and apoptosis in order to minimize the probability of transmission of damaged DNA to daughter cells. Different checkpoints pathways have been identified that operate at the G1/S phase transition, during S phase and at the G2/M boundary. All of them involve the activation of ATM or ATR kinase. ATM initialises the cell cycle block upon treatment with DSB inducing agents such as ionising radiation, whereas ATR is

Results

the signal transducer of DNA lesions evoked by UV light and chemicals interfering with DNA replication. Upon activation, ATM phosphorylates p53 that contributes to p53 stabilisation and functional activation and at the end G1 arrest. ATM phosphorylation and activation of Chk1 and Chk2 kinases provokes G1/S, S and G2/M arrest independent from p53. Chk1 and Chk2 phosphorylate the phosphatases CDC25A and CDC25C targeting them for cytoplasmic degradation and preventing activation of the cdc/cyclin complex. ATM^{-/-} cells are not able to fully activate the cell cycle checkpoint upon ionising radiation.

To analyse cell cycle checkpoint activation upon alkylation, cell cycle distribution was measured by FACS analysis. Exponentially growing cells were treated with 10 μ M MNNG or 1 mM MMS. Untreated ATM^{-/-} cells were dividing slightly faster than ATM^{+/+} cells, which was indicated by a higher S phase fraction. In both cell lines exposure to MNNG did not induce major changes in the cell cycle progression (**Fig. 28**). A slight delay in S phase progression was observed between 3 and 12 h after treatment. Then the delay of DNA synthesis was abrogated and cells entered the G2 phase. An accumulation in G2 phase was observed in both cell lines at 12 to 24 h post-treatment. ATM^{+/+} cells fully recovered 36 h after treatment, while ATM^{-/-} entered apoptosis (**Fig. 28**).

MMS induced a moderate delay in S phase progression both in ATM^{+/+} and ATM^{-/-} cells. The accumulation of cells in S phase persisted until 12 h post-treatment time (**Fig. 29**). The proportion of G2 cells gradually increased starting 9 h after treatment. The maximum of the G2/M block was reached in both cell lines at 18 h post-treatment, when the G2 fraction consisted for 40 % of the population (**Fig. 29**). Following G2/M blockage ATM^{-/-} cells underwent apoptosis, as observed by arising of SubG1 fraction. In contrast ATM^{+/+} cells fully recovered and accumulated in the G1 phase (**Fig. 29**).

Results

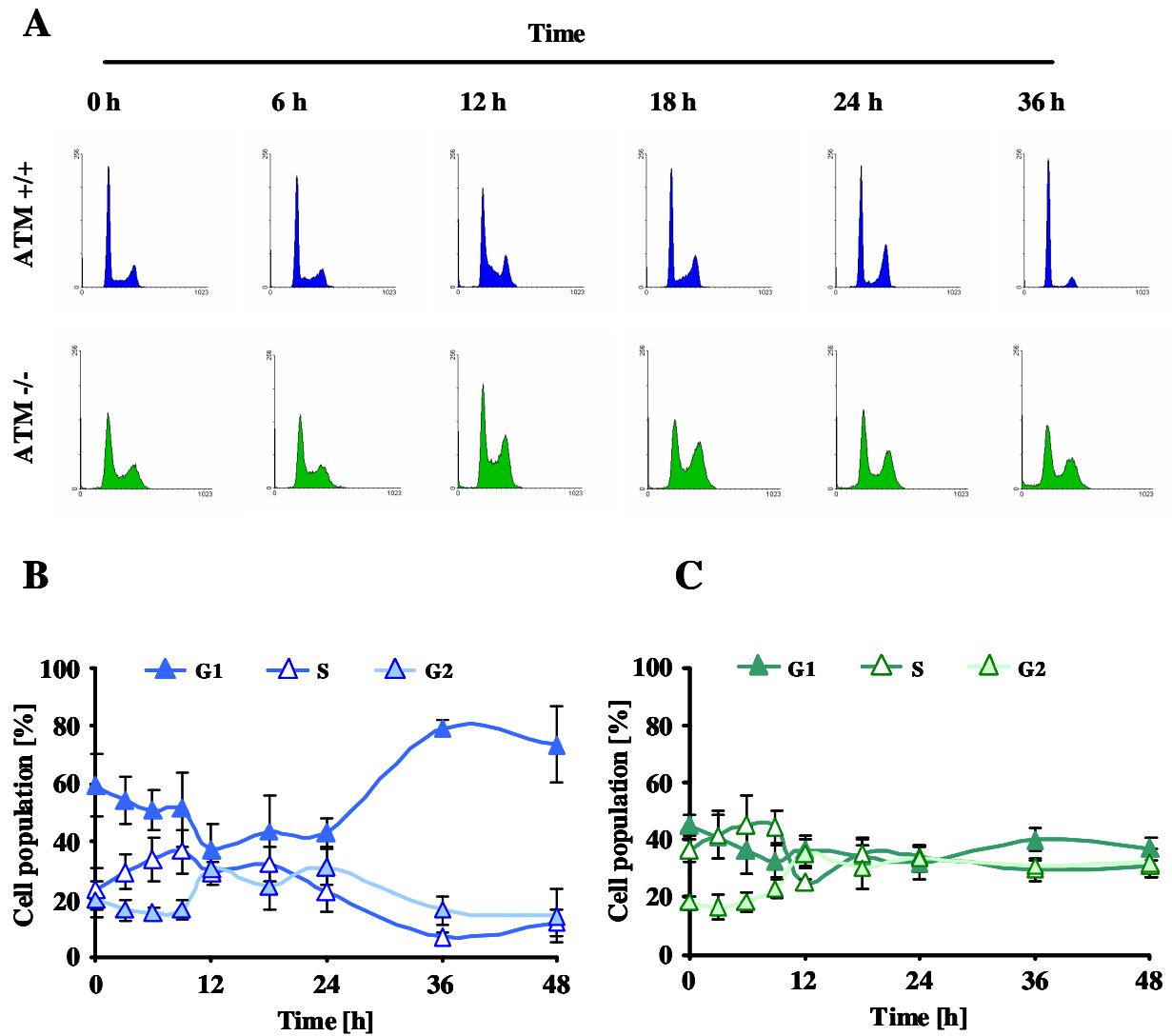


Fig. 28 Cell cycle distribution of ATM +/+ and ATM -/- cells after treatment with 10 μ M MNNG

Cells were harvested at indicated time points, fixed in 70 % ethanol and stained with propidium iodide. DNA content was analysed by FACS and quantified with ModFitLT software. Histograms illustrating cell cycle distribution in a representative experiment are shown in A. The means of three independent experiments \pm SD are shown for ATM +/+ cells in B and ATM -/- cells in C.

Results

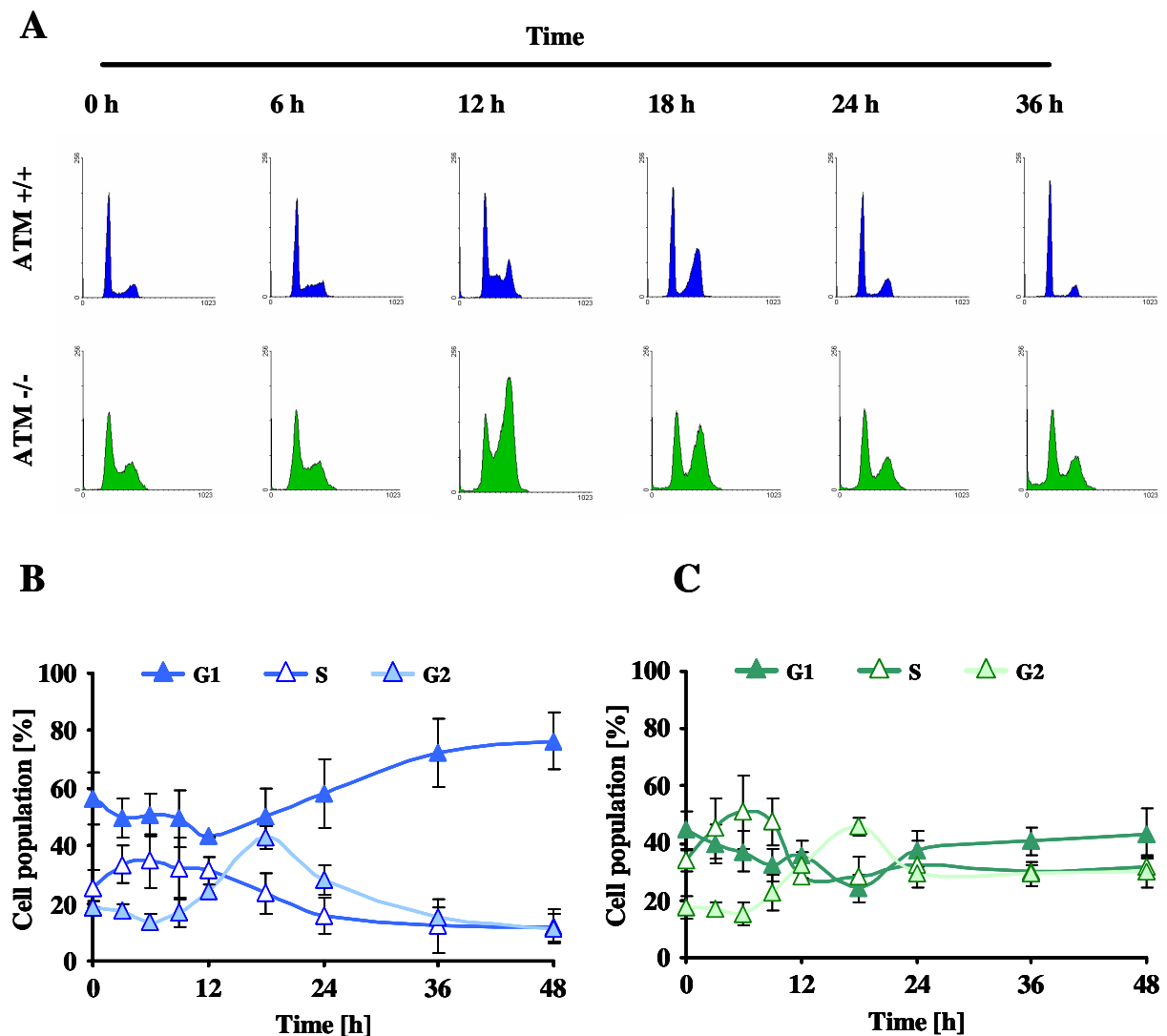


Fig. 29 Cell cycle distribution of ATM +/+ and ATM -/- cells after treatment with 1 mM MMS

Cells were harvested at indicated time points, fixed in 70 % ethanol and stained with propidium iodide. DNA content was analysed by FACS. Cell cycle distribution was quantified with ModFitLT software. Histograms illustrating cell cycle distribution in a representative experiment are shown in A. The means of three independent experiments \pm SD are shown for ATM +/+ cells in B and ATM -/- cells in C.

To consolidate the statement that G2/M checkpoint activation after methylating agent treatment is independent of ATM, an analysis of the cell cycle was carried out in dose dependent manner 24 h after treatment. The G2/M checkpoint activation was detected after MNNG treatment in the dose range of 1 – 20 μ M (**Fig. 30**). Accumulation of cells in the G2 phase was observed already by a low dose treatment of 1 μ M MNNG. The G2 fraction increased in a dose dependent manner and dominated in the population 24 h after application

Results

of 20 μM MNNG. There was no difference the G2/M checkpoint activation between ATM $+/+$ and ATM $-/-$ cells.

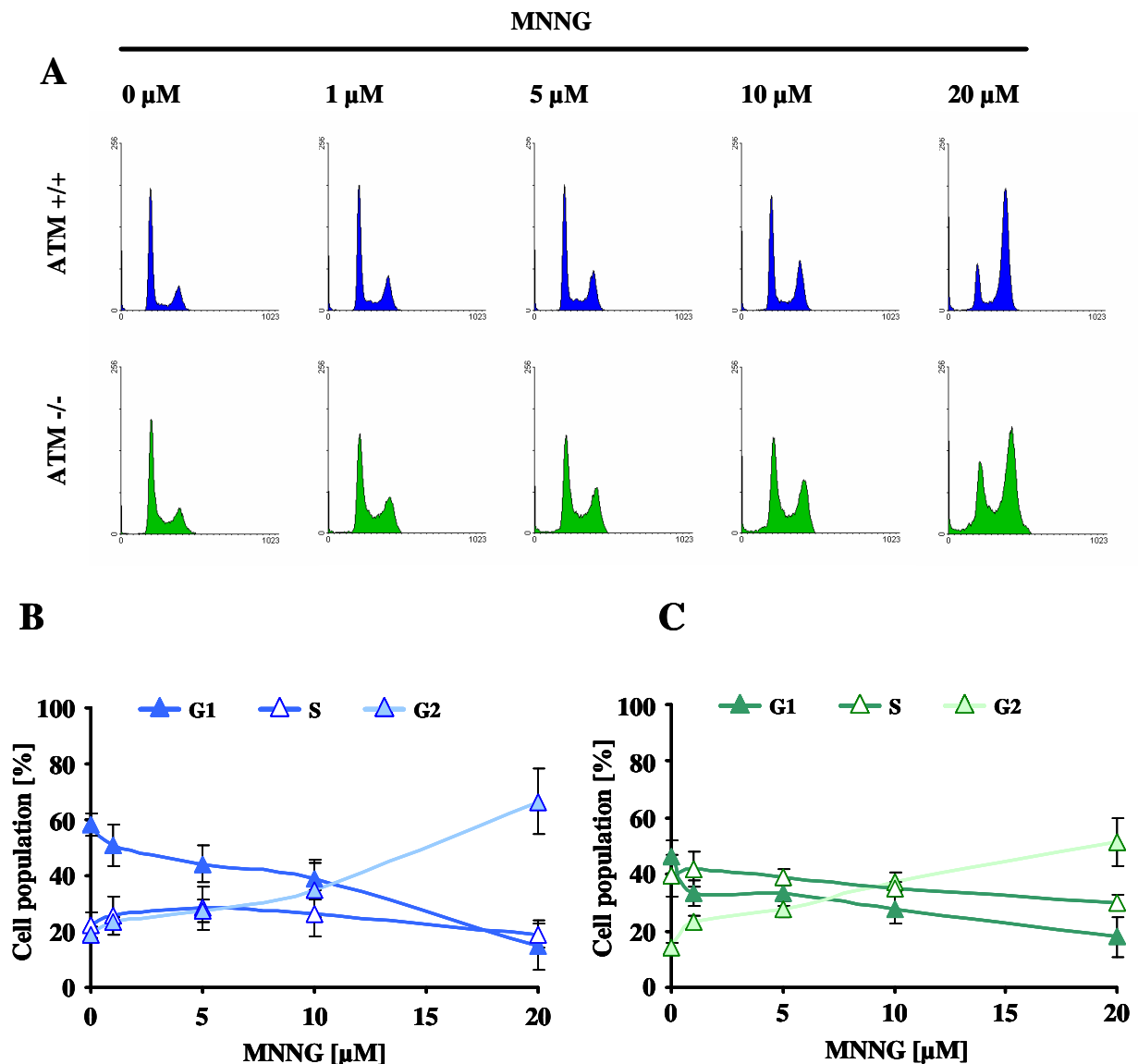


Fig. 30 Cell cycle distribution of ATM $+/+$ and ATM $-/-$ cells as a function of dose 24 h after MNNG treatment

Cells were treated for 1 h with MNNG and then left to recover for 24 h. Cells were collected by trypsinisation, washed with PBS and fixed with 70 % ethanol. DNA was stained with propidium iodide and analysed by FACS. DNA content was quantified with ModFitLT software. DNA histograms of a representative experiment are shown in A. The quantification of cell cycle distribution in three independent experiments is illustrated for ATM $+/+$ cells in B and ATM $-/-$ cells in C.

Results

Cell cycle progression upon MMS treatment was analysed 24 h after pulse treatment within the drug concentration range between 0.5 and 2 mM (**Fig. 31**). A strong G2/M block was induced by doses of MMS (> 1.0 mM) and reached its maximum with > 70 % of the cells within the G2/M phase after treatment with 2.0 mM. ATM $-/-$ fibroblasts induced the G2/M checkpoint as effective as ATM proficient cells. Therefore, hypersensitivity of ATM $-/-$ cells to MMS and MNNG is not mediated by a lack of G2/M checkpoint control. The results show that after treatment with methylating agents the G2/M cell cycle checkpoint is fully controlled by ATR.

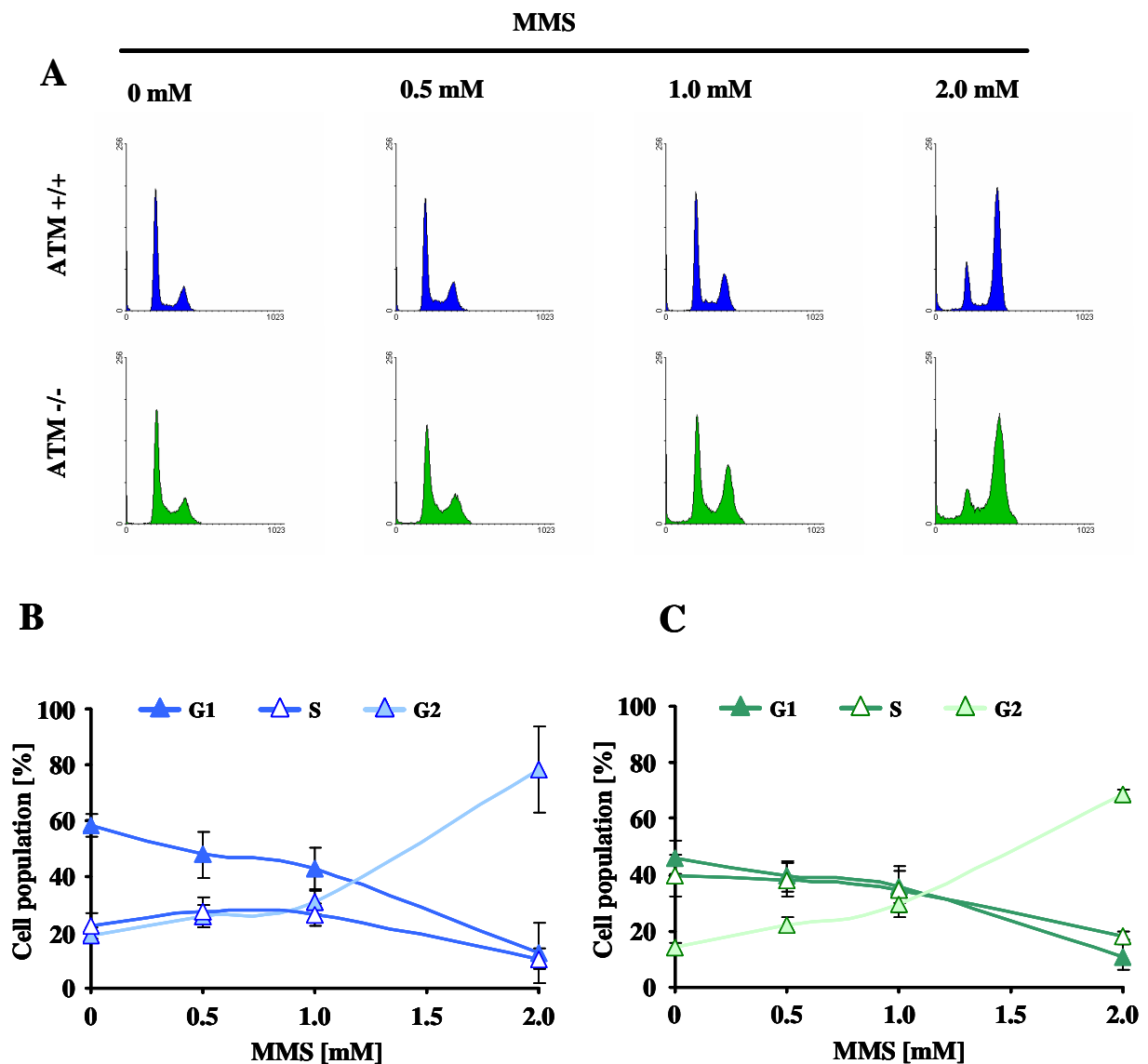


Fig. 31 Cell cycle distribution of ATM $+/+$ and ATM $-/-$ cells 24 h after treatment with different doses of MMS

Cells were processed as in the experiment 3.24. DNA histograms of a representative experiment are shown in A. Cell cycle distribution in ATM $+/+$ (B) and ATM $-/-$ cells (C) quantified in three independent experiments \pm SD.

Results

As already mentioned, checkpoint activation upon genotoxic stress involves two transducer kinases Chk-1 and Chk-2. After DSB induction ATM phosphorylates the Chk-1 kinase at multiple serine residues. In ATM $-/-$ cells Chk-1 phosphorylation is delayed and dependent on ATR. To investigate the molecular regulation of cell cycle checkpoint activation, ATM $+/+$ and ATM $-/-$ fibroblasts were treated with 5 Gy ionising radiation, 10 μ M MNNG or 1 mM MMS. Protein extracts were subjected to SDS page, immunoblotted and Ser345 phosphorylated Chk-1 was detected with specific antibodies. γ -irradiation was included as a positive control to confirm the checkpoint defect in the ATM $-/-$ strain. As shown in **Fig. 32A** the ATM $+/+$ mouse fibroblasts activated efficiently the Chk-1 kinase within 30 min after irradiation whereas as expected, ATM $-/-$ cells missed this activation. In contrast, activation of Chk-1 in ATM $-/-$ cells upon treatment with methylating agents was not disturbed (**Fig. 32B and 32C**). The phosphorylation of Chk-1 after MNNG and MMS treatment was biphasic. Early response took place immediately after mutagen treatment and thereafter the kinase was silenced. The second wave of Chk-1 phosphorylation was observed between 6 and 9 h post-treatment when cells entered S phase and preceded the accumulation of cyclin A. Synthesis of cyclin A is synthesised starts in late S phase and it is expressed until mitosis, when it becomes degraded. The accumulation of cyclin A in ATM $+/+$ and ATM $-/-$ cells occurred between 12 and 24 h after treatment with MNNG and MMS that was paralleled by accumulation of cells in G2 (as shown in Fig. 29 - 30).

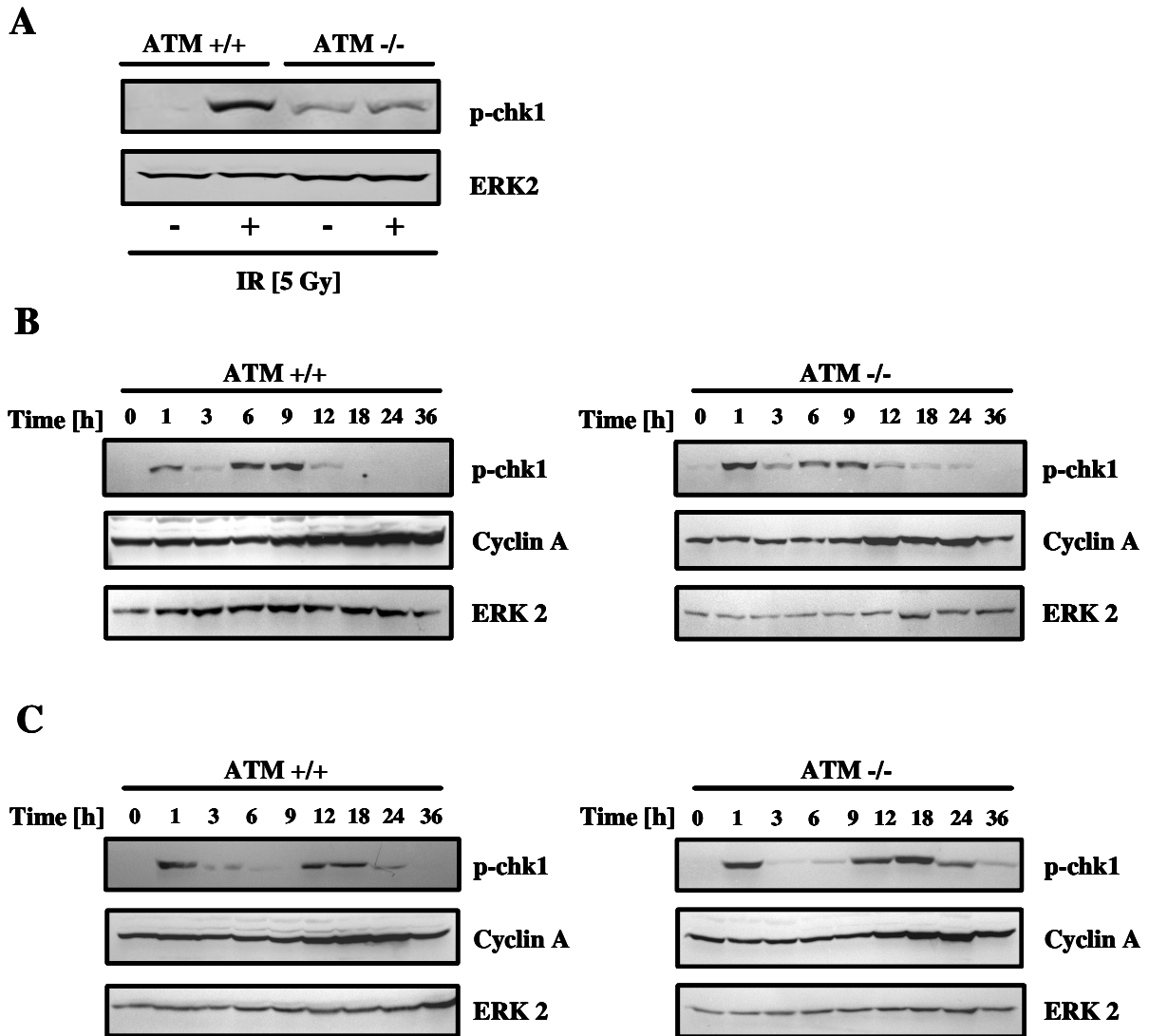


Fig. 32 Chk-1 kinase activation in ATM -/- and ATM +/+ cell upon treatment with 5 Gy ionising radiation (A), 10 μ M MNNG (B) and 1 mM MMS (C)

Cells were seeded in 5 cm cell culture plates, cultivated for 48 h and then treated. Protein extracts were prepared by lysis with hot SDS sample buffer directly on the plates. Cells were harvested 30 minutes after γ -irradiation (A) and for purpose of time kinetics after MNNG (B) and MMS (C) treatment. 10 μ l extracts were subjected to Western Blot analysis. Membranes were incubated with anti-phospho Ser345 Chk-1 and anti-Cyclin A antibodies. Detection of ERK2 is presented to assure equal loading.

3.2 Influence of cytokines on DNA repair and sensitivity of cells to alkylating agents

The first part of the study concentrated on the intracellular processing of lesions induced by methylating agents. It also was shown that O⁶MeG inducing agents such as temozolomide and provoke high frequency of apoptosis. Methylating agents induce MAPK and NFκB signaling pathways that result in differential expression of pro and anti-apoptotic genes such as *fasR*, *fasL*, *c-iap* and *c-jun* (**Fig. 27**). The same signaling cascades are involved in signal transduction from extracellular matrix after activation of membrane receptors by cytokines. Cytokines regulate the cell survival after genotoxic stress by modulation of the MAPK or NFκB pathway (Heron-Milhavet et al., 2001; Kothny-Wilkes et al., 1998). Scattered reports indicate that cytokines may influence DNA repair and apoptosis in an ATM dependent manner. The ATM function is influenced by cytokines such as IGF-I and IL-1. The IGF-I pathway is involved in radiosensitivity of ATM cells. The IGF-IR is under transcriptional control of ATM, and in a feedback loop IGF-I stimulates ATM kinase activity (Macaulay et al., 2001; Peretz et al., 2001; Shahrabani-Gargir et al., 2004). Finally the IL-1 induced *c-jun* transcription is impaired in ATM ^{-/-} cells (Sikpi et al., 1999). To analyse the influence of IGF-I and IL-1 on sensitivity of ATM ^{-/-} cells to methylating agents, WST-1 metabolic assay was performed. In addition, the DNA repair gene expression pattern after cytokine treatment was investigated by DNA microarray analysis.

3.2.1 Modulation of cell survival by IGF-I and IL-1 after MMS treatment in ATM ^{-/-} and ATM ^{+/+} background

All experiments involving cytokines were performed under low serum conditions in order to prevent receptor activation by growth factors within FCS. The cells were plated and cultivated for 24 h in DMEM supplemented with 10 % serum. Afterwards they were washed twice with PBS and supplied with medium containing 0.2 % FCS. Cells were treated with cytokines after 24 h serum deprivation in order to achieve complete silencing of the cellular receptors. Cells were maintained under low serum conditions till the end of the experiment. The indispensable serum deprivation limited the investigation on cytokine effect on methylating agents processing to N-alkylations. Mouse fibroblasts reacted on serum deprivation with a very fast proliferation block. The starving condition did not increase cell death, however cell division was drastic reduced. Previous data showed that cell proliferation is necessary for O⁶MeG induced cell death. The treatment of ATM ^{-/-} and ATM ^{+/+} cells with 20 μM MNNG in 0.2 % FCS medium resulted in 100 % survival of both cell lines as measured by WST-1 assay 96 h after treatment (data not shown).

Results

An equal expression of IGF-I and IL-1 receptors in ATM $+/+$ and ATM $-/-$ cells was proven by analysis of the activation of down stream signaling cascades. Cells were treated with recombinant IGF-I (50 ng/ml) or IL-1 α (10 ng/ml), harvested 30 minutes later and subjected to western blot analysis. Activation of the IGF-IR was detected with antibodies against the phosphorylated form of Akt. IL-1R activation was shown by analysing the phosphorylation of p38 MAP kinase. Both cell lines responded to IGF-I and IL-1 treatment (**Fig. 33**).

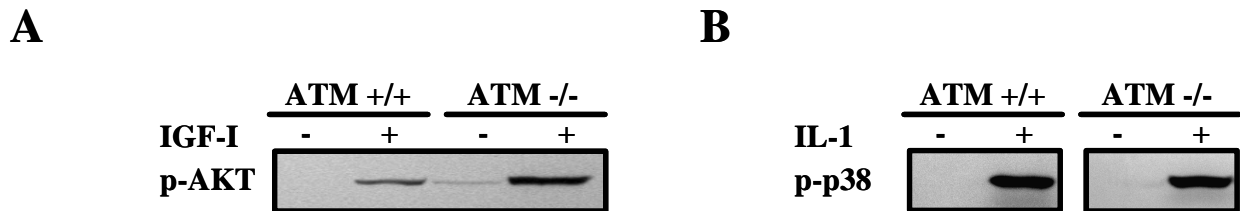


Fig. 33 ATM $+/+$ and ATM $-/-$ cells possess functional IGF-I and IL-1 receptors

- A) Cells were cultivated for 24 h at standard conditions, then the medium was changed for medium with 0.2 % serum and cells were incubated for the next 24 h. Cells were treated with 50 ng/ml IGF-I and harvested 30 min later. Protein extracts were separated on 10 % SDS PAGE and blotted on the nitrocellulose membrane. Membrane was incubated with anti p –Akt antibodies.
- B) Cells were cultivated for 24 h at standard conditions, then the medium was exchanged by medium with 0.2 % serum and cells were incubated for the next 24 h. Cells were treated with 10 ng/ml IL-1 α and harvested 30 min later. Protein extracts were separated on 10 % SDS PAGE and blotted on the nitrocellulose membrane. Membrane was incubated with anti p – p38 MAPK antibodies.

To analyse the influence of cytokines on MMS-induced cytotoxicity, WST-1 assays were performed 24 h after MMS exposure (**Fig 34**). Cells were pre-treated with 50 ng/ml IGF-I or 10 ng/ml IL-1 for 24 h, then the medium was replaced by fresh medium containing mutagen in presence or absence of cytokine. Despite equal activation of receptors, a difference in sensitivity between ATM $-/-$ and ATM $+/+$ cells treated with MMS and cytokines was observed. ATM $-/-$ cells were not influenced by IGF-I and IL-1 stimulation. The ATM $+/+$ survival was increased by pre-treatment with IGF-I, especially after high dose MMS treatment. Treatment with 0.8 mM MMS reduced the survival of ATM $+/+$ cells to 30 % but only to 80 % upon IGF-I stimulation. In opposite, IL-1 reduced only slightly the survival of ATM $+/+$ cells; the difference was statistically not relevant.

Results

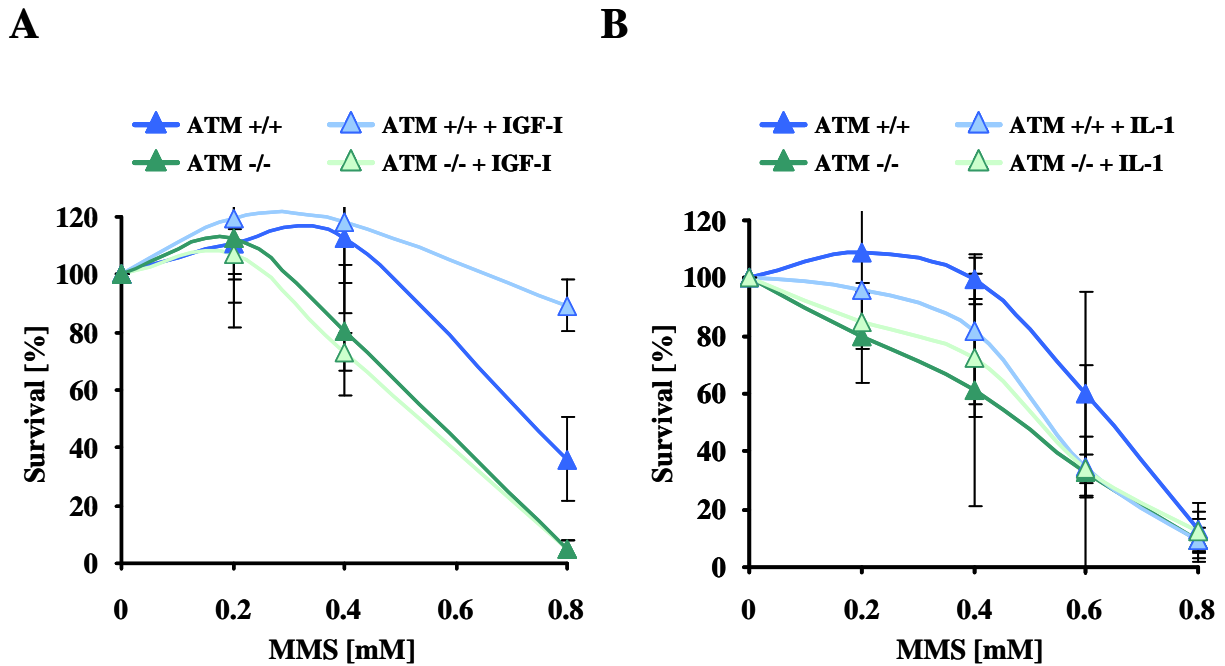


Fig. 34 Survival of ATM +/+ and ATM -/- cells treated for 24 h with different concentrations of MMS in presence or absence of IGF-I (A) or IL-1 (B)

2000 cells were seeded in 96 well micro-titer plates and cultivated for 24 h. Cells were washed twice with PBS and supplemented with fresh medium containing 0.2 % FCS. 24 h later cells were treated with 50 ng/ml IGF-I (A) or 10 ng/ml IL-1 α (B) and incubated for the next 24 h. The medium was discarded and cells were supplied with low serum medium containing mutagen +/- cytokine. WST-1 assay was performed 24 h later.

The increased survival of ATM +/+ cells stimulated with IGF-I was due to a reduced frequency of cell death (**Fig. 35**). The FACS analysis was performed after 24 h MMS exposure. The stimulation with IGF-I was undertaken 24 h before and simultaneously to the treatment. A protective effect was observed in ATM +/+ cells but not in ATM -/- cells. Cells treated with 0.6 mM MMS died by necrosis, apoptosis was not detected. The absence of apoptosis might result from a low ATP content in the cells maintained under low serum conditions, or the apoptotic process was already completed by the time of acquisition.

Results

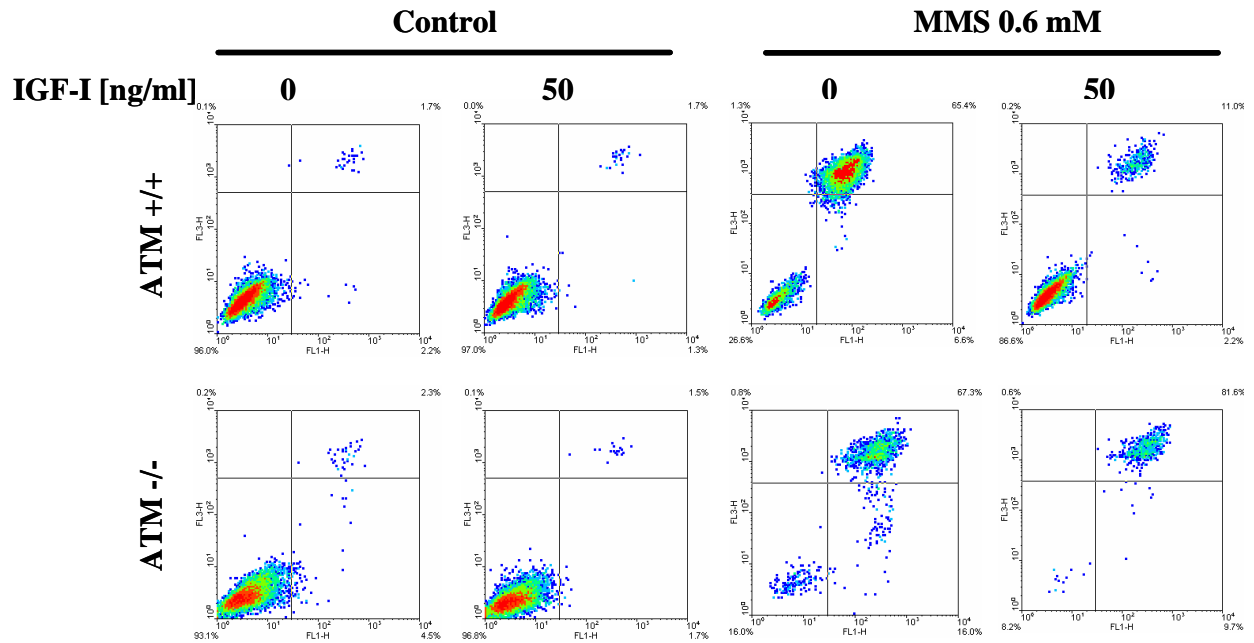


Fig. 35 Apoptosis and necrosis analysed in ATM +/+ and ATM -/- cells treated with 0.6 mM MMS for 24 h with and without IGF-I stimulation

Cells were plated in 3.5 cm cell culture dishes and cultivated for 24 h, thereafter the medium was replaced by fresh medium containing 0.2 % FCS and the cells were incubated for the next 24 h. MMS treatment was carried out 24 h after IGF-I stimulation [50 ng/ml]. Cells were harvested and stained with Annexin V-FITC (X axis) and PI (Y axis) and subjected to FACS analysis. The viable population turns up in lower left quadrant at each plot. The necrotic and apoptotic cells are in the upper right and lower right quadrants respectively. Representative experiment of three is shown.

3.2.2 Influence of IGF-I and IL-1 on DNA repair gene expression

IGF-I and IL-1 signaling involves several transcription factors such as AP-1 or NfκB. The binding sites of these factors are present in different genes involved in DNA repair or apoptosis. The transcription regulation of DNA repair might be responsible for lower sensitivity of the wild type cells to MMS, observed after IGF-I stimulation. IL-1 had no effect on cytotoxicity induced by MMS, however the modulation of other DNA repair pathways can not be excluded. To investigate if IGF-I and IL-1 influence the DNA repair capacity, a microarray approach was undertaken. Self-designed microarrays containing 50 Bp oligonucleotides representing 150 genes involved in DNA repair, replication or transcription was used. Each oligonucleotide was spotted in duplicates. The array contained three housekeeping genes: *GAPDH*, *β-ACTIN* and *α-TUBULIN* that allowed normalisation. The analysis was carried out with the human epithelial tumour cell line KB, which was ATM +/+ p53 -/-. The cells were already used in published studies analysing the effect of IL-12 and IL-1 on sensitivity to UV irradiation (Kothny-Wilkes et al., 1998). The IGF-I responsiveness

Results

of KB cells was confirmed by western blot analysis with anti p-Akt antibodies. Therefore cells were seeded and cultured for 24 h. After this time the medium was replaced by the fresh medium containing 0.2 % FCS. Serum starvation was performed for 24 h, than the cells were stimulated with cytokines. The Akt activation was analysed 30 min after treatment (**Fig. 36A**). IGF-I stimulation led to increased Akt phosphorylation on Ser473, indicating the existence of a functional IGF-I pathway in KB cells. For the microarray analysis RNA was isolated 2 h after treatment with 50 ng/ml IGF-I. The integrity of RNA was proven by gel electrophoresis before every microarray analysis (**Fig. 36B**). The RNA (5 µg) was direct labelled by a reverse transcription reaction with Cy3-dUTP or Cy5-dUTP. The experiment involved dye switch between control and cytokine treatment. The signal of approximately 120 out of 150 genes is presented in **Fig. 36C**. 30 genes were excluded because of low signal intensity. Two genes were up-regulated of factor higher than 2: *NFκB* and *P21*. None of the genes was down-regulated (factor < 0.5).

Results

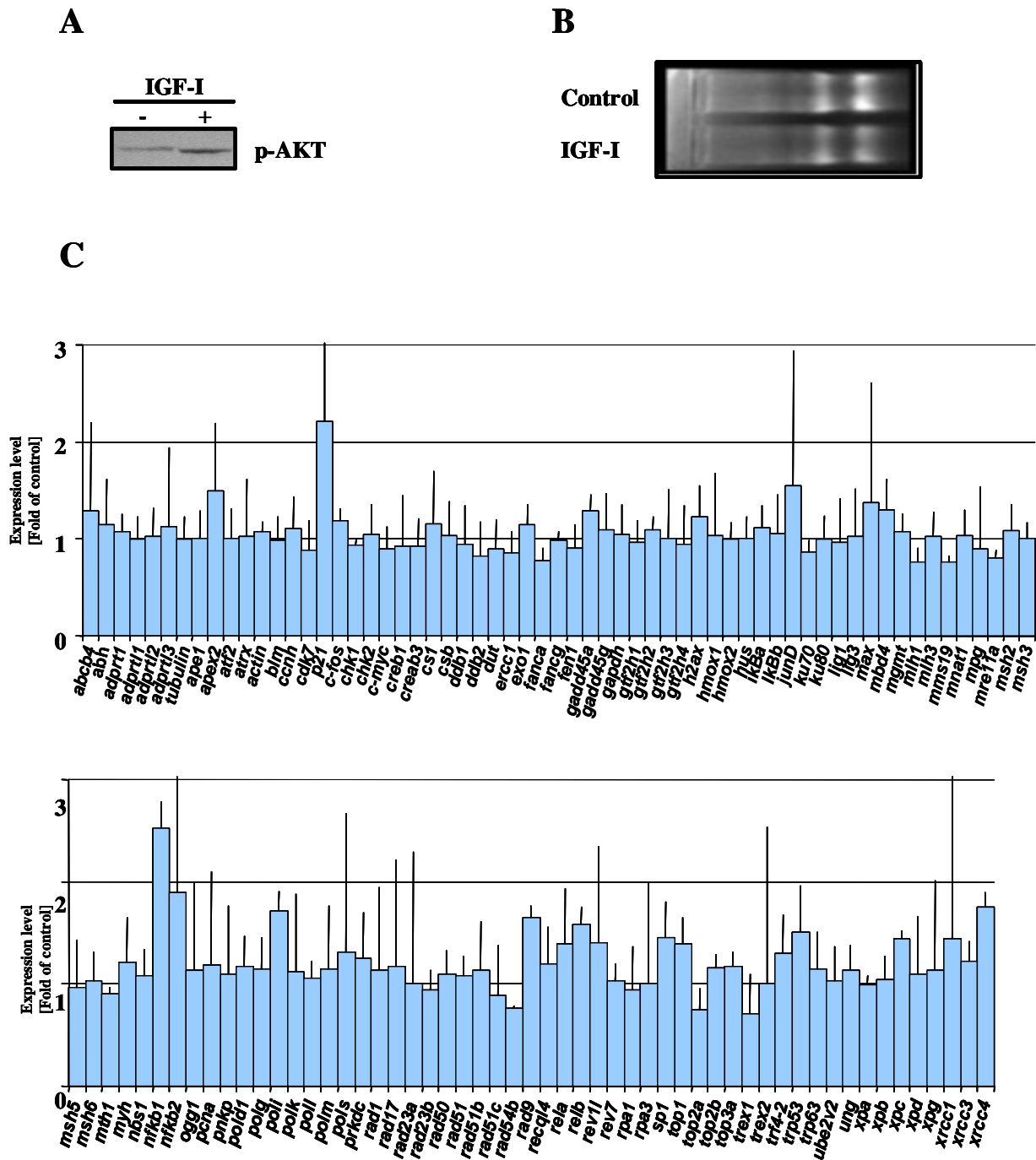


Fig. 36 DNA repair gene expression upon stimulation of KB cells with 50 ng/ml IGF-I

- A) Western Blot analysis of AKT activation in KB cells 30 min after IGF-I treatment.
- B) RNA gel electrophoresis of 5 µg control and IGF-I treated sample.
- C) Microarray analysis of KB cells 2 h after treatment with 50 ng/ml IGF-I.

Results

In order to assure that the experimental conditions were optimal for analysis of IL-1 targets, additional experiments involving the regulation of the known IL-1 target gene *IL-6* were performed. The regulation was analysed on RNA and protein level (**Fig. 37**). KB cells were cultivated under serum starved conditions as described previously and treated with 10 ng/ml IL-1 β . RNA was isolated 1, 3 and 6 h after stimulation and subjected to semi-quantitative RT-PCR. In parallel, the cell culture medium from stimulated cells was collected and the IL-6 production was determined by ELISA immunoassay. *IL-6* gene induction was observed 1 h after treatment, thereafter the RNA level declined to the control level (**Fig. 37 insert**). Induction of IL-6 on the protein level postponed mRNA accumulation, and a 5 fold increase was measured 3 h after IL-1 stimulation.

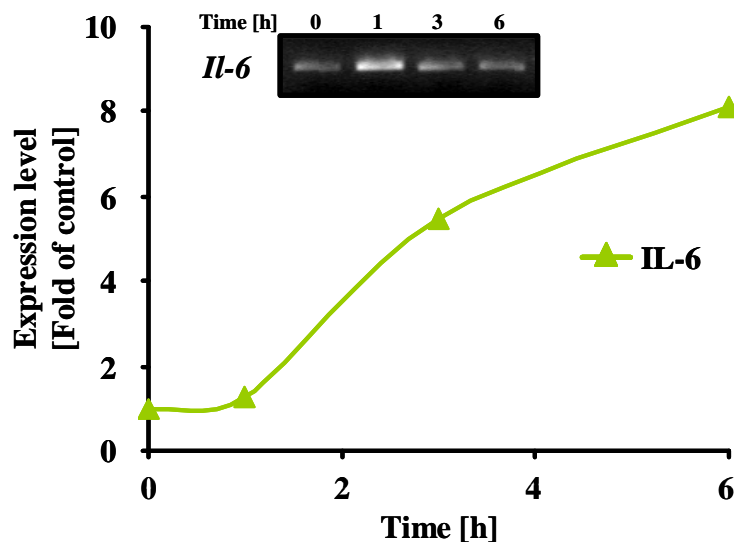


Fig. 37 Regulation of IL-6 on RNA (insert) and protein level (graph) in KB cells treated with 10 ng/ml IL-1

IL-6 immunoassay was carried out with cell culture supernatants of cells treated with IL-1 in serum free conditions. RNA was isolated as described in material section. PCR was performed with 2 μ l template, annealing temperature 56 $^{\circ}$ C, 25 cycles. Expression level is defined as IL-6 level upon treatment with IL-1 compared to the untreated cells.

The microarray analysis was performed in KB cells 2 h after IL-1 stimulation a time point suggested by IL-6 expression experiments (**Fig. 38**). Similar to IGF-I, IL-1 had little effect on the expression of DNA repair genes. *NF κ B*, *I κ B* and *p21* were up-regulated by a factor of 2. A few genes that were characterised by high spot quality and were reproducibly up-regulated by a factor of 1.5 were chosen for further analysis by means of PCR.

Results

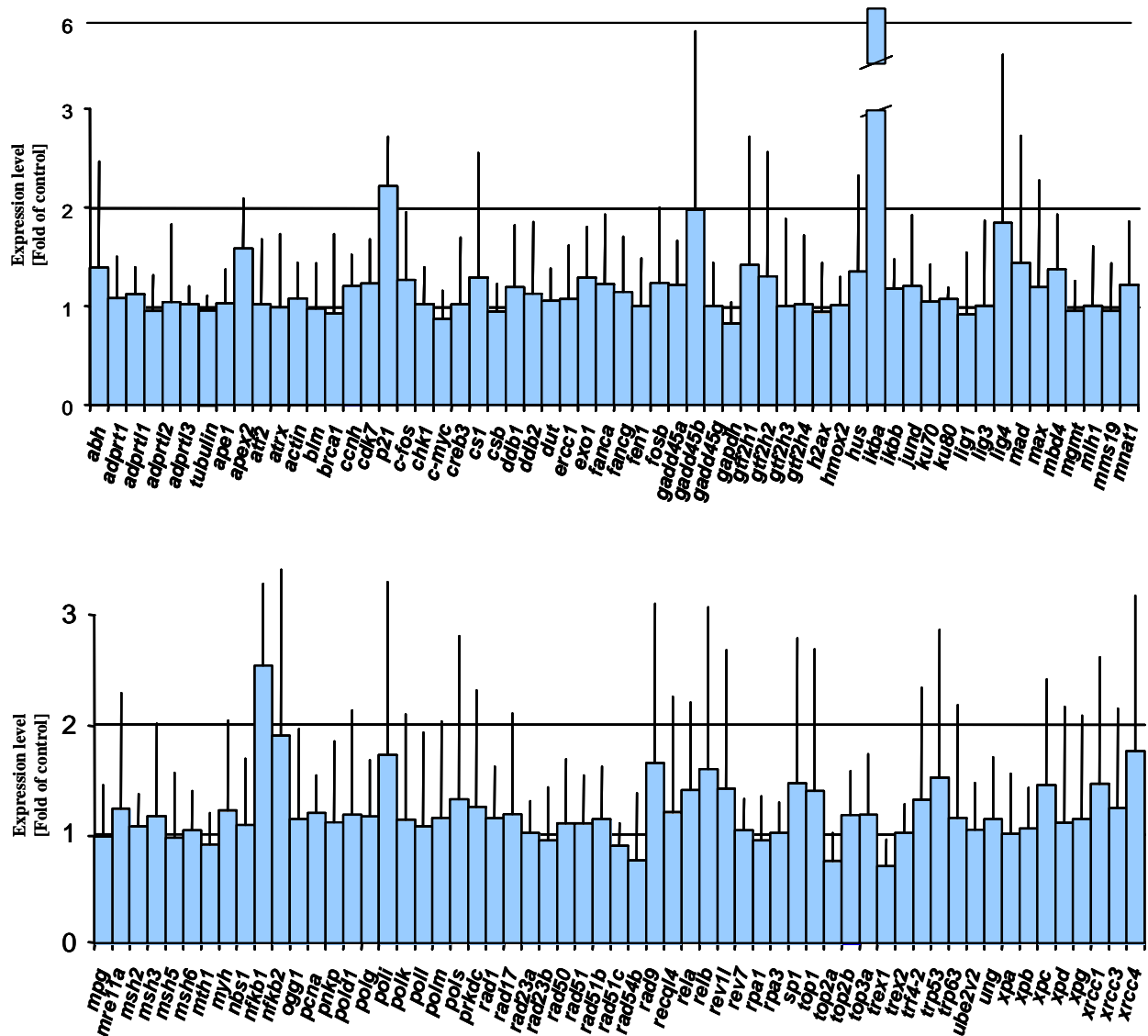


Fig. 38 Microarray analysis of DNA repair gene expression in KB cells 2 h after stimulation with 10 ng/ml IL-1

3.3 IL- 1 regulates APEX2 gene in human keratinocytes

PCR analysis of genes that were chosen based on the microarray analysis confirmed the IL-1 induction of 4 genes (**Fig. 39A**). Among these 4 genes, three well known IL-1 up-regulated genes were found: *NFκB*, *IκB* and *p21*. A new gene, not yet known to be inducible, found to be up-regulated by IL-1 was the *apurinic endonuclease 2 (APEX2)*. Upon IL-1 treatment the mRNA level of *APEX2* increased in all experiments and the induction factor was between 1.5 and 2.2. The induction factors correlated well with the expression pattern obtained by microarray analysis (**Fig. 39B**). The microarray was characterised by higher fidelity but on cost of lower reproducibility.

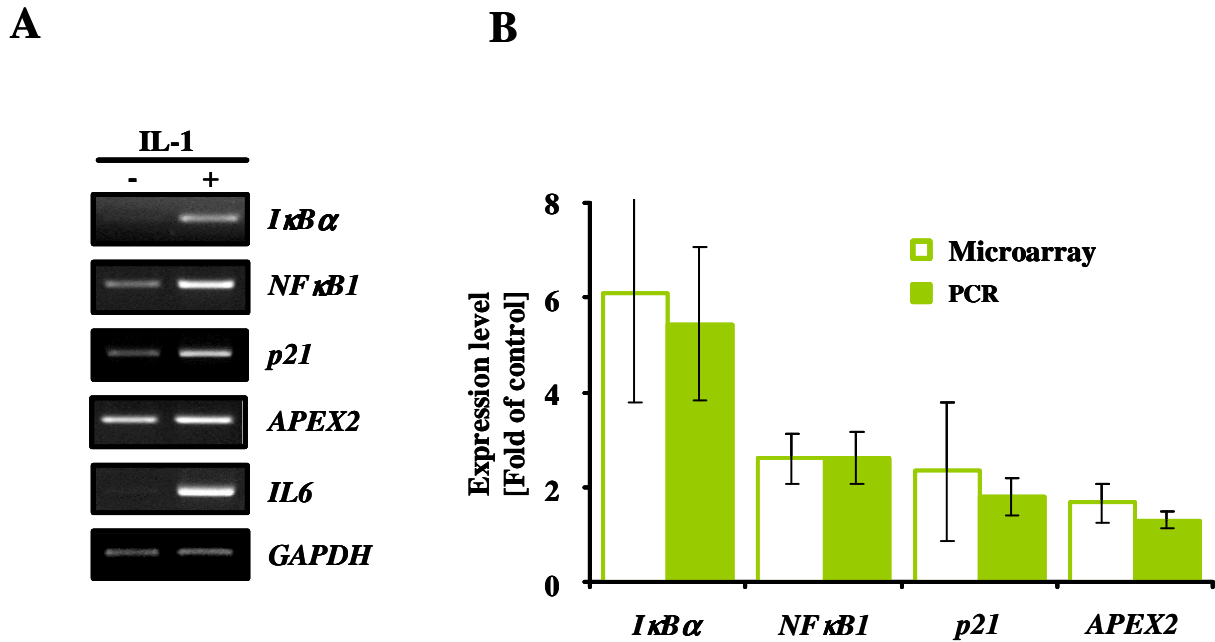


Fig. 39 Induction of *NFκB*, *IκB*, *p21* and *APEX2* in KB cells after IL-1 stimulation was confirmed by semi-quantitative RT-PCR

- A) Following 24 h serum deprivation, KB cells were stimulated with 10 ng/ml IL-1β. RNA was isolated 2 h later. 2 μl of cDNA template was subjected to PCR reaction. *GAPDH* primers were used as loading control. *IL-6* was shown to illustrate the efficiency of IL-1 stimulation.
- B) Comparison of induction factors obtained by means of microarray analysis with RT-PCR. Expression level is defined as *IL-6* level upon treatment with IL-1 compared to the untreated cells. The means of three independent experiments ± SD.

The time course of *APEX2* induction was analysed by real time RT-PCR (**Fig. 40**). KB cells were stimulated with 10 ng/ml IL-1. Cells were harvested at indicated time points up to 24 h after treatment and RNA was processed as previously described. The *APEX2* expression was normalised with the amount of PCR products amplified by *GAPDH* primers. *APEX2* was clearly induced at RNA level 2 h after treatment with IL-1. The maximal RNA accumulation was observed 4 h after treatment and the amount of transcripts gradually decreased to reach the control level 24 h after treatment. The *APEX2* up-regulation was followed by an increase in the protein amount in whole cell extracts (**Fig. 40B**). The protein accumulation was observed starting 8 h after IL-1 addition, reaching its maximum 16 h after IL-1 expression. *APEX2* up-regulation was observed in transformed KB cell line and in spontaneously immortalised keratinocytes, the HaCaT cell line (**Fig. 40B lower panel**).

Results

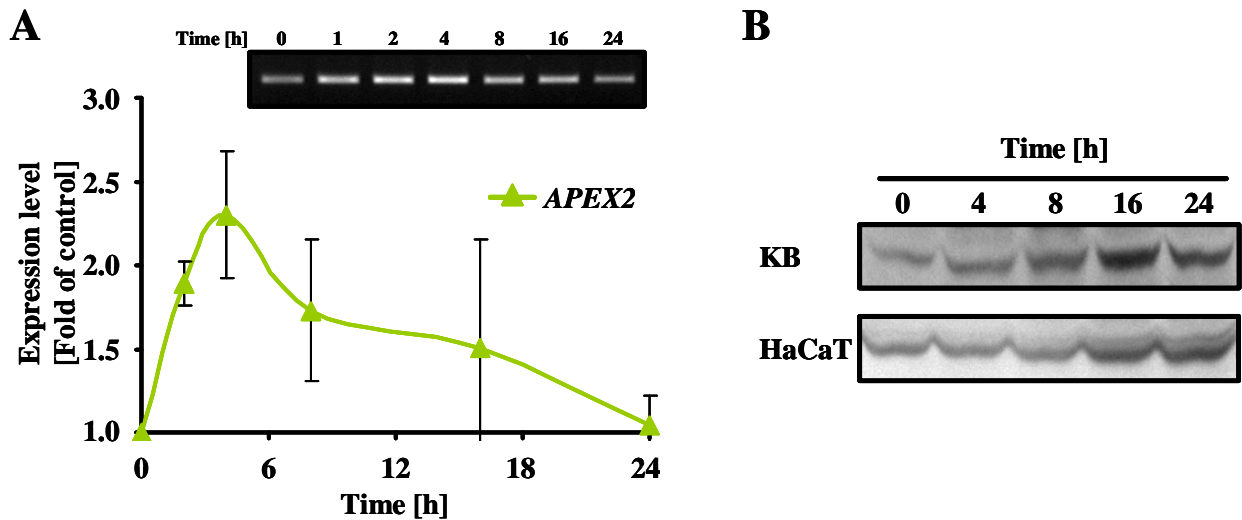


Fig. 40 APEX2 expression on RNA and protein level after stimulation of cells with 10 ng/ml IL-1

- A) APEX2 expression measured by RT – PCR in KB cells. RNA was isolated from stimulated KB cells at indicated time points and processed by real time RT-PCR. The PCR products of representative experiment were loaded on 1 % agarose gel and visualised with ethidium bromide.
- B) APEX2 expression measured by western blot analysis in KB and HaCaT cells at different time points after cytokine treatment. 20 μ g whole cell extracts isolated from KB or HaCaT cells were separated on 10 % SDS PAGE and transferred to nitrocellulose membrane. The membrane was incubated with rabbit polyclonal antibodies against APEX2.

To analyse whether the increased APEX2 mRNA level is achieved by increased transcription or increased mRNA stability, cells were pre-treated with actinomycin D, a RNA polymerase inhibitor. Cells were incubated for 1 h with 2 μ g/ml actinomycin D and then 10 ng/ml IL-1 was added to the medium. Cells were harvested 4 h after cytokine treatment, which was determined in previous experiment to be the time of the highest APEX2 expression. Upon actinomycin D pre-treatment, IL-1 had no effect on APEX2 expression (**Fig. 41**). In addition, inhibition of RNA polymerase blocked the induction of the IL-1 dependent gene *IL-6*. The *GAPDH* level remained not changed in control and IL-1 stimulated cells. This indicates that APEX2 accumulation was the result of *de novo* mRNA synthesis, induced by binding of transcription factors to the promoter. The experiment excludes post-transcriptional regulation as a mechanism of IL-1 dependent induction of APEX2 mRNA.

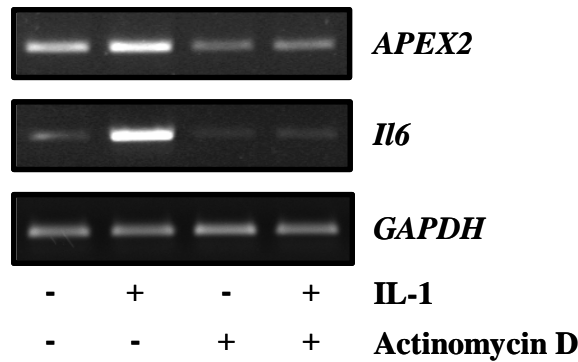


Fig. 41 Influence of actinomycin D on *APEX2* expression in IL-1 stimulated KB cells

Following serum starvation KB cells were treated with 2 µg/ml actinomycin D and incubated for 1 h. IL-1 was added to the medium and the cells were further incubated for 4 h in the presence of actinomycin D. PCR reaction involved 23 cycles with annealing temperature 52°C for *APEX2* primers, 25 x 56°C for *IL-6* and 21 x 56°C *GAPDH*.

3.3.1 *IL-1* gene up-regulation was specific for *APEX2* and did not occur for other BER genes

Apex2 is the second discovered apurinic endonuclease. It is localised in nuclei and mitochondria of mammalian cells. The sequence homology to apurinic endonuclease 1 (ape1) suggests that it participates in base excision repair (BER). In the microarray experiment, IL-1 did not induce any other genes participating in this process. However, it might be the case that the induction of these genes appears at later time points. The array screening was carried out only 2 h after IL-1 stimulation. To investigate BER gene expression in more detail, real time RT-PCR analysis was performed (**Fig. 42**). RNA was isolated from the IL-1 stimulated KB cells at time points between 1 and 24 h. The analysis included genes of long and short patch BER such as *APE1*, *PCNA*, *POLβ*, *FEN1*, *XRCC1* and *LIGIII*. None of those genes was induced by a factor of 2 or higher. The expression of a few of them was elevated ~ 1.5 fold. *PCNA*, *POLβ* and *FEN1* were stimulated by IL-1 and the highest mRNA level was observed 2 - 4 h after treatment. The *APE1* induction was reached its maximum 8 h after cytokine stimulation. *XRCC1* and *LIGIII* were not induced.

Results

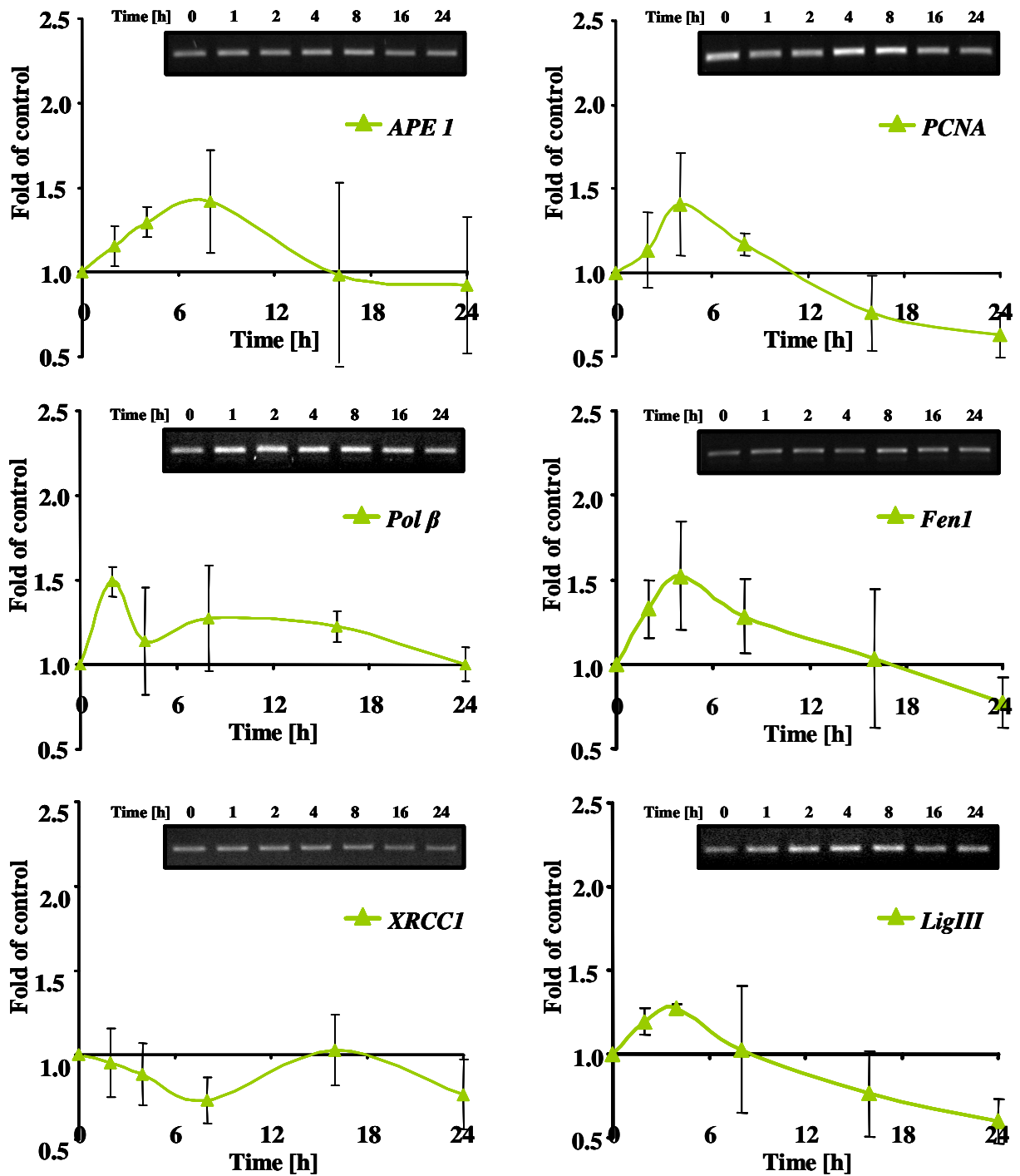


Fig. 42 BER gene expression in KB cells stimulated with 10 ng/ml IL-1

RNA was isolated from stimulated KB cells at indicated time points and processed by two step real time RT-PCR. The PCR products of representative experiment were loaded on 1 % agarose gel and visualised with ethidium bromide.

The expression levels of BER components was analysed additionally on protein level by western blot analysis of whole and nuclear extracts (**Fig. 43**). Proteins were isolated from KB

Results

cells after stimulation with 10 ng/ml IL-1. The increase in mRNA observed for *APE1*, *PCNA* and *FEN1* did not translate on protein expression. The only protein where expression was enhanced by IL-1 was Pol β . Pol β accumulation followed directly the transcription activation and the elevation in the protein level was observed already 4 h after IL-1 treatment. The protein accumulation took place predominantly in the nuclear compartment (**Fig. 43B**).

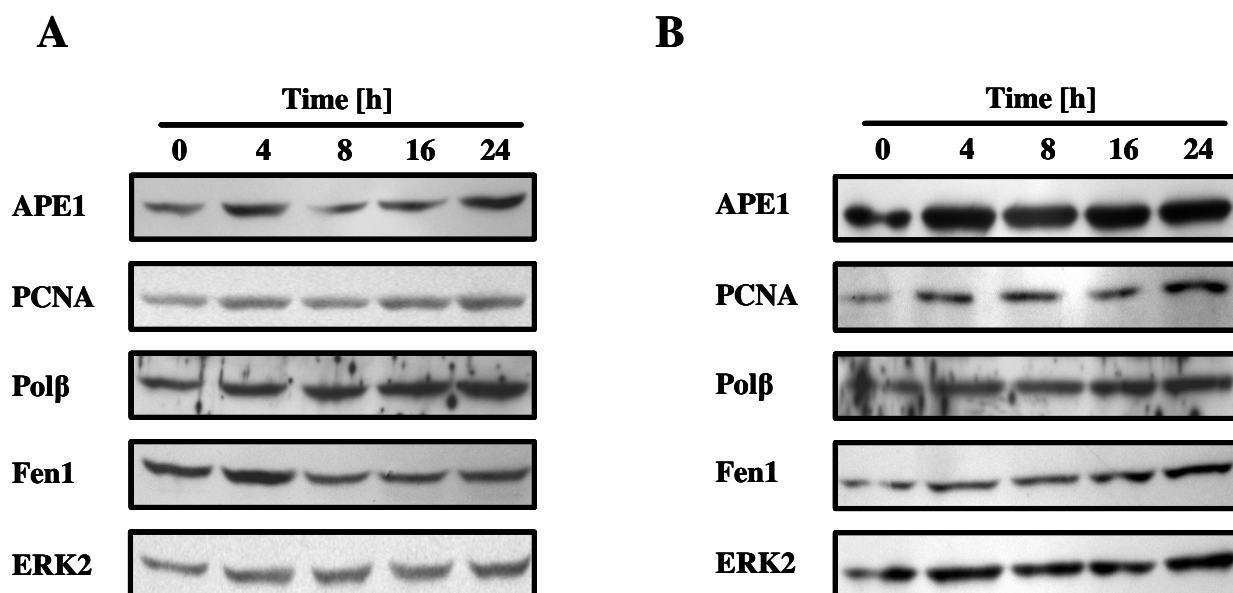


Fig. 43 Western blot analysis of BER proteins in whole (A) and nuclear (B) extracts of KB cells stimulated with 10 ng/ml IL-1

3.3.2 IL-1 increases survival of KB cells exposed to oxidative stress

It was shown above that IL-1 stimulation leads to an accumulation of APEX2 and Pol β . The function of APEX2 is not precisely clear although a participation in post-translational BER has been proposed. To answer the question of how up-regulation of APEX2 influences the cellular sensitivity to these agents, apoptosis in KB cells pre-treated with IL-1 was analysed by FACS (**Fig. 44**). Cells were incubated in medium containing 0.2 % serum for 24 h. Afterwards the cells were stimulated with 10 ng/ml IL-1 and cultivated for the next 24 h, than treated with DNA damaging agents. After treatment cells were cultivated for 48 h in medium with reduced serum content (0.2%). The cells were stained with AnnexinV-FITC and PI. The toxic treatment involved agents inducing DNA damage repaired by BER: ionising radiation, H₂O₂, and the methylating agents MMS and MNNG. A weak protective effect of IL-1 was observed after all treatments applied. The highest decrease in apoptotic frequency was detected in cells treated with H₂O₂.

Results

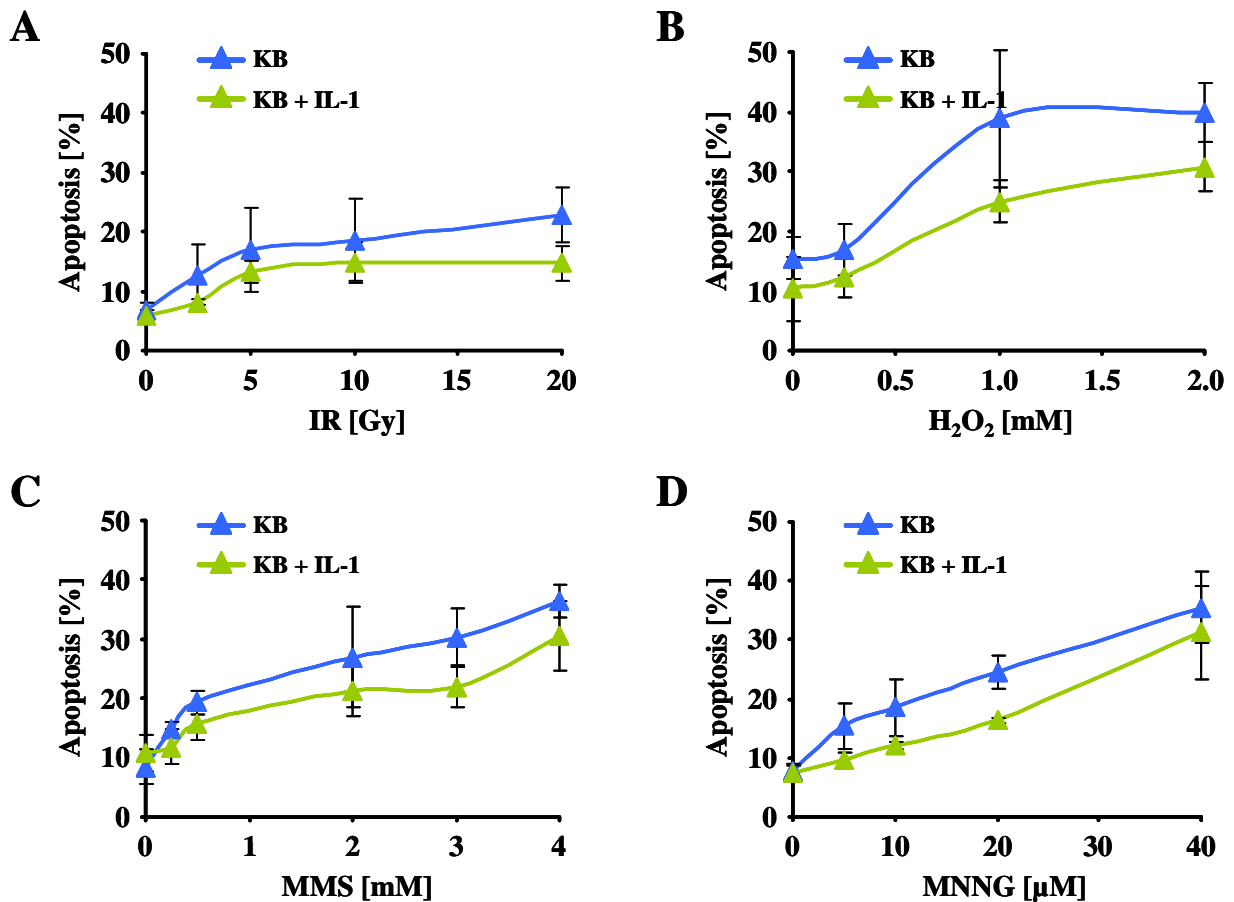


Fig. 44 Frequency of apoptosis in KB cells treated with different genotoxic agents with and without IL-1 stimulation

Cells were pre-treated for 24 h with 10 ng/ml IL-1 and then treated with different doses of ionising radiation (A), H₂O₂ (B), MMS (C) and MNNG (D). The FACS analysis of AnnexinV-FITC/PI stained samples was performed after 48 h cultivation. The data are means of three independent experiments \pm SD.

It is known that IL-1 regulates cell cycle checkpoints through p21 activation (Nalca and Rangnekar, 1998; Osawa et al., 2000). The *P21* induction was also observed in KB cells treated with IL-1 and subjected to microarray and PCR analysis. The p21 accumulation leads to cell cycle arrest in G1 cell cycle phase. Not proliferating cells are less susceptible to apoptosis. To exclude that the decreased cell death of KB cells was provoked by differences in proliferation rate, cell cycle distribution was analysed before and after IL-1 treatment (**Fig. 45**). The day 1 of analysis indicates cells seeded and cultivated for 24 h in medium containing 10 % serum. Cells were washed and supplied with low serum medium for the next 24 h, when the IL-1 stimulation was done (day 2). The cells were treated with toxins 24 h later (day 3). The cells cultivated in serum deprived medium reduced proliferation rate and at the time of treatment over 60 % of population was in the G1 phase. There was no difference between cells stimulated with IL-1 and left untreated (day 3). An equal cell cycle distribution

Results

in control cells and those treated with IL-1 was also shown after treatment with genotoxins (day 4). The analysis involved cells 24 h after treatment with 10 Gy ionising radiation, 1 mM H₂O₂, 10 μM MNNG or 1 mM MMS. Whereas all agents induce different effects on cell cycle distribution, there was no influence of IL-1 detected (see Fig. 46B for quantification of cell cycle distribution).

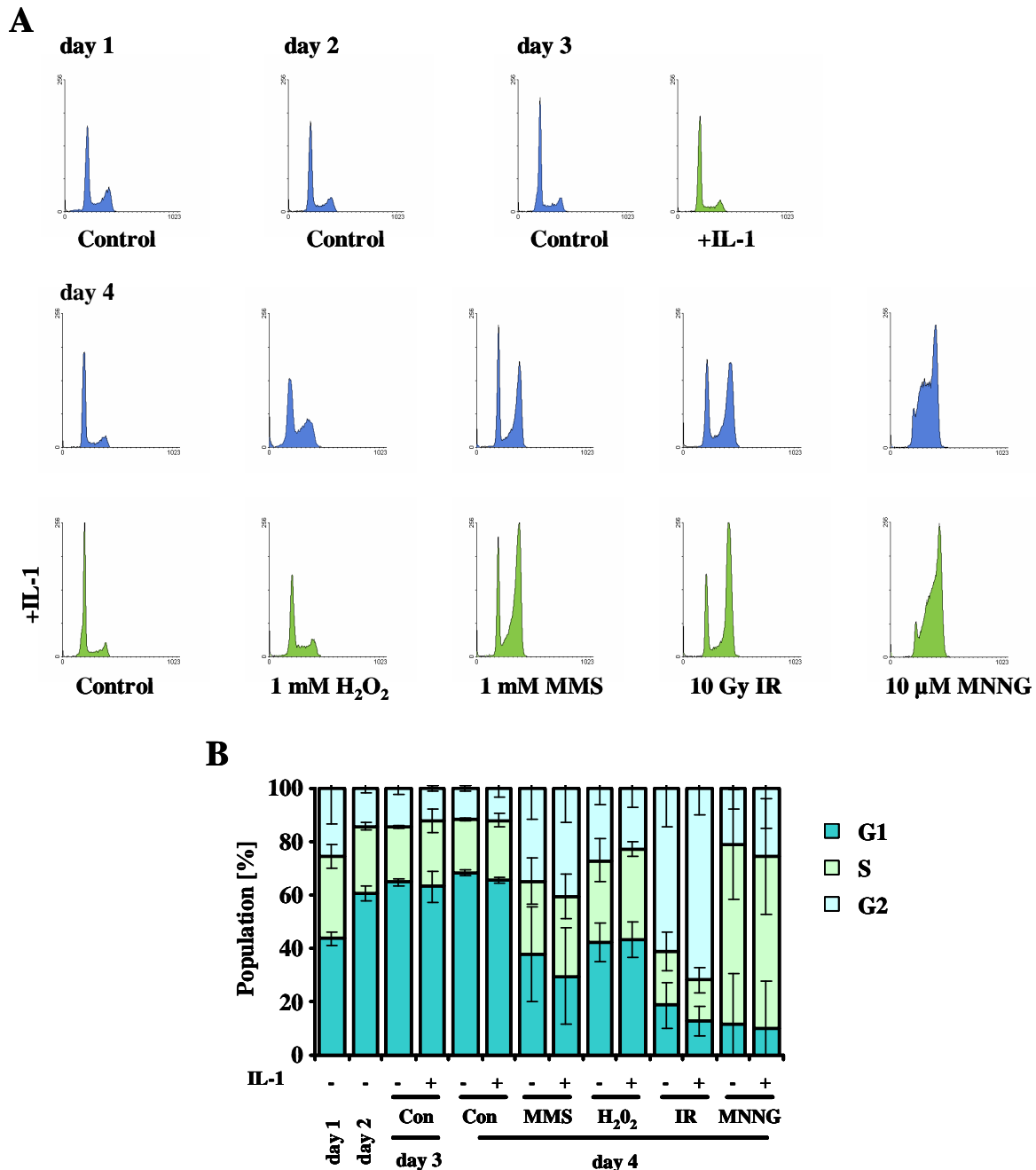


Fig. 45 Cell cycle distribution of KB cells treated with IL-1 and genotoxins

At day 2 cells were treated with 10 ng/ml IL-1 following 24 h serum starvation. The genotoxic treatment was performed at day 3. Cell cycle distribution was measured by FACS based on DNA content. DNA was stained with propidium iodide. The histograms of the representative experiments are shown in A. Mean values of three independent experiments \pm SD are graphical illustrated in B.

Results

The effect of IL-1 on proteins involved within the apoptotic pathway was studied by western blot analysis (Fig. 46). KB cells were stimulated with 10 ng/ml IL-1 and treated 24 h later with 1 mM MMS or 1mM H₂O₂. Cells were harvested at indicated time points between 1 and 48 h after treatment. The analysis included pro and anti-apoptotic proteins that were described to be regulated in an IL-1 dependent manner, such as AKT, p38, Bcl-2 and Bax. Genotoxin treatment led to an activation of p38 kinase. After treatment, p38 kinase was rapidly phosphorylated at Thr180/Tyr182. The active form of p38 was detected 1 and 6 h after treatment. In IL-1 pre-treated cells the basal level of p38 phosphorylation was slightly elevated but it had not influence on the extent of p38 activation upon MMS or H₂O₂ treatment. IL-1 did not influence the expression of Bcl-2 and Bax. The anti-apoptotic AKT pathway was activated by H₂O₂ treatment and the phosphorylation was blocked by IL-1 stimulation. In conclusion, the decreased apoptotic frequency after genotoxic treatment does neither result from IL-1 interaction with the cell cycle nor with the apoptotic pathway. Therefore, the effect of IL-1 is supposed be due to up-regulation of APEX2 and increase of DNA repair capacity.

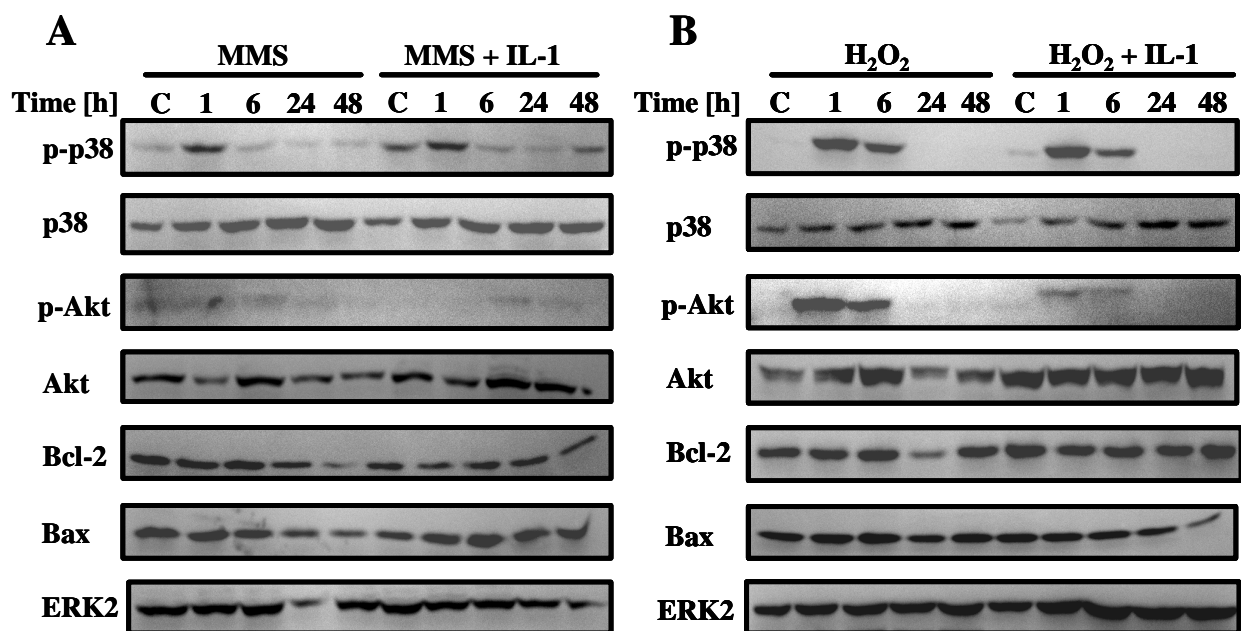


Fig. 46 Influence of IL-1 on major apoptotic proteins in KB cells treated with 1 mM MMS (A) or 1 mM H₂O₂ (B)

Cells were stimulated with IL-1 for 24 h and than treated with MMS or H₂O₂. 20 μ g of whole cell extracts was subjected to western blot.

3.3.3 Influence of *APEX2* over-expression on survival of HeLa cells

In the previous section, it was shown that IL-1 causes an up-regulation of *APEX2* expression. The stimulation of KB cells with IL-1 led to a decrease in apoptosis of cells treated with genotoxic agents and the protective effect was strongest in cells treated with H₂O₂. Cell cycle control and direct interaction of IL-1 with apoptotic proteins was excluded as a reason for the IL-1 action as survival factor. To investigate whereas increased expression of *APEX2* indeed protects cells against oxidative DNA damage, the *APEX2* cDNA was cloned in a mammalian expression vector under the control of the CMV promoter. The cDNA was synthesised using RNA isolated from KB cells. The *APEX2* cDNA was amplified by PCR and cloned into pcDNA3.1/ V5 –His-Topo vector (Invitrogen) according to the manufacture's protocol. The vector was transfected into HeLa-MR cells and the *APEX2* expression was analysed by RT-PCR (**Fig. 47**). Stable clones were selected with G418 (1mg/ml). Only one *APEX2* over-expressing clone (HeLa-Apex2 C4) was obtained from 60 clones picked and tested. The expression was 3 times higher than in the clone transfected with the empty vector (HeLa-Neo C2), which reflected the *APEX2* induction obtained after IL-1 stimulation. The transient transfection was more efficient and the *APEX2* mRNA level was increased with a factor of 30.

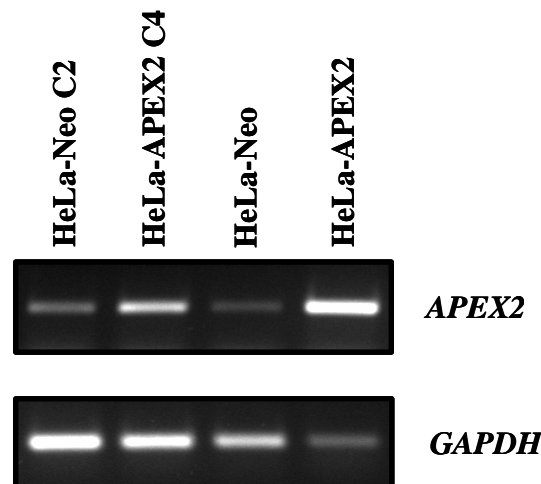


Fig. 47 *APEX2* expression in HeLa cells stably and transiently transfected with pcDNA3.1-*APEX2*

HeLa cells were transfected with pcDNA3.1 empty vector or pcDNA3.1-*APEX2*. Stable clones were selected with G418 and designed as HeLa-NeoC2 and HeLa-Apex2C4. The transiently transfected cells are designed as HeLa-Neo and HeLa-APEX2. RNA was isolated 24 h after transfection.

3.3.4 Sensitivity of HeLa cells over-expressing APEX2 to DNA damaging agents

To investigate the role of APEX2 in cell death induced by genotoxic agents, HeLa cells over-expressing APEX2 were exposed to ionising radiation, H₂O₂, MNNG, MMS, temozolomide and fotemustine. 72 h later cells were harvested and subjected to SubG1 analysis by FACS. The response of HeLa-APEX2 C4 cells is shown in **Fig. 48**, and apoptosis frequency of transient transfected cells is shown in **Fig. 49**. In both cases, APEX2 protected the cells against ionising radiation. The decreased level of apoptosis was observed in a dose range up to 20 Gy (**Fig. 48-49**).

The experiments with MMS and H₂O₂ showed some discrepancy between the responses of selected HeLa-APEX2 C4 clone and transient transfected HeLa-MR cells (**Fig. 48 – 49B and C**). The HeLa-APEX2 C4 strain was killed by MMS and H₂O₂ as effective as mock transfected HeLa-Neo C2. In opposite, transient over-expression of APEX2 protected cells against both agents. The most pronounced effect was observed after treatment with H₂O₂. Apoptosis after treatment with 2.0 mM H₂O₂ was reduced in APEX2 transfected cells from over 40 to 15 %. It was not clear if the protective effect of APEX2 was obtained in transient transfected cells because of higher expression level or the clonal effects between HeLa-Neo C2 and HeLa-APEX2 C4 strains.

In addition, the HeLa-APEX C4 clone was more sensitive to O⁶MeG inducing agents such as MNNG and temozolomide (**Fig. 48 – 49D and E**). The experiment was carried out without MGMT inhibitor and the difference in sensitivity was probably caused by clonal variation in MGMT expression. The transient transfected population was not sensitised towards O⁶MeG by APEX2 over-expression (**Fig. 48 – 49D and E**). Overall the data suggests that APEX2 protects cells from the cytotoxic effect of various genotoxic agents.

Results

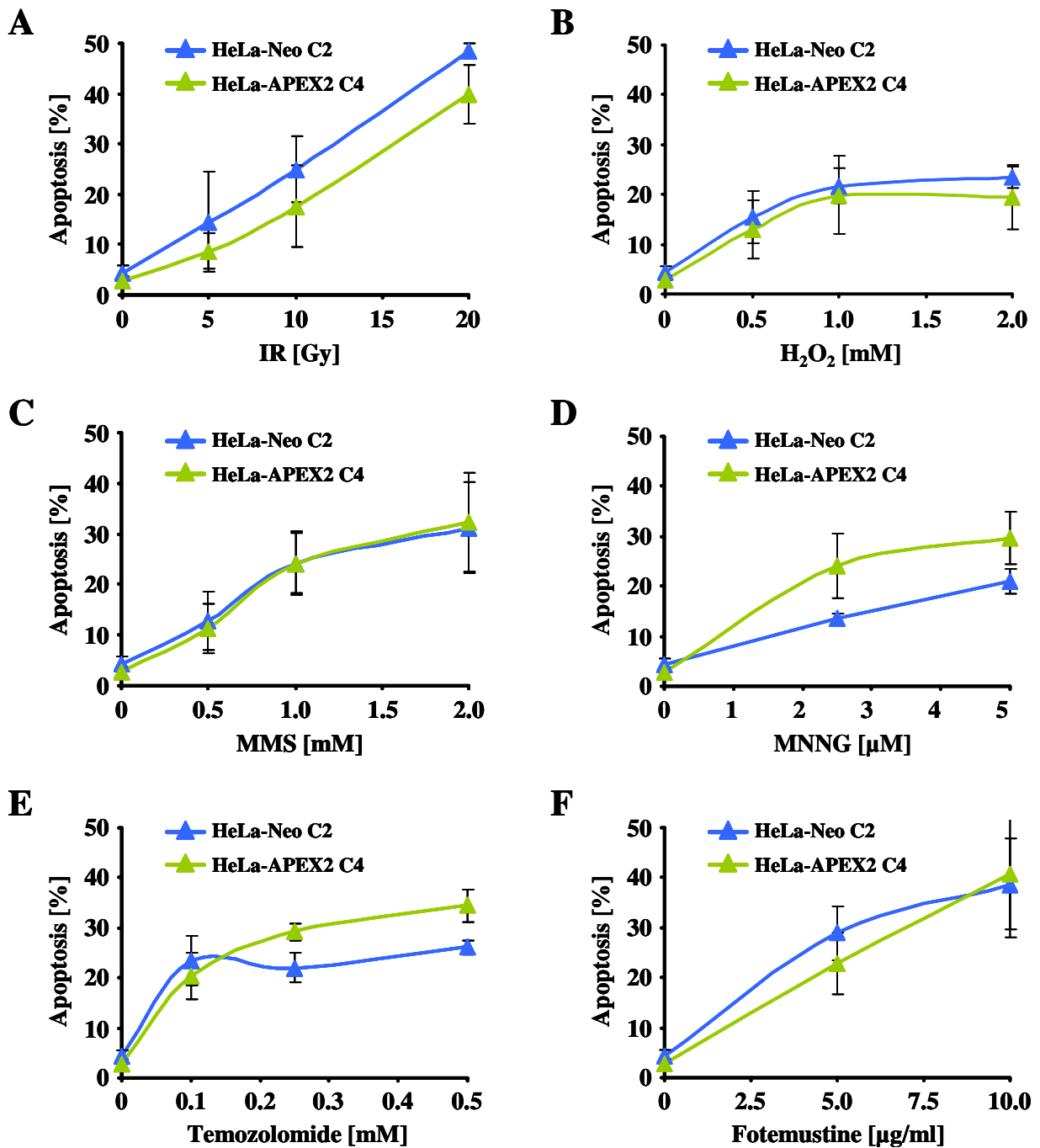


Fig. 48 Apoptosis induced by different genotoxins in HeLa cells transfected with pcDNA3.1-neo and pcDNA3.1-APEX2 vector

SubG1 measurement was performed 72 h after treatment. The results are means of three independent experiments \pm SD.

Results

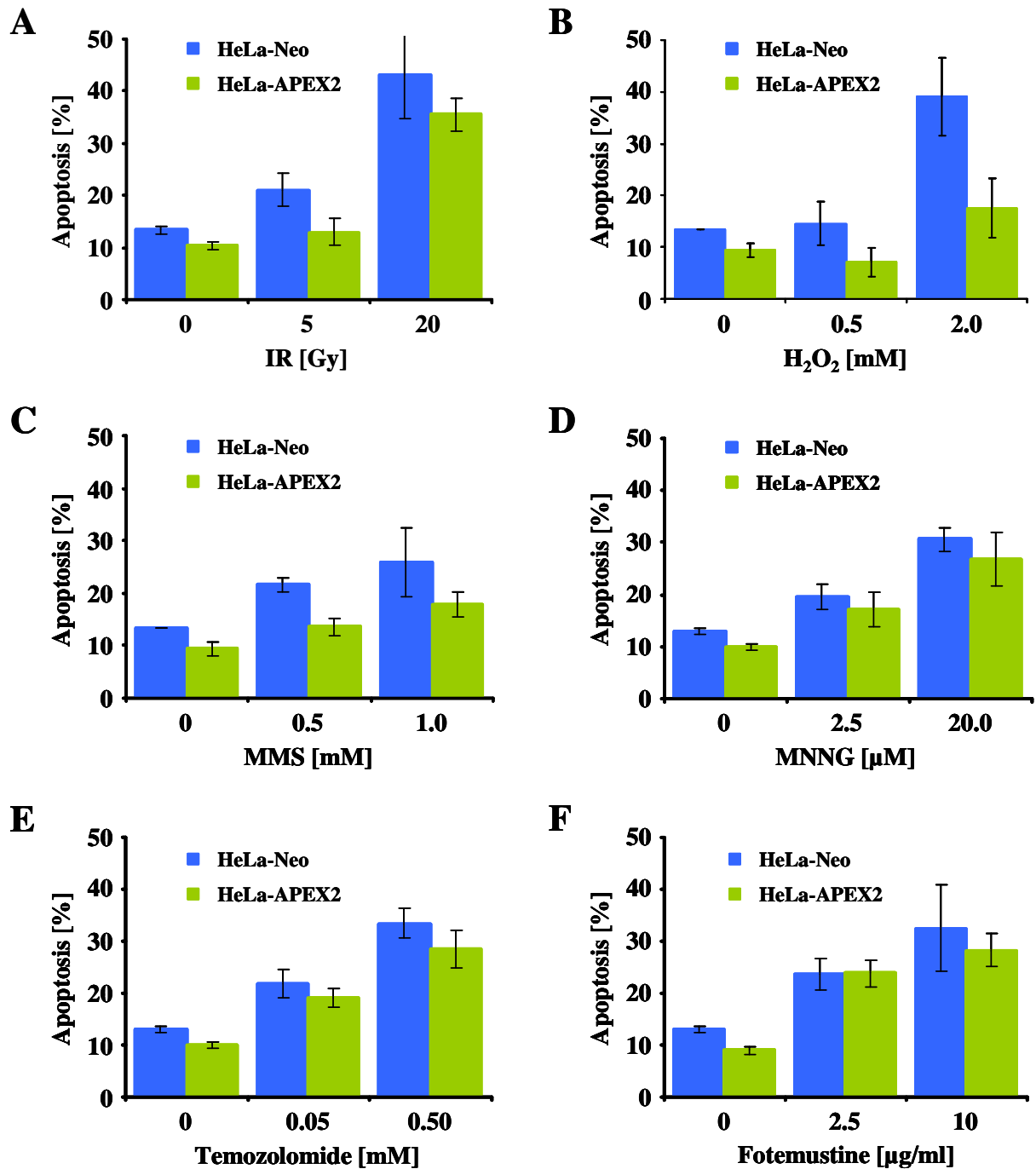


Fig. 49 Frequency of apoptosis measured by SubG1 in HeLa -MR cells transiently transfected with pcDNA3.1 empty or pcDNA3.1-APEX2 vector

HeLa-MR cells were transfected with 8 μg DNA and 20 μl Lipofectamine 2000. The treatment was performed 24 h later. Apoptosis measurement was done 72 h after genotoxic treatment. Results are means of two independent experiments.

4 Discussion

DNA methylating compounds are used as anticancer chemotherapeutics. These compounds include temozolomide, streptozotocin, procarbazine and dacarbazine. They are used in the treatment of gliomas, malignant melanomas, carcinoid tumours and Hodgkin's lymphomas. Clinical studies are still ongoing but it is expected that similar compounds will be used in the treatment of other tumours. Although methylating agents are therapeutically applied, the cellular processing of methylated DNA lesions is still poorly understood. To date, we know that the critical DNA lesion responsible for cell death is O⁶MeG. Processing of O⁶MeG involves the repair protein MGMT as well as the MMR system, but the functional link between DNA damage and apoptosis still remains a mystery. Determination of the signaling pathway evoked by O⁶MeG to trigger apoptosis and the mechanism of resistance against the agents will be of great benefit for tumour therapy. This study focuses on the role of DSB and ATM kinase in the cellular processing of O⁶MeG. Moreover, the influence of the cytokines IL-1 and IGF-I in ATM deficient cells on the sensitivity to methylating agents was investigated. Finally, it was shown that IL-1 modulates survival after genotoxic agents by induction of DNA repair.

4.1 ATM is involved in O⁶MeG processing

4.1.1 ATM deficient cells are hypersensitive to methylating agents

ATM is a serine/threonine kinase that gets activated in the presence of DSBs. The mechanism involves autophosphorylation and dimer dissociation. Activated ATM kinase induces cell cycle checkpoints, DNA repair and apoptosis. Human cells deficient for ATM derived from A-T patients are hypersensitive to the cytotoxic and genotoxic effect of ionising radiation and chemicals inducing DSB. They show higher incidence of apoptosis and increased yield in chromosomal aberrations (Lavin et al., 2005). For O⁶MeG inducing agents contradictory results have been reported.

Human ATM ^{-/-} fibroblasts has been assayed in clonogenic survival experiments with the methylating agents MMS, MNU and MNNG. These agents mostly form N7MeG. The frequency of O⁶MeG formation varies between 0.3 % of total DNA alkylations for MMS, 7 % for MNNG, and 5.9 to 8.2 % for MNU (Beranek, 1990). Some publications report hypersensitivity of different ATM ^{-/-} strains to MNU as well as to MMS. Hypersensitivity to MNU was shown by Teo *et al.* for two different A-T fibroblast strains (Teo and Arlett, 1982). Two out of three A-T lines were significantly more sensitive to MMS treatment in the study

Discussion

of Barfknecht *et al.* (Barfknecht and Little, 1982). In contrast, normal sensitivity to MMS was reported for A-T fibroblasts (altogether 5 different A-T strains and 6 control lines) by Scudiero *et al.* (Scudiero, 1980). MNNG was the most often used agent, but again contradictory results were obtained in studies with this agent. Thus, decreased clonogenic survival has been reported in five different ATM *-/-* fibroblast strains by Scudiero *et al.*, which has not been confirmed by other authors (Adamson *et al.*, 2002; Teo and Arlett, 1982). The reasons for these contradictory results could be ascribed to two reasons. Firstly, different mutations within the ATM gene cause variability in the response of human ATM strains from different patients which manifests itself among the others in the degree of radiosensitivity (Sun *et al.*, 2002; Zhang *et al.*, 2002). Secondly, sensitivity to O⁶MeG inducing agents is tightly correlated with the MGMT and MMR expression, which (particularly the MGMT level) vary considerably among established human cell lines. The cellular background that might influence the sensitivity to methylating agents was not considered by any of the authors. Therefore the involvement of ATM in O⁶MeG processing is still an open question.

To address this question, in the present study, ATM *-/-* fibroblasts derived from ATM knockout mice were utilized. An advantage over the previous studies is that the cells are derived from littermates so that they are of the same genetic background. In contrast, human A-T fibroblasts were compared to fibroblasts of healthy donors of unknown genotype. The murine ATM *-/-* and ATM *+/+* cell pair was also analysed for MGMT and MMR status. ATM *-/-* mouse fibroblasts grew poorly in culture, thus they were also mutated for p53 to balance the proliferation rate with the wild - type cells. The compared strains were therefore ATM *+/+* p53 *-/-* and double knockout ATM *-/-* p53 *-/-* (Elson *et al.*, 1996). The MGMT level was very low in both cell lines. The basal MGMT activities were in the range of 50 to 80 fmol/mg protein and therefore the cells were described as Mex⁻. MGMT in these cells was not inducible by ionising radiation or MNNG treatment. MNNG even further reduced the MGMT activity in ATM *-/-* and ATM *+/+* cells to an undetectable level (**Fig. 7**). Equal MMR capacity in both cell lines was shown by comparison of expression levels of the participating proteins: MSH2, MSH6, MLH1 and PMS2 (**Fig. 8**).

Mouse ATM *-/-* fibroblasts were clearly hypersensitive to O⁶MeG inducing agents (**Fig. 12**). In clonogenic survival experiments ATM *-/-* cells were almost 5 times more sensitive to MNNG than the wild - type fibroblasts when considering the IC₅₀. The survival of ATM *-/-* decreased rapidly upon treatment with MNNG in a dose range of 1 – 10 µM; in this dose range ATM *+/+* cells were only slightly affected. The survival of ATM *-/-* cells was also decreased by MMS. The reduction of survival of ATM *-/-* cells correlated with the amount of

Discussion

O⁶MeG formed. The difference in colony formation between ATM ^{-/-} and ATM ^{+/+} cells was much more pronounced after treatment with MNNG than with MMS. This was measured both in clonogenic survival and in metabolic WST-1 assay (**Fig. 13**). The toxic effect of MMS in ATM ^{-/-} cells increased after permanent drug treatment (**Fig. 14**).

Since O⁶MeG inducing agents are commonly used anticancer drugs, the hypersensitivity of ATM ^{-/-} cells to methylating agents is of particular importance for tumour therapy. Although our analysis of O⁶MeG toxicity was performed only with non - therapeutic chemicals such as MNNG and MMS the results can be applied to explain the effects of methylating drugs that are in clinical use. Thus, it was shown that ATM ^{-/-} cells were also hypersensitive to the O⁶MeG - inducing anticancer drug temozolomide (**Fig. 10**). The sensitization of cells by ATM deficiency was about 4 fold as measured by IC₅₀ in clonogenic survival. It is to be expected that the development of strategies for the inactivation of ATM in tumours will be a highly attractive research area in the future.

ATM knockout cells showed a similar survival level as the wild - type following treatment with the O⁶chloroethylating agent fotemustine (**Fig. 10**). Within the DNA, chloroethyl adducts of guanine are converted to DNA interstrand cross-links (ICL), which are responsible for the induction of cell death. ICL's form DSB, presumably as repair intermediates or at replication forks during bypass that require NER and HR components, but the equal sensitivities of ATM ^{-/-} and ATM ^{+/+} cells to fotemustine indicate that these DSB are not recognised and processed by ATM. Consistent with our data, lack of cross-link sensitivity for ATM ^{-/-} cells was also reported previously by Fedier *et al.* for platinum compounds (Fedier *et al.*, 2003). Concurrently, the sensitivity to the ICL - inducing agent mitomycin C (MMC) was reported for ATR mutated cells, showing that ATR is involved in the processing of these DNA lesions (Alderton *et al.*, 2004).

4.1.2 O⁶MeG is the DNA lesion causing hypersensitivity of ATM ^{-/-} cells to DNA methylating agents

A critical genotoxic and pro-apoptotic DNA lesion induced by methylating agents is O⁶MeG. To check whether O⁶MeG lesions are involved in methylation – hypersensitivity of ATM ^{-/-} cells and to clarify that the sensitivity does not result from N-alkylations, the O⁶MeG repair capacity of the cells was manipulated. O⁶MeG is repaired in a one step reaction by the DNA repair protein MGMT (Mitra and Kaina, 1993; Pegg, 1990). The methyl group is transferred from guanine to the active site of MGMT, where it covalently binds to cytosine leading to irreversible enzyme inactivation. The inactive MGMT gets fastly degraded and the restoration

Discussion

of DNA repair capacity requires *de novo* protein synthesis. MGMT deficient cells designed as Mex⁻ are highly sensitive to O⁶-methylating agents compared to MGMT competent cells designed as Mex⁺ (Kaina et al., 1991). The murine fibroblasts used in our study possessed low basal MGMT activity (67 and 78 fmol/mg protein for ATM ^{+/+} and ATM ^{-/-} respectively), and the residual MGMT was inactivated by pre-treatment with the competitive inhibitor O⁶BG. O⁶BG was highly specific and effective in the inactivation of MGMT (to undetectable level) (**Fig. 17**). O⁶BG treatment gave rise to increased MNNG-induced cell killing, which was clearly more extensive in ATM ^{-/-} compared to ATM ^{+/+} cells (**Fig. 18**). Overall, the sensitizing effect of O⁶BG was low, which was to be expected since the strains expressed low levels of MGMT. Inhibition of MGMT by O⁶BG only sensitized ATM ^{-/-} cells to MMS, which mostly produces N-methylation lesions. However, the low amount of O⁶MeG induced by MMS still contributes to MMS cytotoxicity. The finding that MGMT depleted ATM ^{-/-} cells responded more intensively to the killing effect of MNNG and MMS than MGMT depleted ATM ^{+/+} cells indicates that O⁶MeG is critically involved in ATM ^{-/-} hypersensitivity. MGMT depletion by O⁶BG also provoked an increase in the frequency of apoptosis in ATM ^{-/-} cells, which was not observed in ATM ^{+/+} cells (**Fig. 18**).

On the other hand, transfection-mediated increase of MGMT expression caused a significant increase in survival of ATM ^{-/-} cells treated with MNNG and MMS (**Fig. 19 - 20**). MGMT was stably over-expressed (controlled by a SV40 promoter) resulting in MGMT activities in the selected clones of 635 and 776 fmol/mg protein for ATM ^{-/-} and ATM ^{+/+} respectively. The protective effect of MGMT was determined after treatment with MNNG and MMS by colony formation and by Annexin-V/PI staining. MGMT protection against MNNG was clearly less pronounced in wild - type cells than in the ATM ^{-/-} strain. Collectively, the data support the conclusion that hypersensitivity of ATM ^{-/-} cells to methylating agents is mainly due to un-repaired O⁶MeG.

4.1.3 ATM is dispensable for apoptosis induced by O⁶MeG

The hypersensitivity of ATM ^{-/-} cells to methylating agents was due to the induction of a high frequency of apoptosis (**Fig. 15**). ATM ^{-/-} cells underwent apoptosis already at low dose of MNNG (1 μ M). Apoptosis was amplified by MGMT inhibition (**Fig. 18**). Cell death was induced in a dose dependent manner and 20 μ M MNNG caused apoptosis in almost half the knockout cells. The wild - type cells were nearly completely resistant to MNNG induced apoptosis. MMS was less effective than MNNG in triggering apoptosis, probably due to the

Discussion

lower frequency of O⁶MeG lesions. The methylating agents predominantly induced apoptosis and only caused marginal necrosis.

To exclude the influence of clonal effects on O⁶MeG induced apoptosis, control experiments with the ATM kinase inhibitor caffeine were performed (**Fig. 16**). Caffeine is an unspecific inhibitor of the PI3K family. The affinity of the inhibitor varies between nuclear kinases such that caffeine inhibits preferably ATM, followed by ATR and DNA-PK. Human ATM proficient cells treated with 1 mM caffeine exhibit A-T phenotype such as radiosensitivity, radioresistant DNA synthesis and lack of S and G2 checkpoint induction (Blasina et al., 1999; Sarkaria et al., 1999). Caffeine did not affect apoptosis in ATM ^{-/-} cells treated with MNNG or MMS. In contrast, it increased apoptosis in the ATM ^{+/+} strain. The frequency of apoptosis was elevated in wild - type cells to the level observed in the knockouts. To conclude, ATM is involved in the processing of O⁶MeG and the protective effect depends on the ATM kinase activity.

Clearly, ATM is not required for triggering the apoptotic pathway following treatment of cells with methylating agents. It rather acts protectively, attenuating the genotoxic effect of O⁶MeG lesions. However, published data suggests that ATM may participate in apoptosis induction which is cell type and agent specific. Human ATM ^{-/-} fibroblasts undergo apoptosis with high frequency after low dose ionising radiation. Although cells from A-T patients exhibit diminished and postponed activation of the p53 signal transduction pathway at early times after radiation exposure, it has been proposed that high levels of DNA damage persisting in ATM ^{-/-} cells may up-regulate p53 through an ATM-independent mechanism at late times after irradiation, leading to cell death by apoptosis (Enns et al., 1998). Similar data were obtained in this study for mouse fibroblasts. High level of p53 independent apoptosis was induced in ATM ^{-/-} cells upon ionising radiation (**Fig. 9**). However, Heinzelmann-Schwarz *et al.* used the same fibroblasts in sensitivity studies involving photodynamic therapy (PDT), showing a negative relationship between ATM expression and apoptosis activation. In this study apoptosis was measured by TUNEL assay and caspase 3 – cleavage apoptosis assays. In the subset of dead cells, apoptosis was reduced by loss of ATM (Heinzelmann-Schwarz et al., 2003). This indicates substrate specificity of ATM dependent apoptosis in fibroblasts. Contrary to fibroblasts, where ATM protects against apoptosis, ATM was required for cell death in neuronal cells and in thymocytes. In the developing central nervous system, ATM initiates a p53-dependent apoptotic cascade after DNA damage involving upregulation of Bax (Chong et al., 2000; Herzog et al., 1998; Lee et al., 2001; Lee and McKinnon, 2000). In thymocytes apoptosis induced by ionizing radiation is independent from p53 but involves

Discussion

ATM phosphorylation of c-Abl and E2F1 transcription factor. E2F1 phosphorylation enhanced its stability and increases its transcriptional activity towards p73. P73 is phosphorylated by ATM activated c-Abl and accumulates in damaged cells that leads to induction of apoptotic cell death (Bhandoola et al., 2000; Irwin et al., 2000; Lin et al., 2001; Lissy et al., 2000; Shaul, 2000; Xu and Baltimore, 1996).

4.1.4 Apoptosis induced by O⁶MeG is a late effect

In time course experiments it was shown that apoptosis induced by O⁶MeG is a quite late effect. The first apoptotic cells were detected 24 h after MMS and 48 h after MNNG treatment (**Fig. 21 - 22**). The fraction of apoptotic cells increased with time and reached 30 % in ATM ^{-/-} cells at 96 h post-treatment. The doses, 1 mM MMS and 10 μM MNNG, that were applied in the time course experiments hardly influenced the survival of ATM wild - type cells. The marginal induction of apoptosis in ATM ^{+/+} fibroblasts (less than 15 %) was seen 72- 96 h after treatment.

The delay in apoptosis suggests that not O⁶MeG *per se* is responsible for induction of cell death. It is rather the secondary or tertiary DNA lesion appearing during O⁶MeG processing that provides the apoptotic initiating signal. The fact that ATM ^{-/-} cells are hypersensitive to methylating agents supports the model of Ochs and Kaina (Ochs and Kaina, 2000), which assumes that these downstream secondary lesions are DSB. The authors have shown that DSB are formed in Mex⁻ CHO-9 cells after treatment with low doses of MNNG. The DSB formation preceded the apoptotic cascade. Similar data were obtained by Roos *et al.* for human peripheral lymphocytes. Low dose treatment with MNNG or temozolomide induced apoptosis in CD3/CD28 stimulated lymphocytes. O⁶MeG-triggered apoptosis in proliferating lymphocytes was preceded by a wave of DSBs, which coincided with p53 and Fas receptor up-regulation (Roos et al., 2004). ATM specifically recognises DSBs, and to date ATM has not been shown to have affinity for any other kind of lesions. The protective action of ATM in O⁶MeG processing lends additional support for the model where DSBs arise downstream of O⁶MeG and that these DSBs are the final trigger for apoptosis. Additionally we have shown that treatment with MNNG induces a high frequency of chromosomal aberrations in ATM ^{-/-} fibroblasts. The treatment also elevates the number of SCE's to a higher extend in knockout cells than in the wild - type (Debiak et al., 2004). Both chromosomal aberrations and SCE's results from misrepaired DSB, implicating the repair defect in ATM ^{-/-} cells.

4.1.5 Apoptosis induced by O⁶MeG is executed via the mitochondrial pathway

To determine which apoptotic pathway becomes activated in response to O⁶MeG, caspase activity assays with substrates of caspase-3, -8 and -9 were performed (**Fig. 23**). Unfortunately, the activation of transducer caspases-8 and -9 was too low to enable us to distinguish between mitochondrial or membrane receptor dependent pathways. The involvement of the mitochondrial pathway was shown by determining the cytochrome c release from the mitochondria to the cytosol. Cytochrome c release from the mitochondria was observed in a dose dependent manner following MMS and MNNG treatment in ATM +/+ and ATM -/- cells. The time and dose kinetics of cytochrome c release paralleled caspase-3 proteolytic activation (**Fig. 23**). Our data indicate the involvement of the mitochondrial apoptotic pathway in O⁶MeG induced apoptosis in rodent fibroblasts. This is consistent with the findings of Ochs *et al.* (Ochs and Kaina, 2000; Ochs *et al.*, 2002). However, contrary to our study, Ochs *et al.* ascribed the central role in O⁶MeG triggered apoptosis to the Bcl-2 protein, since they observed a decline in mitochondrial Bcl-2 level before MNNG and MMS triggered apoptosis in CHO-9 cells. Proteosomal Bcl-2 degradation leads to a reduction of the Bcl-2/Bax ratio, causing for the release of pro-apoptotic proteins. Bcl-2 over-expression partly rescued cells from O⁶MeG induced apoptosis (Ochs and Kaina, 2000; Ochs *et al.*, 2002). A change in the Bcl-2/Bax ratio was only observed in ATM +/+ cells following MMS treatment. Bcl-2 decline and Bax up-regulation in the mitochondrial fraction appeared in a dose dependent manner 72 h after MMS treatment. The Bcl-2/Bax ratio remained unchanged in ATM -/- cells and ATM +/+ cells treated with MNNG. In ATM -/- cells, Bcl-2 expression was reduced but the expression of Bax decreased to the same extent, so that the Bcl-2/Bax ratio remained unchanged. The decline of Bcl-2 observed in ATM -/- cells appears to be an unspecific byproduct of cell death due to degradation of the whole mitochondria during the apoptotic process. In contrast to CHO-9 cells, ATM -/- fibroblasts induced the FasR following MNNG treatment, suggesting that in these cells the death receptor-mediated pathway may be partly involved in O⁶MeG induced apoptosis (**Fig. 23**).

4.2 ATM protects cells against O⁶MeG induced apoptosis

We have shown that ATM participates in O⁶MeG processing and protects cells against methylating agent - induced apoptosis. The second part of the study focused on which cellular pathways are regulated by ATM following methylating agents treatment. From radiobiological studies it is known that ATM activates different survival pathways, which include cell cycle checkpoints, DNA repair and transcription factors. In the following section, the participation of ATM in these processes upon the treatment with methylating agents will be discussed.

4.2.1 ATM interactions within the apoptotic pathway upon treatment with O⁶MeG inducing agents

It has been reported that following genotoxic stress, ATM may influence apoptosis by interacting either with the pro-apoptotic MAPK pathway or by attenuating NFκB mediated anti-apoptotic signals. Therefore, we determined the activation of these pathways in ATM -/- cells following O⁶MeG induction. The MAPK pathway consists of 3 subfamilies: ERK, JNK and p38 kinase. ERK's are activated by receptor tyrosine kinases and provide proliferation or differentiation signals. Therefore ERK activation was not addressed in this study. JNK and p38 MAPK are activated by genotoxic stress and are involved in the regulation of different AP-1 components. We observed that methylating agents activate JNK and p38 kinases shortly after treatment (**Fig. 24**). Increased phosphorylation of JNK and p38 kinases was observed 1 h after treatment. Early induction of MAPK's occurred in both ATM +/+ and ATM -/- cells. Activation occurred in a dose dependent manner following MMS and MNNG treatment and was quantitatively equal in both cell lines (**Fig. 25**). Due to similar early activation of JNK and p38 kinases it was concluded that early MAPK activation is not the cause of ATM -/- O⁶MeG hypersensitivity. However, although the level of JNK activation was the same in ATM -/- and ATM +/+ cells, it persisted longer in ATM knockouts than in wild - type cells. In ATM wild - type cells JNK and p38 activation returned to control levels 6 h after alkylation treatment while in ATM knockout cells JNK activation persisted for up to 24 h. The long-term stress kinase activation following methylating agent treatment exposure might contribute to the increased level of apoptosis and the corresponding hypersensitivity of ATM -/- cells. Prolonged JNK phosphorylation in A-T cells has been shown by Bar-Shira *et al.* following neocarzinostatin treatment (Bar-Shira *et al.*, 2002). In that study, neocarzinostatin up-regulated MAP kinase phosphatase – 5 (MKP-5) at transcription level. MKP- 5 dephosphorylates and inactivates JNK and p38. In A-T fibroblasts, MKP-5 was not induced following radiomimetic treatment which resulted in prolonged JNK activation and increased

Discussion

cell death. Decreased phosphatase activity might also be a reason for the prolonged JNK phosphorylation observed in ATM $-/-$ cells after treatment with O⁶MeG inducing agents.

The pro-apoptotic activity of JNK is dependent on transcription. Upon JNK activation, JNK phosphorylates c-Jun and ATF-2, which comprises the AP-1 transcription factor. The long-term activation of JNK in ATM $-/-$ cells following MNNG and MMS treatment, however, had no influence on DNA binding activity of the AP-1 complex. Maximal AP-1 activity was measured 6 h after MNNG and 3 h after MMS treatment and thereafter decreased to control level in both ATM $+/+$ and ATM $-/-$ cells (**Fig. 26**). Nevertheless, the transcriptional activity of AP-1 target genes was regulated in an ATM dependent manner by undefined factors. The expression of *fasL* and *c-jun* increased in ATM $+/+$ fibroblasts starting 24 h after treatment, while the expression in knockouts remained unchanged (**Fig. 27**). Surprisingly, an up-regulation of pro-apoptotic genes took place in the resistant wild-type cells and not in the hypersensitive mutant. This implicates that ATM somehow suppresses apoptosis by additional anti-apoptotic factors. This regulation might possibly be mediated through the NF κ B pathway. Indeed, a defect in NF κ B signaling was shown to contribute to the A-T radiosensitive phenotype, and correction of NF κ B activation in A-T cells resulted in a decrease of apoptosis induced in these cells by γ -irradiation (Jung and Dritschilo, 2001; Jung et al., 1997; Li et al., 2001; Panta et al., 2004; Piret et al., 1999). NF κ B regulation after methylating agent treatment was analysed by determination of the expression levels of its target genes *fasR* and *c-iap* (**Fig. 27**). The expression of the genes was lower in ATM $+/+$ cells 14 h after treatment. In ATM $-/-$ cells the expression levels remained unchanged. We therefore conclude that the hypersensitivity of ATM $-/-$ cells is, at least in part, due to a defect in activating the anti-apoptotic NF κ B pathway. Nevertheless, NF κ B activation following methylating agent treatment has to be investigated in more detail.

4.2.2 ATM does not activate cell cycle checkpoints following methylating agent treatment

ATM takes part in activating the cell cycle checkpoints following ionising radiation. Activated by DSBs ATM phosphorylates p53 on Ser15 and the transducer kinases Chk1 and Chk2. The latter in turn also phosphorylates p53 on Ser20, Cdc25A on Ser123 and Cdc25C on Ser216. Phosphorylation of p53 contributes to its stabilisation and functional activation, which plays a pivotal role in the G1 checkpoint. Phosphorylation of Cdc25A and Cdc25C prevents activation of the cyclin-dependent kinases Cdk2 and Cdc2 leading to G1, S and G2 checkpoints initiation. These cell cycle checkpoints do not function in A-T cells, which leads to the radiosensitive phenotype (Abraham, 2001; Khanna et al., 2001; Shiloh, 2003).

Discussion

In this study, it was shown that ATM is dispensable for checkpoint activation after methylating agent treatment. Thus, murine fibroblasts treated with MMS and MNNG revealed a transient delay in S phase progression that was followed by a G2/M block. The cell cycle arrest in S and G2/M phase was equal in ATM $+/+$ and ATM $-/-$ fibroblasts (**Fig. 28 -29**). ATM was also not required for Chk-1 phosphorylation and Cyclin A accumulation, the mediators of S and G2/M arrest, in methylating agent exposed cells (**Fig. 32**). The substrates specificity suggests that the S and G2/M checkpoints evoked by O⁶MeG were induced by ATR. These data are consistent with findings of Stojic and Caporali (Caporali et al., 2004; Stojic et al., 2004). They reported correct activation of the G2/M checkpoint in ATM $-/-$ cells upon treatment with MNNG and temozolomide. They also observed that Chk-1 and Chk-2 phosphorylation was independent of ATM but was abrogated in ATR or MMR inhibited cells. In contrast, Adamson and Brown reported an ATM dependent induction of the G2/M block following MNNG treatment. They showed that ATM rapidly becomes activated and phosphorylated in response to MNNG. ATM kinase activation by MNNG resulted in phosphorylation of p53, Chk-1 and Chk-2. The work was supported by experiments involving knockout cells as well as pharmacological and siRNA approaches (Adamson et al., 2005). The discrepancy in checkpoint activation might be, at least to some extent, explained by the huge difference in the applied doses. The Adamson and Brown study was performed with MNNG doses 120 times higher (25 μ M) than the dose used by Stojic (0.2 μ M MNNG). Caporali also worked with a relatively low dose of temozolomide (12.5 μ M). In the study discussed here we used 10 μ M MNNG. Since the sensitivity of mouse cells to O⁶MeG is much lower than human cells, this dose may be described as moderate. Additionally, Adamson and Brown did not analyze the MGMT activity, while the other studies were performed in Mex⁻ background. The DNA lesions induced by high MNNG dose in MGMT positive cells are N7 alkylations, while the toxicity of low dose treatment is predominantly provoked by O⁶MeG. One might conclude that O⁶MeG induced checkpoint is ATM independent, while N7 alkylations activate the ATM dependent pathway. However, the data obtained with MMS contradicts this conclusion. MMS predominantly induces N7 alkylations, nevertheless G2/M checkpoint activation occurred to an equal level in ATM $-/-$ and ATM $+/+$ cells in a time and dose dependent manner (**Fig. 31**).

4.3 Influence of cytokines on DNA repair capacity and sensitivity to DNA methylating agents

The aim of the second part of the study was to investigate how the cellular environment influences the response of cells to alkylating genotoxins. Cytokines are the most important

Discussion

signal transducers between cells. The major role of cytokines is dedicated to the immune system although they are also involved in the process of carcinogenesis. Depending on tumour type, cytokines may either promote or inhibit the tumour growth. The mode of action of cytokines is carefully examined in terms of tumour proliferation, transformation, and angiogenesis. Although the outcome of studies on the modulation of DNA repair by cytokines would be with great benefit for chemotherapeutic approaches, the subject was only marginal investigated. Here we examined the influence of IGF-I and IL-1 on the sensitivity of cells to methylating agents. The regulation of DNA repair genes was examined and discussed in relation to the ATM background.

4.3.1 IGF- I protects cells against MMS in an ATM dependent manner

The effect of cytokines on cellular sensitivity was examined by means of WST-1 proliferation assay. The cytokine experiments were performed under serum free conditions in order to eliminate receptor activation by FCS. A disadvantage of serum starvation was the drastic decrease in proliferation rate. Because of that the survival experiments were restricted to the effect of N methylation lesions, as the toxicity of O⁶MeG is strictly dependent on proliferation. The treatment of cells with 20 µM MNNG of serum deprived cultures resulted in 100 % survival as measured by WST-1 assay 72 h after exposure. MMS decreased survival in a dose dependent manner, the ATM ^{-/-} cells reacting more sensitive to the treatment (**Fig. 34A**). IL-1 stimulation did not influence the survival of mice fibroblasts but a protective effect was observed in ATM ^{+/+} fibroblasts stimulated with IGF-I. Reduced sensitivity was observed in survival experiments as well as in apoptosis frequency measurement (**Fig. 35**).

It has been shown that the expression of IGF-IR is strongly reduced in human A-T fibroblasts which contributes to radiosensitive phenotype of these cells (Peretz et al., 2001; Shahrabani-Gargir et al., 2004). Decreased expression of the IGF-IR was not found in ATM ^{-/-} murine fibroblasts. Here, the receptor expression was determined by phosphorylation of Akt kinase which is a downstream target in IGF-IR pathway. Equal Akt activation was observed in ATM ^{-/-} and ATM ^{+/+} cells. Lack of a protective effect of IGF-I in ATM ^{-/-} cells treated with MMS is therefore not due to reduced receptor level but results from impaired downstream ATM dependent signaling.

Previously, Macaulay et al. have shown that mouse melanoma cells transfected with antisense IGF-IR do not activate ATM kinase in response to ionising radiation. In consequence the cells have shown reduced radiation-induced p53 accumulation and p53 Ser18 phosphorylation as well as attenuated radioresistant DNA synthesis (Macaulay et al., 2001). Mouse cells used in

Discussion

our study were p53 mutated. However, IGF-I dependent ATM activation might lead to increased MMS resistance by activation of DNA repair independent of p53. Microarray analysis of IGF-I stimulated cells was performed in order to analyse if the protective effect is due to induction of DNA repair genes. From over 120 genes examined in the assay, the only up-regulated gene was *p21* (**Fig. 36**). p21 is involved in G1 cell cycle checkpoint. A participation of p21 in MMS resistance under experimental conditions applied is unlikely as the cells were already arrested in G1 because of serum deprivation.

Trojanek et al. have demonstrated that IGF-I stimulation supports DSB repair by activation of a protein signaling cascade. The mechanism involves the phosphorylation of IRS-1, the major IGF-IR signaling molecule. Phosphorylated IRS-1 facilitates Rad51 translocation to the nucleus and Rad51 foci formation at the site of DNA damage (Trojanek et al., 2003). The conclusion of the study however is misleading. The authors suggest that IGF-I increases the DSB repair potential in the cells, nevertheless the study concerns Cis-Pt toxicity. The assumption that DSB are the toxic DNA lesion induced by this compound is based on γ H2AX staining. There is, however, some evidence that DNA intrastrand crosslinks are responsible for Cis-Pt toxicity. Moreover, γ H2AX foci appear not exclusively at DSB sites but may also result from stalled DNA replication forks (Fernandez-Capetillo et al., 2004). A similar mechanism might be involved in MMS resistance in IGF-I stimulated ATM +/+ cells.

4.3.2 IL-1 induces APEX2 in human keratinocytes

This study is the first that shows upregulation of DNA repair genes by IL-1. The experiments were performed with the human epithelial carcinoma cell line KB. IL-1 induced the expression of apurinic endonuclease 2 (*APEX2*) on mRNA and protein level (**Fig. 40**). Up-regulation of *APEX2* was induced by transcriptional regulation as it was not abrogated by actinomycin D (**Fig. 41**). *APEX2* is a newly discovered protein of unknown function. The sequence homology to APE1 of the active site is high, but because of different coding regions in C and N terminus the endonuclease activity of *APEX2* is very low (Hadi et al., 2002). Sequence analysis allows the exclusion the Ref-1 function in the *APEX2* molecule. APE1 is a redox regulator transcription factors including AP-1, Nf κ B, ATF and p53 (Fritz, 2000). Oxidized proteins are unable to bind DNA. Ref-1 mediated reduction of cysteine residues in the DNA binding domains of transcription factors restores their DNA binding activity and consequently their transcriptional activity. The Ref-1 function of APE1 is strictly dependent on two cysteine residues at positions 65 and 93, which are highly conserved throughout the different species. *APEX2* possess only one cysteine in the N terminus that corresponds to Cys93 of APE1. The single cysteine is insufficient for the redox function (Fritz et al., 2003).

Discussion

Ide et al. has shown a physical interaction of APEX2 with PCNA, thus they ascribe a role of APEX2 in PCNA dependent base excision repair (BER) (Ide et al., 2003; Tsuchimoto et al., 2001). The BER pathway is responsible for the repair of oxidative DNA lesions such as base modifications and apurinic sites. BER is initiated by DNA glycosylases, that remove the aberrant base from the DNA backbone by hydrolysing the N-glycosidic bond between sugar C1' and the base. Following the glycosylase step, apurinic endonuclease is required to remove the 3' deoxyribose, generating a 3'-hydroxyl group. The resulting single nucleotide gap with a 3'-OH terminus is filled by DNA polymerase β using basepair information from the complementary strand. Finally, the nick is sealed by DNA ligaseIII/XRCC1 complex. In a subpathway of BER (long patch BER), the AP site is processed by Pol δ or Pol ϵ that displace several nucleotides in 5' direction. The resulting flap structure is incised by flap endonuclease 1 (FEN1) and the nick is sealed by DNA ligase I. PCNA interacts with Pol δ/ϵ , FEN1, and DNA ligase I throughout the process, supporting their functions (Christmann et al., 2003). Free radicals are massively produced during the cellular immune response. One might suggest that in order to protect immune cells against oxidative DNA damage, a mechanism involving IL-1 induction of BER was developed. However, the induction of APEX2 was unique among the BER proteins. A slight induction at mRNA level was observed after IL-1 stimulation for *Ape1*, *PCNA*, *Pol β* and *Fen1*, nevertheless their protein levels remained nearly unchanged (**Fig. 42 - 43**).

To address the question of the biological relevance of APEX2 stimulation, apoptosis was measured in KB cells stimulated with IL-1 and, thereafter, treated with oxidative and alkylating agents. A protective effect was examined after treatment with ionising radiation, H₂O₂, MMS and MNNG. A decrease in apoptosis was most pronounced upon treatment with high doses of H₂O₂ (**Fig. 44**). To exclude that the protective effect of IL-1 was due to cell cycle checkpoints induction, cell cycle distribution analysis was carried out. There was no difference in cell cycle distribution upon genotoxic treatment between the cells upon cytokine stimulation and controls. Equal cell cycle distribution was observed also at the time of treatment (**Fig. 45**). Furthermore, IL-1 interactions within the apoptotic pathway were investigated. It has been reported that IL-1 might act in different cell systems as an antiapoptotic factor by stimulation of Akt, p38 or Bcl-2 (chapter1.3.2.3). None of these proteins was differently regulated upon IL-1 stimulation in KB cells upon oxidative stress treatment (**Fig. 46**). Therefore, it may be assumed that the protective effect of IL-1 was due the *APEX2* induction.

Discussion

Over-expression of *APEX2* protected KB cells against various genotoxic agents. A decreased apoptosis levels was observed in transient transfected HeLa-MR cells after treatment with ionising radiation, H₂O₂ and MMS (**Fig. 49**). Stable *APEX2* over-expression was poorly tolerated by transfected cells since only a single positive clone was selected from over 60 clones picked and tested. The clone grew badly and formed only faint colonies. The same phenotype has been reported for *APE1*. Over-expression of h*APE1* in CHO-9 cells was lethal and no positive clones were obtained. Notably, in contrast to h*APE1* stable over-expression of yeast *APE* rendered mammalian cells resistant to the cell killing effect of MMS, H₂O₂ and the radiomimetic drug bleomycin (Fritz et al., 2003; Tomicic et al., 1997).

Interestingly, a study of knockout mice revealed that the role of *APEX2* might be not limited to BER (Ide et al., 2004). *APEX2* null mice were viable but characterised by moderate dyshematopoiesis and a relatively severe defect in lymphopoiesis. A significant accumulation of both thymocytes and mitogen stimulated splenocytes in G2/M phase was seen in *APEX2* null mice compared with the wild - type, indicating that *APEX2* is required for proper cell cycle progression of proliferating lymphocytes. The deficient thymocytes were also shown to be more sensitive to ionising radiation. However, a sensitive phenotype has not been reported for *APEX2* deficient MEF's, additionally pointing out the particular role of *APEX2* in maturation or activation of the immune system. This is supported by the fact that *APEX2* is inducible by IL-1.

4.4 Outlook

In the study reported here, it was shown that ATM and DSBs are involved in the processing of O⁶MeG lesions. ATM deficient cells were hypersensitive to O⁶MeG inducing agents such as MNNG, MMS and the anti - cancer drug temozolomide. That inclines that additional inhibition of ATM kinase might be a great benefit for tumour therapy with methylating agents. The development of strategies for inactivation of ATM in tumours will be a highly attractive area of research in the close future. The other potential target for supporting chemotherapy with methylating agents is ATR. It was shown that some cellular responses, in particular cell cycle checkpoints activation, upon O⁶MeG induction are independent from ATM and might be controlled by ATR. However, the involvement of ATR in O⁶MeG processing needs further attention.

It was also shown in this study that the inflammatory cytokine IL-1 regulates the expression of the DNA repair gene *APEX2*. Up-regulation of *APEX2* results in decreased sensitivity to oxidative agents, such as ionising radiation and H₂O₂. The IL-1 induced *APEX2* up-regulation

Discussion

might be involved in the development of cellular resistance against oxidative DNA damage. Determination of APEX2 expression in inflammatory and normal tumours will show whether APEX2 is a determinant of drug resistance and, therefore, of importance for cancer therapy.

5 Summary

DNA methylating compounds are widely used as anti-cancer chemotherapeutics. The pharmaceutical critical DNA lesion induced by these drugs is O⁶-methylguanine (O⁶MeG). O⁶MeG is highly mutagenic and genotoxic, by triggering apoptosis. Despite the potency of O⁶MeG to induce cell death, the mechanism of O⁶MeG induced toxicity is still poorly understood. Comparing the response of mouse fibroblasts wild-type (wt) and deficient for ataxia telangiectasia mutant protein (ATM), a kinase responsible for both the recognition and the signalling of DNA double-strand breaks (DSBs), it was shown that ATM deficient cells are more sensitive to the methylating agents N-methyl-N'-nitro-N-nitrosoguanidine (MNNG), methyl methanesulfonate (MMS) and the anti-cancer drug temozolomide, in both colony formation and apoptosis assays. This clearly shows that DSBs are involved in O⁶MeG toxicity. By inactivating the O⁶MeG repair enzyme O⁶-methylguanine-DNA methyltransferase (MGMT) with the specific inhibitor O⁶-benzylguanine (O⁶BG), ATM wt and deficient cells became more sensitive to MNNG and MMS. The opposite effect was observed when over-expressing MGMT in ATM ^{-/-} cells. The results show that O⁶MeG is the critical DNA lesion causing death in ATM cells following MNNG treatment, and is partially responsible for the toxicity observed following MMS treatment. Furthermore, by inhibiting the ATM kinase activity with caffeine, it was shown that the resistance of wt cells to MNNG was due to the kinase activity of ATM, as wt cells underwent more apoptosis following methylating agent treatment in the presence of caffeine. Apoptosis and caspase-3 activation were late events, starting 48h after treatment. This lends support to the model where O⁶MeG lesions are converted into DSBs during replication. As ATM wt and deficient cells showed similar G2/M blockage and Chk1 activation following MNNG and MMS treatment, it was concluded that the protective effect of ATM is not due to cell cycle progression control. The hypersensitivity of ATM deficient cells was accompanied by their inability to activate the anti-apoptotic NFκB pathway.

In a second part of this study, it was shown that the inflammatory cytokine IL-1 up-regulates the DNA repair gene apurinic endonuclease 2 (*APEX2*). Up-regulation of *APEX2* occurred by transcriptional regulation as it was abrogated by actinomycin D. *APEX2* mRNA accumulation was accompanied by increase in *APEX2* protein level. IL-1 induced *APEX2* expression as well as transfection of cells with *APEX2* cDNA positively correlated with a decrease in apoptosis after treatment with genotoxic agents, particularly affecting cell death after H₂O₂. This indicates an involvement of *APEX2* in the BER pathway in cells responding to IL-1.

6 References

- Abraham, R.T. (2001) Cell cycle checkpoint signaling through the ATM and ATR kinases. *Genes Dev*, **15**, 2177-2196.
- Adamson, A.W., Beardsley, D.I., Kim, W.J., Gao, Y., Baskaran, R. and Brown, K.D. (2005) Methylator-induced, mismatch repair-dependent G2 arrest is activated through Chk1 and Chk2. *Mol Biol Cell*, **16**, 1513-1526.
- Adamson, A.W., Kim, W.J., Shangary, S., Baskaran, R. and Brown, K.D. (2002) ATM is activated in response to N-methyl-N'-nitro-N-nitrosoguanidine-induced DNA alkylation. *J Biol Chem*, **277**, 38222-38229.
- Alderton, G.K., Joenje, H., Varon, R., Borglum, A.D., Jeggo, P.A. and O'Driscoll, M. (2004) Seckel syndrome exhibits cellular features demonstrating defects in the ATR-signalling pathway. *Hum Mol Genet*, **13**, 3127-3138.
- Ambs, S., Merriam, W.G., Bennett, W.P., Felley-Bosco, E., Ogunfusika, M.O., Oser, S.M., Klein, S., Shields, P.G., Billiar, T.R. and Harris, C.C. (1998) Frequent nitric oxide synthase-2 expression in human colon adenomas: implication for tumor angiogenesis and colon cancer progression. *Cancer Res*, **58**, 334-341.
- Anasagasti, M.J., Olaso, E., Calvo, F., Mendoza, L., Martin, J.J., Bidaurrezaga, J. and Vidal-Vanaclocha, F. (1997) Interleukin 1-dependent and -independent mouse melanoma metastases. *J Natl Cancer Inst*, **89**, 645-651.
- Bachus, K.E., Doty, E., Haney, A.F. and Weinberg, J.B. (1995) Differential effects of interleukin-1 alpha, tumor necrosis factor-alpha, indomethacin, hydrocortisone, and macrophage co-culture on the proliferation of human fibroblasts and peritoneal mesothelial cells. *J Soc Gynecol Investig*, **2**, 636-642.
- Bakkenist, C.J. and Kastan, M.B. (2003) DNA damage activates ATM through intermolecular autophosphorylation and dimer dissociation. *Nature*, **421**, 499-506.
- Bancroft, C.C., Chen, Z., Yeh, J., Sunwoo, J.B., Yeh, N.T., Jackson, S., Jackson, C. and Van Waes, C. (2002) Effects of pharmacologic antagonists of epidermal growth factor receptor, PI3K and MEK signal kinases on NF-kappaB and AP-1 activation and IL-8 and VEGF expression in human head and neck squamous cell carcinoma lines. *Int J Cancer*, **99**, 538-548.
- Banin, S., Moyal, L., Shieh, S., Taya, Y., Anderson, C.W., Chessa, L., Smorodinsky, N.I., Prives, C., Reiss, Y., Shiloh, Y. and Ziv, Y. (1998) Enhanced phosphorylation of p53 by ATM in response to DNA damage. *Science*, **281**, 1674-1677.
- Barfknecht, T.R. and Little, J.B. (1982) Hypersensitivity of ataxia telangiectasia skin fibroblasts to DNA alkylating agents. *Mutat Res*, **94**, 369-382.
- Barlow, C., Hirotsune, S., Paylor, R., Liyanage, M., Eckhaus, M., Collins, F., Shiloh, Y., Crawley, J.N., Ried, T., Tagle, D. and Wynshaw-Boris, A. (1996) Atm-deficient mice: a paradigm of ataxia telangiectasia. *Cell*, **86**, 159-171.

References

- Bar-Shira, A., Rashi-Elkeles, S., Zlochover, L., Moyal, L., Smorodinsky, N.I., Seger, R. and Shiloh, Y. (2002) ATM-dependent activation of the gene encoding MAP kinase phosphatase 5 by radiomimetic DNA damage. *Oncogene*, **21**, 849-855.
- Baskaran, R., Wood, L.D., Whitaker, L.L., Canman, C.E., Morgan, S.E., Xu, Y., Barlow, C., Baltimore, D., Wynshaw-Boris, A., Kastan, M.B. and Wang, J.Y. (1997) Ataxia telangiectasia mutant protein activates c-Abl tyrosine kinase in response to ionizing radiation. *Nature*, **387**, 516-519.
- Becker, K., Dosch, J., Gregel, C.M., Martin, B.A. and Kaina, B. (1996) Targeted expression of human O(6)-methylguanine-DNA methyltransferase (MGMT) in transgenic mice protects against tumor initiation in two-stage skin carcinogenesis. *Cancer Res*, **56**, 3244-3249.
- Becker, K., Gregel, C., Fricke, C., Komitowski, D., Dosch, J. and Kaina, B. (2003) DNA repair protein MGMT protects against N-methyl-N-nitrosourea-induced conversion of benign into malignant tumors. *Carcinogenesis*, **24**, 541-546.
- Becker, K., Gregel, C.M. and Kaina, B. (1997) The DNA repair protein O6-methylguanine-DNA methyltransferase protects against skin tumor formation induced by antineoplastic chloroethylnitrosourea. *Cancer Res*, **57**, 3335-3338.
- Benchekroun, M.N., Parker, R., Dabholkar, M., Reed, E. and Sinha, B.K. (1995) Effects of interleukin-1 alpha on DNA repair in human ovarian carcinoma (NIH:OVCAR-3) cells: implications in the mechanism of sensitization of cis-diamminedichloroplatinum(II). *Mol Pharmacol*, **47**, 1255-1260.
- Beranek, D.T. (1990) Distribution of methyl and ethyl adducts following alkylation with monofunctional alkylating agents. *Mutat Res*, **231**, 11-30.
- Bhandoola, A., Dolnick, B., Fayad, N., Nussenzweig, A. and Singer, A. (2000) Immature thymocytes undergoing receptor rearrangements are resistant to an Atm-dependent death pathway activated in mature T cells by double-stranded DNA breaks. *J Exp Med*, **192**, 891-897.
- Billiau, A. (1996) Interferon-gamma: biology and role in pathogenesis. *Adv Immunol*, **62**, 61-130.
- Binoux, M. (1997) GH, IGFs, IGF-binding protein-3 and acid-labile subunit: what is the pecking order? *Eur J Endocrinol*, **137**, 605-609.
- Biswas, T., Ramana, C.V., Srinivasan, G., Boldogh, I., Hazra, T.K., Chen, Z., Tano, K., Thompson, E.B. and Mitra, S. (1999) Activation of human O6-methylguanine-DNA methyltransferase gene by glucocorticoid hormone. *Oncogene*, **18**, 525-532.
- Bjorkdahl, O., Wingren, A.G., Hedhund, G., Ohlsson, L. and Dohlsten, M. (1997) Gene transfer of a hybrid interleukin-1 beta gene to B16 mouse melanoma recruits leucocyte subsets and reduces tumour growth in vivo. *Cancer Immunol Immunother*, **44**, 273-281.

References

- Blasina, A., Price, B.D., Turenne, G.A. and McGowan, C.H. (1999) Caffeine inhibits the checkpoint kinase ATM. *Curr Biol*, **9**, 1135-1138.
- Bomalaski, J.S., Steiner, M.R., Simon, P.L. and Clark, M.A. (1992) IL-1 increases phospholipase A2 activity, expression of phospholipase A2-activating protein, and release of linoleic acid from the murine T helper cell line EL-4. *J Immunol*, **148**, 155-160.
- Bradford, M.M. (1976) A rapid and sensitive method for the quantitation of microgram quantities of protein utilizing the principle of protein-dye binding. *Anal Biochem*, **72**, 248-254.
- Branch, P., Aquilina, G., Bignami, M. and Karran, P. (1993) Defective mismatch binding and a mutator phenotype in cells tolerant to DNA damage. *Nature*, **362**, 652-654.
- Brown, K.D., Ziv, Y., Sadanandan, S.N., Chessa, L., Collins, F.S., Shiloh, Y. and Tagle, D.A. (1997) The ataxia-telangiectasia gene product, a constitutively expressed nuclear protein that is not up-regulated following genome damage. *Proc Natl Acad Sci U S A*, **94**, 1840-1845.
- Burma, S., Chen, B.P., Murphy, M., Kurimasa, A. and Chen, D.J. (2001) ATM phosphorylates histone H2AX in response to DNA double-strand breaks. *J Biol Chem*, **276**, 42462-42467.
- Canman, C.E., Lim, D.S., Cimprich, K.A., Taya, Y., Tamai, K., Sakaguchi, K., Appella, E., Kastan, M.B. and Siliciano, J.D. (1998) Activation of the ATM kinase by ionizing radiation and phosphorylation of p53. *Science*, **281**, 1677-1679.
- Caporali, S., Falcinelli, S., Starace, G., Russo, M.T., Bonmassar, E., Jiricny, J. and D'Atri, S. (2004) DNA damage induced by temozolomide signals to both ATM and ATR: role of the mismatch repair system. *Mol Pharmacol*, **66**, 478-491.
- Carney, J.P., Maser, R.S., Olivares, H., Davis, E.M., Le Beau, M., Yates, J.R., 3rd, Hays, L., Morgan, W.F. and Petrini, J.H. (1998) The hMre11/hRad50 protein complex and Nijmegen breakage syndrome: linkage of double-strand break repair to the cellular DNA damage response. *Cell*, **93**, 477-486.
- Chan, C.L., Wu, Z., Eastman, A. and Bresnick, E. (1992) Irradiation-induced expression of O6-methylguanine-DNA methyltransferase in mammalian cells. *Cancer Res*, **52**, 1804-1809.
- Chan, J.M., Stampfer, M.J., Ma, J., Gann, P., Gaziano, J.M., Pollak, M. and Giovannucci, E. (2002) Insulin-like growth factor-I (IGF-I) and IGF binding protein-3 as predictors of advanced-stage prostate cancer. *J Natl Cancer Inst*, **94**, 1099-1106.
- Chao, C.C., Lokensgard, J.R., Sheng, W.S., Hu, S. and Peterson, P.K. (1997) IL-1-induced iNOS expression in human astrocytes via NF-kappa B. *Neuroreport*, **8**, 3163-3166.
- Chen, G. and Lee, E. (1996) The product of the ATM gene is a 370-kDa nuclear phosphoprotein. *J Biol Chem*, **271**, 33693-33697.

References

- Chen, G., Yuan, S.S., Liu, W., Xu, Y., Trujillo, K., Song, B., Cong, F., Goff, S.P., Wu, Y., Arlinghaus, R., Baltimore, D., Gasser, P.J., Park, M.S., Sung, P. and Lee, E.Y. (1999a) Radiation-induced assembly of Rad51 and Rad52 recombination complex requires ATM and c-Abl. *J Biol Chem*, **274**, 12748-12752.
- Chen, Z., Malhotra, P.S., Thomas, G.R., Ondrey, F.G., Duffey, D.C., Smith, C.W., Enamorado, I., Yeh, N.T., Kroog, G.S., Rudy, S., McCullagh, L., Mousa, S., Quezado, M., Herscher, L.L. and Van Waes, C. (1999b) Expression of proinflammatory and proangiogenic cytokines in patients with head and neck cancer. *Clin Cancer Res*, **5**, 1369-1379.
- Chizzonite, R., Truitt, T., Kilian, P.L., Stern, A.S., Nunes, P., Parker, K.P., Kaffka, K.L., Chua, A.O., Lugg, D.K. and Gubler, U. (1989) Two high-affinity interleukin 1 receptors represent separate gene products. *Proc Natl Acad Sci U S A*, **86**, 8029-8033.
- Chong, M.J., Murray, M.R., Gosink, E.C., Russell, H.R., Srinivasan, A., Kapsetaki, M., Korsmeyer, S.J. and McKinnon, P.J. (2000) Atm and Bax cooperate in ionizing radiation-induced apoptosis in the central nervous system. *Proc Natl Acad Sci U S A*, **97**, 889-894.
- Christmann, M., Tomicic, M.T., Roos, W.P. and Kaina, B. (2003) Mechanisms of human DNA repair: an update. *Toxicology*, **193**, 3-34.
- Citron, M., Decker, R., Chen, S., Schneider, S., Graver, M., Kleynerman, L., Kahn, L.B., White, A., Schoenhaus, M. and Yarosh, D. (1991) O6-methylguanine-DNA methyltransferase in human normal and tumor tissue from brain, lung, and ovary. *Cancer Res*, **51**, 4131-4134.
- Collett-Solberg, P.F. and Cohen, P. (2000) Genetics, chemistry, and function of the IGF/IGFBP system. *Endocrine*, **12**, 121-136.
- Colotta, F., Re, F., Muzio, M., Bertini, R., Polentarutti, N., Sironi, M., Giri, J.G., Dower, S.K., Sims, J.E. and Mantovani, A. (1993) Interleukin-1 type II receptor: a decoy target for IL-1 that is regulated by IL-4. *Science*, **261**, 472-475.
- Corbett, J.A., Kwon, G., Marino, M.H., Rodi, C.P., Sullivan, P.M., Turk, J. and McDaniel, M.L. (1996) Tyrosine kinase inhibitors prevent cytokine-induced expression of iNOS and COX-2 by human islets. *Am J Physiol*, **270**, C1581-1587.
- Corsini, E., Sangha, N. and Feldman, S.R. (1997) Epidermal stratification reduces the effects of UVB (but not UVA) on keratinocyte cytokine production and cytotoxicity. *Photodermatol Photoimmunol Photomed*, **13**, 147-152.
- Costantino, A., Vinci, C., Mineo, R., Frasca, F., Pandini, G., Milazzo, G., Vigneri, R. and Belfiore, A. (1996) Interleukin-1 blocks insulin and insulin-like growth factor-stimulated growth in MCF-7 human breast cancer cells by inhibiting receptor tyrosine kinase activity. *Endocrinology*, **137**, 4100-4107.
- Costes, V., Portier, M., Lu, Z.Y., Rossi, J.F., Bataille, R. and Klein, B. (1998) Interleukin-1 in multiple myeloma: producer cells and their role in the control of IL-6 production. *Br J Haematol*, **103**, 1152-1160.

References

- Daniels, D.S., Mol, C.D., Arvai, A.S., Kanugula, S., Pegg, A.E. and Tainer, J.A. (2000) Active and alkylated human AGT structures: a novel zinc site, inhibitor and extrahelical base binding. *Embo J*, **19**, 1719-1730.
- Datta, S.R., Dudek, H., Tao, X., Masters, S., Fu, H., Gotoh, Y. and Greenberg, M.E. (1997) Akt phosphorylation of BAD couples survival signals to the cell-intrinsic death machinery. *Cell*, **91**, 231-241.
- Debiak, M., Nikolova, T. and Kaina, B. (2004) Loss of ATM sensitizes against O6-methylguanine triggered apoptosis, SCEs and chromosomal aberrations. *DNA Repair (Amst)*, **3**, 359-368.
- Diem, R., Hobom, M., Grotzsch, P., Kramer, B. and Bahr, M. (2003) Interleukin-1 beta protects neurons via the interleukin-1 (IL-1) receptor-mediated Akt pathway and by IL-1 receptor-independent decrease of transmembrane currents in vivo. *Mol Cell Neurosci*, **22**, 487-500.
- Dinarello, C.A. (1996) Biologic basis for interleukin-1 in disease. *Blood*, **87**, 2095-2147.
- Dinarello, C.A., Ikejima, T., Warner, S.J., Orencole, S.F., Lonnemann, G., Cannon, J.G. and Libby, P. (1987) Interleukin 1 induces interleukin 1. I. Induction of circulating interleukin 1 in rabbits in vivo and in human mononuclear cells in vitro. *J Immunol*, **139**, 1902-1910.
- Dosch, J., Christmann, M. and Kaina, B. (1998) Mismatch G-T binding activity and MSH2 expression is quantitatively related to sensitivity of cells to methylating agents. *Carcinogenesis*, **19**, 567-573.
- Dower, S.K., Sims, J.E., Cerretti, D.P. and Bird, T.A. (1992) The interleukin-1 system: receptors, ligands and signals. *Chem Immunol*, **51**, 33-64.
- Duckett, D.R., Drummond, J.T., Murchie, A.I., Reardon, J.T., Sancar, A., Lilley, D.M. and Modrich, P. (1996) Human MutSalpha recognizes damaged DNA base pairs containing O6-methylguanine, O4-methylthymine, or the cisplatin-d(GpG) adduct. *Proc Natl Acad Sci U S A*, **93**, 6443-6447.
- Dunkern, T., Roos, W. and Kaina, B. (2003) Apoptosis induced by MNNG in human TK6 lymphoblastoid cells is p53 and Fas/CD95/Apo-1 related. *Mutat Res*, **544**, 167-172.
- Dunn, S.E., Ehrlich, M., Sharp, N.J., Reiss, K., Solomon, G., Hawkins, R., Baserga, R. and Barrett, J.C. (1998) A dominant negative mutant of the insulin-like growth factor-I receptor inhibits the adhesion, invasion, and metastasis of breast cancer. *Cancer Res*, **58**, 3353-3361.
- Dupraz, P., Cottet, S., Hamburger, F., Dolci, W., Felley-Bosco, E. and Thorens, B. (2000) Dominant negative MyD88 proteins inhibit interleukin-1beta /interferon-gamma - mediated induction of nuclear factor kappa B-dependent nitrite production and apoptosis in beta cells. *J Biol Chem*, **275**, 37672-37678.
- Ehrlich, L.C., Peterson, P.K. and Hu, S. (1999) Interleukin (IL)-1beta-mediated apoptosis of human astrocytes. *Neuroreport*, **10**, 1849-1852.

References

- el-Deiry, W.S., Harper, J.W., O'Connor, P.M., Velculescu, V.E., Canman, C.E., Jackman, J., Pietenpol, J.A., Burrell, M., Hill, D.E., Wang, Y. and et al. (1994) WAF1/CIP1 is induced in p53-mediated G1 arrest and apoptosis. *Cancer Res*, **54**, 1169-1174.
- Ellingsen, E., Morath, S., Flo, T., Schromm, A., Hartung, T., Thiernemann, C., Espevik, T., Golenbock, D., Foster, D., Solberg, R., Aasen, A. and Wang, J. (2002) Induction of cytokine production in human T cells and monocytes by highly purified lipoteichoic acid: involvement of Toll-like receptors and CD14. *Med Sci Monit*, **8**, BR149-156.
- Elson, A., Wang, Y., Daugherty, C.J., Morton, C.C., Zhou, F., Campos-Torres, J. and Leder, P. (1996) Pleiotropic defects in ataxia-telangiectasia protein-deficient mice. *Proc Natl Acad Sci U S A*, **93**, 13084-13089.
- Endres, S., van der Meer, J.W. and Dinarello, C.A. (1987) Interleukin-1 in the pathogenesis of fever. *Eur J Clin Invest*, **17**, 469-474.
- Enns, L., Barley, R.D., Paterson, M.C. and Mirzayans, R. (1998) Radiosensitivity in ataxia telangiectasia fibroblasts is not associated with deregulated apoptosis. *Radiat Res*, **150**, 11-16.
- Estrov, Z., Manna, S.K., Harris, D., Van, Q., Estey, E.H., Kantarjian, H.M., Talpaz, M. and Aggarwal, B.B. (1999) Phenylarsine oxide blocks interleukin-1beta-induced activation of the nuclear transcription factor NF-kappaB, inhibits proliferation, and induces apoptosis of acute myelogenous leukemia cells. *Blood*, **94**, 2844-2853.
- Fedier, A., Schlamming, M., Schwarz, V.A., Haller, U., Howell, S.B. and Fink, D. (2003) Loss of atm sensitises p53-deficient cells to topoisomerase poisons and antimetabolites. *Ann Oncol*, **14**, 938-945.
- Fernandez-Capetillo, O., Lee, A., Nussenzweig, M. and Nussenzweig, A. (2004) H2AX: the histone guardian of the genome. *DNA Repair (Amst)*, **3**, 959-967.
- Fischer-Posovszky, P., Tornqvist, H., Debatin, K.M. and Wabitsch, M. (2004) Inhibition of death-receptor mediated apoptosis in human adipocytes by the insulin-like growth factor I (IGF-I)/IGF-I receptor autocrine circuit. *Endocrinology*, **145**, 1849-1859.
- Fritz, G. (2000) Human APE/Ref-1 protein. *Int J Biochem Cell Biol*, **32**, 925-929.
- Fritz, G., Grosch, S., Tomicic, M. and Kaina, B. (2003) APE/Ref-1 and the mammalian response to genotoxic stress. *Toxicology*, **193**, 67-78.
- Fritz, G. and Kaina, B. (1992) Stress factors affecting expression of O6-methylguanine-DNA methyltransferase mRNA in rat hepatoma cells. *Biochim Biophys Acta*, **1171**, 35-40.
- Fritz, G., Tano, K., Mitra, S. and Kaina, B. (1991) Inducibility of the DNA repair gene encoding O6-methylguanine-DNA methyltransferase in mammalian cells by DNA-damaging treatments. *Mol Cell Biol*, **11**, 4660-4668.

References

- Garcia-Monzon, C., Moreno-Otero, R., Pajares, J.M., Garcia-Sanchez, A., Lopez-Botet, M., de Landazuri, M.O. and Sanchez-Madrid, F. (1990) Expression of a novel activation antigen on intrahepatic CD8+ T lymphocytes in viral chronic active hepatitis. *Gastroenterology*, **98**, 1029-1035.
- Gatei, M., Sloper, K., Sorensen, C., Syljuasen, R., Falck, J., Hobson, K., Savage, K., Lukas, J., Zhou, B.B., Bartek, J. and Khanna, K.K. (2003) Ataxia-telangiectasia-mutated (ATM) and NBS1-dependent phosphorylation of Chk1 on Ser-317 in response to ionizing radiation. *J Biol Chem*, **278**, 14806-14811.
- Gatti, R.A., Berkel, I., Boder, E., Braedt, G., Charmley, P., Concannon, P., Ersoy, F., Foroud, T., Jaspers, N.G., Lange, K. and et al. (1988) Localization of an ataxia-telangiectasia gene to chromosome 11q22-23. *Nature*, **336**, 577-580.
- Gerson, S.L. (2002) Clinical relevance of MGMT in the treatment of cancer. *J Clin Oncol*, **20**, 2388-2399.
- Gerson, S.L. (2004) MGMT: its role in cancer aetiology and cancer therapeutics. *Nat Rev Cancer*, **4**, 296-307.
- Gerson, S.L., Trey, J.E., Miller, K. and Berger, N.A. (1986) Comparison of O6-alkylguanine-DNA alkyltransferase activity based on cellular DNA content in human, rat and mouse tissues. *Carcinogenesis*, **7**, 745-749.
- Giovannucci, E. (2001) Insulin, insulin-like growth factors and colon cancer: a review of the evidence. *J Nutr*, **131**, 3109S-3120S.
- Glassner, B.J., Weeda, G., Allan, J.M., Broekhof, J.L., Carls, N.H., Donker, I., Engelward, B.P., Hampson, R.J., Hersmus, R., Hickman, M.J., Roth, R.B., Warren, H.B., Wu, M.M., Hoeijmakers, J.H. and Samson, L.D. (1999) DNA repair methyltransferase (Mgmt) knockout mice are sensitive to the lethal effects of chemotherapeutic alkylating agents. *Mutagenesis*, **14**, 339-347.
- Goldberg, M., Stucki, M., Falck, J., D'Amours, D., Rahman, D., Pappin, D., Bartek, J. and Jackson, S.P. (2003) MDC1 is required for the intra-S-phase DNA damage checkpoint. *Nature*, **421**, 952-956.
- Goldmacher, V.S., Cuzick, R.A., Jr. and Thilly, W.G. (1986) Isolation and partial characterization of human cell mutants differing in sensitivity to killing and mutation by methylnitrosourea and N-methyl-N'-nitro-N-nitrosoguanidine. *J Biol Chem*, **261**, 12462-12471.
- Greenfeder, S.A., Nunes, P., Kwee, L., Labow, M., Chizzonite, R.A. and Ju, G. (1995) Molecular cloning and characterization of a second subunit of the interleukin 1 receptor complex. *J Biol Chem*, **270**, 13757-13765.
- Griswold, D.E., Connor, J.R., Dalton, B.J., Lee, J.C., Simon, P., Hillegass, L., Sieg, D.J. and Hanna, N. (1991) Activation of the IL-1 gene in UV-irradiated mouse skin: association with inflammatory sequelae and pharmacologic intervention. *J Invest Dermatol*, **97**, 1019-1023.

References

- Grombacher, T., Mitra, S. and Kaina, B. (1996) Induction of the alkyltransferase (MGMT) gene by DNA damaging agents and the glucocorticoid dexamethasone and comparison with the response of base excision repair genes. *Carcinogenesis*, **17**, 2329-2336.
- Ha, L., Ceryak, S. and Patierno, S.R. (2003) Chromium (VI) activates ataxia telangiectasia mutated (ATM) protein. Requirement of ATM for both apoptosis and recovery from terminal growth arrest. *J Biol Chem*, **278**, 17885-17894.
- Haas, S. and Kaina, B. (1995) c-Fos is involved in the cellular defence against the genotoxic effect of UV radiation. *Carcinogenesis*, **16**, 985-991.
- Hadi, M.Z., Ginalski, K., Nguyen, L.H. and Wilson, D.M., 3rd. (2002) Determinants in nuclease specificity of Ape1 and Ape2, human homologues of Escherichia coli exonuclease III. *J Mol Biol*, **316**, 853-866.
- Hankinson, S.E., Willett, W.C., Colditz, G.A., Hunter, D.J., Michaud, D.S., Deroo, B., Rosner, B., Speizer, F.E. and Pollak, M. (1998) Circulating concentrations of insulin-like growth factor-I and risk of breast cancer. *Lancet*, **351**, 1393-1396.
- Hannan, M.A., Hellani, A., Al-Khodairy, F.M., Kunhi, M., Siddiqui, Y., Al-Yussef, N., Pangué-Cruz, N., Siewertsen, M., Al-Ahdal, M.N. and Aboussekhra, A. (2002) Deficiency in the repair of UV-induced DNA damage in human skin fibroblasts compromised for the ATM gene. *Carcinogenesis*, **23**, 1617-1624.
- Harper, J.W., Adami, G.R., Wei, N., Keyomarsi, K. and Elledge, S.J. (1993) The p21 Cdk-interacting protein Cip1 is a potent inhibitor of G1 cyclin-dependent kinases. *Cell*, **75**, 805-816.
- Harris, L.C., Potter, P.M., Tano, K., Shiota, S., Mitra, S. and Brent, T.P. (1991) Characterization of the promoter region of the human O6-methylguanine-DNA methyltransferase gene. *Nucleic Acids Res*, **19**, 6163-6167.
- Hata, K., Van Thiel, D.H., Herberman, R.B. and Whiteside, T.L. (1992) Phenotypic and functional characteristics of lymphocytes isolated from liver biopsy specimens from patients with active liver disease. *Hepatology*, **15**, 816-823.
- Heinzelmann-Schwarz, V., Fedier, A., Hornung, R., Walt, H., Haller, U. and Fink, D. (2003) Role of p53 and ATM in photodynamic therapy-induced apoptosis. *Lasers Surg Med*, **33**, 182-189.
- Heron-Milhavet, L., Karas, M., Goldsmith, C.M., Baum, B.J. and LeRoith, D. (2001) Insulin-like growth factor-I (IGF-I) receptor activation rescues UV-damaged cells through a p38 signaling pathway. Potential role of the IGF-I receptor in DNA repair. *J Biol Chem*, **276**, 18185-18192.
- Heron-Milhavet, L. and LeRoith, D. (2002) Insulin-like growth factor I induces MDM2-dependent degradation of p53 via the p38 MAPK pathway in response to DNA damage. *J Biol Chem*, **277**, 15600-15606.

References

- Herzog, K.H., Chong, M.J., Kapsetaki, M., Morgan, J.I. and McKinnon, P.J. (1998) Requirement for Atm in ionizing radiation-induced cell death in the developing central nervous system. *Science*, **280**, 1089-1091.
- Hoar, D.I. and Sargent, P. (1976) Chemical mutagen hypersensitivity in ataxia telangiectasia. *Nature*, **261**, 590-592.
- Hofseth, L.J., Saito, S., Hussain, S.P., Espey, M.G., Miranda, K.M., Araki, Y., Jhappan, C., Higashimoto, Y., He, P., Linke, S.P., Quezado, M.M., Zurer, I., Rotter, V., Wink, D.A., Appella, E. and Harris, C.C. (2003) Nitric oxide-induced cellular stress and p53 activation in chronic inflammation. *Proc Natl Acad Sci U S A*, **100**, 143-148.
- Holman, S.R. and Baxter, R.C. (1996) Insulin-like growth factor binding protein-3: factors affecting binary and ternary complex formation. *Growth Regul*, **6**, 42-47.
- Honma, S., Shimodaira, K., Shimizu, Y., Tsuchiya, N., Saito, H., Yanaihara, T. and Okai, T. (2002) The influence of inflammatory cytokines on estrogen production and cell proliferation in human breast cancer cells. *Endocr J*, **49**, 371-377.
- Hu, S., Peterson, P.K. and Chao, C.C. (1997) Cytokine-mediated neuronal apoptosis. *Neurochem Int*, **30**, 427-431.
- Huang, Y.T., Sheen, T.S., Chen, C.L., Lu, J., Chang, Y., Chen, J.Y. and Tsai, C.H. (1999) Profile of cytokine expression in nasopharyngeal carcinomas: a distinct expression of interleukin 1 in tumor and CD4+ T cells. *Cancer Res*, **59**, 1599-1605.
- Ide, Y., Tsuchimoto, D., Tominaga, Y., Iwamoto, Y. and Nakabeppu, Y. (2003) Characterization of the genomic structure and expression of the mouse Apex2 gene. *Genomics*, **81**, 47-57.
- Ide, Y., Tsuchimoto, D., Tominaga, Y., Nakashima, M., Watanabe, T., Sakumi, K., Ohno, M. and Nakabeppu, Y. (2004) Growth retardation and dyslymphopoiesis accompanied by G2/M arrest in APEX2-null mice. *Blood*, **104**, 4097-4103.
- Ioannou, Y.A. and Chen, F.W. (1996) Quantitation of DNA fragmentation in apoptosis. *Nucleic Acids Res*, **24**, 992-993.
- Irwin, M., Marin, M.C., Phillips, A.C., Seelan, R.S., Smith, D.I., Liu, W., Flores, E.R., Tsai, K.Y., Jacks, T., Vousden, K.H. and Kaelin, W.G., Jr. (2000) Role for the p53 homologue p73 in E2F-1-induced apoptosis. *Nature*, **407**, 645-648.
- Ito, R., Kitadai, Y., Kyo, E., Yokozaki, H., Yasui, W., Yamashita, U., Nikai, H. and Tahara, E. (1993) Interleukin 1 alpha acts as an autocrine growth stimulator for human gastric carcinoma cells. *Cancer Res*, **53**, 4102-4106.
- Jerome, L., Shiry, L. and Leyland-Jones, B. (2003) Deregulation of the IGF axis in cancer: epidemiological evidence and potential therapeutic interventions. *Endocr Relat Cancer*, **10**, 561-578.

References

- Jimi, E., Nakamura, I., Ikebe, T., Akiyama, S., Takahashi, N. and Suda, T. (1998) Activation of NF-kappaB is involved in the survival of osteoclasts promoted by interleukin-1. *J Biol Chem*, **273**, 8799-8805.
- Jin, L., Yuan, R.Q., Fuchs, A., Yao, Y., Joseph, A., Schwall, R., Schnitt, S.J., Guida, A., Hastings, H.M., Andres, J., Turkel, G., Polverini, P.J., Goldberg, I.D. and Rosen, E.M. (1997) Expression of interleukin-1beta in human breast carcinoma. *Cancer*, **80**, 421-434.
- Jobling, S.A., Auron, P.E., Gurka, G., Webb, A.C., McDonald, B., Rosenwasser, L.J. and Gehrke, L. (1988) Biological activity and receptor binding of human prointerleukin-1 beta and subpeptides. *J Biol Chem*, **263**, 16372-16378.
- Jung, M. and Dritschilo, A. (2001) NF-kappa B signaling pathway as a target for human tumor radiosensitization. *Semin Radiat Oncol*, **11**, 346-351.
- Jung, M., Kondratyev, A., Lee, S.A., Dimtchev, A. and Dritschilo, A. (1997) ATM gene product phosphorylates I kappa B-alpha. *Cancer Res*, **57**, 24-27.
- Kaina, B. (2004) Mechanisms and consequences of methylating agent-induced SCEs and chromosomal aberrations: a long road traveled and still a far way to go. *Cytogenet Genome Res*, **104**, 77-86.
- Kaina, B. and Christmann, M. (2002) DNA repair in resistance to alkylating anticancer drugs. *Int J Clin Pharmacol Ther*, **40**, 354-367.
- Kaina, B., Fritz, G. and Coquerelle, T. (1993) Contribution of O6-alkylguanine and N-alkylpurines to the formation of sister chromatid exchanges, chromosomal aberrations, and gene mutations: new insights gained from studies of genetically engineered mammalian cell lines. *Environ Mol Mutagen*, **22**, 283-292.
- Kaina, B., Fritz, G., Mitra, S. and Coquerelle, T. (1991) Transfection and expression of human O6-methylguanine-DNA methyltransferase (MGMT) cDNA in Chinese hamster cells: the role of MGMT in protection against the genotoxic effects of alkylating agents. *Carcinogenesis*, **12**, 1857-1867.
- Kaina, B., Ziouta, A., Ochs, K. and Coquerelle, T. (1997) Chromosomal instability, reproductive cell death and apoptosis induced by O6-methylguanine in Mex-, Mex+ and methylation-tolerant mismatch repair compromised cells: facts and models. *Mutat Res*, **381**, 227-241.
- Karran, P. and Bignami, M. (1992) Self-destruction and tolerance in resistance of mammalian cells to alkylation damage. *Nucleic Acids Res*, **20**, 2933-2940.
- Kastan, M.B., Zhan, Q., el-Deiry, W.S., Carrier, F., Jacks, T., Walsh, W.V., Plunkett, B.S., Vogelstein, B. and Fornace, A.J., Jr. (1992) A mammalian cell cycle checkpoint pathway utilizing p53 and GADD45 is defective in ataxia-telangiectasia. *Cell*, **71**, 587-597.

References

- Khanna, K.K., Keating, K.E., Kozlov, S., Scott, S., Gatei, M., Hobson, K., Taya, Y., Gabrielli, B., Chan, D., Lees-Miller, S.P. and Lavin, M.F. (1998) ATM associates with and phosphorylates p53: mapping the region of interaction. *Nat Genet*, **20**, 398-400.
- Khanna, K.K. and Lavin, M.F. (1993) Ionizing radiation and UV induction of p53 protein by different pathways in ataxia-telangiectasia cells. *Oncogene*, **8**, 3307-3312.
- Khanna, K.K., Lavin, M.F., Jackson, S.P. and Mulhern, T.D. (2001) ATM, a central controller of cellular responses to DNA damage. *Cell Death Differ*, **8**, 1052-1065.
- Kim, S.T., Lim, D.S., Canman, C.E. and Kastan, M.B. (1999) Substrate specificities and identification of putative substrates of ATM kinase family members. *J Biol Chem*, **274**, 37538-37543.
- Kimata, H. and Fujimoto, M. (1994) Growth hormone and insulin-like growth factor I induce immunoglobulin (Ig)E and IgG4 production by human B cells. *J Exp Med*, **180**, 727-732.
- Knupfer, H., Stanitz, D., Brauckhoff, M., Schmidt, R., Knupfer, M.M. and Preiss, R. (2001) IL-1 receptor type I expression in breast cancer. *Breast*, **10**, 411-415.
- Kokkinakis, D.M., Ahmed, M.M., Delgado, R., Fruitwala, M.M., Mohiuddin, M. and Albores-Saavedra, J. (1997) Role of O6-methylguanine-DNA methyltransferase in the resistance of pancreatic tumors to DNA alkylating agents. *Cancer Res*, **57**, 5360-5368.
- Kol, S., Ben-Shlomo, I., Ando, M., Payne, D.W. and Adashi, E.Y. (1997) Interleukin-1 beta stimulates ovarian phosphoipase A2 (PLA2) expression and activity: up-regulation of both secretory and cytosolic PLA2. *Endocrinology*, **138**, 314-321.
- Kooijman, R.K., Scholtens, L.E., Rijkers, G.T. and Zegers, B.J. (1995) Differential expression of type I insulin-like growth factor receptors in different stages of human T cells. *Eur J Immunol*, **25**, 931-935.
- Kool, J., Hamdi, M., Cornelissen-Steijger, P., van der Eb, A.J., Terleth, C. and van Dam, H. (2003) Induction of ATF3 by ionizing radiation is mediated via a signaling pathway that includes ATM, Nibrin1, stress-induced MAPkinases and ATF-2. *Oncogene*, **22**, 4235-4242.
- Kothny-Wilkes, G., Kulms, D., Poppelmann, B., Luger, T.A., Kubin, M. and Schwarz, T. (1998) Interleukin-1 protects transformed keratinocytes from tumor necrosis factor-related apoptosis-inducing ligand. *J Biol Chem*, **273**, 29247-29253.
- Koyama, N., Harada, N., Takahashi, T., Mita, S., Okamura, H., Tominaga, A. and Takatsu, K. (1988) Role of recombinant interleukin-1 compared to recombinant T-cell replacing factor/interleukin-5 in B-cell differentiation. *Immunology*, **63**, 277-283.
- Kozlov, S., Gueven, N., Keating, K., Ramsay, J. and Lavin, M.F. (2003) ATP activates ataxia-telangiectasia mutated (ATM) in vitro. Importance of autophosphorylation. *J Biol Chem*, **278**, 9309-9317.

References

- Kuhn, K., Hashimoto, S. and Lotz, M. (2000) IL-1 beta protects human chondrocytes from CD95-induced apoptosis. *J Immunol*, **164**, 2233-2239.
- Kulik, G., Klippel, A. and Weber, M.J. (1997) Antiapoptotic signalling by the insulin-like growth factor I receptor, phosphatidylinositol 3-kinase, and Akt. *Mol Cell Biol*, **17**, 1595-1606.
- Kumar, S., Votta, B.J., Rieman, D.J., Badger, A.M., Gowen, M. and Lee, J.C. (2001) IL-1- and TNF-induced bone resorption is mediated by p38 mitogen activated protein kinase. *J Cell Physiol*, **187**, 294-303.
- Kupper, T.S. and Groves, R.W. (1995) The interleukin-1 axis and cutaneous inflammation. *J Invest Dermatol*, **105**, 62S-66S.
- Kurt-Jones, E.A., Beller, D.I., Mizel, S.B. and Unanue, E.R. (1985) Identification of a membrane-associated interleukin 1 in macrophages. *Proc Natl Acad Sci U S A*, **82**, 1204-1208.
- Kurtz, A., Jelkmann, W. and Bauer, C. (1982) A new candidate for the regulation of erythropoiesis. Insulin-like growth factor I. *FEBS Lett*, **149**, 105-108.
- Kurzrock, R., Wetzler, M., Estrov, Z. and Talpaz, M. (1995) Interleukin-1 and its inhibitors: a biologic and therapeutic model for the role of growth regulatory factors in leukemias. *Cytokines Mol Ther*, **1**, 177-184.
- Kusano, K., Miyaura, C., Inada, M., Tamura, T., Ito, A., Nagase, H., Kamei, K. and Suda, T. (1998) Regulation of matrix metalloproteinases (MMP-2, -3, -9, and -13) by interleukin-1 and interleukin-6 in mouse calvaria: association of MMP induction with bone resorption. *Endocrinology*, **139**, 1338-1345.
- Lachman, L.B., Dinarello, C.A., Llansa, N.D. and Fidler, I.J. (1986) Natural and recombinant human interleukin 1-beta is cytotoxic for human melanoma cells. *J Immunol*, **136**, 3098-3102.
- Lackinger, D. and Kaina, B. (2000) Primary mouse fibroblasts deficient for c-Fos, p53 or for both proteins are hypersensitive to UV light and alkylating agent-induced chromosomal breakage and apoptosis. *Mutat Res*, **457**, 113-123.
- Laemmli, U.K. (1970) Cleavage of structural proteins during the assembly of the head of bacteriophage T4. *Nature*, **227**, 680-685.
- Lage, H., Christmann, M., Kern, M.A., Dietel, M., Pick, M., Kaina, B. and Schadendorf, D. (1999) Expression of DNA repair proteins hMSH2, hMSH6, hMLH1, O6-methylguanine-DNA methyltransferase and N-methylpurine-DNA glycosylase in melanoma cells with acquired drug resistance. *Int J Cancer*, **80**, 744-750.
- Lavin, M.F., Birrell, G., Chen, P., Kozlov, S., Scott, S. and Gueven, N. (2005) ATM signaling and genomic stability in response to DNA damage. *Mutat Res*, **569**, 123-132.

References

- Lavin, M.F., Khanna, K.K., Beamish, H., Spring, K., Watters, D. and Shiloh, Y. (1995) Relationship of the ataxia-telangiectasia protein ATM to phosphoinositide 3-kinase. *Trends Biochem Sci*, **20**, 382-383.
- Lavin, M.F. and Shiloh, Y. (1997) The genetic defect in ataxia-telangiectasia. *Annu Rev Immunol*, **15**, 177-202.
- Lazar-Molnar, E., Hegyesi, H., Toth, S. and Falus, A. (2000) Autocrine and paracrine regulation by cytokines and growth factors in melanoma. *Cytokine*, **12**, 547-554.
- Lee, J.H. and Paull, T.T. (2004) Direct activation of the ATM protein kinase by the Mre11/Rad50/Nbs1 complex. *Science*, **304**, 93-96.
- Lee, J.H. and Paull, T.T. (2005) ATM activation by DNA double-strand breaks through the Mre11-Rad50-Nbs1 complex. *Science*, **308**, 551-554.
- Lee, S.A., Dritschilo, A. and Jung, M. (2001a) Role of ATM in oxidative stress-mediated c-Jun phosphorylation in response to ionizing radiation and CdCl₂. *J Biol Chem*, **276**, 11783-11790.
- Lee, Y., Chong, M.J. and McKinnon, P.J. (2001b) Ataxia telangiectasia mutated-dependent apoptosis after genotoxic stress in the developing nervous system is determined by cellular differentiation status. *J Neurosci*, **21**, 6687-6693.
- Lee, Y. and McKinnon, P.J. (2000) ATM dependent apoptosis in the nervous system. *Apoptosis*, **5**, 523-529.
- Lee, Z.H., Lee, S.E., Kim, C.W., Lee, S.H., Kim, S.W., Kwack, K., Walsh, K. and Kim, H.H. (2002) IL-1 α stimulation of osteoclast survival through the PI 3-kinase/Akt and ERK pathways. *J Biochem (Tokyo)*, **131**, 161-166.
- Lefebvre, P. and Laval, F. (1986) Enhancement of O⁶-methylguanine-DNA-methyltransferase activity induced by various treatments in mammalian cells. *Cancer Res*, **46**, 5701-5705.
- Lefebvre, P. and Laval, F. (1989) Potentiation of N-methyl-N¹-nitro-N-nitrosoguanidine-induced O⁶-methylguanine-DNA-methyltransferase activity in a rat hepatoma cell line by poly (ADP-ribose) synthesis inhibitors. *Biochem Biophys Res Commun*, **163**, 599-604.
- Lefebvre, P., Zak, P. and Laval, F. (1993) Induction of O⁶-methylguanine-DNA-methyltransferase and N³-methyladenine-DNA-glycosylase in human cells exposed to DNA-damaging agents. *DNA Cell Biol*, **12**, 233-241.
- Li, B.D., Khosravi, M.J., Berkel, H.J., Diamandi, A., Dayton, M.A., Smith, M. and Yu, H. (2001a) Free insulin-like growth factor-I and breast cancer risk. *Int J Cancer*, **91**, 736-739.
- Li, N., Banin, S., Ouyang, H., Li, G.C., Courtois, G., Shiloh, Y., Karin, M. and Rotman, G. (2001b) ATM is required for IkappaB kinase (IKK κ) activation in response to DNA double strand breaks. *J Biol Chem*, **276**, 8898-8903.

References

- Li, Q., Bostick-Bruton, F. and Reed, E. (1998) Effect of interleukin-1 alpha and tumour necrosis factor-alpha on cisplatin-induced ERCC-1 mRNA expression in a human ovarian carcinoma cell line. *Anticancer Res*, **18**, 2283-2287.
- Lim, D.S., Kim, S.T., Xu, B., Maser, R.S., Lin, J., Petrini, J.H. and Kastan, M.B. (2000) ATM phosphorylates p95/nbs1 in an S-phase checkpoint pathway. *Nature*, **404**, 613-617.
- Lim, D.S., Kirsch, D.G., Canman, C.E., Ahn, J.H., Ziv, Y., Newman, L.S., Darnell, R.B., Shiloh, Y. and Kastan, M.B. (1998) ATM binds to beta-adaptin in cytoplasmic vesicles. *Proc Natl Acad Sci U S A*, **95**, 10146-10151.
- Lin, W.C., Lin, F.T. and Nevins, J.R. (2001) Selective induction of E2F1 in response to DNA damage, mediated by ATM-dependent phosphorylation. *Genes Dev*, **15**, 1833-1844.
- Ling, Z., Chen, M.C., Smismans, A., Pavlovic, D., Schuit, F., Eizirik, D.L. and Pipeleers, D.G. (1998) Intercellular differences in interleukin 1beta-induced suppression of insulin synthesis and stimulation of noninsulin protein synthesis by rat pancreatic beta-cells. *Endocrinology*, **139**, 1540-1545.
- Liss, C., Fekete, M.J., Hasina, R., Lam, C.D. and Lingem, M.W. (2001) Paracrine angiogenic loop between head-and-neck squamous-cell carcinomas and macrophages. *Int J Cancer*, **93**, 781-785.
- Lissy, N.A., Davis, P.K., Irwin, M., Kaelin, W.G. and Dowdy, S.F. (2000) A common E2F-1 and p73 pathway mediates cell death induced by TCR activation. *Nature*, **407**, 642-645.
- Loechler, E.L., Green, C.L. and Essigmann, J.M. (1984) In vivo mutagenesis by O6-methylguanine built into a unique site in a viral genome. *Proc Natl Acad Sci U S A*, **81**, 6271-6275.
- London, S.J., Yuan, J.M., Travlos, G.S., Gao, Y.T., Wilson, R.E., Ross, R.K. and Yu, M.C. (2002) Insulin-like growth factor I, IGF-binding protein 3, and lung cancer risk in a prospective study of men in China. *J Natl Cancer Inst*, **94**, 749-754.
- Lovett, D., Kozan, B., Hadam, M., Resch, K. and Gemsa, D. (1986) Macrophage cytotoxicity: interleukin 1 as a mediator of tumor cytostasis. *J Immunol*, **136**, 340-347.
- Lowry, O.H., Rosebrough, N.J., Farr, A.L. and Randall, R.J. (1951) Protein measurement with the Folin phenol reagent. *J Biol Chem*, **193**, 265-275.
- Macaulay, V.M., Salisbury, A.J., Bohula, E.A., Playford, M.P., Smorodinsky, N.I. and Shiloh, Y. (2001) Downregulation of the type 1 insulin-like growth factor receptor in mouse melanoma cells is associated with enhanced radiosensitivity and impaired activation of Atm kinase. *Oncogene*, **20**, 4029-4040.
- Madge, L.A. and Pober, J.S. (2000) A phosphatidylinositol 3-kinase/Akt pathway, activated by tumor necrosis factor or interleukin-1, inhibits apoptosis but does not activate NFkappaB in human endothelial cells. *J Biol Chem*, **275**, 15458-15465.

References

- Majano, P.L., Garcia-Monzon, C., Lopez-Cabrera, M., Lara-Pezzi, E., Fernandez-Ruiz, E., Garcia-Iglesias, C., Borque, M.J. and Moreno-Otero, R. (1998) Inducible nitric oxide synthase expression in chronic viral hepatitis. Evidence for a virus-induced gene upregulation. *J Clin Invest*, **101**, 1343-1352.
- March, C.J., Mosley, B., Larsen, A., Cerretti, D.P., Braedt, G., Price, V., Gillis, S., Henney, C.S., Kronheim, S.R., Grabstein, K. and et al. (1985) Cloning, sequence and expression of two distinct human interleukin-1 complementary DNAs. *Nature*, **315**, 641-647.
- Martin, M.U. and Wesche, H. (2002) Summary and comparison of the signaling mechanisms of the Toll/interleukin-1 receptor family. *Biochim Biophys Acta*, **1592**, 265-280.
- Matsuoka, S., Rotman, G., Ogawa, A., Shiloh, Y., Tamai, K. and Elledge, S.J. (2000) Ataxia telangiectasia-mutated phosphorylates Chk2 in vivo and in vitro. *Proc Natl Acad Sci U S A*, **97**, 10389-10394.
- Maya, R., Balass, M., Kim, S.T., Shkedy, D., Leal, J.F., Shifman, O., Moas, M., Buschmann, T., Ronai, Z., Shiloh, Y., Kastan, M.B., Katzir, E. and Oren, M. (2001) ATM-dependent phosphorylation of Mdm2 on serine 395: role in p53 activation by DNA damage. *Genes Dev*, **15**, 1067-1077.
- McMahan, C.J., Slack, J.L., Mosley, B., Cosman, D., Lupton, S.D., Brunton, L.L., Grubin, C.E., Wignall, J.M., Jenkins, N.A., Brannan, C.I. and et al. (1991) A novel IL-1 receptor, cloned from B cells by mammalian expression, is expressed in many cell types. *Embo J*, **10**, 2821-2832.
- Melchionna, R., Chen, X.B., Blasina, A. and McGowan, C.H. (2000) Threonine 68 is required for radiation-induced phosphorylation and activation of Cds1. *Nat Cell Biol*, **2**, 762-765.
- Miller, L.J., Kurtzman, S.H., Anderson, K., Wang, Y., Stankus, M., Renna, M., Lindquist, R., Barrows, G. and Kreutzer, D.L. (2000) Interleukin-1 family expression in human breast cancer: interleukin-1 receptor antagonist. *Cancer Invest*, **18**, 293-302.
- Mitra, S. and Kaina, B. (1993) Regulation of repair of alkylation damage in mammalian genomes. *Prog Nucleic Acid Res Mol Biol*, **44**, 109-142.
- Moore, M.H., Gulbis, J.M., Dodson, E.J., Demple, B. and Moody, P.C. (1994) Crystal structure of a suicidal DNA repair protein: the Ada O6-methylguanine-DNA methyltransferase from *E. coli*. *Embo J*, **13**, 1495-1501.
- Mosley, B., Urdal, D.L., Prickett, K.S., Larsen, A., Cosman, D., Conlon, P.J., Gillis, S. and Dower, S.K. (1987) The interleukin-1 receptor binds the human interleukin-1 alpha precursor but not the interleukin-1 beta precursor. *J Biol Chem*, **262**, 2941-2944.
- Muta, K., Krantz, S.B., Bondurant, M.C. and Wickrema, A. (1994) Distinct roles of erythropoietin, insulin-like growth factor I, and stem cell factor in the development of erythroid progenitor cells. *J Clin Invest*, **94**, 34-43.

References

- Nalca, A. and Rangnekar, V.M. (1998) The G1-phase growth-arresting action of interleukin-1 is independent of p53 and p21/WAF1 function. *J Biol Chem*, **273**, 30517-30523.
- Nikulina, M.A., Sandhu, N., Shamim, Z., Andersen, N.A., Oberson, A., Dupraz, P., Thorens, B., Karlsen, A.E., Bonny, C. and Mandrup-Poulsen, T. (2003) The JNK binding domain of islet-brain 1 inhibits IL-1 induced JNK activity and apoptosis but not the transcription of key proapoptotic or protective genes in insulin-secreting cell lines. *Cytokine*, **24**, 13-24.
- Ochs, K. and Kaina, B. (2000) Apoptosis induced by DNA damage O6-methylguanine is Bcl-2 and caspase-9/3 regulated and Fas/caspase-8 independent. *Cancer Res*, **60**, 5815-5824.
- Ochs, K., Lips, J., Profittlich, S. and Kaina, B. (2002) Deficiency in DNA polymerase beta provokes replication-dependent apoptosis via DNA breakage, Bcl-2 decline and caspase-3/9 activation. *Cancer Res*, **62**, 1524-1530.
- O'Connor, P.J. and Saffhill, R. (1979) The action of rat cytosol enzymes on some methylated nucleic acid components produced by the carcinogenic N-nitroso compounds. *Chem Biol Interact*, **26**, 91-102.
- Olivecrona, H., Hilding, A., Ekstrom, C., Barle, H., Nyberg, B., Moller, C., Delhanty, P.J., Baxter, R.C., Angelin, B., Ekstrom, T.J. and Tally, M. (1999) Acute and short-term effects of growth hormone on insulin-like growth factors and their binding proteins: serum levels and hepatic messenger ribonucleic acid responses in humans. *J Clin Endocrinol Metab*, **84**, 553-560.
- O'Neill, J.P. (2000) DNA damage, DNA repair, cell proliferation, and DNA replication: how do gene mutations result? *Proc Natl Acad Sci U S A*, **97**, 11137-11139.
- O'Neill, T., Dwyer, A.J., Ziv, Y., Chan, D.W., Lees-Miller, S.P., Abraham, R.H., Lai, J.H., Hill, D., Shiloh, Y., Cantley, L.C. and Rathbun, G.A. (2000) Utilization of oriented peptide libraries to identify substrate motifs selected by ATM. *J Biol Chem*, **275**, 22719-22727.
- Onozaki, K., Matsushima, K., Aggarwal, B.B. and Oppenheim, J.J. (1985) Human interleukin 1 is a cytotoxic factor for several tumor cell lines. *J Immunol*, **135**, 3962-3968.
- Osawa, Y., Hachiya, M., Araki, S., Kusama, T., Matsushima, K., Aoki, Y. and Akashi, M. (2000) IL-1 induces expression of p21(WAF1) independently of p53 in high-passage human embryonic fibroblasts WI38. *J Biochem (Tokyo)*, **127**, 883-893.
- Panta, G.R., Kaur, S., Cavin, L.G., Cortes, M.L., Mercurio, F., Lothstein, L., Sweatman, T.W., Israel, M. and Arsura, M. (2004) ATM and the catalytic subunit of DNA-dependent protein kinase activate NF-kappaB through a common MEK/extracellular signal-regulated kinase/p90(rsk) signaling pathway in response to distinct forms of DNA damage. *Mol Cell Biol*, **24**, 1823-1835.
- Pegg, A.E. (1990) Properties of mammalian O6-alkylguanine-DNA transferases. *Mutat Res*, **233**, 165-175.

References

- Pegg, A.E. (1999) DNA repair pathways and cancer prevention. *Adv Exp Med Biol*, **472**, 253-267.
- Pegg, A.E., Dolan, M.E. and Moschel, R.C. (1995) Structure, function, and inhibition of O6-alkylguanine-DNA alkyltransferase. *Prog Nucleic Acid Res Mol Biol*, **51**, 167-223.
- Peretz, S., Jensen, R., Baserga, R. and Glazer, P.M. (2001) ATM-dependent expression of the insulin-like growth factor-I receptor in a pathway regulating radiation response. *Proc Natl Acad Sci U S A*, **98**, 1676-1681.
- Piret, B., Schoonbroodt, S. and Piette, J. (1999) The ATM protein is required for sustained activation of NF-kappaB following DNA damage. *Oncogene*, **18**, 2261-2271.
- Poppelmann, B., Klimmek, K., Strozyk, E., Voss, R., Schwarz, T. and Kulms, D. (2005) NF{kappa}B-dependent down-regulation of tumor necrosis factor receptor-associated proteins contributes to interleukin-1-mediated enhancement of ultraviolet B-induced apoptosis. *J Biol Chem*, **280**, 15635-15643.
- Povey, A.C., Hall, C.N., Cooper, D.P., O'Connor, P.J. and Margison, G.P. (2000) Determinants of O(6)-alkylguanine-DNA alkyltransferase activity in normal and tumour tissue from human colon and rectum. *Int J Cancer*, **85**, 68-72.
- Preuss, I., Thust, R. and Kaina, B. (1996) Protective effect of O6-methylguanine-DNA methyltransferase (MGMT) on the cytotoxic and recombinogenic activity of different antineoplastic drugs. *Int J Cancer*, **65**, 506-512.
- Ralston, S.H. and Grabowski, P.S. (1996) Mechanisms of cytokine induced bone resorption: role of nitric oxide, cyclic guanosine monophosphate, and prostaglandins. *Bone*, **19**, 29-33.
- Roos, W., Baumgartner, M. and Kaina, B. (2004) Apoptosis triggered by DNA damage O6-methylguanine in human lymphocytes requires DNA replication and is mediated by p53 and Fas/CD95/Apo-1. *Oncogene*, **23**, 359-367.
- Rossi, S.C. and Topal, M.D. (1991) Mutagenic frequencies of site-specifically located O6-methylguanine in wild-type Escherichia coli and in a strain deficient in adenine methyltransferase. *J Bacteriol*, **173**, 1201-1207.
- Rozen, F., Zhang, J. and Pollak, M. (1998) Antiproliferative action of tumor necrosis factor-alpha on MCF-7 breastcancer cells is associated with increased insulin-like growth factor binding protein-3 accumulation. *Int J Oncol*, **13**, 865-869.
- Rubin, R. and Baserga, R. (1995) Insulin-like growth factor-I receptor. Its role in cell proliferation, apoptosis, and tumorigenicity. *Lab Invest*, **73**, 311-331.
- Saffhill, R. and Hall, J.A. (1985) The incorporation of O6-methyldeoxyguanosine monophosphate and O4-methyldeoxythymidine monophosphate into polynucleotide templates leads to errors during subsequent in vitro DNA synthesis. *Chem Biol Interact*, **56**, 363-370.

References

- Sarkaria, J.N., Busby, E.C., Tibbetts, R.S., Roos, P., Taya, Y., Karnitz, L.M. and Abraham, R.T. (1999) Inhibition of ATM and ATR kinase activities by the radiosensitizing agent, caffeine. *Cancer Res*, **59**, 4375-4382.
- Savitsky, K., Bar-Shira, A., Gilad, S., Rotman, G., Ziv, Y., Vanagaite, L., Tagle, D.A., Smith, S., Uziel, T., Sfez, S. and et al. (1995a) A single ataxia telangiectasia gene with a product similar to PI-3 kinase. *Science*, **268**, 1749-1753.
- Savitsky, K., Sfez, S., Tagle, D.A., Ziv, Y., Sartiell, A., Collins, F.S., Shiloh, Y. and Rotman, G. (1995b) The complete sequence of the coding region of the ATM gene reveals similarity to cell cycle regulators in different species. *Hum Mol Genet*, **4**, 2025-2032.
- Sawada, K., Krantz, S.B., Dessypris, E.N., Koury, S.T. and Sawyer, S.T. (1989) Human colony-forming units-erythroid do not require accessory cells, but do require direct interaction with insulin-like growth factor I and/or insulin for erythroid development. *J Clin Invest*, **83**, 1701-1709.
- Scudiero, D.A. (1980) Decreased DNA repair synthesis and defective colony-forming ability of ataxia telangiectasia fibroblast cell strains treated with N-methyl-N'-nitro-N-nitrosoguanidine. *Cancer Res*, **40**, 984-990.
- Sell, C., Baserga, R. and Rubin, R. (1995) Insulin-like growth factor I (IGF-I) and the IGF-I receptor prevent etoposide-induced apoptosis. *Cancer Res*, **55**, 303-306.
- Shafman, T., Khanna, K.K., Kedar, P., Spring, K., Kozlov, S., Yen, T., Hobson, K., Gatei, M., Zhang, N., Watters, D., Egerton, M., Shiloh, Y., Kharbanda, S., Kufe, D. and Lavin, M.F. (1997) Interaction between ATM protein and c-Abl in response to DNA damage. *Nature*, **387**, 520-523.
- Shahrabani-Gargir, L., Pandita, T.K. and Werner, H. (2004) Ataxia-telangiectasia mutated gene controls insulin-like growth factor I receptor gene expression in a deoxyribonucleic acid damage response pathway via mechanisms involving zinc-finger transcription factors Sp1 and WT1. *Endocrinology*, **145**, 5679-5687.
- Shaul, Y. (2000) c-Abl: activation and nuclear targets. *Cell Death Differ*, **7**, 10-16.
- Shiloh, Y. (2001) ATM and ATR: networking cellular responses to DNA damage. *Curr Opin Genet Dev*, **11**, 71-77.
- Shiloh, Y. (2003) ATM: ready, set, go. *Cell Cycle*, **2**, 116-117.
- Shiloh, Y. and Becker, Y. (1981) Kinetics of O6-methylguanine repair in human normal and ataxia telangiectasia cell lines and correlation of repair capacity with cellular sensitivity to methylating agents. *Cancer Res*, **41**, 5114-5120.
- Shiraishi, A., Sakumi, K. and Sekiguchi, M. (2000) Increased susceptibility to chemotherapeutic alkylating agents of mice deficient in DNA repair methyltransferase. *Carcinogenesis*, **21**, 1879-1883.

References

- Shumate, M.L., Yumet, G., Ahmed, T.A. and Cooney, R.N. (2005) Interleukin-1 (IL-1) inhibits the induction of insulin-like growth factor-I (IGF-I) by growth hormone (GH) in CWSV-1 hepatocytes. *Am J Physiol Gastrointest Liver Physiol*.
- Sikpi, M.O., Wang, Y. and Mallya, S.M. (1999) Heightened induction of c-jun mRNA by PMA, EGF and IL-1 in ataxia telangiectasia lymphoblasts. *Int J Radiat Biol*, **75**, 893-901.
- Silber, J.R., Bobola, M.S., Ghatan, S., Blank, A., Kolstoe, D.D. and Berger, M.S. (1998) O6-methylguanine-DNA methyltransferase activity in adult gliomas: relation to patient and tumor characteristics. *Cancer Res*, **58**, 1068-1073.
- Silber, J.R., Mueller, B.A., Ewers, T.G. and Berger, M.S. (1993) Comparison of O6-methylguanine-DNA methyltransferase activity in brain tumors and adjacent normal brain. *Cancer Res*, **53**, 3416-3420.
- Simonart, T. and Van Vooren, J.P. (2002) Interleukin-1 beta increases the BCL-2/BAX ratio in Kaposi's sarcoma cells. *Cytokine*, **19**, 259-266.
- Sims, J.E., March, C.J., Cosman, D., Widmer, M.B., MacDonald, H.R., McMahan, C.J., Grubin, C.E., Wignall, J.M., Jackson, J.L., Call, S.M. and et al. (1988) cDNA expression cloning of the IL-1 receptor, a member of the immunoglobulin superfamily. *Science*, **241**, 585-589.
- Singer, II, Kawka, D.W., Scott, S., Weidner, J.R., Mumford, R.A., Riehl, T.E. and Stenson, W.F. (1996) Expression of inducible nitric oxide synthase and nitrotyrosine in colonic epithelium in inflammatory bowel disease. *Gastroenterology*, **111**, 871-885.
- Singer, C.F., Kronsteiner, N., Hudelist, G., Marton, E., Walter, I., Kubista, M., Czerwenka, K., Schreiber, M., Seifert, M. and Kubista, E. (2003) Interleukin 1 system and sex steroid receptor expression in human breast cancer: interleukin 1alpha protein secretion is correlated with malignant phenotype. *Clin Cancer Res*, **9**, 4877-4883.
- Smith, G.C., Cary, R.B., Lakin, N.D., Hann, B.C., Teo, S.H., Chen, D.J. and Jackson, S.P. (1999) Purification and DNA binding properties of the ataxia-telangiectasia gene product ATM. *Proc Natl Acad Sci U S A*, **96**, 11134-11139.
- Soares, H.D., Morgan, J.I. and McKinnon, P.J. (1998) Atm expression patterns suggest a contribution from the peripheral nervous system to the phenotype of ataxia-telangiectasia. *Neuroscience*, **86**, 1045-1054.
- Soon, L., Flechner, L., Gutkind, J.S., Wang, L.H., Baserga, R., Pierce, J.H. and Li, W. (1999) Insulin-like growth factor I synergizes with interleukin 4 for hematopoietic cell proliferation independent of insulin receptor substrate expression. *Mol Cell Biol*, **19**, 3816-3828.
- Srivenugopal, K.S., Yuan, X.H., Friedman, H.S. and Ali-Osman, F. (1996) Ubiquitination-dependent proteolysis of O6-methylguanine-DNA methyltransferase in human and murine tumor cells following inactivation with O6-benzylguanine or 1,3-bis(2-chloroethyl)-1-nitrosourea. *Biochemistry*, **35**, 1328-1334.

References

- Stewart, G.S., Maser, R.S., Stankovic, T., Bressan, D.A., Kaplan, M.I., Jaspers, N.G., Raams, A., Byrd, P.J., Petrini, J.H. and Taylor, A.M. (1999) The DNA double-strand break repair gene hMRE11 is mutated in individuals with an ataxia-telangiectasia-like disorder. *Cell*, **99**, 577-587.
- Stojic, L., Mojas, N., Cejka, P., Di Pietro, M., Ferrari, S., Marra, G. and Jiricny, J. (2004) Mismatch repair-dependent G2 checkpoint induced by low doses of SN1 type methylating agents requires the ATR kinase. *Genes Dev*, **18**, 1331-1344.
- Sun, X., Becker-Catania, S.G., Chun, H.H., Hwang, M.J., Huo, Y., Wang, Z., Mitui, M., Sanal, O., Chessa, L., Crandall, B. and Gatti, R.A. (2002) Early diagnosis of ataxia-telangiectasia using radiosensitivity testing. *J Pediatr*, **140**, 724-731.
- Suzuki, A., Kusakai, G., Kishimoto, A., Lu, J., Ogura, T., Lavin, M.F. and Esumi, H. (2003) Identification of a novel protein kinase mediating Akt survival signaling to the ATM protein. *J Biol Chem*, **278**, 48-53.
- Suzuki, A., Kusakai, G., Kishimoto, A., Shimojo, Y., Ogura, T., Lavin, M.F. and Esumi, H. (2004) IGF-1 phosphorylates AMPK-alpha subunit in ATM-dependent and LKB1-independent manner. *Biochem Biophys Res Commun*, **324**, 986-992.
- Suzuki, K., Kodama, S. and Watanabe, M. (1999) Recruitment of ATM protein to double strand DNA irradiated with ionizing radiation. *J Biol Chem*, **274**, 25571-25575.
- Takikawa, O., Oku, T., Yasui, H. and Yoshida, R. (1993) Synergism between IFN-gamma and IL-1 alpha/beta in growth inhibition of an allografted tumor. *J Immunol*, **151**, 2070-2076.
- Teo, I.A. and Arlett, C.F. (1982) The response of a variety of human fibroblast cell strains to the lethal effects of alkylating agents. *Carcinogenesis*, **3**, 33-37.
- Thissen, J.P. and Verniers, J. (1997) Inhibition by interleukin-1 beta and tumor necrosis factor-alpha of the insulin-like growth factor I messenger ribonucleic acid response to growth hormone in rat hepatocyte primary culture. *Endocrinology*, **138**, 1078-1084.
- Thomas, G.R., Chen, Z., Leukinova, E., Van Waes, C. and Wen, J. (2004) Cytokines IL-1 alpha, IL-6, and GM-CSF constitutively secreted by oral squamous carcinoma induce down-regulation of CD80 costimulatory molecule expression: restoration by interferon gamma. *Cancer Immunol Immunother*, **53**, 33-40.
- Thornberry, N.A., Bull, H.G., Calaycay, J.R., Chapman, K.T., Howard, A.D., Kostura, M.J., Miller, D.K., Molineaux, S.M., Weidner, J.R., Aunins, J. and et al. (1992) A novel heterodimeric cysteine protease is required for interleukin-1 beta processing in monocytes. *Nature*, **356**, 768-774.
- Tomicic, M., Eschbach, E. and Kaina, B. (1997) Expression of yeast but not human apurinic/aprimidinic endonuclease renders Chinese hamster cells more resistant to DNA damaging agents. *Mutat Res*, **383**, 155-165.

References

- Trojanek, J., Ho, T., Del Valle, L., Nowicki, M., Wang, J.Y., Lassak, A., Peruzzi, F., Khalili, K., Skorski, T. and Reiss, K. (2003) Role of the insulin-like growth factor I/insulin receptor substrate 1 axis in Rad51 trafficking and DNA repair by homologous recombination. *Mol Cell Biol*, **23**, 7510-7524.
- Tsuchimoto, D., Sakai, Y., Sakumi, K., Nishioka, K., Sasaki, M., Fujiwara, T. and Nakabeppu, Y. (2001) Human APE2 protein is mostly localized in the nuclei and to some extent in the mitochondria, while nuclear APE2 is partly associated with proliferating cell nuclear antigen. *Nucleic Acids Res*, **29**, 2349-2360.
- Turner, B.C., Haffty, B.G., Narayanan, L., Yuan, J., Havre, P.A., Gumbs, A.A., Kaplan, L., Burgaud, J.L., Carter, D., Baserga, R. and Glazer, P.M. (1997) Insulin-like growth factor-I receptor overexpression mediates cellular radioresistance and local breast cancer recurrence after lumpectomy and radiation. *Cancer Res*, **57**, 3079-3083.
- Uziel, T., Lerenthal, Y., Moyal, L., Andegeko, Y., Mittelman, L. and Shiloh, Y. (2003) Requirement of the MRN complex for ATM activation by DNA damage. *Embo J*, **22**, 5612-5621.
- van de Winkel, J.G. and Capel, P.J. (1993) Human IgG Fc receptor heterogeneity: molecular aspects and clinical implications. *Immunol Today*, **14**, 215-221.
- van't Hof, R.J., Armour, K.J., Smith, L.M., Armour, K.E., Wei, X.Q., Liew, F.Y. and Ralston, S.H. (2000) Requirement of the inducible nitric oxide synthase pathway for IL-1-induced osteoclastic bone resorption. *Proc Natl Acad Sci U S A*, **97**, 7993-7998.
- van't Hof, R.J. and Ralston, S.H. (1997) Cytokine-induced nitric oxide inhibits bone resorption by inducing apoptosis of osteoclast progenitors and suppressing osteoclast activity. *J Bone Miner Res*, **12**, 1797-1804.
- Varon, R., Vissinga, C., Platzer, M., Cerosaletti, K.M., Chrzanowska, K.H., Saar, K., Beckmann, G., Seemanova, E., Cooper, P.R., Nowak, N.J., Stumm, M., Weemaes, C.M., Gatti, R.A., Wilson, R.K., Digweed, M., Rosenthal, A., Sperling, K., Concannon, P. and Reis, A. (1998) Nibrin, a novel DNA double-strand break repair protein, is mutated in Nijmegen breakage syndrome. *Cell*, **93**, 467-476.
- Verhasselt, B., Van Damme, J., van Larebeke, N., Put, W., Bracke, M., De Potter, C. and Mareel, M. (1992) Interleukin-1 is a motility factor for human breast carcinoma cells in vitro: additive effect with interleukin-6. *Eur J Cell Biol*, **59**, 449-457.
- von Wronski, M.A. and Brent, T.P. (1994) Effect of 5-azacytidine on expression of the human DNA repair enzyme O6-methylguanine-DNA methyltransferase. *Carcinogenesis*, **15**, 577-582.
- Wang, J., Ando, T. and Dunn, A.J. (1997) Effect of homologous interleukin-1, interleukin-6 and tumor necrosis factor-alpha on the core body temperature of mice. *Neuroimmunomodulation*, **4**, 230-236.
- Wang, Y., Kato, T., Ayaki, H., Ishizaki, K., Tano, K., Mitra, S. and Ikenaga, M. (1992) Correlation between DNA methylation and expression of O6-methylguanine-DNA methyltransferase gene in cultured human tumor cells. *Mutat Res*, **273**, 221-230.

References

- Wang, Z., Lee, K.B., Reed, E. and Sinha, B.K. (1996) Sensitization by interleukin-1alpha of carboplatinum anti-tumor activity against human ovarian (NIH:OVCAR-3) carcinoma cells in vitro and in vivo. *Int J Cancer*, **68**, 583-587.
- Watters, D., Kedar, P., Spring, K., Bjorkman, J., Chen, P., Gatei, M., Birrell, G., Garrone, B., Srinivasa, P., Crane, D.I. and Lavin, M.F. (1999) Localization of a portion of extranuclear ATM to peroxisomes. *J Biol Chem*, **274**, 34277-34282.
- Watts, G.S., Pieper, R.O., Costello, J.F., Peng, Y.M., Dalton, W.S. and Futscher, B.W. (1997) Methylation of discrete regions of the O6-methylguanine DNA methyltransferase (MGMT) CpG island is associated with heterochromatinization of the MGMT transcription start site and silencing of the gene. *Mol Cell Biol*, **17**, 5612-5619.
- Weizman, N., Shiloh, Y. and Barzilai, A. (2003) Contribution of the Atm protein to maintaining cellular homeostasis evidenced by continuous activation of the AP-1 pathway in Atm-deficient brains. *J Biol Chem*, **278**, 6741-6747.
- Wibley, J.E., Pegg, A.E. and Moody, P.C. (2000) Crystal structure of the human O(6)-alkylguanine-DNA alkyltransferase. *Nucleic Acids Res*, **28**, 393-401.
- Wolf, J.S., Chen, Z., Dong, G., Sunwoo, J.B., Bancroft, C.C., Capo, D.E., Yeh, N.T., Mukaida, N. and Van Waes, C. (2001) IL (interleukin)-1alpha promotes nuclear factor-kappaB and AP-1-induced IL-8 expression, cell survival, and proliferation in head and neck squamous cell carcinomas. *Clin Cancer Res*, **7**, 1812-1820.
- Wolf, M., Bohm, S., Brand, M. and Kreymann, G. (1996) Proinflammatory cytokines interleukin 1 beta and tumor necrosis factor alpha inhibit growth hormone stimulation of insulin-like growth factor I synthesis and growth hormone receptor mRNA levels in cultured rat liver cells. *Eur J Endocrinol*, **135**, 729-737.
- Woods, K.V., El-Naggar, A., Clayman, G.L. and Grimm, E.A. (1998) Variable expression of cytokines in human head and neck squamous cell carcinoma cell lines and consistent expression in surgical specimens. *Cancer Res*, **58**, 3132-3141.
- Wu, X., Ranganathan, V., Weisman, D.S., Heine, W.F., Ciccone, D.N., O'Neill, T.B., Crick, K.E., Pierce, K.A., Lane, W.S., Rathbun, G., Livingston, D.M. and Weaver, D.T. (2000a) ATM phosphorylation of Nijmegen breakage syndrome protein is required in a DNA damage response. *Nature*, **405**, 477-482.
- Wu, X., Rathbun, G., Lane, W.S., Weaver, D.T. and Livingston, D.M. (2000b) Interactions of the Nijmegen breakage syndrome protein with ATM and BRCA1. *Cold Spring Harb Symp Quant Biol*, **65**, 535-545.
- Xie, K., Huang, S., Wang, Y., Beltran, P.J., Juang, S.H., Dong, Z., Reed, J.C., McDonnell, T.J., McConkey, D.J. and Fidler, I.J. (1996) Bcl-2 protects cells from cytokine-induced nitric-oxide-dependent apoptosis. *Cancer Immunol Immunother*, **43**, 109-115.
- Xu, Y., Ashley, T., Brainerd, E.E., Bronson, R.T., Meyn, M.S. and Baltimore, D. (1996) Targeted disruption of ATM leads to growth retardation, chromosomal fragmentation during meiosis, immune defects, and thymic lymphoma. *Genes Dev*, **10**, 2411-2422.

References

- Xu, Y. and Baltimore, D. (1996) Dual roles of ATM in the cellular response to radiation and in cell growth control. *Genes Dev*, **10**, 2401-2410.
- Yamada, K., Takane-Gyotoku, N., Yuan, X., Ichikawa, F., Inada, C. and Nonaka, K. (1996) Mouse islet cell lysis mediated by interleukin-1-induced Fas. *Diabetologia*, **39**, 1306-1312.
- Yang, D.Q. and Kastan, M.B. (2000) Participation of ATM in insulin signalling through phosphorylation of eIF-4E-binding protein 1. *Nat Cell Biol*, **2**, 893-898.
- Yuan, S.S., Chang, H.L., Hou, M.F., Chan, T.F., Kao, Y.H., Wu, Y.C. and Su, J.H. (2002) Neocarzinostatin induces Mre11 phosphorylation and focus formation through an ATM- and NBS1-dependent mechanism. *Toxicology*, **177**, 123-130.
- Yuan, S.S., Chang, H.L. and Lee, E.Y. (2003a) Ionizing radiation-induced Rad51 nuclear focus formation is cell cycle-regulated and defective in both ATM(-/-) and c-Abl(-/-) cells. *Mutat Res*, **525**, 85-92.
- Yuan, S.S., Yang, Y.K., Chen, H.W., Chung, Y.F., Chang, H.L. and Su, J.H. (2003b) Neocarzinostatin-induced Rad51 nuclear focus formation is cell cycle regulated and aberrant in AT cells. *Toxicol Appl Pharmacol*, **192**, 231-236.
- Zha, J., Harada, H., Yang, E., Jockel, J. and Korsmeyer, S.J. (1996) Serine phosphorylation of death agonist BAD in response to survival factor results in binding to 14-3-3 not BCL-X(L). *Cell*, **87**, 619-628.
- Zhang, Y., Ma, W.Y., Kaji, A., Bode, A.M. and Dong, Z. (2002) Requirement of ATM in UVA-induced signaling and apoptosis. *J Biol Chem*, **277**, 3124-3131.
- Zhang, Z. and Fuller, G.M. (1997) The competitive binding of STAT3 and NF-kappaB on an overlapping DNA binding site. *Biochem Biophys Res Commun*, **237**, 90-94.
- Zhao, S., Weng, Y.C., Yuan, S.S., Lin, Y.T., Hsu, H.C., Lin, S.C., Gerbino, E., Song, M.H., Zdzienicka, M.Z., Gatti, R.A., Shay, J.W., Ziv, Y., Shiloh, Y. and Lee, E.Y. (2000) Functional link between ataxia-telangiectasia and Nijmegen breakage syndrome gene products. *Nature*, **405**, 473-477.
- Zhou, B.B., Chaturvedi, P., Spring, K., Scott, S.P., Johanson, R.A., Mishra, R., Mattern, M.R., Winkler, J.D. and Khanna, K.K. (2000) Caffeine abolishes the mammalian G(2)/M DNA damage checkpoint by inhibiting ataxia-telangiectasia-mutated kinase activity. *J Biol Chem*, **275**, 10342-10348.